GENERAL ATOMIC

GA-A14214
UC-77

THORIUM UTILIZATION PROGRAM

QUARTERLY PROGRESS REPORT FOR THE PERIOD ENDING NOVEMBER 30, 1976

Prepared under
Contract EY-76-C-03-0167
Project Agreement No. 53
for the San Francisco Operations Office
U.S. Energy Research and Development Administration

GENERAL ATOMIC PROJECT 3225

DATE PUBLISHED: DECEMBER 1976

DISCLAIMER

QUARTERLY REPORT SERIES*

GA-A13178 - June 1974 through August 1974

GA-A13255 - September 1974 through November 1974

GA-A13366 - December 1974 through February 1975

GA-A13510 - March 1975 through May 1975

GA-A13593 - June 1975 through August 1975

GA-A13746 - September 1975 through November 1975

GA-A13833 - December 1975 through February 1976

GA-A13949 - March 1976 through May 1976

GA-A14085 - June 1976 through August 1976

*Prior to GA-A13178, the Thorium Utilization Program was reported in the Base Program Quarterly Progress Report.

ABSTRACT

This publication continues the quarterly series presenting results of work performed under the National HTGR Fuel Recycle Program (also known as the Thorium Utilization Program) at General Atomic Company. Results of work on this program prior to June 1974 were included in a quarterly series on the HTGR Base Program.

The work reported includes the development of unit processes and equipment for reprocessing of High-Temperature Gas-Cooled Reactor (HTGR) fuel, the design and development of an integrated pilot line to demonstrate the head end of HTGR reprocessing using unirradiated fuel materials, and design work in support of Hot Engineering Tests (HET). Work is also described on trade-off studies concerning the required design of facilities and equipment for the large-scale recycle of HTGR fuels in order to guide the development activities for HTGR fuel recycle.

INTRODUCTION

This report covers the work performed by General Atomic Company under U.S. Energy Research and Development Administration Contract EY-76-C-03-0167, Project Agreement No. 53. The work done under this project agreement is part of the program for development of recycle technology for High-Temperature Gas-Cooled Reactor (HTGR) fuels described in the "National Program Plan for HTGR Fuel Recycle Development" (GCR-76/19).

The objective of the program is to provide a demonstration plant for the recycle of HTGR fuels. This plant will demonstrate facility and equipment design and operating procedures which are licensable and commercially feasible for the reprocessing and refabrication of spent fuel from HTGRs. Work at General Atomic Company is concentrating on the following National Program tasks: Program Management and Analysis (Task 100); Reprocessing Technology Development (Task 200); Refabrication Technology Development (Task 300); HTGR Recycle Demonstration Facility (HRDF) design support (Task 600).

Task 100, Program Management and Analysis, includes the functions of overall planning, scheduling, budgeting, reporting, management control of the program, and coordination of activities.

Task 200, Reprocessing Technology Development, includes the definition of flowsheets, the development of components, and the definition of operating techniques, remote maintenance and or disassembly techniques, and coordination of fuel shipping and storage activities. Operations which must be developed include crushing of the fuel elements; burning the graphite in a fluidized bed-burner; separation of the fertile and fissile

particles; crushing the SiC coating on fissile particles; burning the crushed particles; dissolution of thorium and uranium in the burned, crushed particles; separation of the undissolved solids (SiC hulls, etc.) from the leachate; separation of the thorium and uranium from the fission products by solvent extraction; separation and purification of the thorium and uranium by solvent extraction; process and facility off-gas treatments to ensure releases are environmentally acceptable and in compliance with regulations; and the primary treatment of solid, liquid, and gaseous wastes from the process.

Task 300, Refabrication Technology Development, includes the definition of flowsheets, the development of components, and the definition of operating techniques, remote maintenance and/or disassembly techniques, and coordination of fuel shipping and storage activities. The refabrication begins with aqueous uranyl nitrate solution from the reprocessing facility and ends with fuel elements prepared for shipment to the reactor. The principal operations to be developed are loading the ion-exchange resin with uranium, resin carbonization, resin conversion, coating the converted resin with pyrolytic carbon and SiC, fuel rod fabrication, fuel element assembly, fuel and fuel element inspection, scrap recovery, and waste handling.

Task 600, HTGR Recycle Demonstration Facility, includes the design, construction, proof-testing, and operation of a demonstration facility for the recycle of HTGR fuel. The plant is to include all fuel cycle operations from the receiving of spent fuel elements from the reactors to shipping the refabricated fuel elements back to the reactors. The preconceptual design studies and the early conceptual design are to be used to guide the development work for reprocessing and refabrication processes and equipment. The results of the research and development tasks will in turn be used to guide the detailed design of HRDF.

CONTENTS

FIGURES

FIGURES (Continued)

FIGURES (Continued)

FIGURES (Continued)

FIGURES (Continued)

TABLES

TABLES (Continued)

TABLES (Continued)

1. SUMMARY

Program activities remained on schedule during the quarter with head-end reprocessing line equipment shakedown and modifications continuing. Fuel element size reduction system (UNIFRAME) demonstrations have been completed for the primary and secondary crushers. These demonstrations have resulted in design modifications to the primary crusher toggles and cheek plate assemblies and the addition of a fuel element chute and side/guide/clamp plate chamfers. No design modifications have been finalized for the secondary crusher. "Blinding" was experienced on the vibratory screener-separator during Phase I testing of this equipment. Various screener modifications are being evaluated and this work will continue during the next quarter.

The prototype 40-cm primary burner was used to obtain experimental heat transfer coefficients and expanded slugging bed heights for various bed materials. The 40-cm-diameter burner exhibits better bed mixing than the 20-cm-diameter burner, simplifying the startup procedure. The experimental test programs on the 20-cm primary burner with alternate fines feeders was completed, resulting in the selection of a single hopper gravity flow fines recycle system.

System shakedown (Phase I) of the 20-cm secondary burner was completed. Two full-cycle burner runs resulted in the measurement of heat transfer coefficients of feed and product material, and testing of partially automated burner sequencing. Design modifications are being made to the distributor plate, transport blowers, and roll crusher side plates. Sufficient data were obtained to allow run sequence automation to proceed.

Design of the engineering-scale dissolver-leacher for incorporation into the engineering-scale head-end line was initiated. After a review of commercially available centrifuges, a purchase order was placed for a vertical continuous unit. Bench-scale and pilot plant dissolution runs were made to determine the potential advantage of using a heel operating mode for sol gel ThO_2 kernel dissolution, with preliminary results indicating that operating with a 40% heel can reduce the dissolution time by a factor of three. Other bench-scale studies were made on the stripping of macroreticular resin used for solvent cleanup. Disodium EDTA and oxalic acid were tested as potential alternate stripping agents but were found to be inferior to the nitric acid - hydrofluoric acid mixture. Additional tests were made to determine the effects of SiC and heavy metal carbides in leacher feed on the fission product zirconium decontamination factor during the subsequent solvent extraction processing. The presence of heavy metal carbides was found to have a definite adverse effect, but SiC had no discernible effect.

Two solvent extraction runs were successfully completed during the quarter. Run 56 was used to test the operability of the intertie between the 1A centrifugal contactor and the 1S pulsed column. Run 57 represented the first cycle of the Acid-Thorex flowsheet.

Component and system qualification testing continues on the dry solids handling system. The inlet filter on the secondary burner product removal system successfully contained material when the line flooded. Conveying line bend erosion is being monitored; five of six in-bunker multitube metal filters have been preloaded; effective volumes of two bunkers have been measured using level sensors; the primary burner feeder has been calibrated; and the weigh cell calibration is in progress. Two of the six pneumatic transfer subsystems have been tested. The primary burner product removal system worked successfully but the secondary burner product removal system plugged, apparently by the initial surge of material from the burner.

Gaseous fission product release treatment has been reviewed and several changes are necessary to the proposed treatment scheme. Work on the HRDF material balance for the head-end process and the gaseous fission product distribution has been completed. A preliminary effort was made to establish the target decontamination factors and design basis for HRDF which are compatible with the current EPA proposed standards and the current development stage of the technology.

The HET-Reprocessing system design criteria were completed and compiled into the initial draft of the Criteria Document for the HTGR Fuel Recycle Hot Engineering Test. The conceptual design was initiated on the HET-Reprocessing systems under GA responsibility.

Two candidate fuel handling canister designs have been prepared. One design has each fuel element stored in a fuel handling canister which has a bolted closure sealed with a gasket or O-ring. Four of these canisters would be stacked in a long inner container which would have a bolted closure and is the primary containment for the system. The other design has each element stored in a mild steel canister which is sealed by welding the cover. This canister becomes the primary containment.

As part of the Reprocessing Flowsheet Review and Material Balance activity, HRDF flowsheets for the reprocessing head-end and off-gas treatment systems were revised to incorporate process and design improvements developed at GA and other sites during the past year. The Reprocessing Yields and Material Throughput Study continues with definition of HRDF feed material characteristics and the projected paths of material through the reprocessing unit operations and to side streams, i.e., off-gas, waste. The analytical work on the Spent Fuel Element Decay Heat and Source Term Analysis Report was completed.

2. FUEL ELEMENT CRUSHING

Individual testing of the major equipment items is in progress on the fuel element size reduction system (UNIFRAME) for the cold engineering-scale reprocessing line. Parametric studies on the primary crusher utilizing scrap unfueled fuel elements as feed led to the selection of the proper nip angle and close side settings. The product characteristics and operational capabilities of the primary crusher were determined through a series of crushing tests on unfueled full and half-size H-327 graphite fuel elements and a half-size control rod element. Crushed materials from the primary crusher tests were utilized to observe the product characteristics and operational capabilities of the secondary crusher. The differences in products from the various types and configurations of elements, the product size distributions, and material throughput rates were observed for both crushers.

Checkout of lift fixtures for the primary and secondary crusher Pitman assemblies and the primary stationary jaw were completed as a part of the demonstration of remote maintenance capabilities.

2.1. UNIFRAME FUEL ELEMENT SIZE REDUCTION SYSTEM

The major size reduction equipment and subsystems are shown assembled and ready for operation in Figs. 2-1 and 2-2. In Fig. 2-2 the vibratory screener-separator and the crusher for oversized screener product are seen mounted beneath the UNIFRAME isolation valve body and the tertiary crusher transition section.

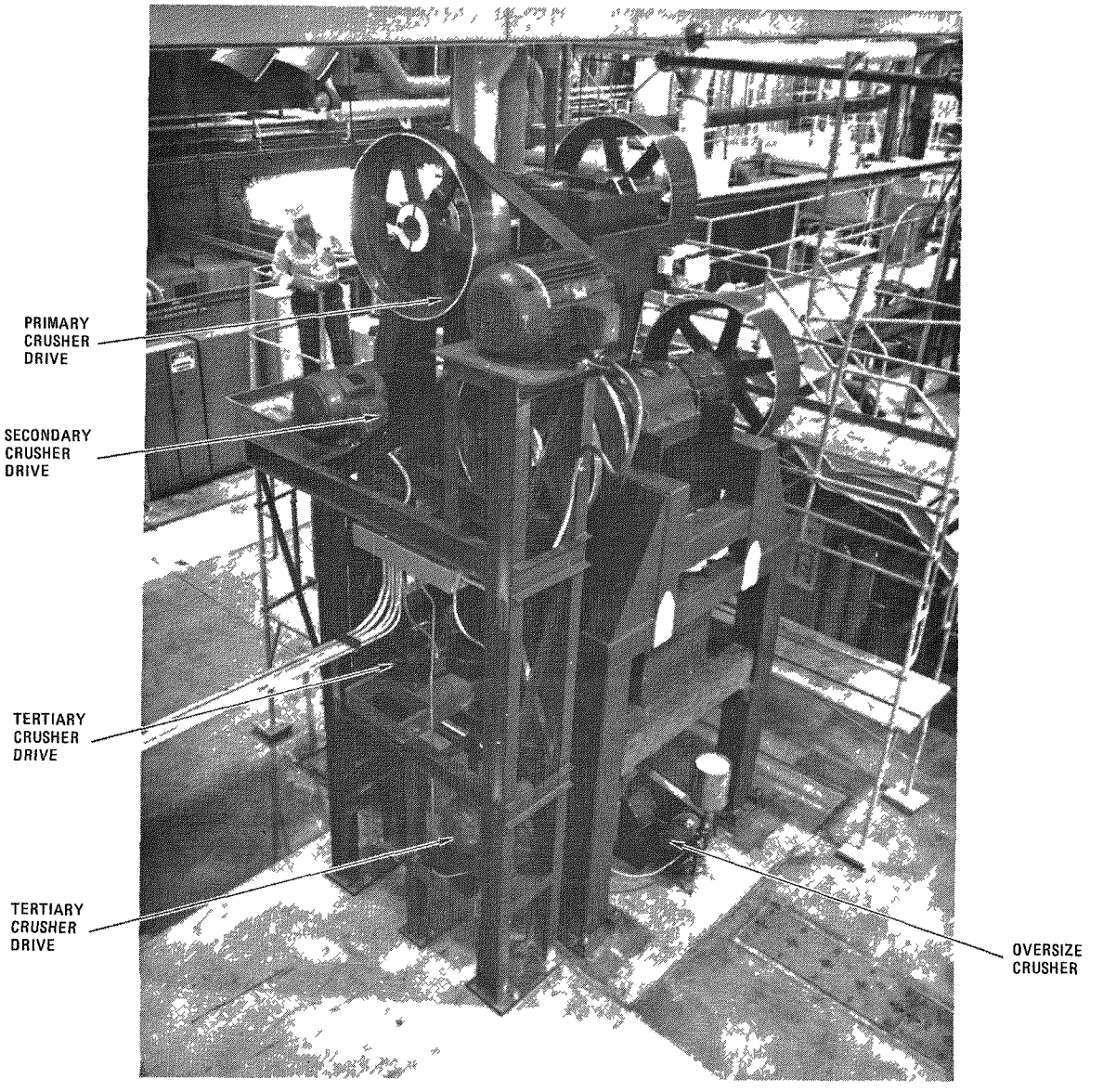

Fig. 2-1. UNIFRAME size reduction system with ventilation enclosure partially removed

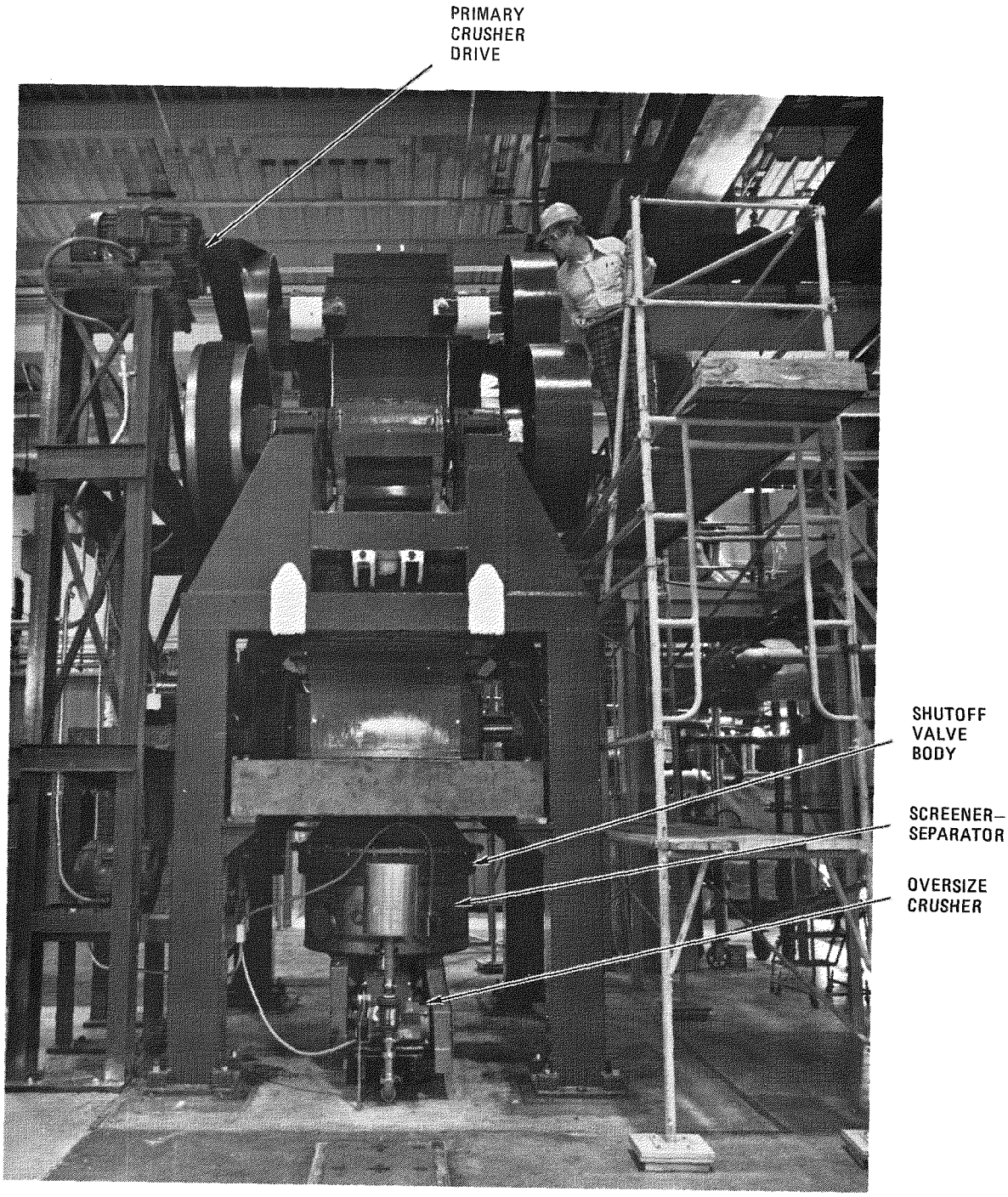

Fig. 2-2. UNIFRAME size reduction system

2.2. CURRENT STATUS OF DESIGN

2.2.1. Documentation

The documentation for the UNIFRAME is complete with the exception of the Design Report (DR521001), which is scheduled for January 1979. All other control documents are continuously upgraded to reflect changes brought about by installation and operating experience, test results, and other programmatical results. Supporting documents such as interim reports, procedural documents, etc., are prepared as required.

2.3. CURRENT STATUS OF TESTING

The experimental work to be conducted on the UNIFRAME fuel element size reduction system in the HTGR Fuel Reprocessing Cold Pilot Plant is described by the "Activity Plan - Fuel Element Size Reduction System" (AP-521001).

Phase I of the Activity Plan experimental work encompasses tests whose major objective is the individual demonstration of design and operational capabilities of each major equipment item. The Phase I tests on the primary and secondary crushers have been completed, and the tertiary crusher is currently being readied for its Phase I tests.

2.3.1. Primary Crusher Tests

During preoperational assembly and checkout, it was found that the 5-cm (2-in.) close side setting (CSS) specified in the design for the primary crusher had not been attained and that the actual CSS measured ∿3 cm (∿1.2 in.). Forty-one cm (16 in.) toggles were ordered to replace the original 46-cm (18-in.) toggles. The smaller toggles, used with shims between the pushing block and the pushing beam, allowed flexibility in the choice of the CSS and permitted the CSS to be set to the desired 5 cm (2 in.).

The discrepancy between the as-built CSS of 3 cm (1.2 in.) and the design CSS of 5 cm (2 in.) was investigated and determined to be the result of the accumulation of minor design and manufacturing variances and manufacturing tolerance buildup.

The changeover in the primary crusher from 45.7 cm (18 in.) to 40.6 cm (16 in.) toggles provided an opportunity to examine the solid, dry film lubricant system which had been applied to the toggle pin joints. The system used was molybdenum disulfide (MoS_2) and antimony trioxide (Sb_2O_3) with a polyimide binder. The dry film system was applied only to the shaft surfaces.

After careful disassembly, both shafts and each bore were closely examined for evidence of wear or breakdown of the dry film lubricant. Since the appearance of the bores and shaft surfaces was inconclusive, the lubricant system was stripped from half the diameter for the full length of the two shafts. The stripping was done by the use of glass beads and was "soft" enough to remove the coating without damaging the substrate or destroying wear evidence. Figure 2-3 is a composite photograph of one shaft with the toggle positions identified. The upper portion of the shaft shows the dry film lubricant as it was after disassembly. The lower portion has been stripped of lubricant. The shiny, glazed-appearing areas are highly burnished regions of the coating. The more matte regions are either lightly burnished or unscathed. Figure 2-4 is a closeup view of the demarcation between the "as-run" and the stripped dry film lubricant. This photograph illustrates a typical condition of the underlying surfaces on both toggle shafts and clearly indicates that there is no wear damage to the steel substrate. The observations and comments of the supplier of the dry film lubricant are as follows:

> "The coating, applied in accordance with MSFC 50M60434, appeared to have performed exceptionally well in preventing galling or spalling of the metal. The shiny black bands indicate areas where the contact

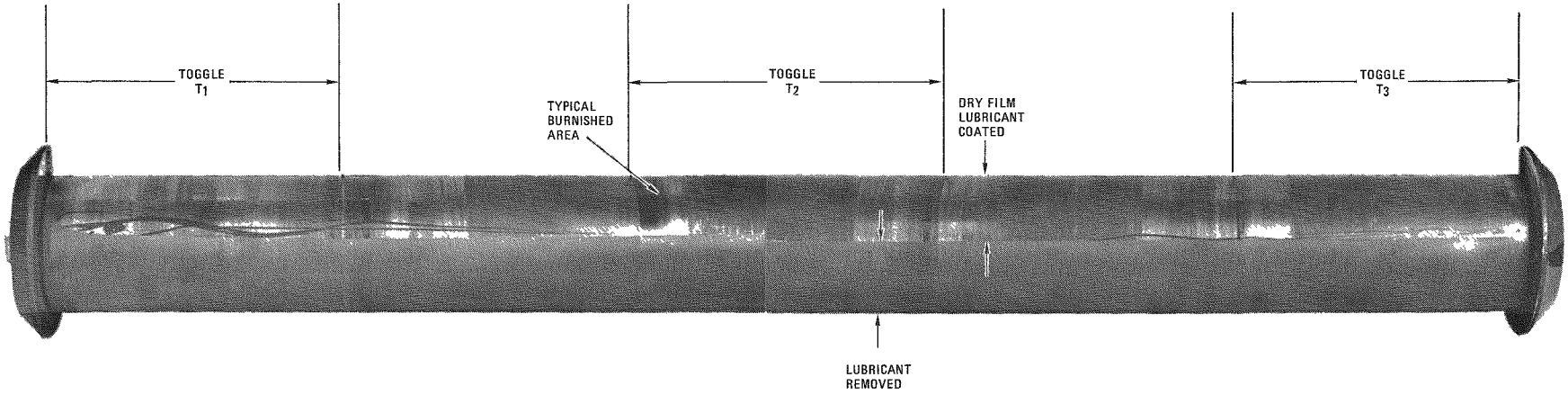

Fig. 2-3. Primary Pitman toggle shaft. Dry film lubricant has been removed from bottom half of shaft

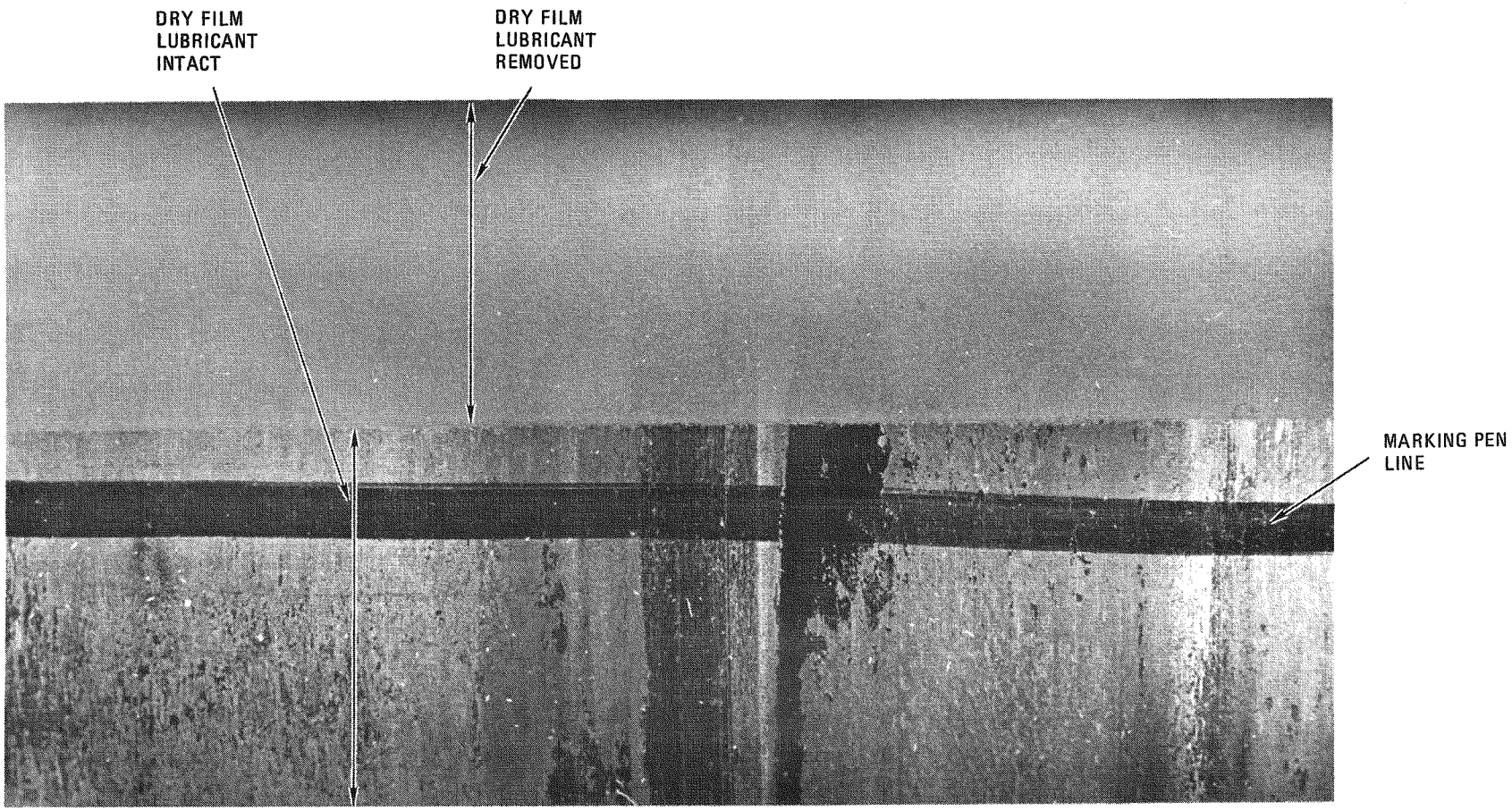

Fig. 2-4. Primary crusher toggle shaft showing absence of substrate damage

loading was extremely high. This is exactly the film appearance found on McMillan (LFW-1) test races which have been run-in at loads up to 150,000 psi.

The other light grey areas on the shafts appeared to be scuffed from general handling, assembly, or disassembly. Again, there is nothing abnormal in appearance to be noted."

All bushing bores in the toggles, pushing block, and Pitman casting showed evidence only of varied degrees of transfer of the dry film lubricant from the shaft to the bores. Debris and wipings from each bore and shaft journal have been collected and are available for analysis, if required. In the absence of shaft wear, these analyses have been deferred.

Initial checkout of the crusher was initiated with the 45.7-cm (18-in.) toggles and the 3-cm (1.2-in.) CSS. A nip angle of 18° was selected based on earlier experimental work (Ref. 2-1). Initial crushing using partial, unfilled blocks met with limited success.

Parametric studies on the primary crusher were then undertaken to establish the proper nip angles and CSS's for consistent crushing. Table 2-1 gives a summary of these parametric studies and the results.

To permit adjustments of the primary crusher to a minimum nip angle of 13°, a modification in the height of the cheek plate assemblies of the stationary jaw was required. In addition, a fuel element entry chute (see Fig. 2-5) was fabricated and installed above the primary crusher. This unit was intended to eliminate the potential loss of material which might occur at initial crushing contact due to the higher position of the fuel block resulting from the reduced nip angle. Figure 2-6 shows the primary stationary jaw and the entry chute mounted in the maintenance fixture. The truncation of the cheek plates to reduce their height is evident.

TABLE 2-1
UNIFRAME PRIMARY CRUSHER PHASE I PARAMETRIC STUDIES[a]

Test	Close Side Setting [cm (in.)]	Nip Angle[b] (deg)	Feed Material	Results
CP-A	3.0 (1.2)	18	Full length segments of standard fuel elements	Partial crushing
CP-B	3.0 (1.2)	16	Uncrushed material from previous test (CP-A)	Partial crushing
CP-C	3.0 (1.2)	18	Standard fuel element	Partial crushing
CP-D	3.0 (1.2)	16	Uncrushed material from previous test (CP-C)	Partial crushing
CP-E	5.3 (2.1)	18	1/2 standard fuel element	Partial crushing (stalled crusher)
CP-F	5.3 (2.1)	16	Uncrushed material from previous test (CP-E)	Partial crushing
CP-G	9.7 (3.8)	17	Uncrushed material from previous test (CP-F)	Partial crushing
CP-H	9.7 (3.8)	13	Uncrushed material from previous test (CP-G)	Complete crushing (as charged)
CP-I	9.7 (3.8)	13	1/3 standard fuel element	Complete crushing (9 sec)
CP-J	9.7 (3.8)	15	Uncrushed material from previous test (CP-D) (20.4 kg)	Partial crushing
CP-K	9.7 (3.8)	14	Uncrushed material from previous test (CP-J) (20.4 kg)	Complete crushing (7.5 sec)
CP-L	5.3 (2.1)	14	1/2 standard fuel element cut vertically (39.7 kg)	Complete crushing (19.5 sec)
CP-M	5.3 (2.1)	14.5	1/2 standard fuel element cut horizontally; no coolant holes, partial fuel holes (70.3 kg)	Complete crushing (6 min 15 sec)
CP-N	5.3 (2.1)	14.5	1/2 standard fuel element cut horizontally; no fuel holes, complete coolant holes (61.2 kg)	Complete crushing (5 min 45 sec)

TABLE 2-1 (Continued)

Test	Close Side Setting [cm (in.)]	Nip Angle[b] (deg)	Feed Material	Results
CP-O	5.3 (2.1)	14.5	Standard fuel element; last two rows of fuel holes removed by vertical cut (83.0 kg)	Complete crushing (4 min 5 sec)
CP-P	5.3 (2.1)	14.5	Standard fuel element; last five rows of fuel holes removed by vertical cut (73.5 kg)	Complete crushing (3 min 5 sec)

[a] Crusher speed = 200 rpm.

[b] Measured at the close side setting.

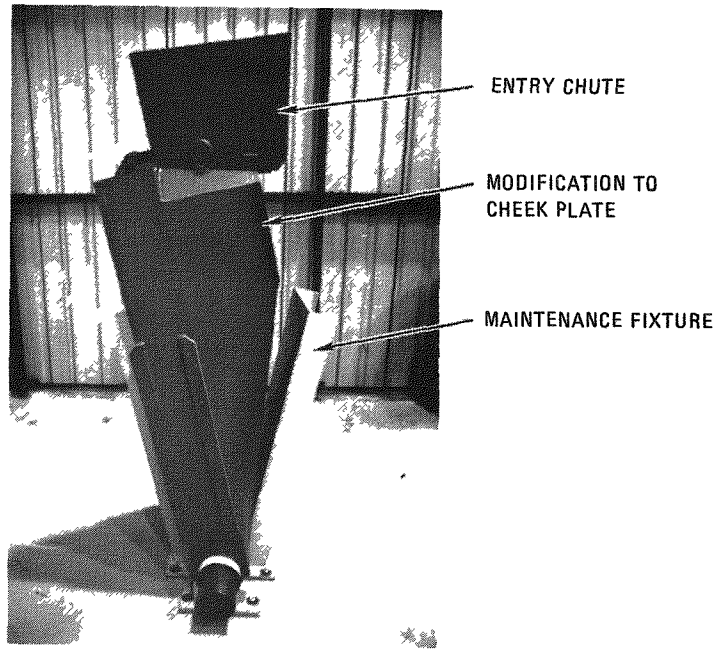

Fig. 2-5. Primary crusher stationary jaw showing modifications and entry chute

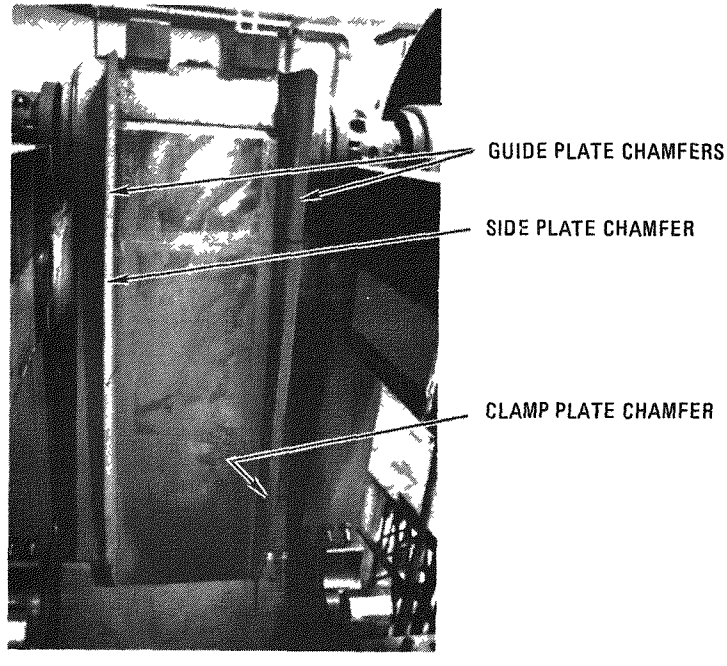

Fig. 2-6. Primary Pitman assembly showing chamfered side plates

Complete crushing occurred at nip angles of 14.5° or less. Although all nip angles were not tested at each of the CSS's, the results and observations of the crushing behavior were consistent enough to conclude that this was the maximum nip angle that could be used at any of the CSS's and still produce a reasonable probability for complete crushing of the fuel element. At nip angles above 14.5°, the fuel elements were only partially crushed. The remaining material merely slid up and down with the action of the Pitman. A slight tendency for slippage was observed at the 14.5° nip angle, but it was not pronounced enough to prevent the materials from being crushed. Instead, it resulted in longer time periods to complete the crushing.

The results of these studies led to the selection of a 5-cm (2-in.) CSS and a 14° nip angle as the parameters for subsequent tests to demonstrate the primary crusher product characteristics. A 5-cm (2-in.) CSS was selected because it was expected to yield a crushed product sufficiently reduced in size to be acceptable for secondary crusher feed. The 14° nip angle was selected because it provided a combination of a high probability for complete crushing with an acceptable crusher gape (feed opening).

Using these settings, three unfueled full-size H-327 graphite fuel elements, three unfueled half-size H-327 fuel elements, and one half-size H-327 control rod element were separately crushed and their products collected to study the primary crusher product characteristics. The unfueled half-size H-327 fuel elements provided a comparison with the unfueled full-size H-327 fuel elements to indicate if significant crushed product differences could be expected from the processing of whole, partial, broken, or damaged fuel elements. The unfueled half-size H-327 control rod element provided a comparison with the unfueled half-size H-327 fuel element to indicate if significant crushed product differences could be expected from the processing of different types of elements. Table 2-2 gives a summary of the tests undertaken to determine the primary crusher product characteristics.

TABLE 2-2
UNIFRAME PRIMARY CRUSHER PHASE I PRODUCT CHARACTERISTICS
Crusher Speed = 200 rpm; Close Side Setting = 5.3 cm (2.1 in.);
Nip Angle = 14° measured at CSS

Test	Feed Material	Results
PC-1	One-half of a standard H-327 fuel element, cut horizontally, 39.2 cm (15-7/16 in.) long, 43.1 kg	Complete crushing (1 min 2 sec)
PC-2	One-half of a standard H-327 fuel element, cut horizontally, 39.4 cm (15-1/2 in.) long, 44.5 kg	Complete crushing (28 sec)
PC-3A	One-half of a standard H-327 fuel element, cut horizontally, 40 cm (15-3/4 in.) long, 45.4 kg	Complete crushing; abnormal operating conditions imposed due to jammed material
PC-3B	One-half of a standard H-327 fuel element, cut horizontally, 39.8 cm (15-11/16 in.) long, 44.2 kg	Complete crushing (24 sec)
PC-4	One-half of a H-327 control rod element, cut horizontally, 39.4 cm (15-1/2 in.) long, 42.4 kg	Complete crushing (32 sec)
PC-7	One whole standard H-327 fuel element, 90.7 kg	Complete crushing (3 min 26 sec)
PC-8	One whole standard H-327 fuel element, 89.4 kg	Complete crushing (1 min 28 sec)
PC-9	One whole standard H-327 fuel element, 89.4 kg	Complete crushing (1 min 16 sec

In one of the tests (PC-3A), the element fractured along the fuel and coolant hole planes in a pattern which allowed the crushing force to wedge the fragments between the two side plates of the Pitman assembly. The material thus captured moved with the action of the Pitman without sliding up or down or falling further into the crushing cavity. Contact of the captured materials with the stationary jaw wear surface was of insufficient force to produce further crushing. This phenomonon was unrelated to the conditions of slippage which occurred at nip angles greater than 14.5°; that slippage was caused by the vertical crushing forces exceeding the frictional forces. The adjustable stationary jaw was moved to a smaller nip angle, providing recontact of the material with both crushing surfaces, and crushing was reinstituted to completion. This procedure for clearing a similarly jammed element has been included in the Operating Procedures (OP-521001), by an amendment to the section on abnormal operation.

In order to reduce the tendency to wedge or bridge, a design change was incorporated which put a 1.27 cm (1/2 in.) by 2.22 cm (7/8 in.) chamfer on the top interior edges of the guide plates, clamp plate, and side plate. These chamfers can be seen in Fig. 2-6.

The test was repeated (PC-3B) because of the possibility that the crushed product from test PC-3A would have atypical size distribution characteristics due to the abnormal operation. In the repeat test and all the other tests, no further jamming occurrence or tendency to jam was observed.

Determination of primary crusher product characteristics from crushing H-327 control rod elements was limited to a single test at this time because of the shortage of available control rod elements.

Material throughput rates varied from ∿42 to ∿111 kg/min in the replicate tests on half-size fuel elements and from ∿26 to ∿61 kg/min in the replicate tests on full-size fuel elements. The throughput rate for the single half-size control rod element was ∿79 kg/min. The large variability in throughputs on replicate tests and overlapping rates between

sizes and types of elements indicated no definite relationships between throughput and size or type of element. However, all the throughput rates were well above the requirement for processing an entire fuel element in less than 15 min.

In all the tests, materials were totally confined to the crushing cavity and no material holdup was detected.

Determination of the product size distributions from each of the tests has been completed. The larger-size product was manually separated and passed through various ring size openings to determine the distribution of ring size material from 2.55 to 15.2 cm (1 to 6 in.) in 2.54 cm (1 in.) increments. Product smaller than 2.54 cm (1 in.) ring size was separated by hand screening into plus and minus 0.476 cm (3/16 in.) mesh fractions. Results of the product size characterizations are shown in Table 2-3.

Graphical representations of the product size distributions resulting from the replicate tests on half-size and full-size fuel elements are shown in Figs. 2-7 and 2-8, respectively. These figures show that a reasonable consistency of product was obtained from the replicate crushing tests on each size of fuel element even at the larger ring size fractions where a single piece could make a difference of several percent.

In general, the difference between the half-size and full-size fuel element three-run averages for each size fraction was insignificant. However, the product from the single test of primary crushing a half-size control rod element was larger (see Figs. 2-9 and 2-10). Owing to the large-diameter control rod holes and the smaller number of coolant and fuel holes, the fracture planes of the control rod element produced larger fragments.

Product from the tests which was greater than 15.2 cm (6 in.) ring size was measured to establish the nominal ring size. Measurement data are given in Table 2-4. Material greater than 15.2 cm (6 in.) nominal ring size was found in product from two of the runs: PC-4, the half-size control rod

TABLE 2-3
UNIFRAME PRIMARY CRUSHER PRODUCT CHARACTERIZATION STUDIES
Close Side Setting 5.3 cm (2.1 in.); Nip Angle = 14°; Crusher Speed = 200 rpm

Half-Size Fuel Element Tests

Ring Size [cm (in.)]	PC-1		PC-2		PC-3B		Avg	
	Wt %	Cum. Wt %	Wt %	Cum. Wt %	Wt %	Cum. Wt %	Wt %	Cum. Wt %
+15.4 (+6)	1.5	100.0	6.8	100.0	3.3	100.0	3.9	100.0
-15.4 (-6) +12.7 (+5)	0	98.5	2.3	93.2	8.4	96.7	3.6	96.1
-12.7 (-5) +10.2 (+4)	11.2	98.5	6.9	90.9	0.9	88.3	6.3	92.5
-10.2 (-4) +7.6 (+3)	10.6	87.3	14.2	84.0	14.1	87.4	13.0	86.2
-7.6 (-3) +5.1 (+2)	12.2	76.7	11.8	69.8	13.9	73.3	12.6	73.2
-5.1 (-2) +2.5 (+1)	17.9	64.5	19.4	58.0	15.4	59.4	17.6	60.6
-2.5 (-1) +0.48[(a)]	39.4	46.6	32.3	38.6	36.3	44.0	36.0	73.0
-0.48[(a)]	7.2	7.2	6.3	6.3	7.7	7.7	7.0	7.0

Control Rod Element Tests

Ring Size [cm (in.)]	PC-4	
	Wt %	Cum. Wt %
+15.4 (+6)	25.6	100.0
-15.4 (-6) +12.7 (+5)	4.6	74.4
-12.7 (-5) +10.2 (+4)	9.6	69.8
-10.2 (-4) +7.6 (+3)	16.6	60.2
-7.6 (-3) +5.1 (+2)	12.2	43.6
-5.1 (-2) +2.5 (+1)	10.5	31.4
-2.5 (-1) +0.48[(a)]	17.7	20.9
-0.48[(a)]	3.2	3.2

Full-Size Fuel Element Tests

Ring Size [cm (in.)]	PC-7		PC-8		PC-9		Avg.	
	Wt %	Cum. Wt %	Wt %	Cum. Wt %	Wt %	Cum. Wt %	Wt %	Cum. Wt %
+15.4 (+6)	0	100.0	0	100.0	2.7	100.0	0.9	100.0
-15.4 (-6) +12.7 (+5)	1.6	100.0	1.0	100.0	0	97.3	0.9	99.1
-12.7 (-5) +10.2 (+4)	6.8	98.4	7.6	99.0	8.0	97.3	7.4	98.2
-10.2 (-4) +7.6 (+3)	11.7	91.6	8.2	91.4	14.6	89.3	11.5	90.8
-7.6 (-3) +5.1 (+2)	13.8	79.9	15.0	83.2	11.0	74.7	13.3	79.3
-5.1 (-2) +2.5 (+1)	16.8	66.1	17.9	68.2	16.1	63.7	16.9	66.0
-2.5 (-1) +0.48[(a)]	39.5	49.3	40.9	50.3	38.3	47.6	39.6	49.1
-0.48[(a)]	9.8	9.8	9.4	9.4	9.3	9.3	9.5	9.5

[(a)] Screen size.

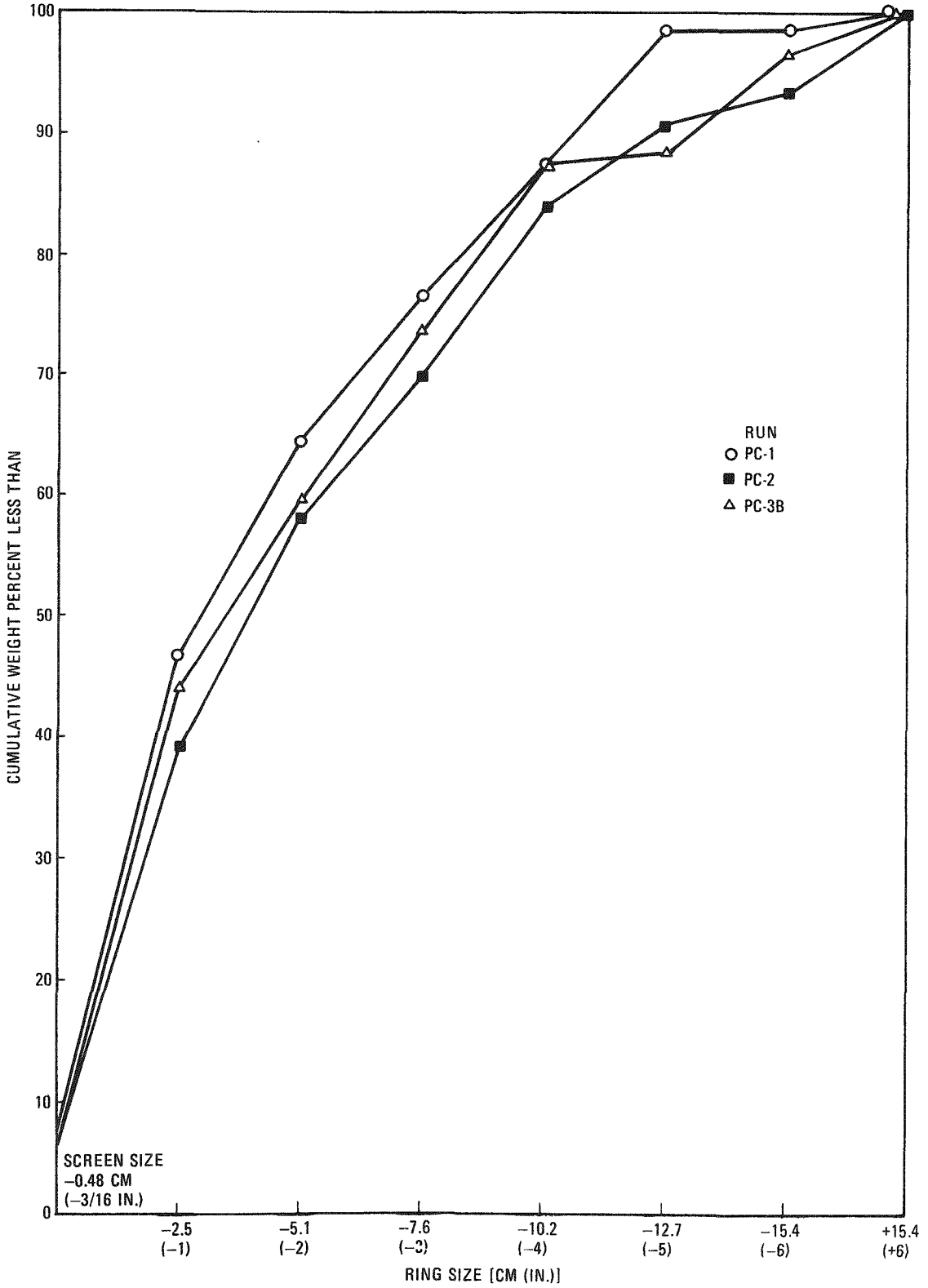

Fig. 2-7. Product size distributions in half-size H-327 fuel element tests

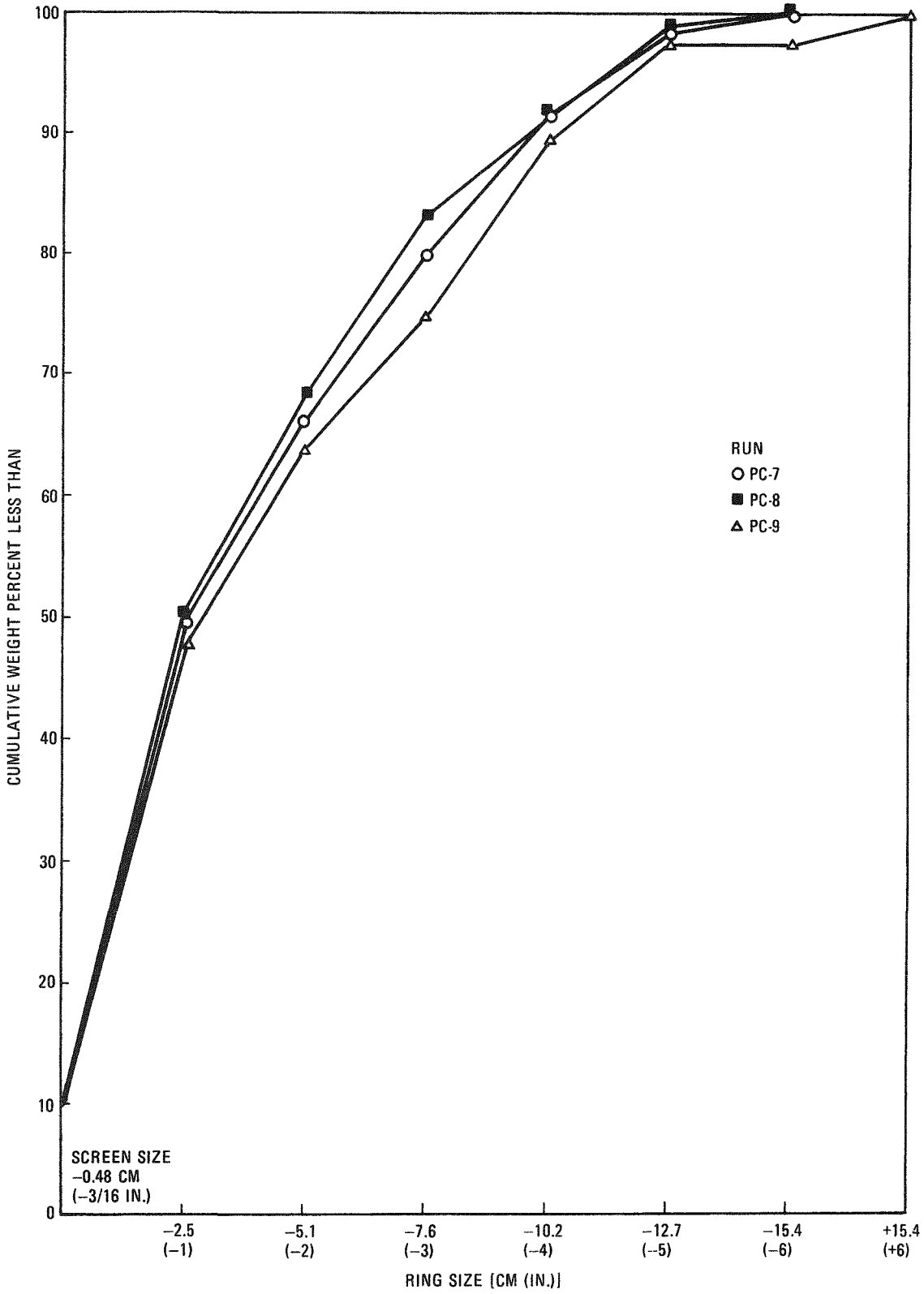

Fig. 2-8. Product size distributions in full-size H-327 fuel element tests

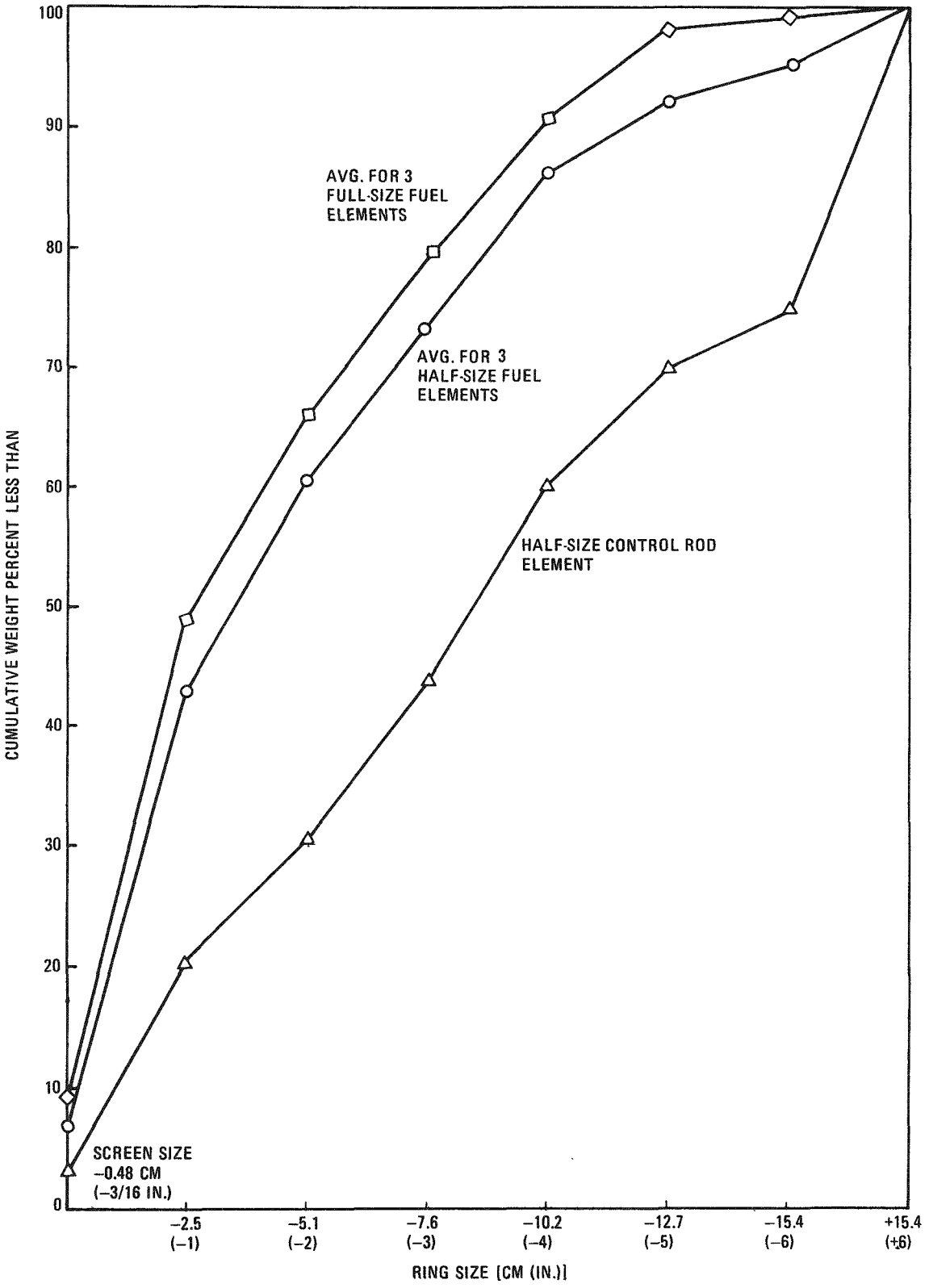

Fig. 2-9. Product size distributions in UNIFRAME primary crusher tests

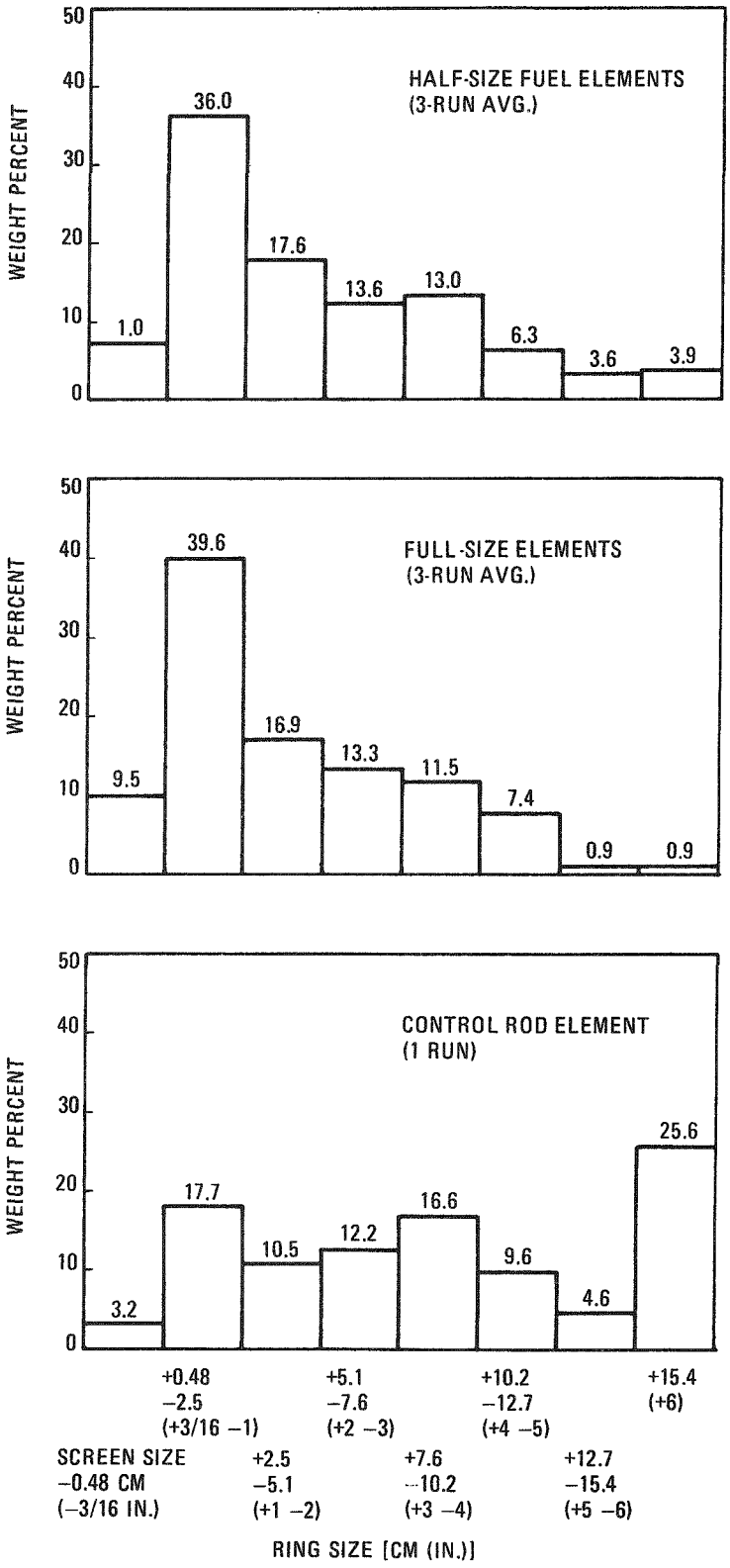

Fig. 2-10. Weight percent of each size fraction in UNIFRAME primary crusher tests

TABLE 2-4
UNIFRAME PRIMARY CRUSHER TESTS - CHARACTERISTICS OF MATERIAL
GREATER THAN 15 CM (6 IN.) RING SIZE

Nominal Ring Size [cm (in.)]	Max. Length [cm (in.)]	Max. Width [cm (in.)]	Max. Thickness [cm (in.)]	Weight (kg)	Wt % of Total Product
		Run PC-1			
15 (6)	28 (11)	15.9 (6-1/4)	2.2 (7/8)	0.638	1.5
		Run PC-2			
15 (6)	28 (11)	16.5 (6-1/2)	2.9 (1-1/8)	1.044	2.3
15 (6)	23 (9)	16.5 (6-1/2)	6.4 (2-1/2)	1.064	2.4
15 (6)	20 (8)	16.5 (6-1/2)	5.1 (2)	0.919	2.1
Total 5				3.027	6.8
		Run PC-3B			
15 (6)	29 (11-1/2)	16.5 (6-1/2)	5.7 (2-1/4)	1.419	3.3
		Run PC-4			
20 (8)	39 (15-1/2)	21.0 (8-1/4)	7.0 (2-3/4)	3.426	7.9
20 (8)	22 (8-1/2)	20.0 (7-7/8)	5.4 (2-1/8)	1.793	4.2
Total 20				5.219	12.1
18 (7)	39 (15-1/2)	18.1 (7-1/8)	6.4 (2-1/2)	3.155	7.3
15 (6)	26 (10-1/4)	15.6 (6-1/8)	6.4 (2-1/2)	1.463	3.4
15 (6)	23 (9-1/4)	15.9 (6-1/4)	4.8 (1-7/8)	1.227	2.8
Total 15				2.690	25.6
Total Run				11.064	25.6
		Run PC-7			
None					0
		Run PC-8			
None					0
		Run PC-9			
18 (7)	20 (8)	17.8 (7)	7.0 (2-3/4)	1.285	2.7

element test, and PC-9, a full-size fuel element test. The quantity of fragments of this size was small, i.e., three pieces in PC-4 and one piece in PC-9. Typical material greater than 15.2 cm (6-in.) ring size is illustrated in Figs. 2-11 and 2-12. Portions of the control rod holes were present in all of the 15.2 cm (6-in.) ring size material produced in the half-size control rod element test.

Crushed products from the primary crusher tests were used as feed for the Phase I testing of the secondary crusher.

2.3.2. Secondary Crusher Tests

Crushed materials from the primary crusher parametric tests were utilized to observe the operation of the secondary crusher prior to demonstrating its product characteristics (see Table 2-5). Material produced with a 9.7 cm (3.8 in.) CSS on the primary crusher failed to be crushed completely in the secondary crusher. The smaller fragments were crushed readily, but the larger fragments with all dimensions >7.6 cm (>3 in.) merely rode up and down with the motion of the Pitman. This was attributed to the fact that these pieces were unable to enter the crushing cavity to a point where the probability for crushing is high. This was experimentally determined on the primary crusher as a <14.5° nip angle. The secondary crusher has a curved wear plate presenting a varying nip angle which reaches 14.5° at a point where the gape (feed opening) is ∿7.4 cm (∿2.9 in.) at the maximum open Pitman position. This reduces the probability of crushing fuel element materials which are greater than 7.4 cm (2.9 in.) in all dimensions. This was borne out by subsequent tests utilizing feed materials produced with a 5.3 cm (2.1 in.) CSS on the primary crusher.

Crushed materials from the tests demonstrating the primary crusher product characteristics were utilized as feed for tests to demonstrate the secondary crusher product characteristics. These runs are summarized in Table 2-6. These feed materials provided comparison of secondary crusher products from unfueled half-size fuel and control rod elements and full-size fuel elements which had been processed through the primary crusher.

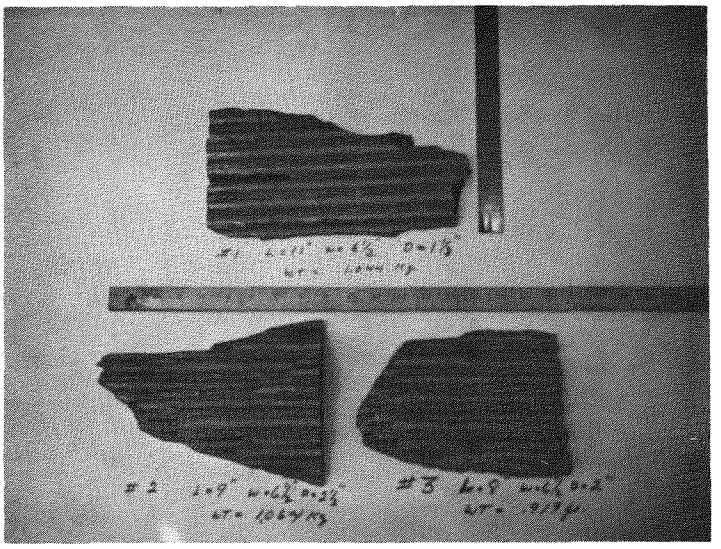

Fig. 2-11. +15-cm ring size material from test PC-2, primary crushing of an unfueled half-size H-327 fuel element

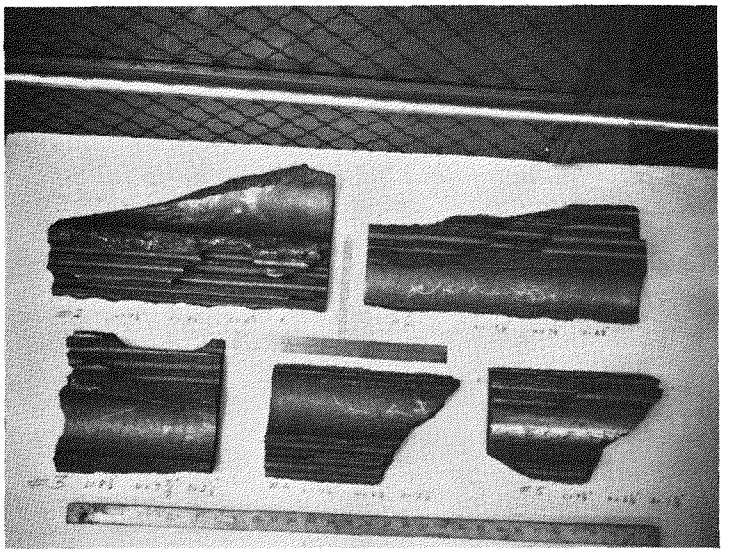

Fig. 2-12. +15-cm ring size material from test PC-4, primary crushing of an unfueled half-size H-327 control rod element

TABLE 2-5
UNIFRAME SECONDARY CRUSHER OPERATION TESTS
Crusher Speed = 300 rpm; Close Side Setting = 0.635 cm (0.25 in.)

Test	Feed Material	Results
SP-A	From primary crusher test CP-H; 9.7 cm (3.8 in.) CSS, 51.3 kg	Failed to crush largest pieces
SP-B	From primary crusher test CP-L; 5.3 cm (2.1 in.) CSS, 39.7 kg	Complete crushing (1 min 43 sec)
SP-C	From primary crusher test CP-M; 5.3 cm (2.1 in.) CSS, 70.4 kg	Shutdown after 4 min 8 sec due to overheated bearing
SP-D	From primary crusher test DC-1; 5.3 cm (2.1 in.) CSS, 44.9 kg	Complete crushing (1 min 25 sec)

TABLE 2-6
UNIFRAME SECONDARY CRUSHER PHASE I PRODUCT CHARACTERISTICS
Crusher Speed = 300 rpm; Close Side Setting = 0.635 cm (0.25 in.)

Test	Feed Material	Results
SC-13	From primary crusher test PC-1; 5.3 cm (2.1 in.) CSS, 1/2 std. fuel element	Complete crushing (1 min 29 sec)
SC-14	From primary crusher test PC-2; 5.3 cm (2.1 in.) CSS, 1/2 std. fuel element, 45 kg	Complete crushing (1 min 35 sec)
SC-15	From primary crusher test PC-3B; 5.3 cm (2.1 in.) CSS, 1/2 std. fuel element, 44 kg	Complete crushing; abnormal operating conditions imposed due to "bridged" material (1 min 43 sec)
SC-16	From primary crusher test PC-4; 5.3 cm (2.1 in.) CSS, 1/2 control rod element, 44 kg	Complete crushing (2 min 46 sec)
SC-19	From primary crusher test PC-7; 5.3 cm (2.1 in.) CSS, full-size fuel element, 91 kg	Complete crushing; abnormal operating conditions imposed due to "bridged" material (3 min 32 sec)
SC-20	From primary crusher test PC-8; 5.3 cm (2.1 in.) CSS, full-size fuel element, 90 kg	Complete crushing (3 min 19 sec)
SC-21	From primary crusher test PC-9; 5.3 cm (2.1 in.) CSS, full-size fuel element, 85 kg	Complete crushing; abnormal operating conditions imposed due to "bridged" material (3 min 48 sec)

In general, secondary crushing was without major problems. However, in three of the seven runs fuel element fragments in the secondary crushing cavity formed bridges connected loosely by interlocking of bridges formed at the fracture planes between coolant and fuel holes, (see Fig. 2-13). These bridges formed masses which were greater than 7.4 cm (2.9 in.) in all dimensions and therefore were unable to enter the crushing cavity to the point where the probability for crushing is high. In no case did this occur with a single fragment. In run SC-15, an additional 9 kg of primary crusher product was charged on top of the bridge in an effort to reinstitute crushing. This was unsuccessful. The bridged material was then removed from the crusher and recharged as individual pieces. These pieces crushed readily and in a normal fashion. In the other two runs (SC-19 and -21) in which bridges were formed, the bridges were disturbed utilizing a steel rod which separated the interlocking pieces. This technique reinstituted crushing to completion. It is apparent that bridging of material in the secondary crusher is inevitable with the current design and that means for eliminating this problem must be devised.

Each of the products from the secondary crushing tests was inspected for large fragments (see Table 2-7). Only two pieces greater than 1.9 cm (3/4 in.) ring size were found in the 442 kg of materials processed in the seven tests.

The products were separated into the plus and minus 0.476 cm (3/16 in.) fractions by hand screening. After primary and secondary crushing, the products from half-size and full-size fuel elements remained similar in size distributions (Tabel 2-7). The product from the single half-size control rod was somewhat smaller than the product from the standard fuel elements. This is opposite the tendency observed in the primary tests, where the control rod product was larger.

Average secondary crushing throughput rates were ∿27 kg/min for half-size fuel elements, ∿25 kg/min for full-size fuel elements, and ∿16 kg/min for the half-size control rod element. The somewhat larger control rod

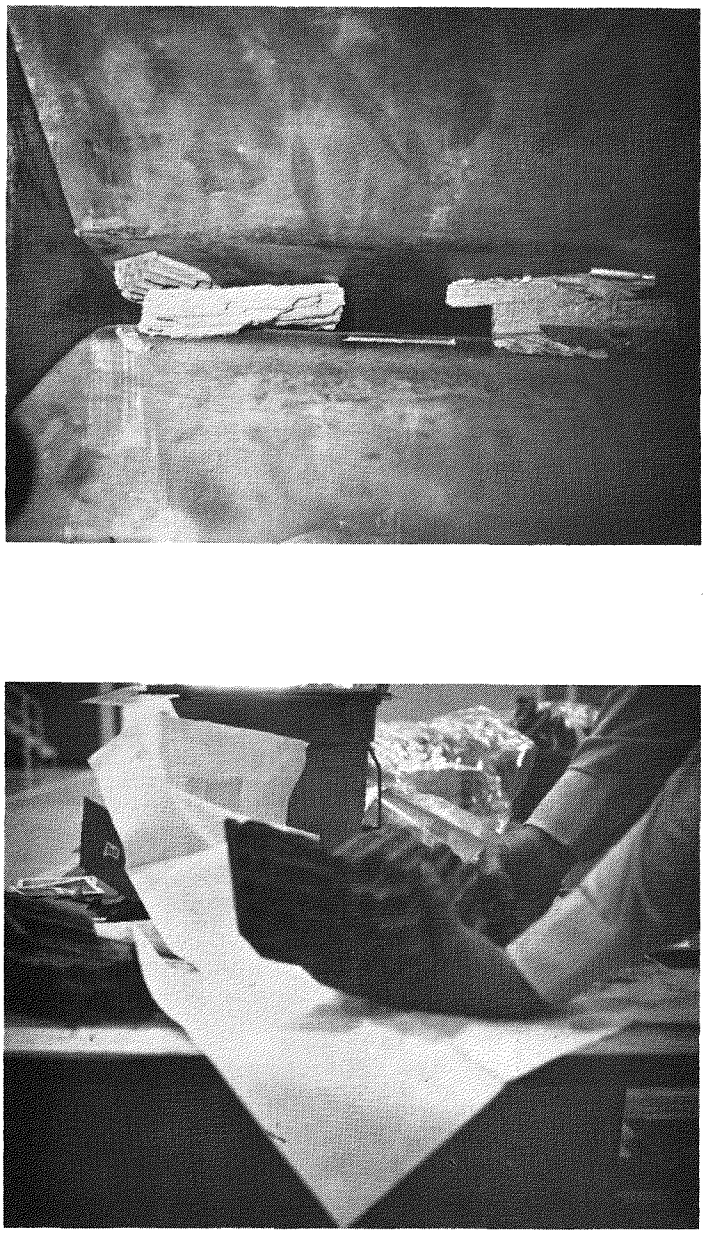

Fig. 2-13. Formation of bridges in fuel element fragments: (top) bridged fragments in test SC-15 and (bottom) typical interlocking to form bridges

TABLE 2-7
UNIFRAME SECONDARY CRUSHER PHASE I PRODUCT CHARACTERIZATION STUDIES
Crusher Speed = 300 rpm; Close Side Setting = 0.635 cm (0.25 in.)

Half-Size Fuel Element Tests				
Size [cm (in.)]	SC-13	SC-14	SC-15	Average
-2.54 +0.476 (-1 +3/16)	51.6 wt %	49.2 wt %	49.1 wt %	50.0 wt %
-0.476 (-3/16)	48.4 wt %	40.8 wt %	50.9 wt %	50.0 wt %

Half-Size Control Rod Element Test	
Size [cm (in.)]	SC-16
-2.54 + 0.476 (-1 +3/16)	45.6 wt %
-0.476 (-3/16)	54.4 wt %

Full-Size Fuel Element Tests				
Size [cm (in.)]	SC-19	SC-20	SC-21	Average
-2.54 +0.476 (-1 +3/16)	52.1 wt %	51.4 wt %	49.9 wt %	51.1 wt %
-0.476 (-3/16)	47.9 wt %	48.6 wt %	50.1 wt %	48.9 wt %

	Longest Piece [cm (in.)]			Widest Piece [cm (in.)]		
Run	Length	Width	Thickness	Length	Width	Thickness
SC-13	6.7 (2-5/8)	0.64 (1/4)	0.64 (1/4)	3.8 (1-1/2)	1.6 (5/8)	0.32 (1/8)
SC-14	7.9 (3-1/8)	0.95 (3/8)	0.32 (1/8)	2.9 (1-1/8)	3.8 (1-1/2)	0.48 (3/16)
SC-15	4.4 (1-3/4)	0.95 (3/8)	0.64 (1/4)	2.9 (1-1/8)	1.6 (5/8)	0.64 (1/4)
SC-16	5.1 (2)	0.95 (3/8)	0.48 (3/16)	4.0 (1-9/16)	1.6 (5/8)	0.32 (1/8)
SC-19	7.3 (2-7/8)	0.79 (5/16)	2.2 (7/8)	5.1 (2)	1.9 (3/4)	0.32 (1/8)
SC-20	7.6 (3)	0.48 (3/16)	0.64 (1/4)	1.9 (3/4)	2.2 (7/8)	0.48 (3/16)
SC-21	4.8 (1-7/8)	0.95 (3/8)	0.95 (3/8)	2.2 (7/8)	1.9 (3/4)	0.64 (1/4)

product after primary crushing apparently increased its process time for secondary crushing. All crushing rates were well above those necessary to process a fuel element in less than 15 min.

In all the tests, materials were totally confined to the crushing cavity. The configuration of the cavity was more than adequate to contain materials fed at rates equivalent to the primary crusher discharge rates (i.e., ∿26 to ∿110 kg/min).

Material holdup, aside from the bridging situations, was confined to an occasional small fragment (<10 g estimated) which appeared to have stuck to one of the wear plates in the narrow section of the cavity. In all cases these fragments were crushed with the succeeding charge. In addition, a small quantity of material was wedged into the clearance between the stationary jaw and the cheek plates.

2.3.3. Tertiary Crusher Tests

Preparations for conducting the Phase I testing of the tertiary crusher are under way. Fabrication of a charging chute and a product catch pan to allow individual testing of this major equipment item is essentially complete. Testing will begin early in the next quarter.

2.3.4. Oversize Monitor Tests

2.3.4.1. Screener-Separator

The screener-separator has been fitted with a dust enclosure and a support stand for individual testing of this major equipment item. Shakedown operations revealed blinding of the perforated plate. Alternate designs are under study, and design modifications are under way for testing to avoid blinding prior to commencing the Phase I tests of this unit.

2.3.4.2. Oversize Pulverizer

Testing of the oversize pulverizer is scheduled for the next quarter.

2.4. REMOTE HANDLING SYSTEM

Handling fixtures required to demonstrate remote maintenance capabilities were designed and fabricated for the UNIFRAME system. During the current quarter efforts have been directed toward checkout of lift fixtures for the Pitman assemblies and the primary fixed jaw, checkout of the shroud shutoff valve, and completion of the design and operating reports.

2.4.1. Prototype Size Reduction System

Tests of the following UNIFRAME jaw fixtures were completed during the quarter:

1. Lift Fixture - Primary Pitman Assembly
2. Lift Fixture - Primary Fixed Jaw
3. Lift Fixture - Secondary Pitman Assembly

These tests included interface checkout and operational verification. This involved mounting of each fixture on its jaw in accordance with the operating procedures to verify compatibility of the interfaces and included adjustments where necessary. The operational tests involved checkout of each fixture operation in accordance with the operating procedures. Adjustments of limit switches and other electrical components were also included in the checkout. Initial operator training and familiarization were performed in conjunction with the checkout tests. All tests were completed satisfactorily, and no significant operational problems were noted.

2.4.2. Crusher Shroud Shutoff Valve (Fig. 2-14)

Fabrication of the valve body and the slide valve assembly were completed on schedule during the quarter. Interface checkout and functional verification were performed along with initial installation and mounting adjustment. No problems were noted, and the valve performed satisfactorily in all operating modes. Complete operational checkout will be performed later in the program in conjunction with other UNIFRAME testing.

2.4.3. Secondary Pitman Lift Fixture (Fig. 2-15)

UNIFRAME checkout operations have necessitated the removal of the various jaws for inspection and adjustment purposes. The appropriate lift fixtures have been used to aid jaw handling. During the removal of the secondary Pitman assembly, the secondary Pitman lift fixture was damaged. The damage occurred to the toggle lift hook drive assembly (Fig. 2-16).

Since these lift operations were performed after satisfactory completion of the fixture checkout, it is not clear why the damage occurred. Preliminary analysis has indicated that the limit switch which controls the upper travel limit for the toggle hook was not adjusted properly. It was noted that interface testing had been carried out to adapt the secondary Pitman fixture for possible use in handling the primary Pitman jaw. These tests involved limit switch adjustments which were not compatible with the functions involving the secondary Pitman removal. Adjustment of the lower limit switch was confirmed; however, adjustment of the upper limit switch was not. It appears likely that adjustments were made but not noted. When operators later attempted to remove the secondary Pitman, the lift fixture was operated based on the assumption that the initial checkout limit switch adjustments had not been disturbed. When the fixture was cycled to raise the toggle to its "up" position for removal, it appears

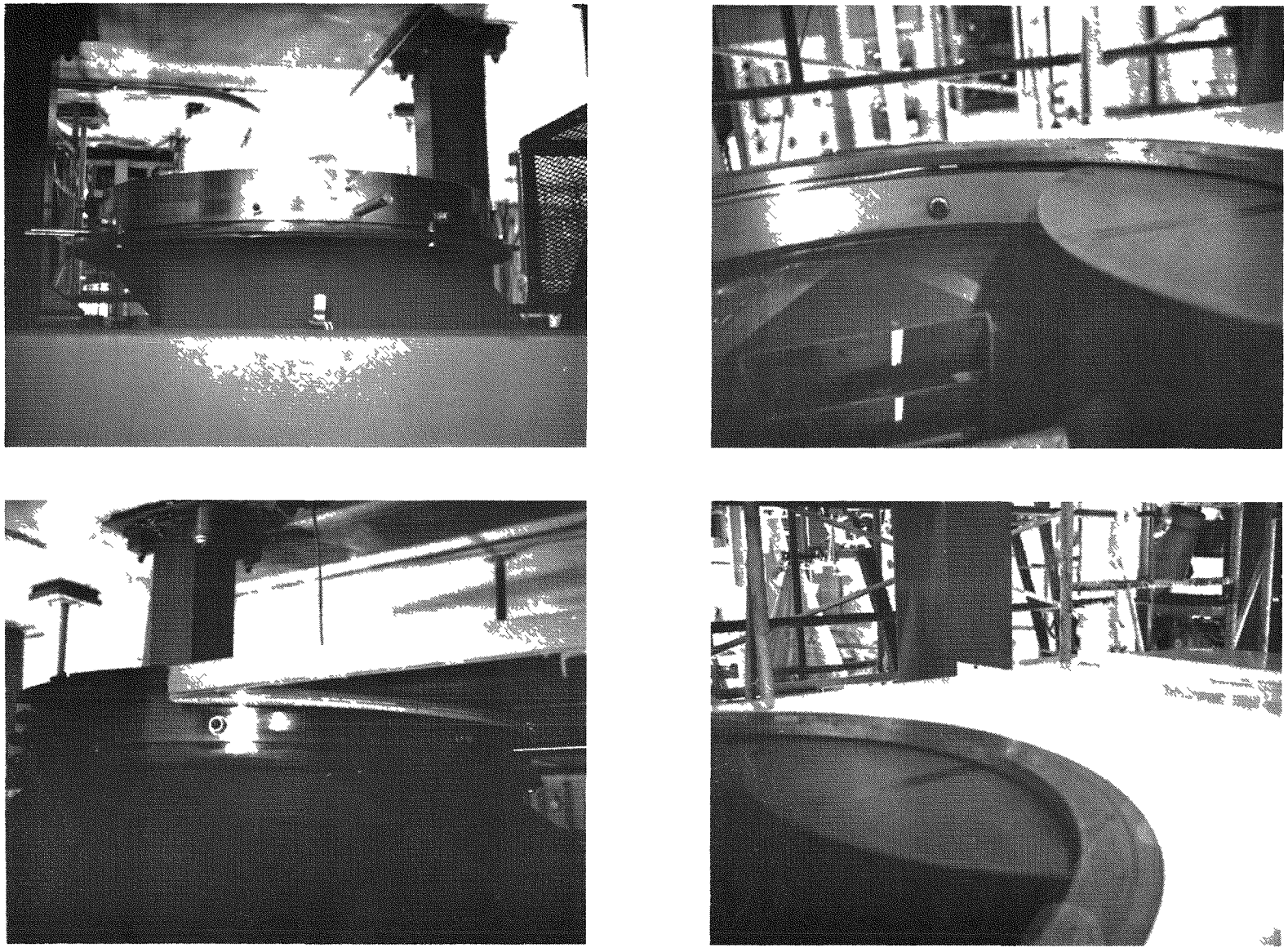

Fig. 2-14. Crusher shroud shutoff valve

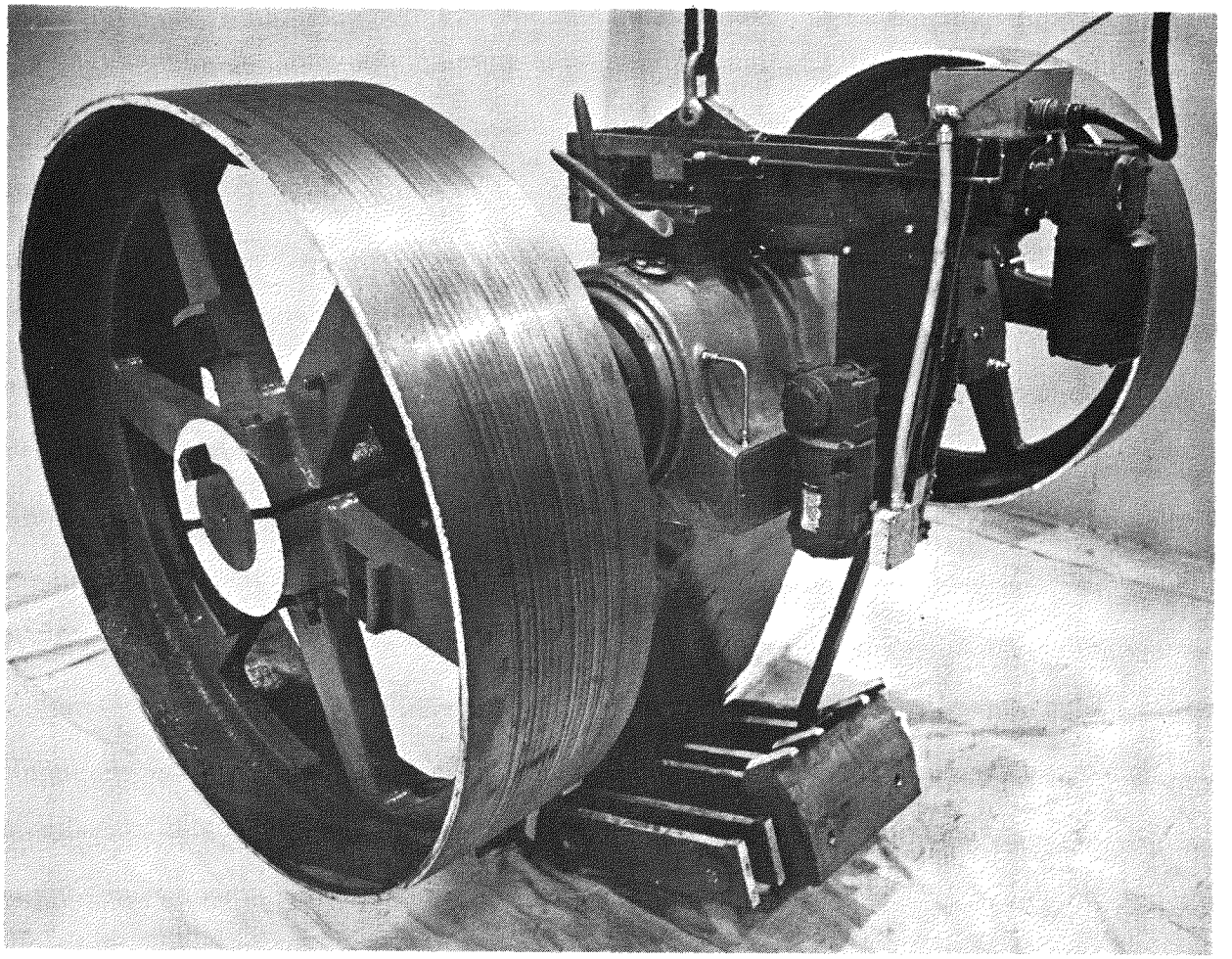

35-135-200-6A

Fig. 2-15. Secondary Pitman lift fixture

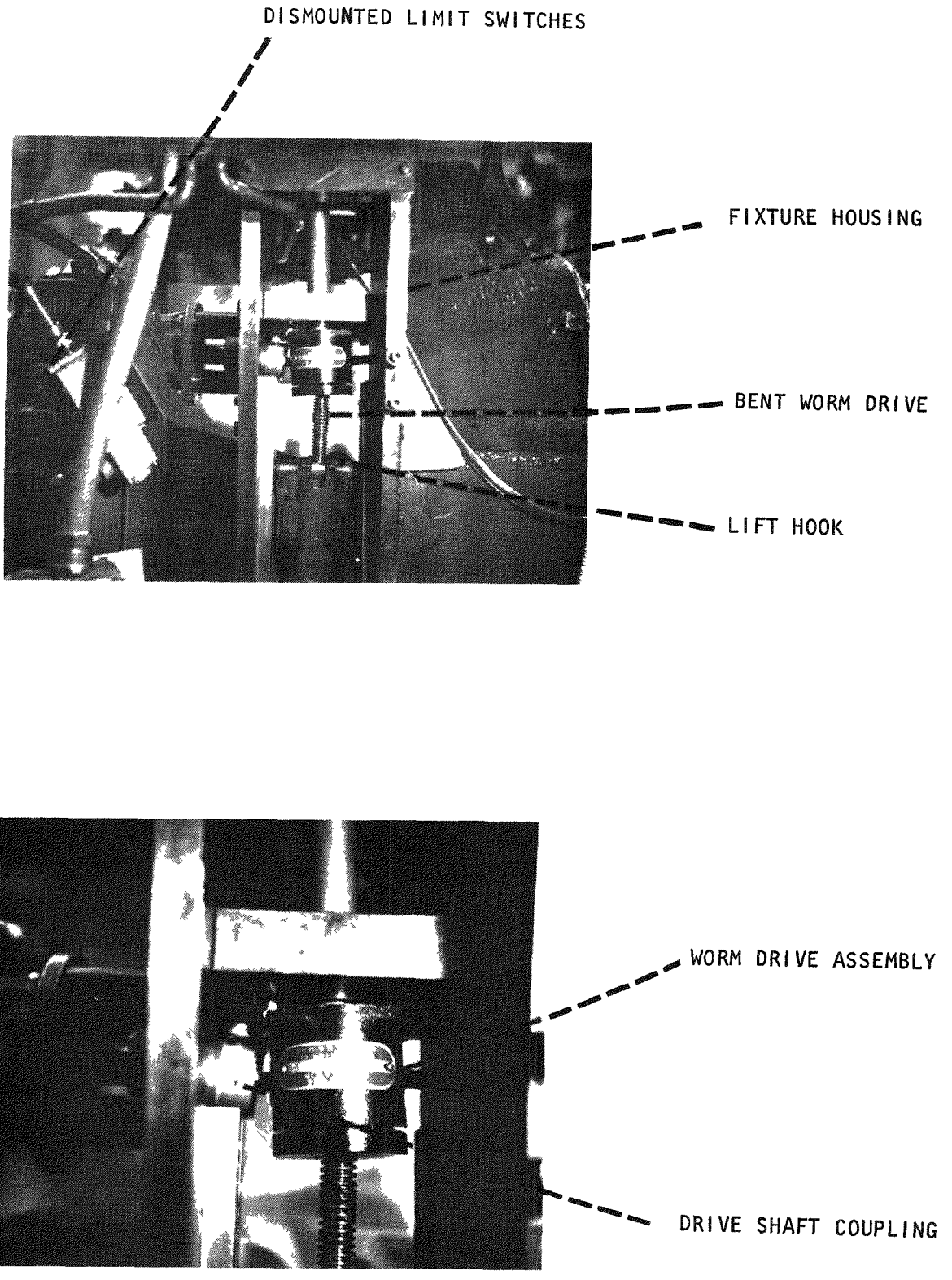

Fig. 2-16. Toggle lift hook drive assembly - secondary Pitman lift fixture

that the limit switch was not contacted and the drive motor continued to operate beyond its upper limit. Figure 2-17 shows the travel still required to contact the upper limit switch prior to motor cutoff. Figures 2-16 and 2-18 show the resulting damage to the worm drive housing and the motor shaft coupling.

Additionally, it can be seen in Fig. 2-19 that the toggle lift arm broke the temporary lubrication system drain valve, rendering it inoperable. Since the valve is not a prototypical feature and would normally not be encountered this is not viewed as a serious condition.

Figure 2-20 is a layout showing the relationship of the various components in the failure mode. It can be seen that a direct line of action can be drawn through the drive pivot, hook/pin interface, and toggle pivot. This provides a straight tension load path which resulted in an overload and subsequent destruction of the hook drive system.

Further evaluation will be performed to:

1. Identify specific equipment operation failure.
2. Identify specific errors in operating procedures or operator performance.
3. Recommend appropriate corrective action to prevent recurrence of the problem.

2.4.4. Semiremote Handling Systems - Design and Operating Reports

A report covering the UNIFRAME remote fixture is in the final management review and printing process.

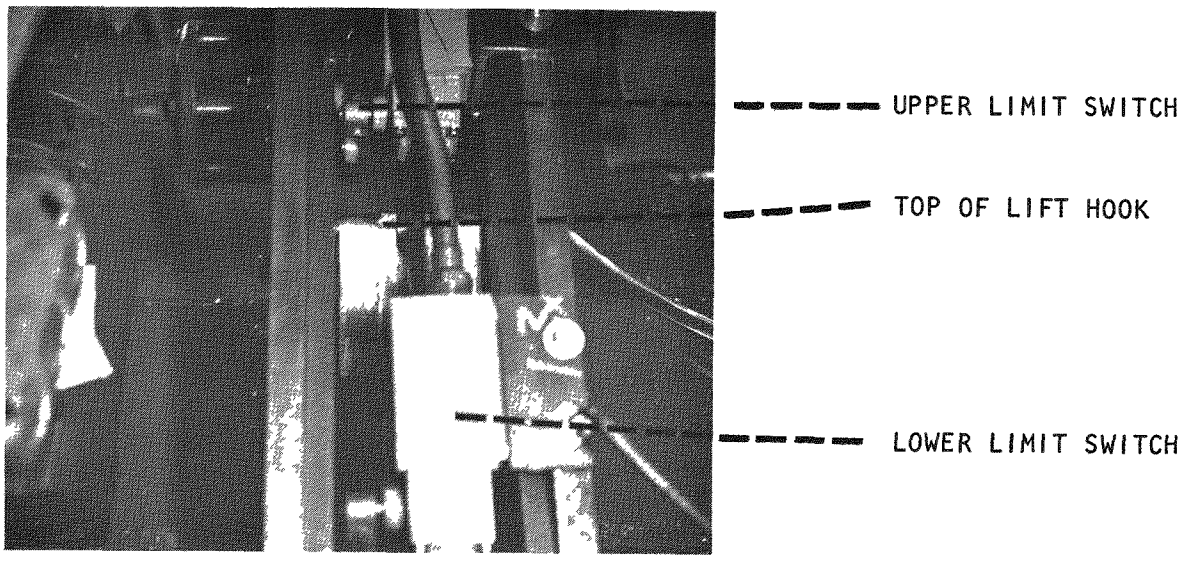

Fig. 2-17. Upper limit switch positioning - secondary Pitman lift fixture

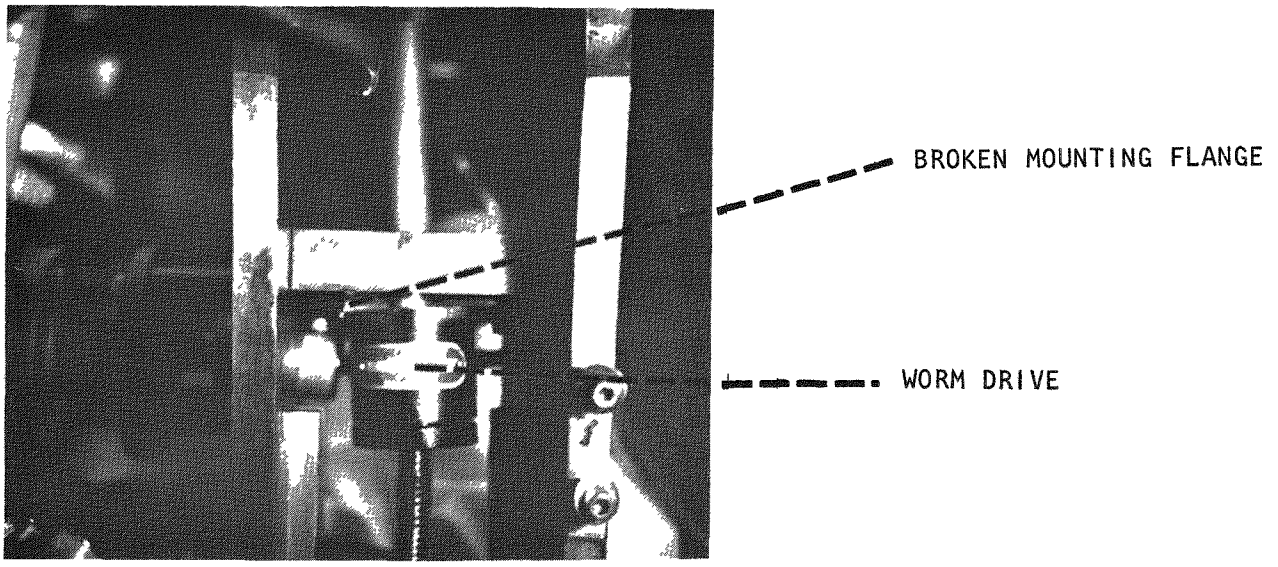

Fig. 2-18. Worm drive assembly - secondary Pitman lift fixture

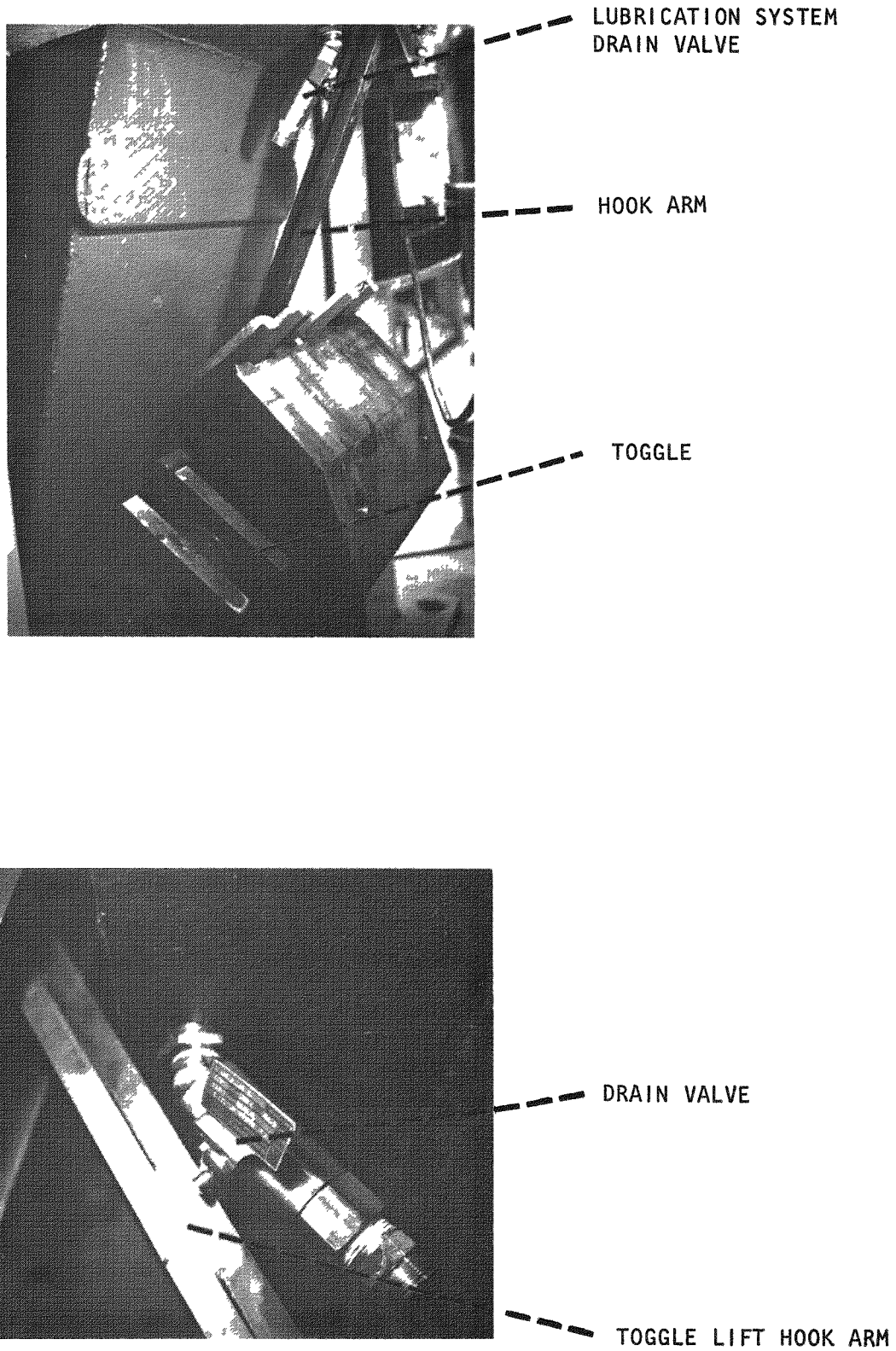

Fig. 2-19. Secondary Pitman jaw showing lubrication drain valve damage

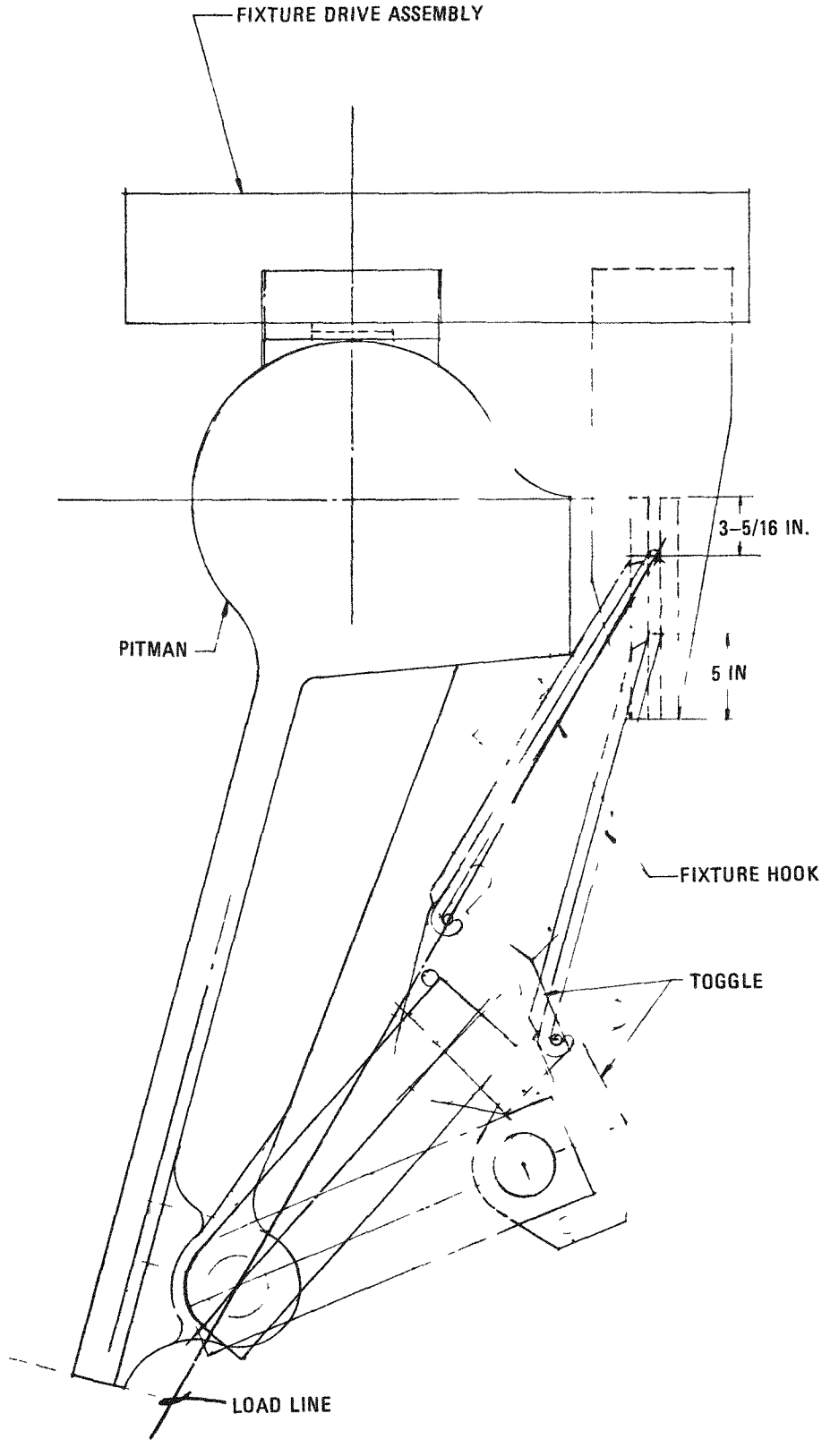

Fig. 2-20. Secondary Pitman lift fixture layout

REFERENCES

2-1. Baxter, B. J., A. Gasparovic, and A. H. Bond, "Primary Jaw Crusher Development, Interim Report," ERDA Report GA-A12864, General Atomic Company, February 28, 1974.

2-2. Baxter, B. J., et al., "Conceptual Design for a Prototype Fuel Element Size Reduction System Designated UNIFRAME, Design Status Report," ERDA Report GA-A13275, General Atomic Company, September 1, 1975.

3. CRUSHED FUEL ELEMENT BURNING

3.1. SUMMARY

3.1.1. 40-cm Primary Burner

During the current quarter, a series of six heatup tests with the 40-cm primary burner were completed. These tests verified the reliability of the induction heating system. Four of the heatup tests were extended to obtain data for experimental heat transfer coefficients of both simulated fresh feed and fuel particle (simulated product) beds.

Preliminary data analysis shows that the acceptance criteria for induction heating can be met. Heating the bed to 700°C required less than 2 hours in all cases during which no interruptions occurred. The clamp heater functioned acceptably in heatup by maintaining the clamp-to-hub ΔT at <112°C. Use of either the single lower induction coil or both the upper and lower coils resulted in similar heatup times. The single coil was the optimum choice as the larger beds required for the use of both coils resulted in excessive bed material carryover and periods of nonisothermal bed temperatures.

3.1.2. 20-cm Primary Burner

The 20-cm primary burner alternate fines recycle system test phase was completed and the results indicate that above-bed fines recycle using the gravity fines transport system was the best choice of the fines recycle alternatives tested. The alternate configurations studied were: (1 and 2) a pressurized dual-parallel hopper system, recycling material to either the

above-bed or in-bed region of the burner, (3) a gravity single-hopper rotary airlock system recycling material to the above-bed region, and (4) a pressurized tri-series hopper system recycling material to the above-bed region.

The gravity system yielded the minimum final fines inventory, fuel particle breakage, agglomeration, noncombustible fines elutriation, and final bed carbon of all the fines recycle system alternatives studied. The gravity system was also the simplest to operate. The fabrication cost of the gravity system was less than half the cost of the other systems. Also, the gravity system appears to be the most reliable as the single moving part (the rotary valve) is capable of feeding fines with large quantities of fuel particles or fresh feed material. Thus, the gravity system was preferred in all respects, greatly increasing potential simplicity, performance, economics, and reliability of the primary burning process.

3.2. PROTOTYPE 40-CM PRIMARY BURNER

3.2.1. Experimental Work

Removal of the outer induction shroud corrected the problem of excessive magnetic susception and heat loss, and the prototype 40-cm primary burner was then successfully operated in six heatup tests. In three of the heatup tests, heating to the 700°C auto-ignition temperature was studied with the single lower induction coil being used to heat beds of crushed graphite, TRISO coated fertile fuel particles, and mixed graphite (83%) and fuel particles (17%) simulating fresh feed. Two additional heatup tests involved the use of both the lower and upper coils to heat beds of particles and simulated fresh feed to 700°C. In the sixth heatup test, both the upper and lower coils were used to heat a fuel particle bed to three temperatures: 200°, 400°, and 700°C. Portions of the bed were removed at each temperature in order to study the effects of the discharge material temperature on product removal and transport. These runs completed the first series of tests for the 40-cm primary burner.

3.2.2. Experimental Results

The 2-hour maximum heatup time required in the acceptance criteria for induction heating the 40-cm vessel can be easily met if no interruptions occur. The average time required in the three uninterrupted bed heatups was 1 hour, 23 minutes. A heatup interrupted by problems involving feeding from the feed bunker required 2 hours. Another test was interrupted for 50 minutes while a blown fuse was located and replaced, requiring 2 hours, 20 minutes for heatup.

Similar heatup times resulted from the use of either the single lower coil or both the upper and lower coils. However, the larger bed required for the use of both coils resulted in the carryover of excessive amounts of fuel particles during the fuel particle bed heatup and in nonisothermal bed temperatures during the initial portion of the fresh feed bed heatup. This indicates that use of the single lower coil is preferable for heatup.

Significant improvement in bed mixing was noted in the 40-cm-burner tests compared with past 20-cm-burner runs, especially in the case of the lower coil fresh feed bed heatup. Only $\sim$0.3 m/s ($\sim$1 ft/sec) velocity was required to initiate mixing of the ambient fresh feed bed in the lower coil of the 40-cm vessel. The transfer of wall heat into the bed began without high initial gas flows. The 20-cm burner has required >0.67 m/s (>2.2 ft/sec) velocity to induce its ambient beds to mix and draw heat from the wall. The improved mixing in the 40-cm-diameter tube may be attributed to the decreased wall effects (decreased gas bypassing in bubbles at the wall).

This improved mixing substantially simplified heatup. Adjustments to total gas flow to compensate for bed temperature increases were not required as they are at high velocities. This reduces the probability of operator error causing excessive bed carryover due to slow or incorrect flow adjustments and also reduces the complexity of the system automation.

The improved mixing and concurrent increase in potential heat transfer may allow reductions in the superficial velocities required at peak burn rate. This would decrease the maximum slug height, plant gas flows, and the required burner height. However, this improvement is dependent upon the effect of bed diameter on heat transfer. With the 40-cm burner, the additional CO_2 diluent may be required for cooling rather than mixing. This will be determined in future tests.

3.2.3. Future Work

The 40-cm burner clamp/plenum section is to be removed, inspected, and re-installed prior to initiation of combustion tests in the next quarter. Preliminary results of these tests as well as results of the heat transfer studies from the six heatup runs will be available in the next quarterly report.

3.3. 20-CM PRIMARY BURNER

3.3.1. Experimental Work

Modules 5 and 6 of the 20-cm primary burner Activity Plan have been successfully completed. The purpose of these modules was to determine the optimum method of recycle fines transport to the burner. The first 9 of 11 planned experiments were performed during the previous reporting period (Ref. 3-1). These experiments involved in-bed and above-bed fines recycle using the pressurized dual-parallel hopper transport system. Eight of the nine experiments were statistically analyzed to determine preferred control levels and also to select the optimum fines injection point. The above-bed injection was selected as the preferred location for recycling fines with the alternative systems subsequently tested.

Two alternative fines transport systems were tested in the current quarter, both recycling fines above the bed. The first alternative system tested was the system consisting of a single aerated hopper and a rotary

valve (or airlock). Four runs were performed with this equipment. The remaining alternative fines recycle system tested consisted of a series of three hoppers, two of which were pressurized. Three runs were performed with the series hopper system (see Figs. 3-1 and 3-2).

The tests which were conducted in modules 5 and 6 were similar to those of modules 1 through 4 (Ref. 3-1) except that fines recycle was incorporated. These two modules can be characterized as shown in Table 3-1.

TABLE 3-1
CHARACTERISTICS OF MODULES 5 AND 6

Module	Type of Operation	Type of Feed	Principal Objectives
5	Semi-continuous "equilibrium phase"	Recycle fines	Determine effect of methods of fines injection on burner performance
6	Semi-continuous "bed burnout phase"	Recycle fines	Determine effect of induction-heated assist, fines burnout, and off-gas O_2 concentration on final bed carbon and temperature profiles

The module 5 and 6 runs were conducted with 32-kg startup beds of simulated fresh [∿83% <0.476 cm (<3/16 in.)] graphite and ∿17% TRISO fertile particles. Startup was done at ∿1.1 m/s (∿3.6 ft/sec). These were all optimum conditions established for startup in modules 1 through 4 (Ref. 3-1). The equilibrium O_2 and velocity, as well as the tailburn off-gas O_2 allowed, were varied in the ranges established in modules 1 through 4.

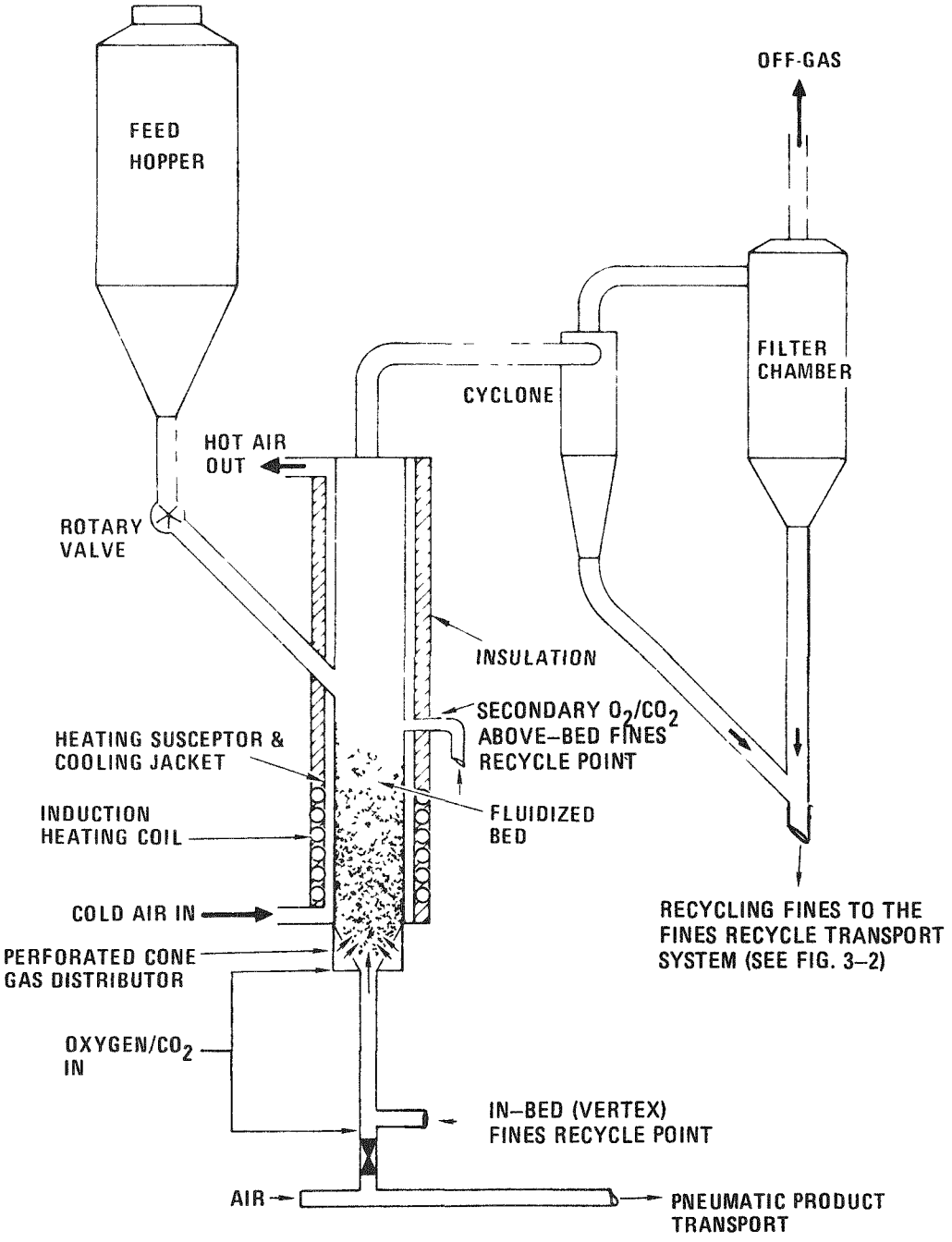

Fig. 3-1. Primary burner configuration

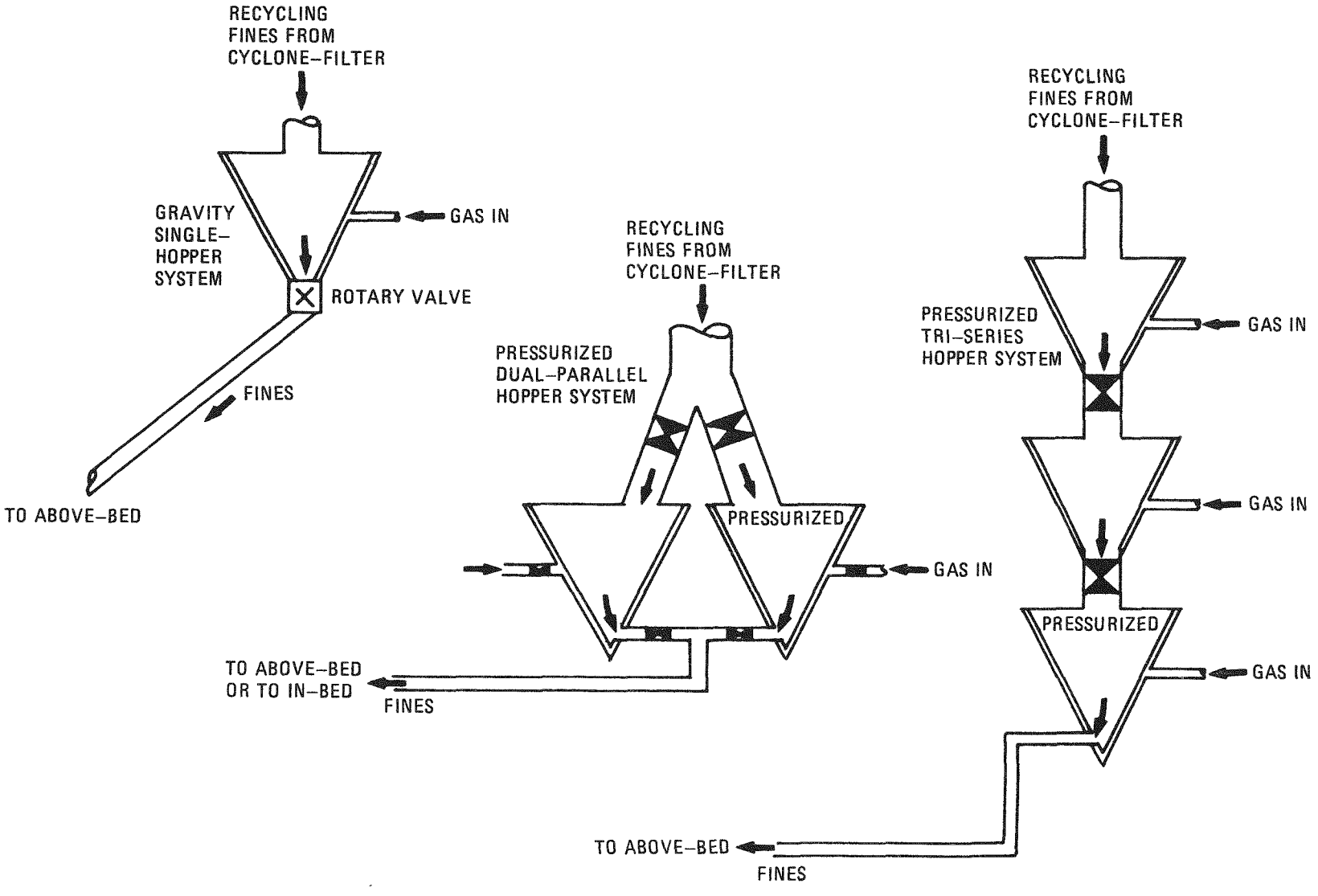

Fig. 3-2. Three fines recycle systems tested

A statistical design technique was used to set up the experiments. Statistical analysis was then used to evaluate the module 5 "equilibrium phase" of the runs to determine recommended operating levels. The results of the experiments are summarized in Section 3.3.2.

3.3.2. Experimental Results

Tables 3-2 and 3-3 show the most significant experimental results of in-bed fines recycle using the pressurized dual-parallel hopper fines transport system compared with above-bed fines recycle using the pressurized dual-parallel hopper system, the pressurized tri-series hopper system, and the gravity single-hopper system. Table 3-3 data show that minimum fuel particle breakage, noncombustible fines elutriation, final fines hopper inventory, particle agglomeration, final bed carbon, and bed material carryover occur when using above-bed recycle by means of the gravity transport system. Table 3-2 shows an apparent increase in heat transfer with above-bed recycle as minimum radial and axial temperature differences were found in the runs using above-bed recycle.

The specifics of the results may best be presented by discussing results of comparison of in-bed versus above-bed recycle; comparison of the gravity, series, and parallel fines transport systems all recycling above the bed; operating levels recommended by the statistical analysis; and, finally, other major results of particular interest.

3.3.2.1. In-Bed Versus Above-Bed Fines Recycle (Parallel Hoppers)

Tables 3-2 and 3-3 show that in-bed fines recycle drastically increased fuel particle carryover into the recycle loop, thereby breaking more particles and increasing noncombustible oxide buildup in the fines. Agglomeration of unbroken fuel particles also increased with in-bed fines recycle. In addition to these negative aspects, final bed carbon was highest with in-bed recycle, indicating poorer bed burnout. Bed heat transfer also was affected negatively by in-bed recycle; both the heat transfer zone and the

TABLE 3-2
20-CM PRIMARY BURNER TEMPERATURE DIFFERENTIALS - AVERAGED EXPERIMENTAL RESULTS FOR MODULES 5 AND 6

Measured Variable	Experimental Results	
	In-Bed Recycle	Above-Bed Recycle[a]
Module 5 averages		
Axial temperature difference, °C	39	32
Median radial temperature difference, °C	118	112
Module 6 averages		
Axial temperature difference, °C		
Overall	39	36
Not induction heated	35	55
Induction heated	43	27
No fines tailburn	35	48
Fines tailburn	43	30
Median radial temperature difference, °C	91	82
Not induction heated	110	120
Induction heated	72	71
No fines tailburn	80	123
Fines tailburn	102	70

[a]Gravity and parallel hopper systems. Series runs excluded due to intermittent fines flow and inordinate end-run fines inventory.

TABLE 3-3
20-CM PRIMARY BURNER PARTICLE BREAKAGE AND RESIDUAL INVENTORY DATA

Averages for Modules 5 and 6	In-Bed Recycle	Above-Bed Recycle		
	Vertex Parallel Hoppers	Above-Bed Parallel Hoppers	Above-Bed Series	Above-Bed Gravity
Fines inventory, kg[(a)]	1.4	1.4	6.8	0.21
Particle breakage, wt %	5.3	1.7	0.82	0.56
Non-combustibles in fines (-355 m), g	1172	332	222	146
Fuel particles in fines hoppers, g	1609	<3	23	<1
Particle agglomeration, wt %	0.015	0.009	0.006	0.001
Final bed carbon, wt %[(a)]	1.2	0.60	0.39	0.36

[(a)] Tailburned results only.

temperature gradients were minimized by above-bed recycle. The final fines inventories for in-bed and above-bed recycle using the parallel pressurized hopper system were similar when fines were burned out. Hence, in-bed recycle using parallel pressurized hoppers will burn fines as well as above-bed recycle, but above-bed recycle is preferable in all other effects on the burner system measured in this study.

3.3.2.2. Gravity Versus Parallel and Series Hopper Above-Bed Recycle

Gravity fines recycle resulted in the least final fines inventory; fuel particle elutriation, breakage, and agglomeration; oxide buildup in fines; and final bed carbon of any of the recycle systems tested. The gravity system was the simplest to operate and its single moving part (the rotary valve) increased the reliability of the system. This system is capable of feeding fines with large quantities of fuel particles or fresh feed material. The fabrication cost of the gravity system is less than half the cost of either of the other transport systems. On this basis the gravity system was chosen as the optimum fines recycle technique for further long-term testing.

3.3.2.3. Operating Levels Recommended

Table 3-4 indicates the level at which the independent or "controlled" variables should be held to reduce the values of the dependent or "measured" variables based upon the statistical analysis. The form is similar to the summation table in Ref. 3-1. The "high-H" and "low-L" terms indicate whether the particular controlled variable should be high or low within the range of values given for each independent variable. The occurrence of an H/L in a row with an L/H means that a "high-H" level of the first variable should combine with a "low-L" level of the other variable, and vice versa.

TABLE 3-4
20-CM PRIMARY BURNER STATISTICAL ANALYSIS OF IN-BED AND ABOVE-BED FINES RECYCLE WITH OPERATING LEVELS[a] FOR MINIMIZING DEPENDENT VARIABLES

Dependent Variable	Independent Variable			
	Bed Velocity, U_T [m/s (ft/sec)] L = 1.01 (3.3) H = 1.09 (3.6)	Secondary O_2, V_s (SLPM) L ≤ 40 H ≤ 80	Delay Time[b] (minutes) L = 0 H = 30	In-Bed O_2, V_o (SLPM) L = 300 H = 350
Axial bed ΔT				
Parallel hoppers, vertex recycle	L	L	L	L
Parallel hoppers, above-bed recycle	L	H	L	L
Radial bed ΔT				
Parallel hoppers, vertex recycle	L	L	--	L
Parallel hoppers, above-bed recycle	L	H	--	L
Off-gas				
CO				
Parallel hoppers, vertex recycle	H	L	--	H
O_2				
Parallel hoppers, vertex bed recycle	L	L	--	L
CO				
Parallel hoppers, above-bed recycle	H/L	L/H	--	H/L
O_2				
Parallel hoppers, above-bed recycle	H/L	L/H	--	H/L
Fines inventory				
Parallel hoppers, vertex recycle	H/L	H/L	--	H/L
Parallel hoppers, above-bed recycle	H/L	H/L	--	H/L
Noncombustible fines elutriation				
Parallel hoppers, vertex recycle	L	L	--	L
Parallel hoppers, above-bed recycle	L	L	--	L
Particle breakage (loss)				
Parallel hoppers, vertex recycle	L	H	--	L
Parallel hoppers, above-bed recycle	L/H	L/H	--	L/H
Particle agglomeration				
Parallel hoppers, vertex recycle	L/H	H/L	--	L/H
Parallel hoppers, above-bed recycle	L/H	H/L	--	L/H

[a] L = low within test range and H = high within test range.

[b] Delay time to start fines recycle after O_2 ramp.

The best fines recycle system tested was gravity above-bed recycle; hence, the levels shown for above-bed recycle were the ones considered. Also considered were qualitative results observed in module 6, the tail-burning phase which was not statistically analyzed.

The combined results indicate that for optimum operation with above-bed gravity fines recycle: (1) fines recycle should be started immediately after the oxygen ramp is completed, (2) total in-bed oxygen, above-bed oxygen, and in-bed velocity should be matched (i.e., at high burn rate, use high above-bed oxygen flow and high in-bed velocity), and (3) induction heating should be used and fines recycle should be continued throughout the final product bed tailburning.

The suggested operating conditions were selected from the tabulated results by ranking the dependent variables in order of importance, as follows: fines inventory (most important), particle breakage, noncombustible fines elutriation, particle agglomeration, off-gas CO and O_2, radial ΔT, and axial ΔT (least important). (Particle agglomeration was ranked relatively lower than in modules 1 through 4 because of the very low (<0.02 wt %) amounts of agglomeration formed.)

3.3.2.4. Other Major Results

Fuel particle agglomeration was found to be very much lower in the fines recycle runs than in runs without fines recycle. Nonrecycle run results show agglomeration to be from 0.02 to 0.2 wt % of final beds, while a range of only 0.001 to 0.015 wt % agglomerates was noted in this work. The apparent explanation is that fines recycle (whether in-bed or above-bed) improves bed mixing, thus avoiding any local or temporal stagnation which can allow fuel particles to be fused by eutectic compounds. This mixing improvement was significant as the higher particle breakage resulting from fines recycle should have provided more impurities to form the eutectics which may bond agglomerates.

An average oxygen ramp rate of 16 SLPM/minute was used in these runs without any noticeable adverse effects (a maximum of 8 SLPM/minute was used in the study reported in Ref. 3-1). Ramp rates in excess of ∿20 SLPM/minute appeared to cause an initial bed temperature overshoot.

3.3.3 Future Work

Studies during the next quarter on the 20-cm primary burner will include module 7 of the Activity Plan. Several runs will study system automation. Module 7 runs will be conducted with the gravity recycle system and will include a run of at least 48 hours duration.

3.4. 40-CM PRIMARY BURNER DESIGN EVALUATION

3.4.1. Introduction

The transformation of the current engineering-scale crushed fuel element burner in the cold pilot plant to a reliable and maintainable piece of equipment which is prototypical to the HRDF design requires a periodic and systematic review of the equipment design, required function, and anticipated performance. A design evaluation (Refs. 3-2 and 3-3) of the burner has been initiated with the dual purpose of performing a critical analysis of the current design with regard to the intended function and of establishing a design data base from which evolutionary changes in subsystem or component design may logically proceed.

3.4.2. Required Data

To facilitate a systematic evaluation of the design, data concerning the system must be collected. This data package will contain the following information as it applies to the system under consideration:

1. System definition.
2. Functional level diagram.
3. Functional Analysis System Technique (FAST) diagrams.

4. Analysis of manufacturing processes, time, and cost.
5. Material selection and failure mode analysis.
6. Design envelope and tolerance study.
7. Design environment specification.

Based on the data collected, an evaluation of the suitability of component and subsystem design will be initiated.

3.4.3. System Definition

The first step toward collecting the set of required data listed above is to establish the boundaries under consideration. Instrumentation and auxiliary features which have only a development testing function and are not prototypical to a commercial installation are excluded. System boundaries are identified in Fig. 3-3. Feed or product bunkers, CO_2 and O_2 storage, and coolers are not included in the evaluation. The induction heating capacitor banks and M-G set, although not shown in Fig. 3-3, are to be included as part of the burner system.

3.4.4. Functional Level Diagram

Based on the system definition, a functional level diagram (FLD) is developed which depicts the relationship between the system, subsystems, and components. The utility of the diagram arises from recognizing a "functional distinction" between components and aggregates of components. Generally, the distinction is made by level, each functional level being related to the overall function performed by the system, with the highest level describing more completely the intended function of the equipment.

The block diagram type format is employed in the primary burner system FLD as shown in Fig. 3-4. The primary burner system is divided into six subsystems:

1. Structural
2. Fluidizing

3. Insulation
4. Heating
5. Cooling
6. Solid handling

Each subsystem uses the functional levels of assembly, subassembly, and components to provide a further categorization of the burner system. In several instances, further breakdown into parts is made so that the same FLD can be utilized during a course of maintenance action, by depicting the relationships between parts and components and therefore the sequence of disassembly or assembly.

In Fig. 3-4 the drawing number associated with each assembly, subassembly, component, or part is identified at the bottom of each block of the FLD. This permits further details about the item in the block to be obtained without tracing the item down from a higher level assembly drawing.

3.5. SEMIREMOTE HANDLING SYSTEMS

Handling fixtures required to demonstrate capabilities for remote maintenance of selected prototype equipment have been designed and fabricated as part of the overall head-end development program. During the current quarter, efforts have been directed toward completion of the design and operating reports.

3.5.1. Handling Equipment - Primary Burner

All scheduled design and development work on the handling equipment has been completed. Current activities will be directed toward preparation of burner assembly and disassembly procedures.

3.5.2. Semiremote Handling Systems - Design and Operating Reports

A report covering the burner remote fixture is in the final management review and printing process.

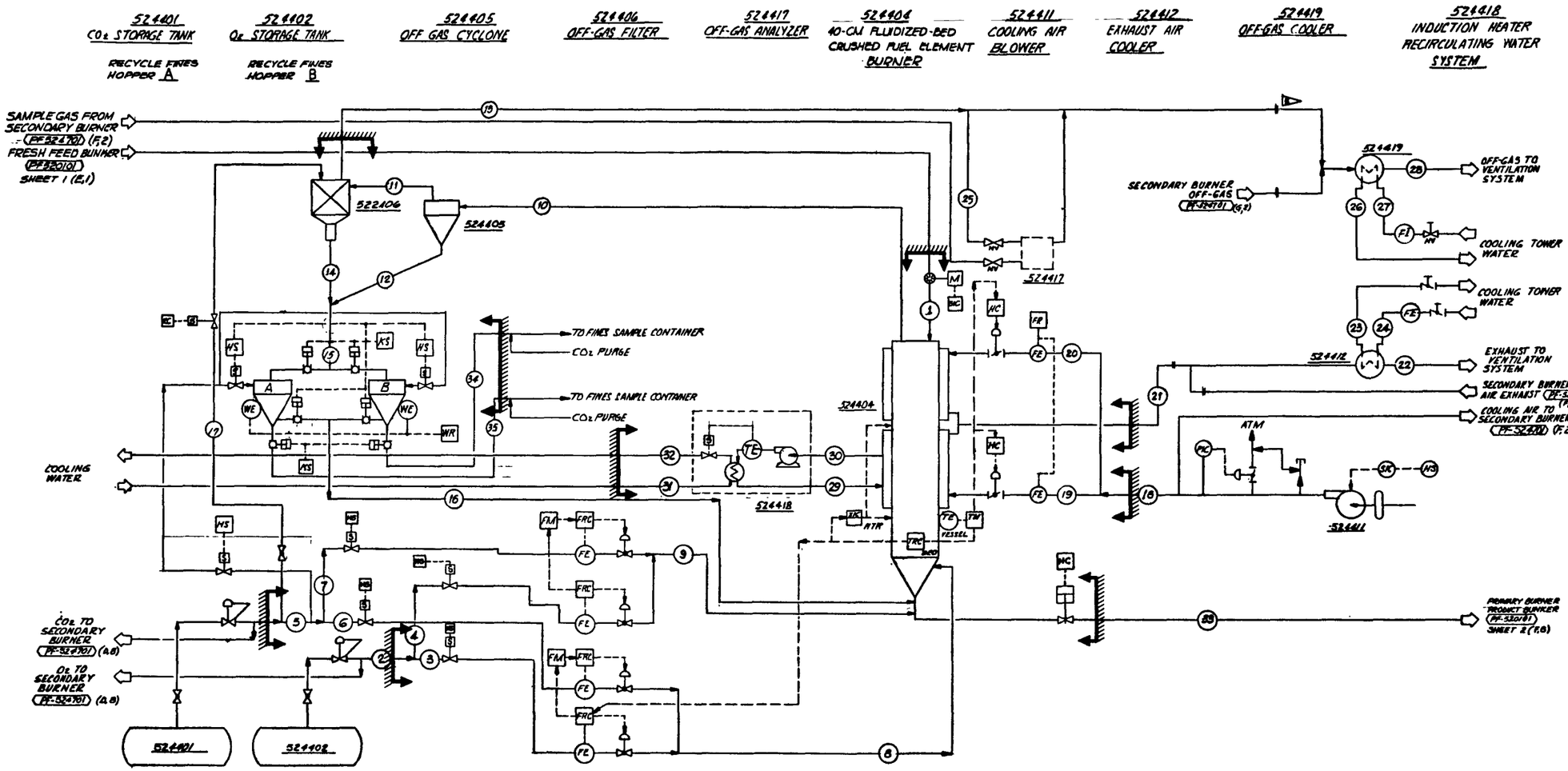

NOTES

1. SYMBOLS & TERMINOLOGY PER GA GUIDE STANDARDS GA 3-3 & GA 2-1
2. BURNABLE CARBON ONLY
3. INTERMITTENT FLOW ONLY (~ 1 SEC. DURATION PER MIN)
4. PERFORMANCE CHARACTERISTICS OF HEAT EXCHANGER NOT AVAILABLE
5. FLANGES FOR POSSIBLE BLINDING TO PERMIT OPERATING BURNER ISOLATION FROM SHUTDOWN BURNER.

Fig. 3-3. System definition for 40-cm primary burner design evaluation

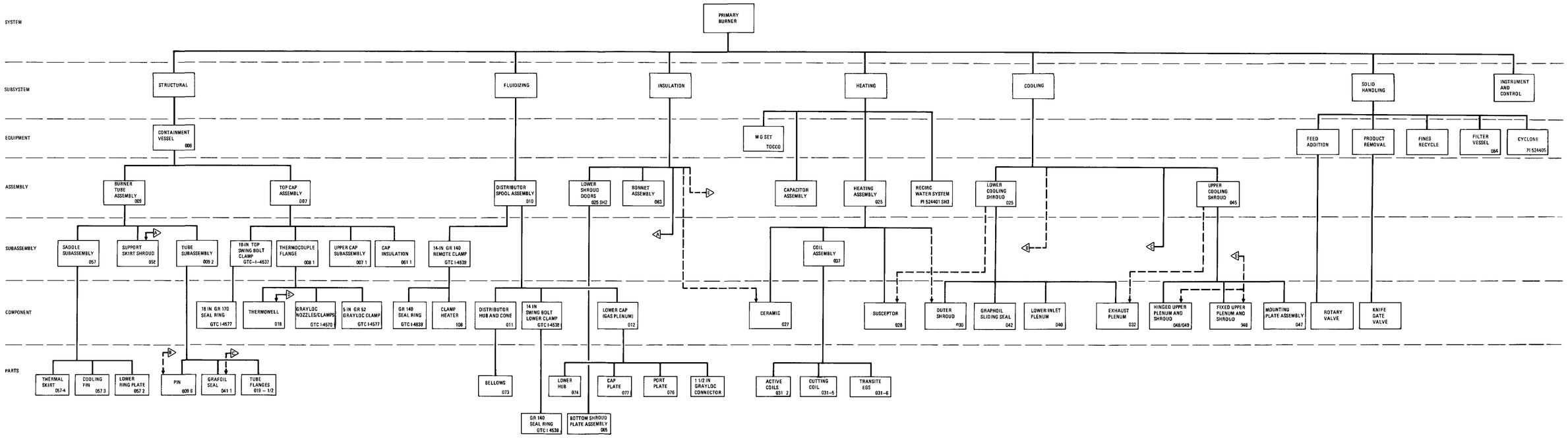

Fig. 3-4. 40-cm primary burner functional level diagram

REFERENCES

3-1. "Thorium Utilization Program Quarterly Progress Report for the Period Ending August 31, 1976," ERDA Report GA-A14085, General Atomic Company, September 30, 1976.

3-2. "Valve Control - Valve Analysis Workshop Seminar," General Atomic unpublished data.

3-3. "Value Control Project No. 68," General Atomic unpublished data, June 1974.

4. PARTICLE CLASSIFICATION, CRUSHING, AND BURNING

4.1. INTRODUCTION

HTGR fuel reprocessing includes steps for classifying, crushing, and burning irradiated SiC coated fuel particles. Current efforts directed toward development of engineering-scale pilot plant equipment include tests of the 20-cm secondary burner with FSV carbide kernel fertile particles, preparation of the 10-cm secondary burner for initial tests with fissile particles, testing of roll crushers with both fertile and fissile particles, and scale-up verification tests with the Alpine zig-zag classifier. WAR fissile particles, resin-derived UC_2 kernels, FSV fissile particles, VSM Th-UC_2 kernels, and FSV carbide kernel fertile particles will be crushed and burned in the secondary burner. LHTGR fertile particles are BISO-coated ThO_2 kernels; the outer carbon coating burns off in the primary burner. Scale-up data are obtained by analysis of data from the 10-cm and 20-cm secondary burners.

Testing in this quarter has included checkout and shakedown of the fertile particle roll crusher and the 20-cm secondary burner. Heat transfer coefficients of feed and product material were measured during these tests. Initial automation of the burner cycle was accomplished with the groundwork laid for more extensive automated control. Future tests will include process optimization and verification of the operating cycle with fertile particles. Burning of fissile particles will be tested in mid-1977 after disassembly of the burner with the remote tooling.

4.2. 20-CM SECONDARY BURNER

Two full-cycle burner runs were made as specified in Phase I of the 20-cm secondary burner test plan (AP524701) for the purpose of system

shakedown. Some problems were uncovered which have since been corrected. The distributor plate hole design allowed "weeping" and "jetting" of the bed to occur. A new design has now been installed. Product removal was discontinuous due to low transport flow as required by solids handling tests. Higher design transport velocities will now be used.

Heat transfer characteristics of feed and product material measured as part of the burner shakedown runs indicate very high heat transfer capabilities of this material. These data are discussed in Section 4.2.4.

A quantity of 125 kg of FSV TRISO fertile Type 5A fuel particles was screened to -850 μ/+425 μ, sampled for uncrushed and crushed properties, and split into two identical 60-kg batches, one for each run of Phase I. This material was crushed in a roll crusher to make feed for the secondary burner. The physical properties and composition of the particles before and after crushing are shown in Table 4-1, and their size distributions are shown on Fig. 4-1.

The roll crusher dimensions include a 0.48-mm (0.019 in.) gap and 102 mm (4 in.) diameter by 102 mm (4 in.) long rolls. Roll crushing was satisfactory until side plates wore excessively, allowing particles to go through uncrushed. A design modification was made which included hard facing the side plates to reduce wear.

Details of these two burner shakedown runs are discussed in Sections 4.2.1. and 4.2.2. Section 4.2.3 summarizes the conclusions from both runs.

4.2.1. Run 1

4.2.1.1. Operation

Figures 4-2 through 4-4 show the parameters such as gas flow, composition, and temperature as a function of run time.

TABLE 4-1
FEED MATERIAL CHARACTERISTICS, PHASE I OF
THE 20-CM 2° BURNER TEST PLAN

Uncrushed Feed

Bulk ρ = 2.17 g/cm^3

Tap ρ = 2.31 g/cm^3

Crushed Feed

Bulk ρ = 2.27 g/cm^3

Tap ρ = 2.12 g/cm^3

Angle of response = 29°

d_{SV} = 212 μm

57.1% ThC_2 = 34,260 g

21.2% C = 12,660 g

21.8% SiC = 13,080 g

<0.1% unbroken particles, determined by screen and microscopic examination

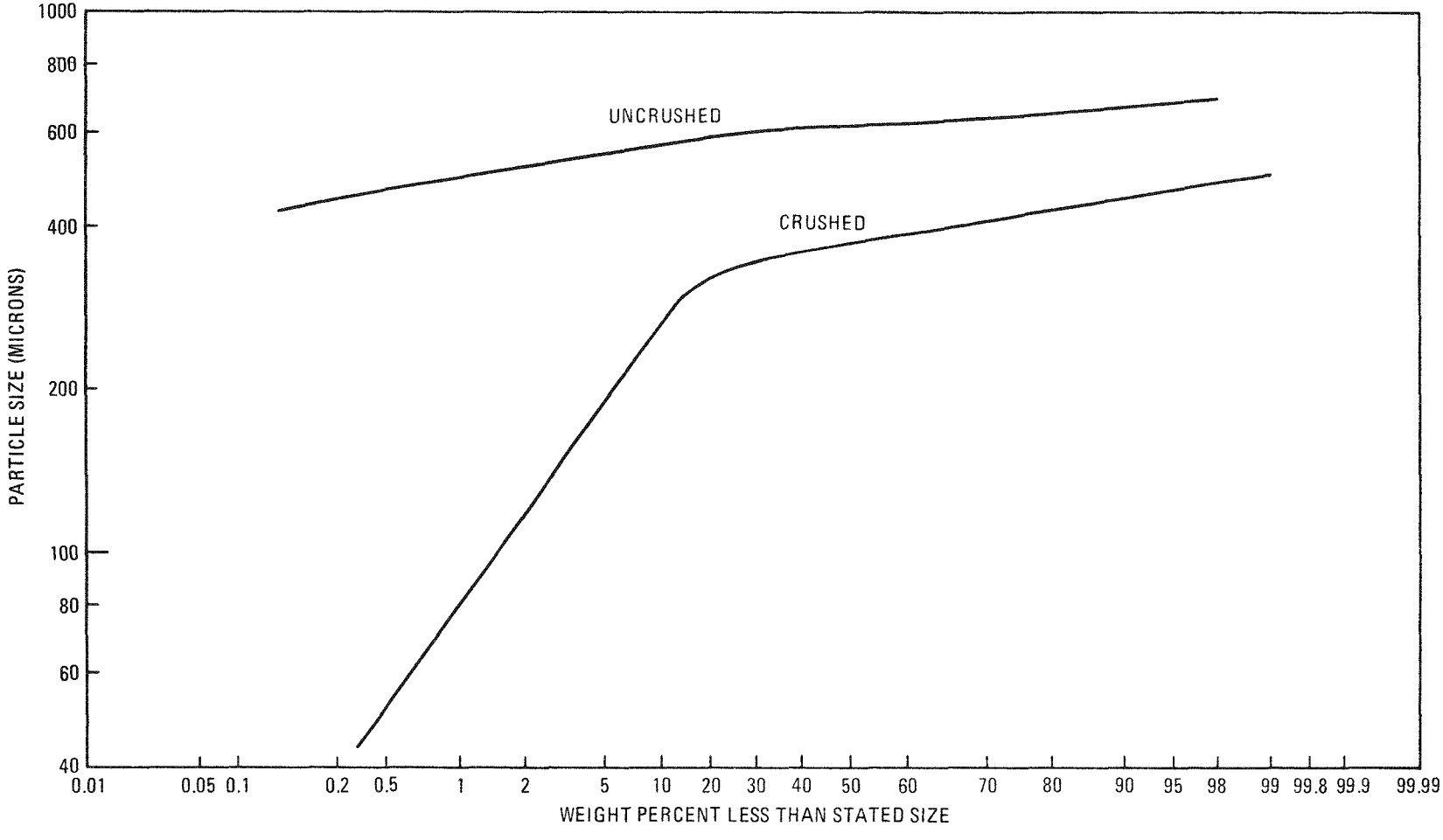

Fig. 4-1. Crushed and uncrushed feed size distributions, 20-cm secondary burner Phase I

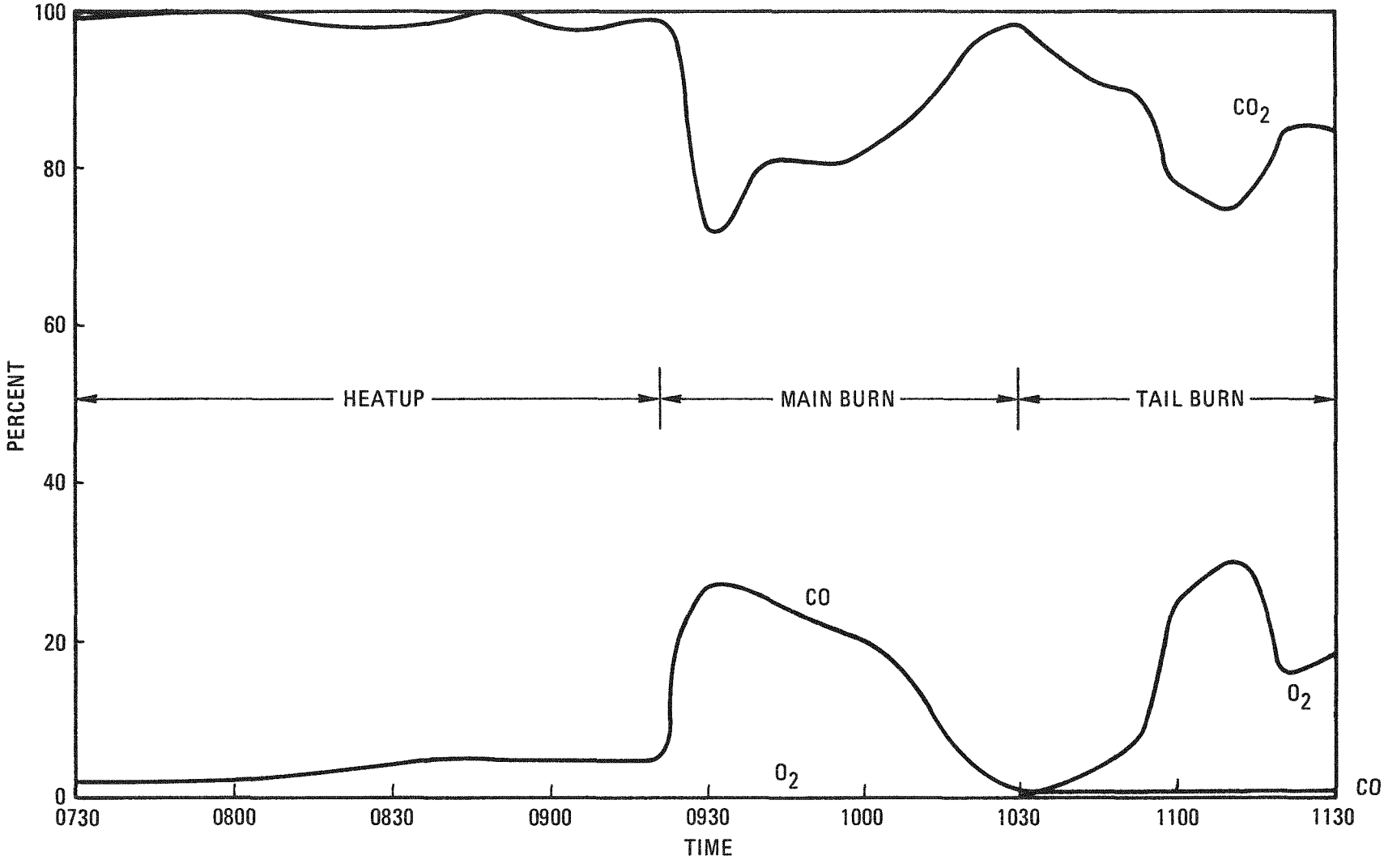

Fig. 4-2. Off-gas composition versus time, 20-cm secondary burner Run 1

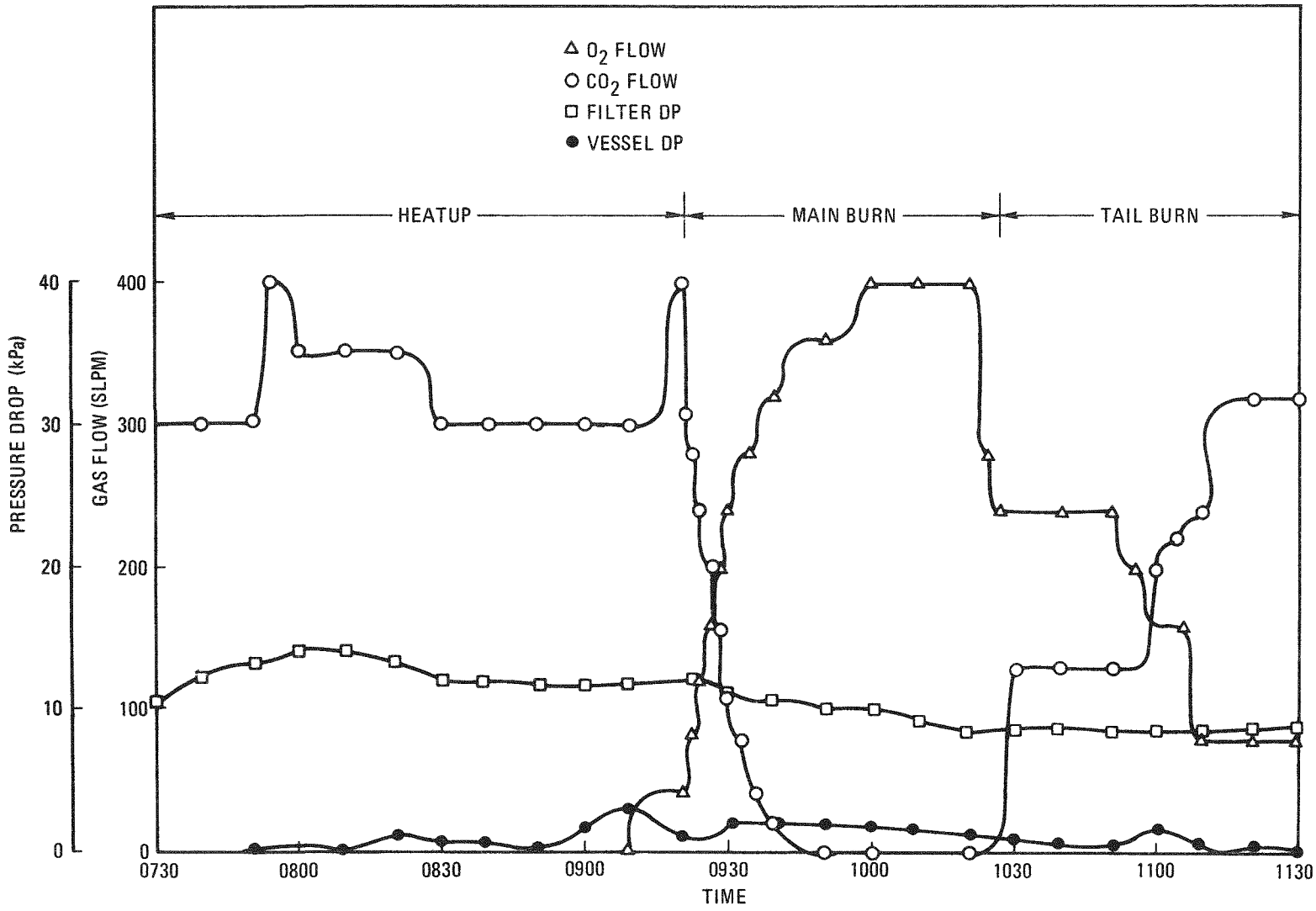

Fig. 4-3. Gas flow and pressure drop versus time, 20-cm secondary burner Run 1

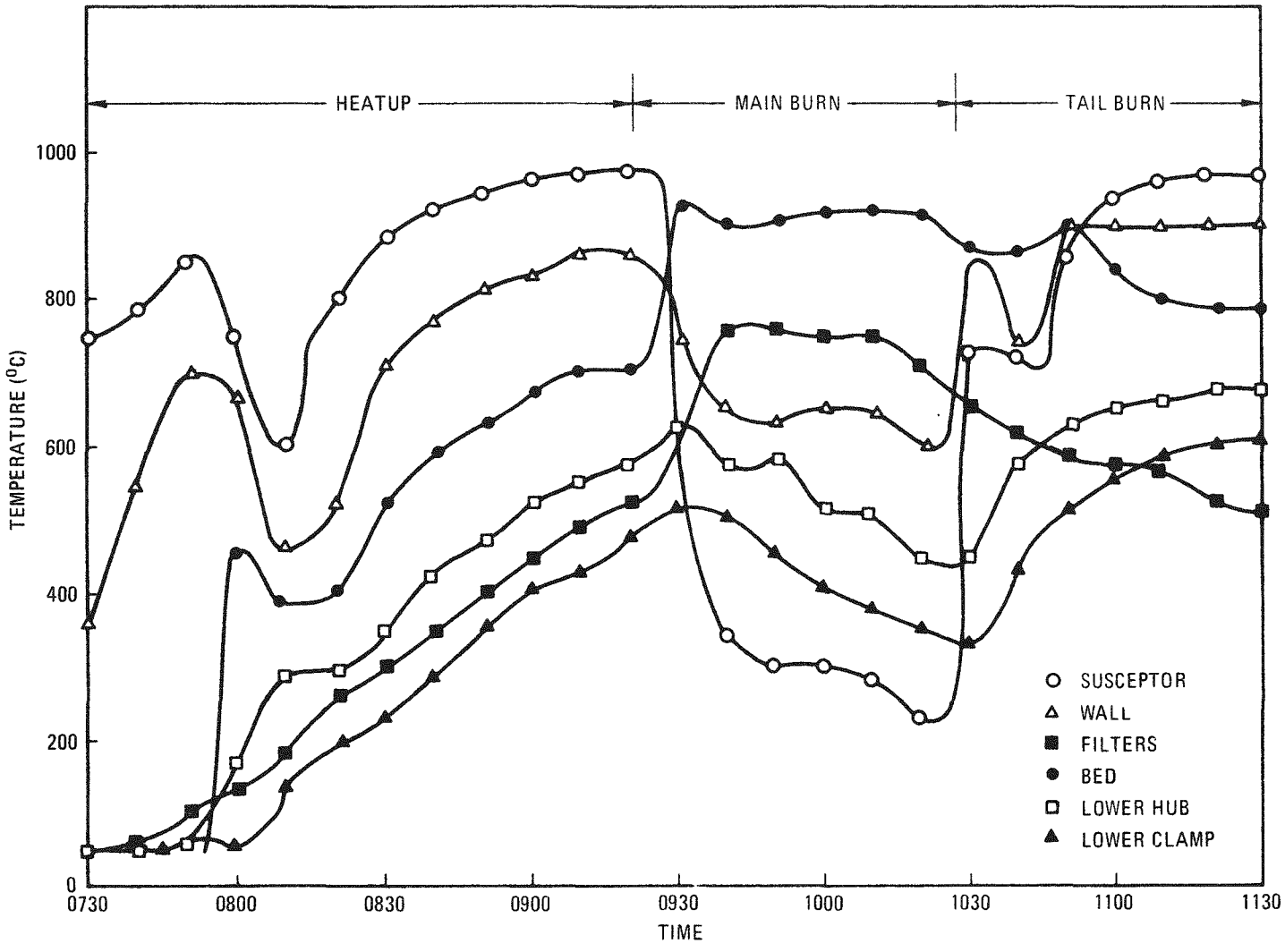

Fig. 4-4. Temperatures versus time, 20-cm secondary burner Run 1

Initial actions included crushing the feed material into the feed hopper. The crusher was actuated at 22-rpm roll speed using ∿30% voltage on a variable speed 520-W (3/4-hp) dc motor and gear reducer. Whole particles were then choke fed to the crusher, which subsequently stalled. An increase in motor voltage to 50% coupled with manual starting of crushing action allowed crushing to proceed at 36-rpm roll speed. The motor is evidently not capable of crushing at 30% voltage. The crushing rate is shown in Fig. 4-5. A purge of 15-SLPM CO_2 gas was provided continuously to the vented feed hopper to avoid material oxidation prior to introduction of the burner.

Feed material was added to the burner using the gravity pneumatic feeder at 40-SLPM CO_2 flow. The burner was being purged at 240-SLPM CO_2 during this time. Four minutes were required to add the entire batch of 60 kg of crushed fuel particles.

Heatup was then begun on automatic control at 70-kW maximum output limit. After 30 min of heating, the lowest bed thermocouple had not responded, indicating a lack of axial bed mixing. When the inlet gas flow was readjusted to 400 SLPM, the lower bed temperature rapidly rose to 450°C. This caused the lower Gray-loc hubs to heat rapidly, with an attendant increase in the clamp-to-hub temperature differential. In order to keep the differential below the design limit of 170°C, it was necessary to manually decrease the induction power to 50 kW for about 10 min followed by a return to the 70-kW limit.

After a total heatup time of 100 min, the bed reached 700°C. Filter blowback was actuated at 272 kPa (40 psi), with each of three banks receiving a 1-sec pulse every 30 sec for an overall rate of one pulse per 10 sec. This kept the filter pressure drop below 2.5 kPa (10 in. H_2O) throughout the run.

Ignition was effected by raising the inlet O_2 concentration from zero to 20% and then stepping up to 100% in discrete steps over a 20-min period. Induction power dropped off automatically as the bed heated above 860°C.

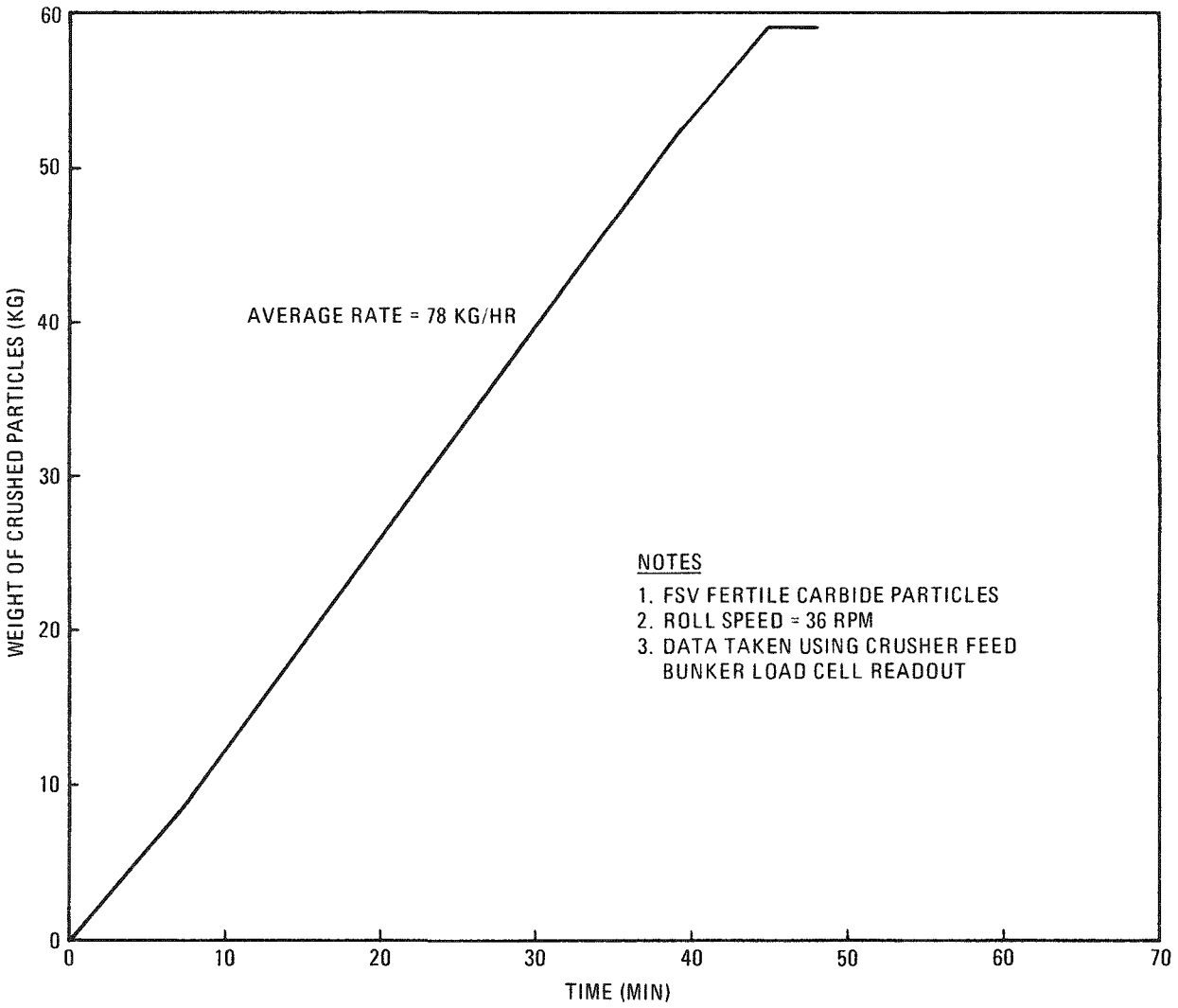

Fig. 4-5. Particle crusher throughput, 20-cm secondary burner Run 1

Cooling air to the upper jacket was on automatic, with a 650°C filter temperature setpoint. Lower cooling air was controlled manually during this run. Cooling air flows overran the chart span, so rates are not available for this run.

Bed slugging was greater initially with maximum pressure variations of over 15 kPa (60 in. H_2O) at 6-sec intervals, while late in the run they were a maximum of 7.5 kPa (30 in. H_2O) at 6-sec intervals.

The full burn rate ended after 50 min when the concentration of CO in the off-gas decreased to zero. Inlet oxygen concentration was then reduced to 60% to preclude the possibility of a pure oxygen front penetrating the bed and reacting with fine carbon on the filter surface. Ten minutes after this was done, oxygen did begin to exit from the burner, increasing to 20% over the next 20 min. In the following 20 min, the inlet oxygen concentration had to be decreased to 20% to keep the outlet below the run limit of 20%; at this time the burn rate had dropped to a negligible point (>4 g/min carbon burn rate).

The induction heater had come back on automatically as the bed temperature dropped below 860°C and was able to hold the bed at 790°C during this low combustion rate period.

At the end of the run the upper end of the burner was vibrated to dislodge any fine particulates adhering to the wall. Particulates are filtered out of the burner off-gas stream by sintered metal filters in the upper end of the burner. The filters are periodically blown back to return material to the fluidized bed. A significant amount of material, 200 g or 0.4% of the product, reentered the bed and was burned after the filter region was vibrated. A permanent method of vibrating the burner filter region would be of definite benefit in lowering product carbon content.

A series of product heat transfer tests were then carried out, followed by product removal at room temperature. Use of too low a transport velocity caused choking flow in vertical portions of the conveying line and subsequent plugging.

4.2.1.2. Analysis

Disassembly of the lower end of the burner revealed material both above and below the distributor plate. This probably resulted from the fact that the drilled hole size was too large combined with insufficient pressure drop existing across the plate. This problem has been investigated in depth and is reported in Section 4.2.5.3.

The product material properties are shown in Table 4-2. A thorium material balance closed within 4%, which is probably within the limits of the sampling error. The product contained just under 1 wt % unbroken fuel particles. The product size distribution is shown in Fig. 4-6.

Following this initial run, welds identified in the maintenance procedures, MM524701, were inspected using a liquid dye penetrant technique. No cracks were found in any locations.

4.2.2. Run 2

4.2.2.1. Operation

Figures 4-7 through 4-9 contain data gathered during the burn run.

Feed material was crushed at 36-rpm roll speed with a throughput as shown in Fig. 4-10. Four minutes were required to add the 60-kg bed of crushed fuel particles. Induction heating proceeded while a 400-SLPM CO_2 gas stream fluidized the bed. A total of only 65 min was required to heat the fluid bed from ambient to 700°C. This reduction in time is attributed to the use of a higher fluidizing gas rate that yielded better bed mixing.

TABLE 4-2
PRODUCT MATERIAL CHARACTERISTICS FOR 20-CM SECONDARY BURNER
RUNS 1 AND 2 WITH FSV FERTILE PARTICLE FEED

Run 1

74.9% ThO_2 = 33,742 g
1.7% C = 766 g
23.4% SiC = 10,542 g

Initial product	=	42,810 g
Material above distributor plate	=	720 g
Material in gas plenum	=	1,520 g
		45,050 g

Bulk ρ = 2.37 g/cm^3
Tap ρ = 3.03 g/cm^3
Angle of repose = 34.5°

$$\frac{Th_{out}}{Th_{in}} = 0.96$$

Run 2

Initial product	=	44,173 g	(1.4% C)	
Material above distributor plate	=	930 g	(7.7% C)	Overall 1.6% C
Material in gas plenum	=	1,758 g	(2.2% C)	
		46,861 g		

Bulk ρ = 2.67 g/cm^3
Tap ρ = 3.43 g/cm^3
Angle of repose = 37°

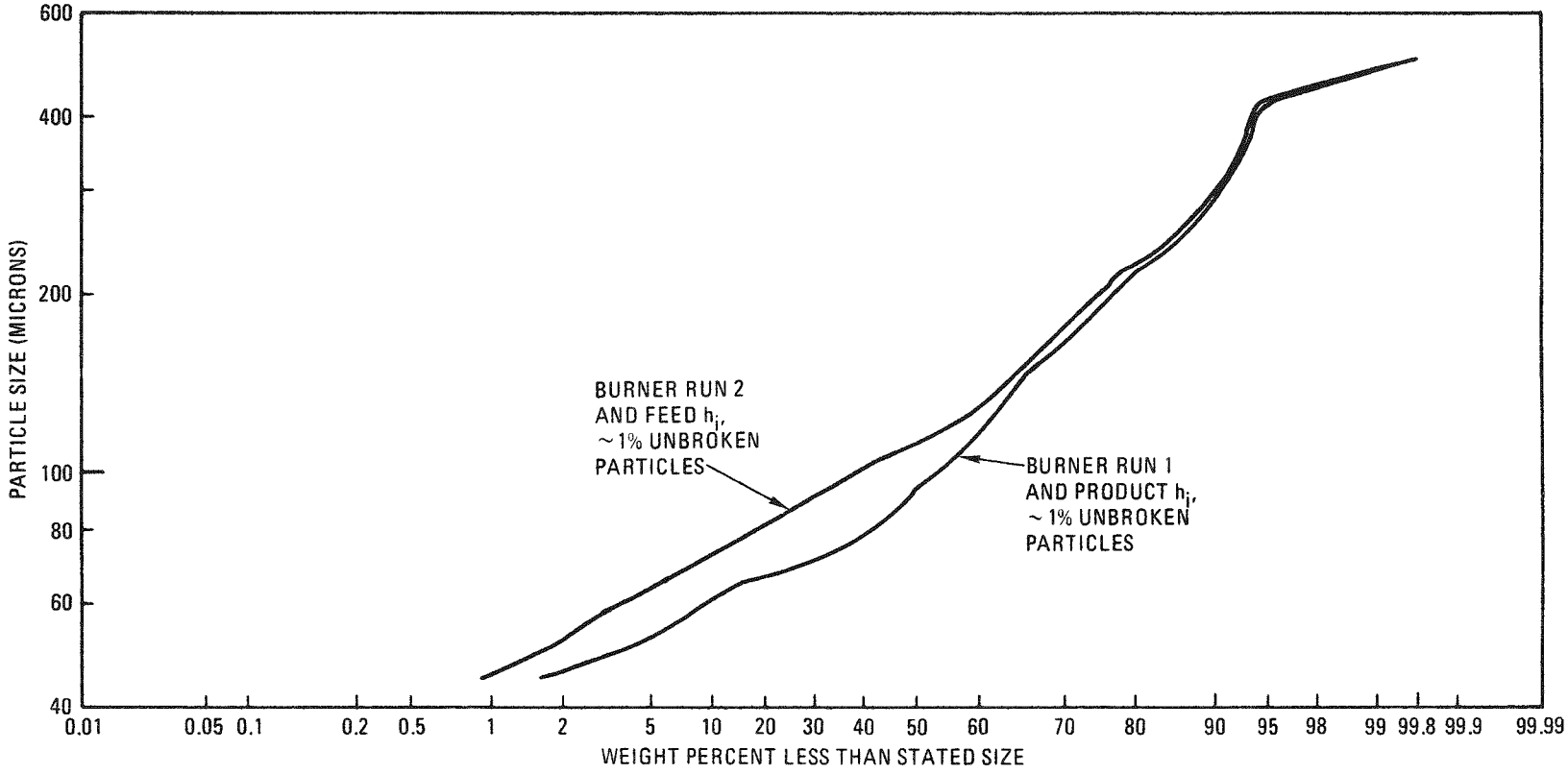

Fig. 4-6. Product size distribution, 20-cm secondary burner Runs 1 and 2

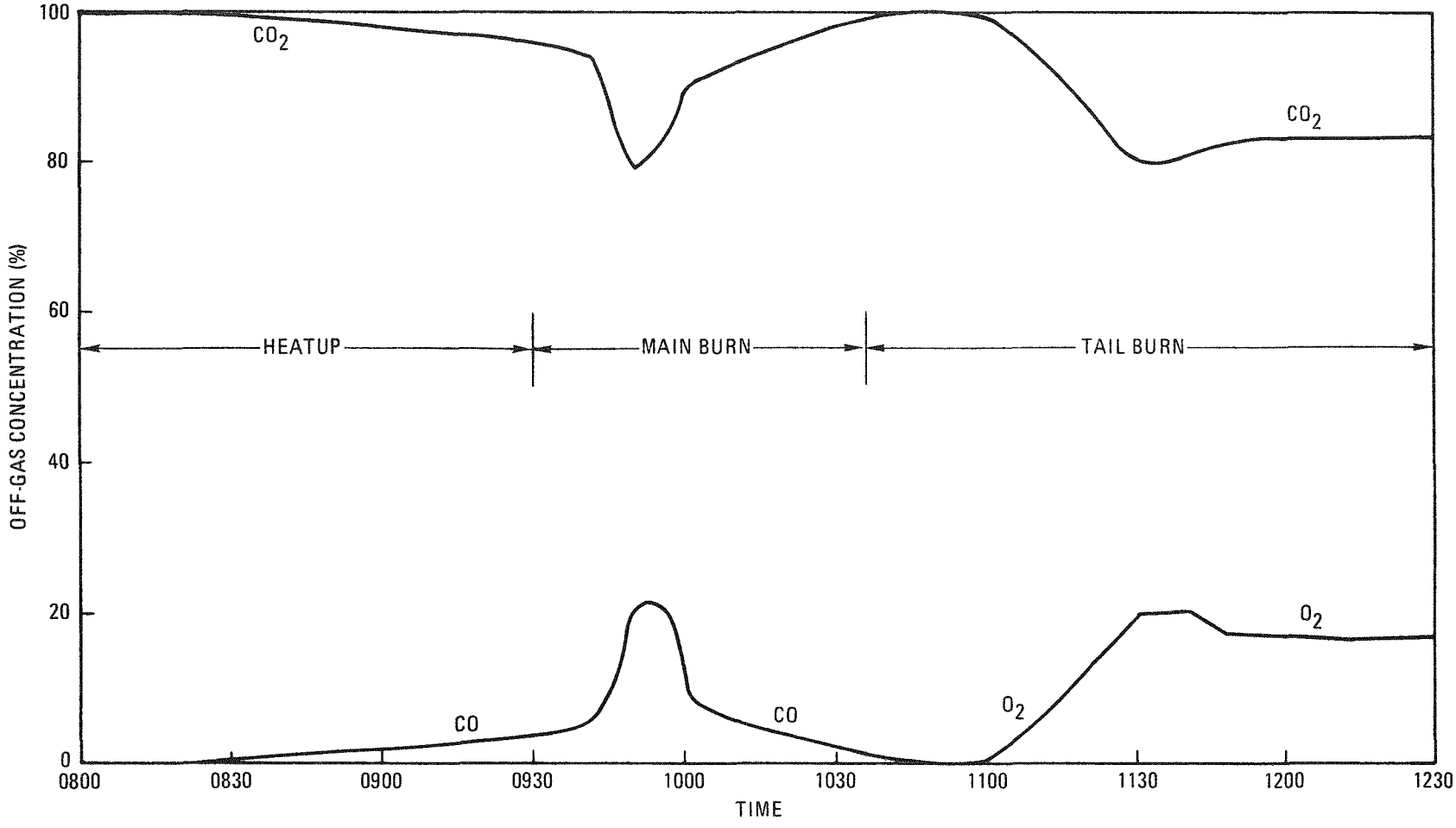

Fig. 4-7. Off-gas composition versus time, 20-cm secondary burner Run 2

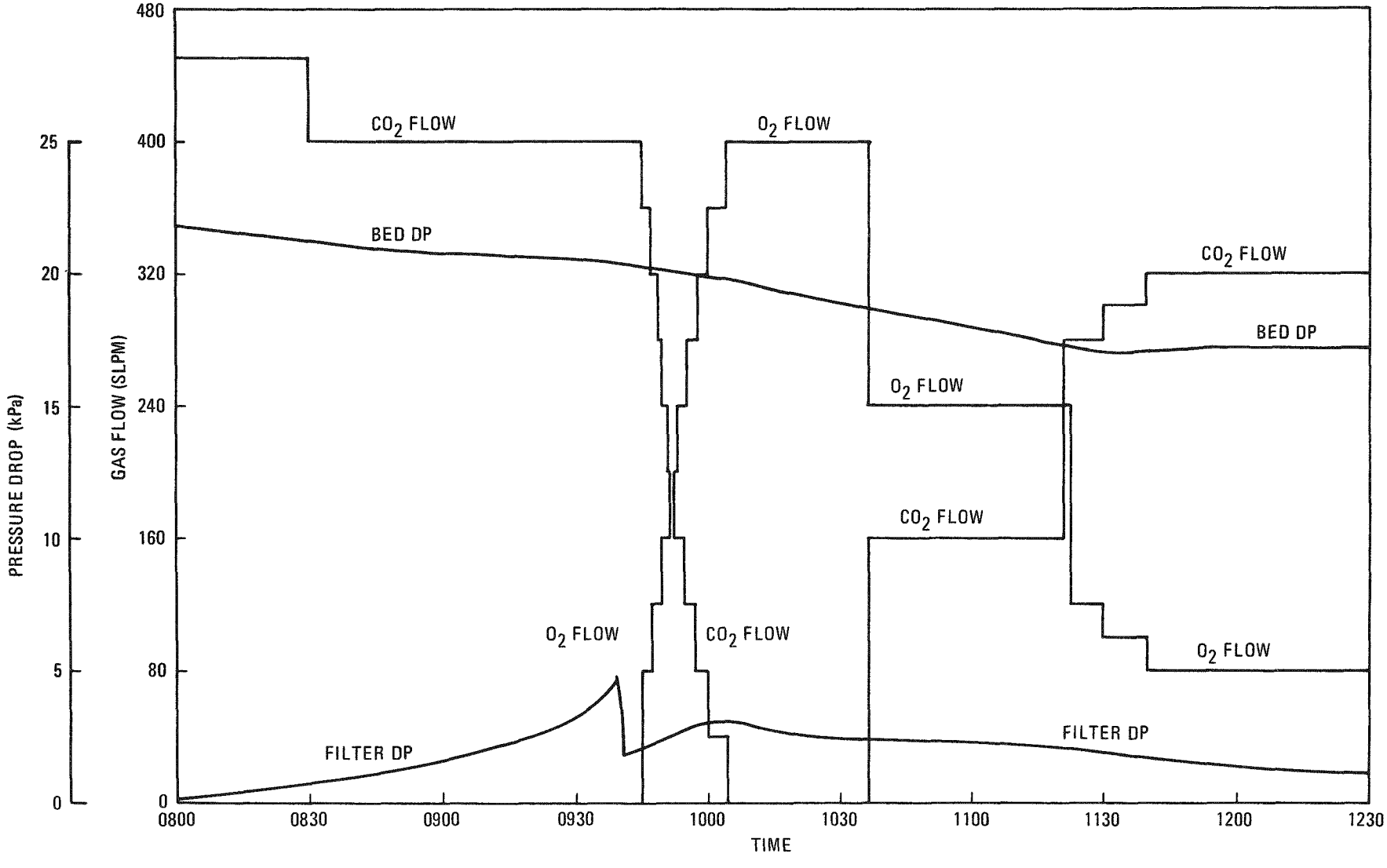

Fig. 4-8. Gas flow and pressure drop versus time, 20-cm secondary burner Run 2

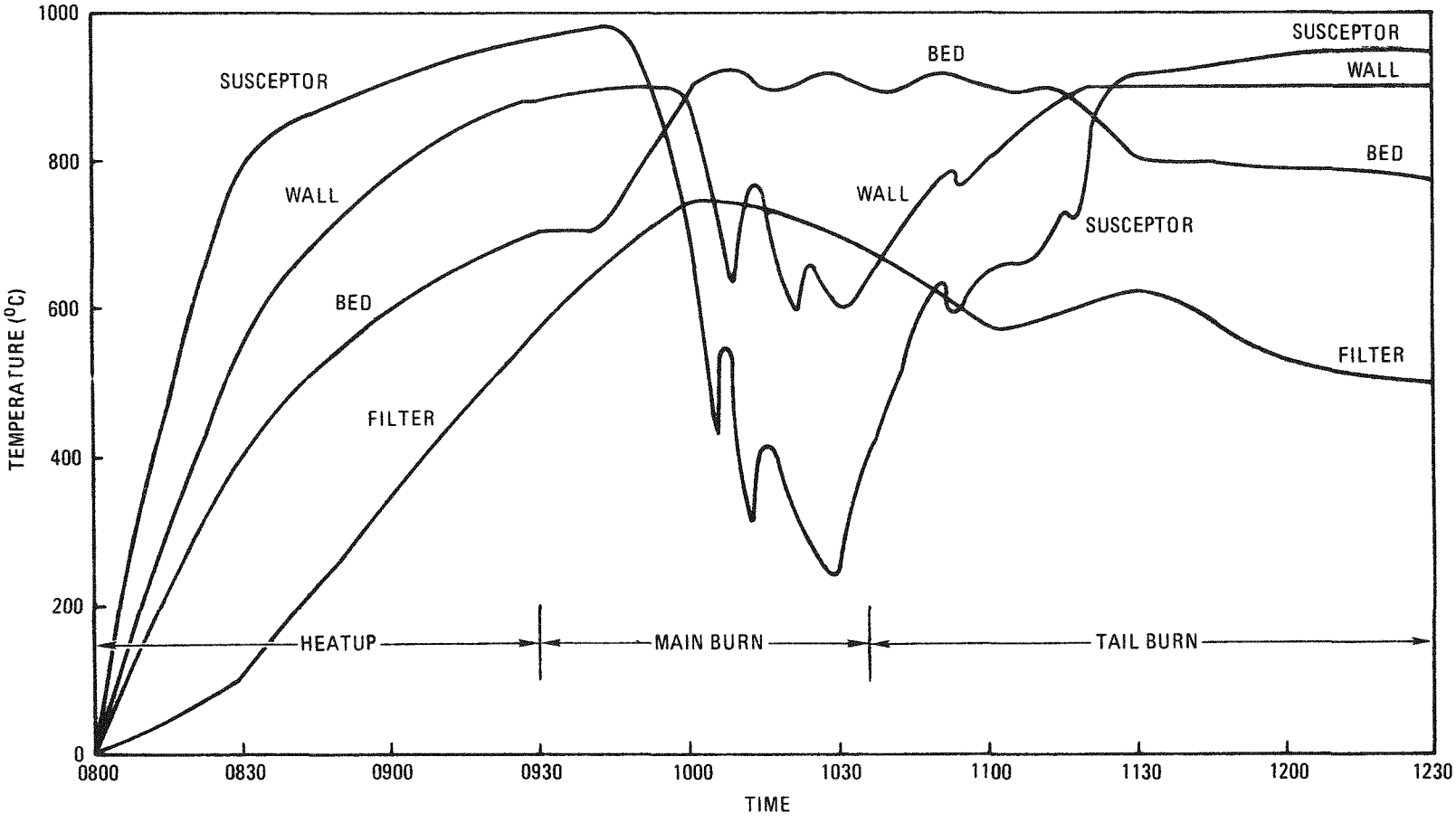

Fig. 4-9. Temperature versus time, 20-cm secondary burner Run 2

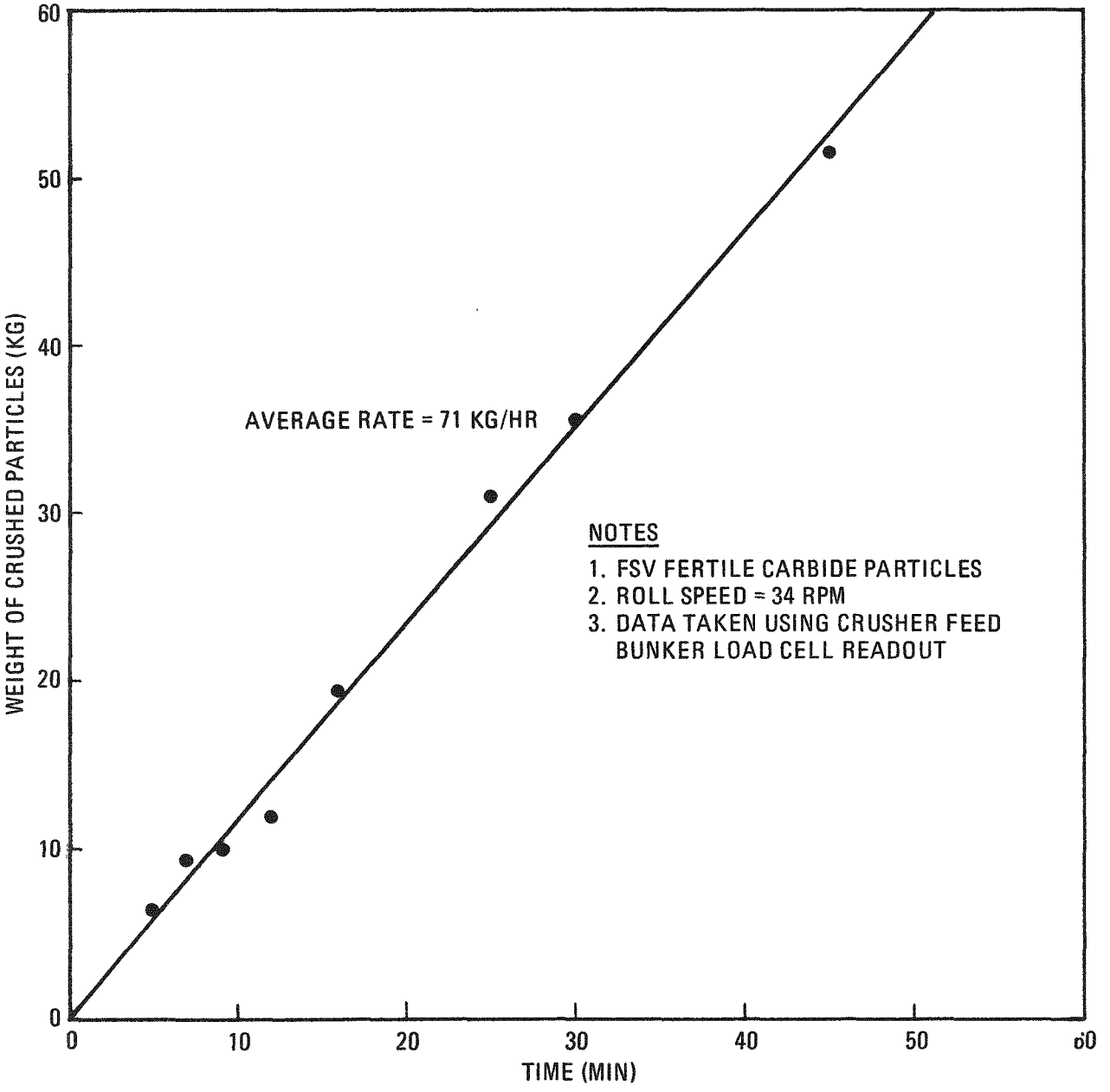

Fig. 4-10. Particle crusher throughput, 20-cm secondary burner Run 2

Clamp-to-hub temperature differentials were under the 170°C limit throughout the heatup period. The automatic induction heater control system continued to work very well.

The fluid bed was then used for a series of heat transfer coefficient measurements using CO_2 gas. During these measurements, an estimated 2.5 kg of carbon were displaced from the burner via a $CO_2 + C \rightarrow 2CO$ reaction. There were initially 15.9 kg of burnable carbon in the feed.

Ignition was again at 700°C, with a stepped ramp of oxygen taking 20 min to reach 100% inlet oxygen. A flow totaling channel kept the total oxygen flow at 400 SLPM throughout the run. The operator adjusted only the desired oxygen flow; the totalizer then adjusted the CO_2 flow rate. Induction power and cooling air were both on automatic control. The lower cooling air controller was not tuned well enough, resulting in an oscillation in bed temperature of ±25°C within a period of about 10 min. Further tuning should decrease this cycling.

Filter blowback was set at the same interval as in the first test. Using 340-kPa (50-psi) blowback, the maximum filter pressure drop was 3 kPa (12 in. H_2O). The burner alignment mechanism (Peaucellier cells) worked well without binding, allowing the burner to grow down in a vertical direction only.

Inlet oxygen was reduced to 60% when off-gas CO decreased to zero. Off-gas oxygen appeared 25 min later and was controlled to <20% by reduction of inlet oxygen. Bed temperature was kept at 780°C by the induction heater. Burning was terminated 2 hr after finishing the pure oxygen burn period. No material holdup was observed in the filter chamber.

The bed was cooled to 100°C, followed by pneumatic product transport. Insufficient transport gas was again responsible for choking flow in vertical sections leading to line plugging.

4.2.2.2. Analysis

As shown in Table 4-2, the burner had material both above and below the distributor plate after product removal. Product size distribution is shown in Figs. 4-6 and 4-11.

One weight percent unbroken particles was again found in the product. The roll gap was checked using a strip of solder dropped through the rotating crusher rolls. It indicated no change in gap since it had last been checked before Run 1. Disassembly of the crusher has revealed wear on the side plates adjacent to the crushing section of the rolls. This wear and roll surface dimensional variations are currently being investigated to determine the cause of the uncrushed particles in both burner run products.

4.2.3. Conclusions

Activity Plan AP524701 details ten acceptance criteria for Phase I operation. These are discussed below:

1. No feed or product line blockage - The product line was blocked in both runs due to insufficient blower capacity. See Section 7 for discussion.
2. Feed time less than 15 min. - It was 4 min.
3. Product removal time less than 30 min. - See criterion 1.
4. Bed heatup to 700°C in 1 hr, able to idle at 800°C - It takes 1 hr 5 min to heat to 700°C; can idle at 780°C.
5. Cooling system keeps bed at 900° ± 25°C - Yes.
6. Control system functions properly - Yes.
7. Distributor plate functions properly - No; new design required; see Section 4.2.5.
8. Filter pressure drop <12.5 kPa (<50 in. H_2O) - Yes.

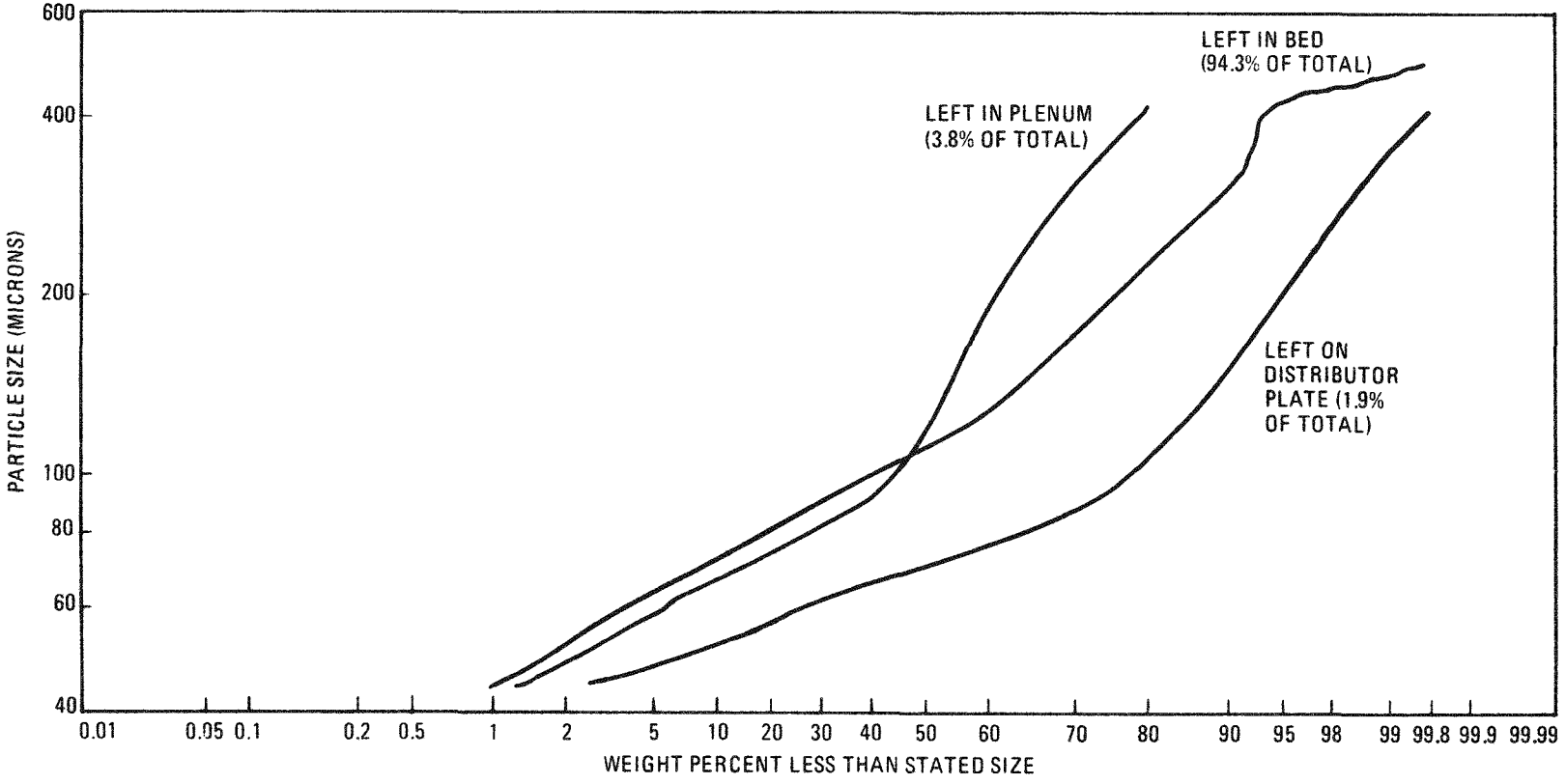

Fig. 4-11. Product size distribution, 20-cm secondary burner Run 2

9. No appreciable vessel leaks or cracks - Checked out acceptably.

10. No shroud frame deformation - Acceptable.

Criteria 1, 3, and 7 were not met but corrective action was initiated. Criterion 4 was determined to be acceptable, and criteria 2, 5, 6, 8, 9, and 10 were met.

Several problem areas were found in Phase I, including the distributor plate, the use of undersized product transport blowers, and the roll crusher side plate wear. These deficiencies are all being corrected and will be retested during Phase II. The distributor plate redesign is discussed in Section 4.2.5. Modifications to the roll crusher are discussed in Section 4.4.

Sufficient data were obtained concerning automatic control to allow run sequence automation to proceed. Off-gas filter performance has been good, with low pressure drop at the present blowback rate. Phase II includes variations in this filter blowback rate in an attempt to minimize both filter pressure drop and blowback gas requirements.

4.2.4. 20-cm Secondary Burner Heat Transfer Coefficients

Heat transfer coefficients were measured using both crushed feed and burned product from the 20-cm secondary burner during Runs 1 and 2. The tests simulated the use of several burner wall temperature limitations since heatup and tail-burn of the secondary burner are limited by wall temperature. Fluidizing gas flow was varied only at the 900°C wall temperature.

The purpose of the tests was to yield basic characteristics of the fluid bed in the range of normal operation. This provides input to future burner design efforts and improves knowledge of the present design.

4.2.4.1. Experimental Procedure

Feed heat transfer coefficients were measured using Run 2 feed, while product measurements were obtained using Run 1 product. Bed material characteristics are shown in Table 4-1 and Figs. 4-1 and 4-6. The automatically controlled induction heater was actuated, causing the system to heat up to yield a steady-state temperature profile. When the temperature stopped changing, data on induction power input, heat losses, and temperature distributions were logged (see Table 4-3). The heater and/or gas flow setting was then varied to yield another data point.

4.2.4.2. Calculation Procedure

The overall heat transfer coefficient across the burner wall and fluid bed interface is determined as follows:

$$U = \frac{Q}{A\ \overline{\Delta T}} \quad ,$$

where Q/A is the heat flux through the wall and $\overline{\Delta T}$ is the average difference between the outside wall temperature and the bed temperature.

The inside heat transfer coefficient, h_i, is calculated as follows:

$$U = \frac{1}{\frac{1}{h_i} + \frac{t}{K}}$$

or

$$h_i = \frac{K}{\frac{K}{U} - T} \quad ,$$

where t = wall thickness = 0.64 cm,

k = wall conductivity,

TABLE 4-3
HEAT TRANSFER DATA AND RESULTS
CRUSHED FSV FERTILE PARTICLE HEAT TRANSFER COEFFICIENT MEASUREMENTS

	CO_2 Flow (SLPM)	Max. Wall Temp. (°C)	Induction Power (kW)	Coil Water Flow (LPM)	Coil ΔT (°F)	Capacitor Water Flow (LPM)	Capacitor ΔT (°F)	Average Wall-to-Bed ΔT (°C)	Heat Flow Area (cm^2)	Net Heat Flow (kW)	U $\left(\frac{cal}{sec\text{-}cm^2\text{-}^oC}\right)$	h_i $\left(\frac{cal}{sec\text{-}cm^2\text{-}^oC}\right)$	U $\left(\frac{cm}{sec}\right)$	Bed. Temp. (°C)	U $\left(\frac{Btu}{hr\text{-}ft^2\text{-}^oF}\right)$	h_i $\left(\frac{Btu}{hr\text{-}ft^2\text{-}^oF}\right)$
Feed																
1	400	900	68	45	10	7.5	8	85	4780	48	0.0284	0.0394	70	760	210	291
2	360	900	65	45	10	7.5	8	82	4620	45	0.0285	0.0395	63	765	211	292
3	320	900	63	45	10	7.5	8	79	4620	42	0.0276	0.0379	57	770	204	280
4	280	900	59	45	10	7.5	8	76	4455	38	0.0270	0.0368	50	775	199	271
Product																
5	400	900	68	45	10	7.5	8	78	5115	47	0.0279	0.0385	71	775	206	284
6	440	900	75	45	10	7.5	8	85	5280	54	0.0288	0.0400	78	770	213	295
7	360	900	58	45	9	7.5	8	69	4950	38	0.0267	0.0362	65	790	197	267
8	360	850	53	45	8	7.5	6	63	5115	37	0.0276	0.0379	62	745	204	280
9	360	800	50	45	8	7.5	5	66	5115	34	0.0242	0.0326	59	700	179	241
10	360	750	45	45	8	7.5	5	71	5115	29	0.0192	0.0245	57	655	142	181

k = 0.065 cal/cm-sec-°C at 900°C,
= 0.060 cal/cm-sec-°C at 800°C,
= 0.055 cal/cm-sec-°C at 700°C.

The total heat input, Q, is defined as:

Q = induction power - coil water heatup - capacitor water heatup - electrical line losses - heat conducted out of both ends of susceptor - heat conducted out of both ends of burner wall.

Induction power is measured using a kilowatt meter at the motor generator. Water flows and temperatures are part of the recorded data. Axial heat conduction from the susceptor and wall is calculated using plots of temperatures, shown typically in Fig. 4-12. The total heat conduction was ∿0.5 kW. Electrical line losses were ∿0.3 kW.

Both the area of heat transfer, A, and the average temperature difference between the bed and wall, ΔT, must be taken from temperature profiles, shown typically in Fig. 4-12. The heat transfer area and points are defined as those points where the bed and wall temperatures cross. Heat is flowing into the bed in the region where the wall temperature is above the bed temperature. The average temperature difference is obtained by step-wise integrated averaging of the temperature difference. The number of data points and the interpolated temperature profiles have a significant effect on the calculated value for ΔT.

Calculation of U and h_i is then possible from knowledge of Q, A, ΔT, k, and t. Experimental data and results are given in Table 4-3 and are plotted in Figs. 4-13 and 4-14. A typical set of calculations is shown in Table 4-4.

In the range investigated, an increase in the heat transfer coefficient occurs as a result of higher velocity or higher bed temperature, with the latter having a much stronger effect. It should be noted

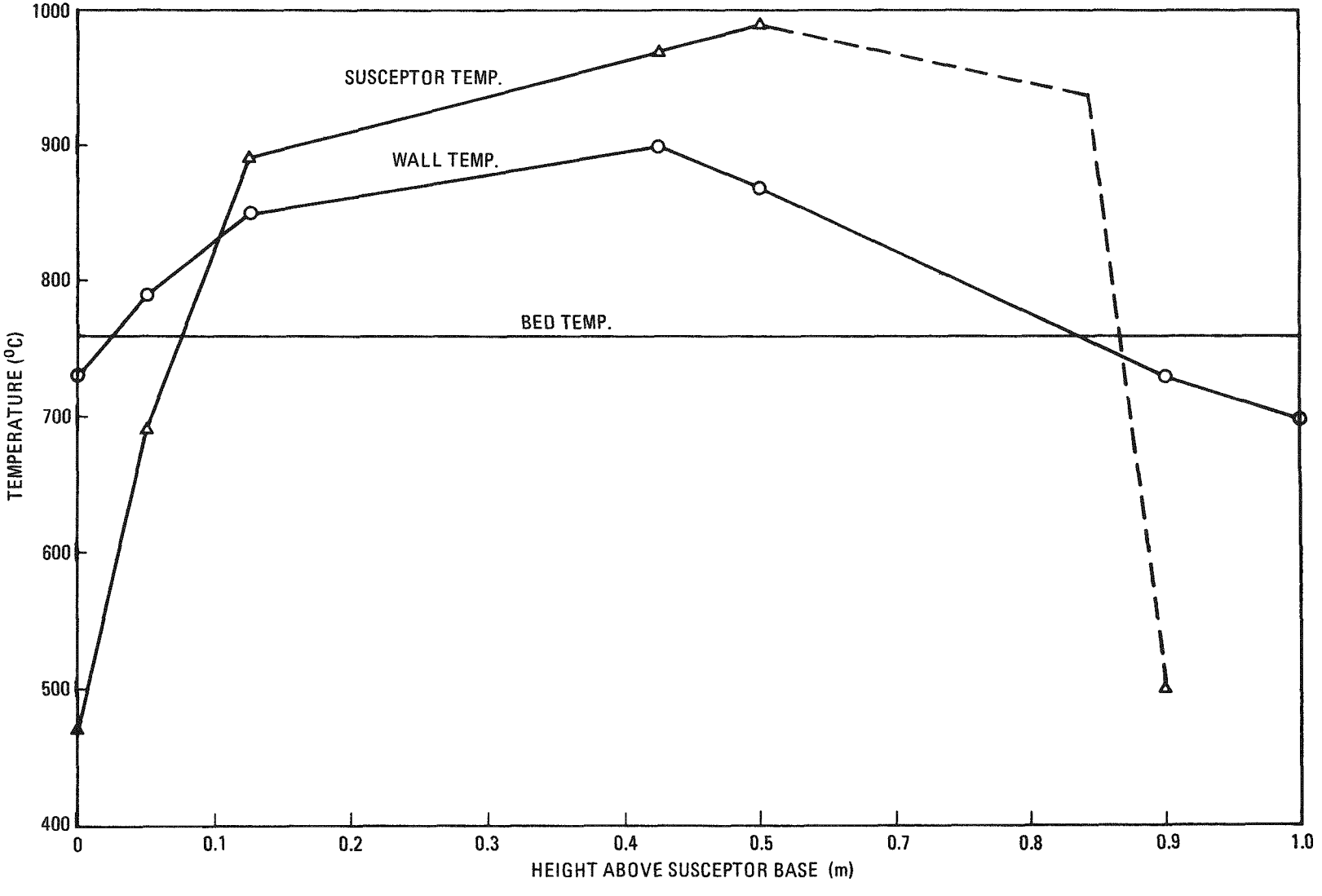

Fig. 4-12. Feed heatup No. 1 temperature profile

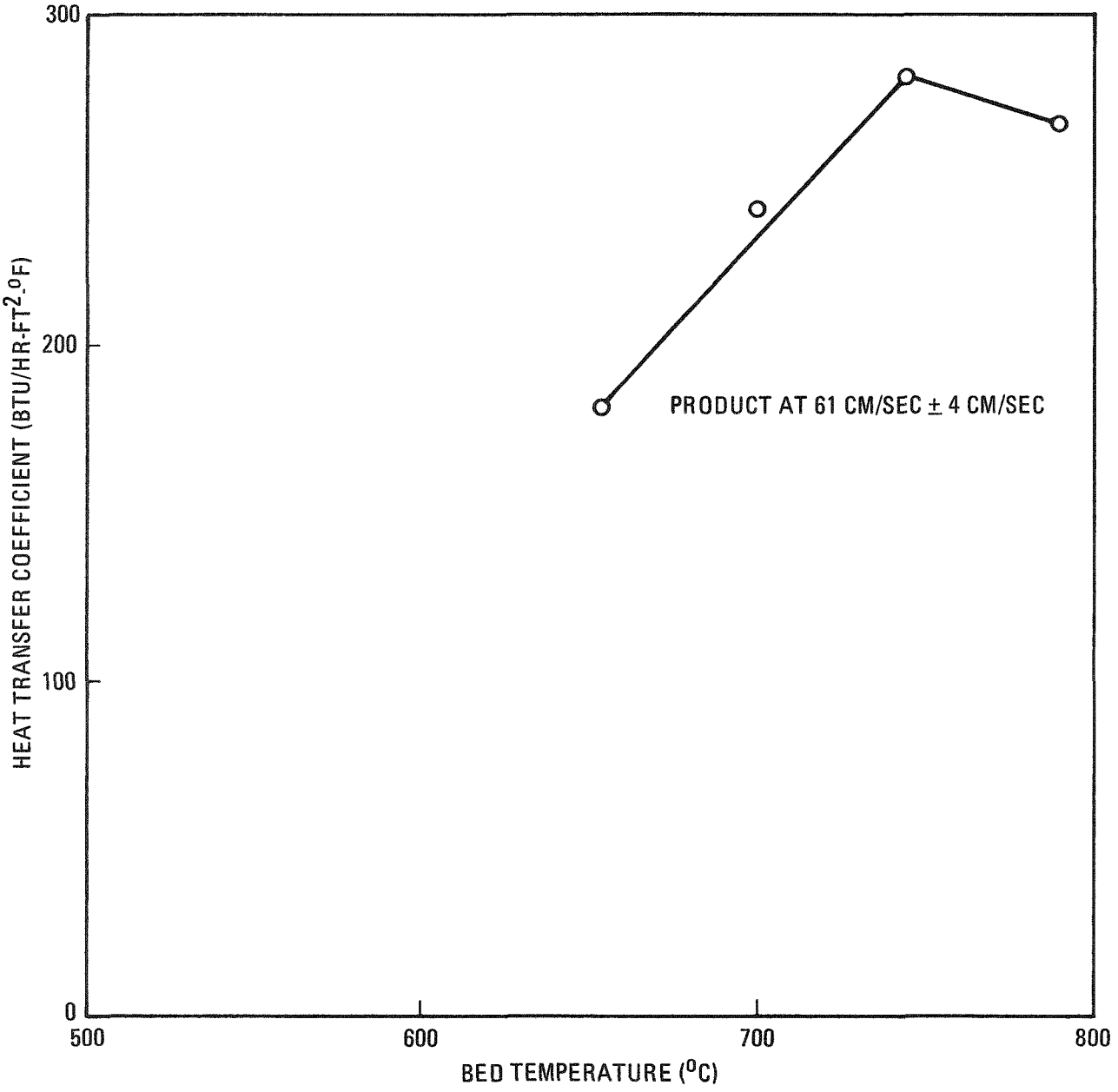

Fig. 4-13. Effect of temperature on heat transfer coefficient

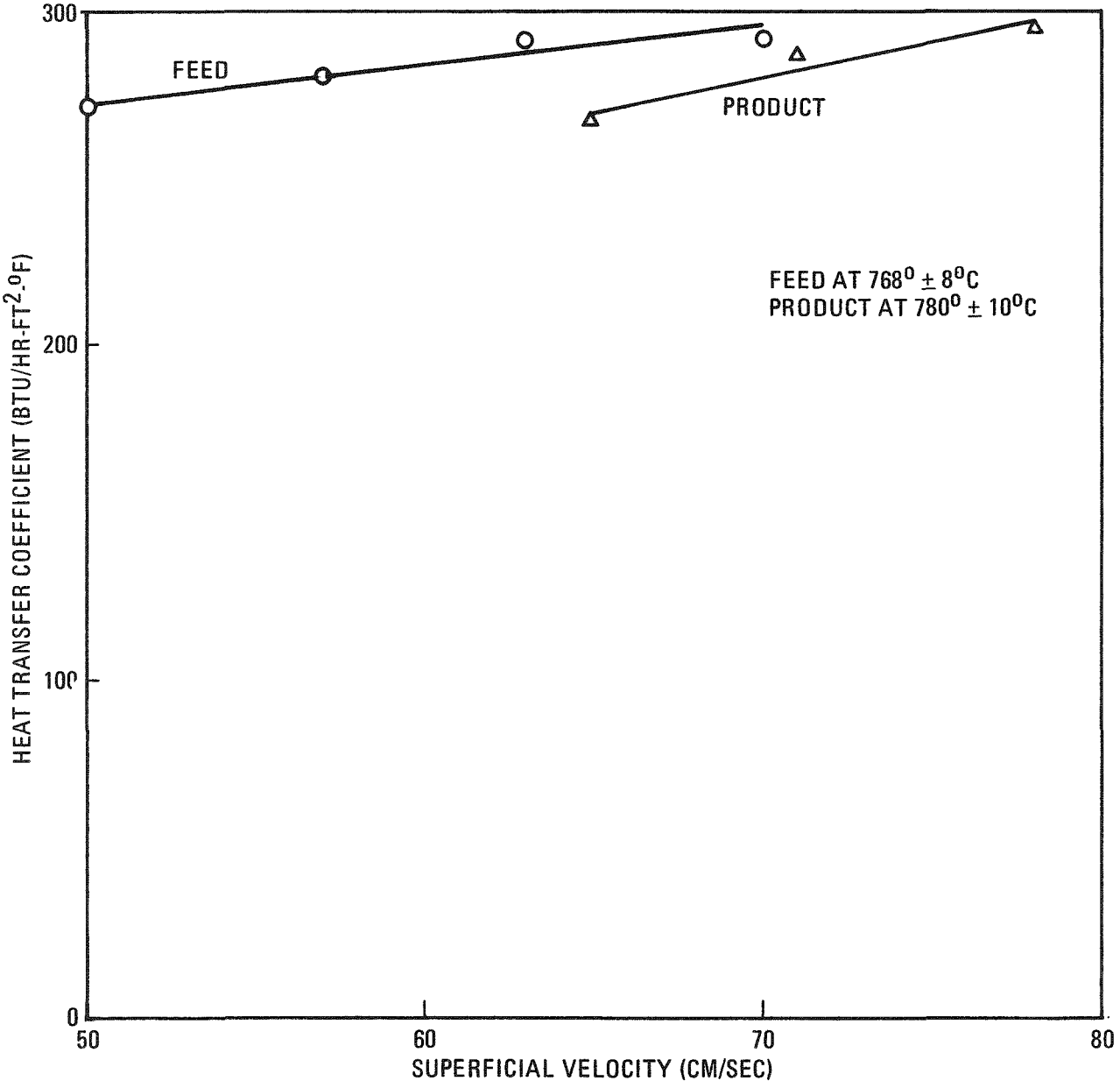

Fig. 4-14. Effect of velocity on heat transfer coefficient

TABLE 4-4
FEED HEAT TRANSFER COEFFICIENT
(see Fig. 4-3 for temperature profile)

Wall temp.	= 900°C max.
Bed temp.	= 760°C
Gas flow	= 400 SLPM CO_2 (70 cm/sec)
Induction power	= 68 kW
Cooling water losses	= 20 kW
Net heat flow	= 48 kW (11,500 cal/sec)
Heat flow area	= 4780 cm^2 (29-in. height)
Mean wall-bed ΔT	= 87°C
Max. wall-bed ΔT	= 140°C

$$U = \frac{Q}{A\ \Delta\overline{T}} = \frac{11,500}{(4780)87} = 0.0277\ \frac{cal}{cm^2\text{-sec-}^oC}\ \left(204\ \frac{Btu}{hr\text{-}ft^2\text{-}^oF}\right)$$

$$h_i = \frac{k}{\frac{k}{u} - t} = \frac{0.065}{\frac{0.065}{0.0277} - 0.64} = 0.0381\ \frac{cal}{cm^2\text{-sec}^oC}\ \left(281\ \frac{Btu}{hr\text{-}ft^2\text{-}^oF}\right)$$

or, using max. ΔT rather than mean ΔT
and using total susceptor area:

Total susceptor area = 5280 cm^2 (81-cm height)
Max. ΔT = 140°C

$$U = \frac{11,500}{5280(140)} = 0.0156\ \frac{cal}{cm^2\text{-sec-}^oC}\ \left(115\ \frac{Btu}{hr\text{-}ft^2\text{-}^oF}\right)$$

$$h_i = \frac{0.065}{\frac{0.005}{0.0156} - 0.64} = 0.0184\ \frac{cal}{cm^2\text{-sec-}^oC}\ \left(136\ \frac{Btu}{hr\text{-}ft^2\text{-}^oF}\right)$$

that increases in velocity and bed temperature give rise to higher heat losses from the bed, so that the actual heating rate (and equilibrium temperature) may be lower with increased velocity (even though the heat transfer coefficient is higher).

4.2.5. 20-cm Secondary Burner Distributor Plate Redesign

Several problems have been encountered relating to the distributor plate in Runs 1 and 2 of 20-cm secondary burner Activity Plan 524701. These led to redesign of the plate based on analysis of the evidence gathered in these two burner runs and experience previously gained during 10-cm secondary burner development work conducted from 1973 to 1975.

4.2.5.1. 20-cm Secondary Burner Operating Experience

The original distributor plate design is shown in Fig. 4-15. It has 121 holes 1370 to 1500 μm (0.054 to 0.059 in.) in diameter on a combination triangular and radial hole layout. Figure 4-16 shows the calculated and observed room temperature pressure drop across the plate as a function of CO_2 gas flow.

Operation of this plate during heatup tests using 820-μm-diameter BISO-coated ThO_2 fuel particles was satisfactory. Only a very small weight of material (<20 g) was found in the inlet gas plenum (beneath the distributor plate). This is believed to have resulted from the large hole size relative to the size of the particles.

Fluidization characteristics were acceptable during these BISO particle heatups, with maximum axial bed temperature differences of ±10°C. Product removal was successful using the product removal valve coupled with the penumatic transport system. The distributor plate sweep tube was used for final cleanout. No material was found above the plate when the burner was dismantled for inspection.

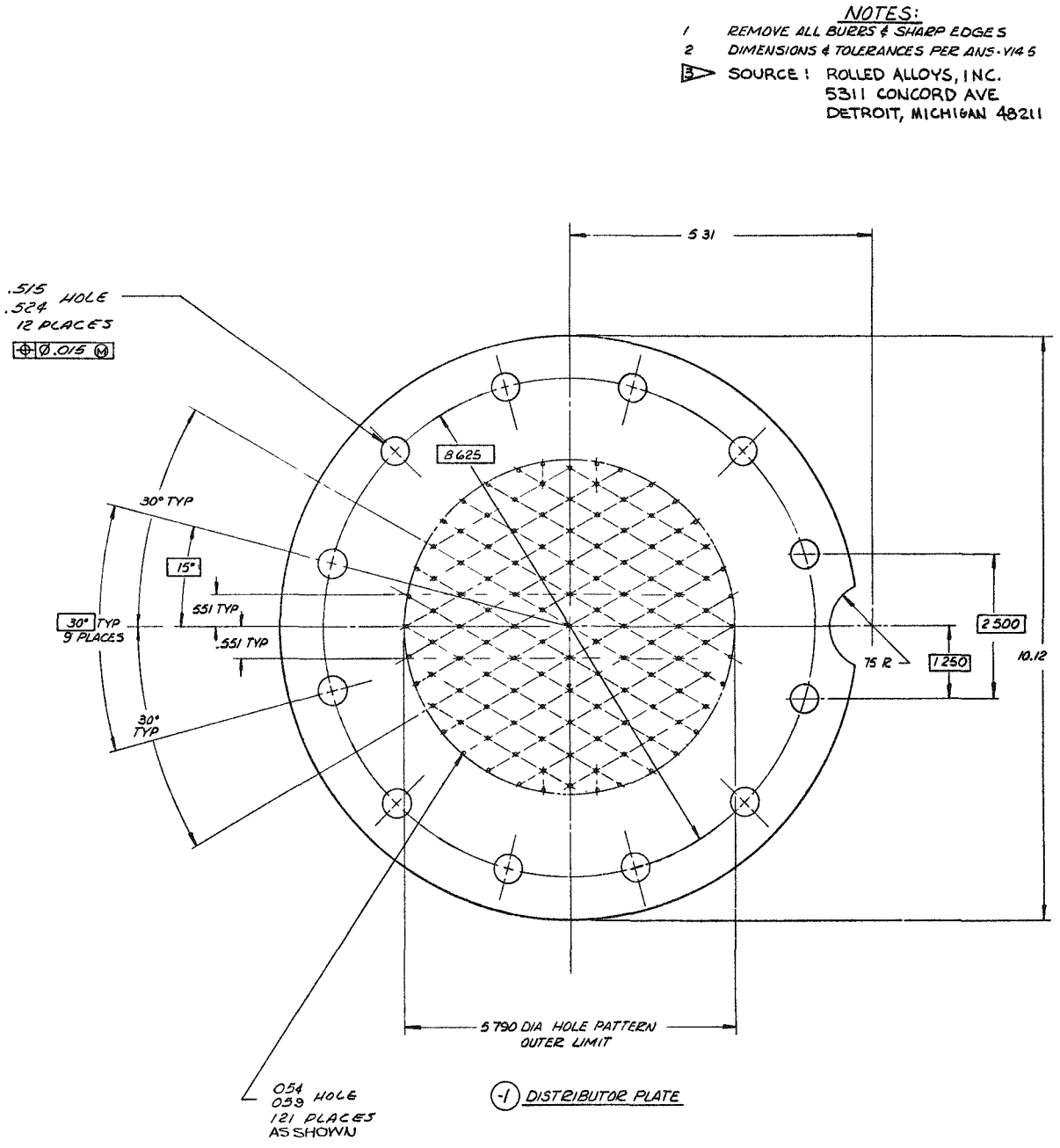

Fig. 4-15. Original distributor plate for 20-cm secondary burner (all dimensions in inches)

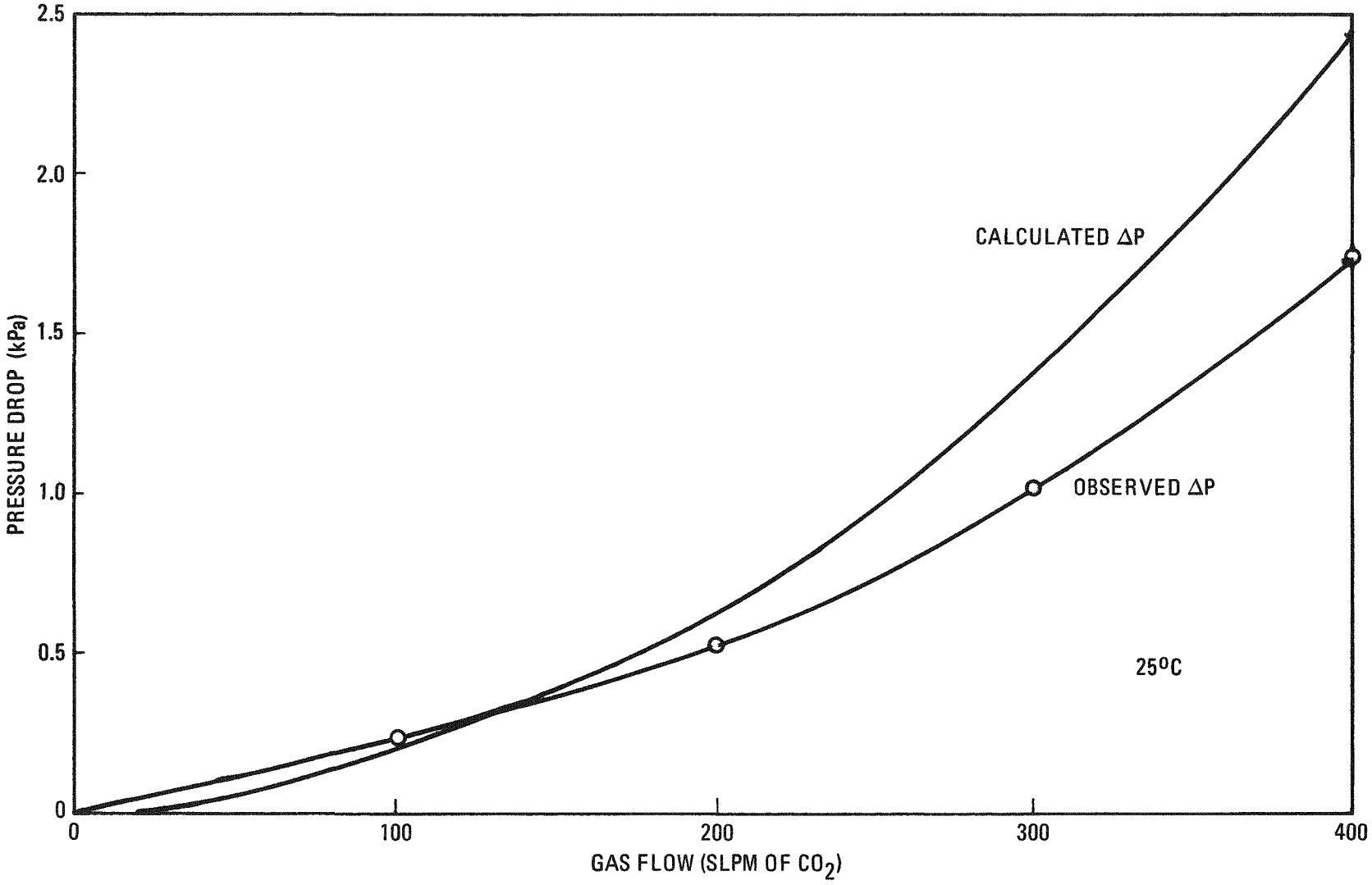

Fig. 4-16. Pressure drop across original distributor plate

Phase I of the Activity Plan was completed using 60-kg batches of crushed TRISO fertile FSV type fuel particles having an initial size distribution as shown in Fig. 4-1.

Operation of the burner throughout Run 1 was smooth and trouble-free. This was followed by a series of product heat transfer tests using the product ash. Product removal was hampered by low transport gas flow rates, so that discontinuous dumping was required. The material was required to remain in the burner without an upflow gas purge through the distributor plate owing to emptying of the CO_2 supply tank over a weekend.

Final product removal was then carried out, followed by lower burner disassembly for inspection. It was determined that the gas coming through the distributor plate holes had "jetted" through the shallow bed, thus ending any fluidization of the bed. This material amounted to 720 g. Inspection of the lower plenum revealed that 1520 g of material had drained in past the distributor plate.

Run 2 yielded similar results with jetting holes evident. A total of 930 g were left on the plate, while 1758 g drained into the plenum. (There was no time when flow did not go up through the plate in this run.)

4.2.5.2. Pertinent Experience on 10-cm Secondary Burner

As reported in Refs. 4-1 and 4-2, a gas distributor having 21 holes 1.7 mm (0.067 in.) in diameter was tried during two runs on the 10-cm secondary burner. Gas jetting was noted following product removal but there was no pneumatic transporter at that time, only a vented can to allow gravity bed drainage out of the product removal valve.

Another distributor having 71 holes 0.64 mm (0.025 in.) in diameter (see Fig. 4-17) was then designed and tested. Reduced individual jet strength led to decreased heel weights when dumping into the vented can. Figure 4-18 shows the room temperature calculated and observed distributor plate pressure drop as a function of gas flow rate.

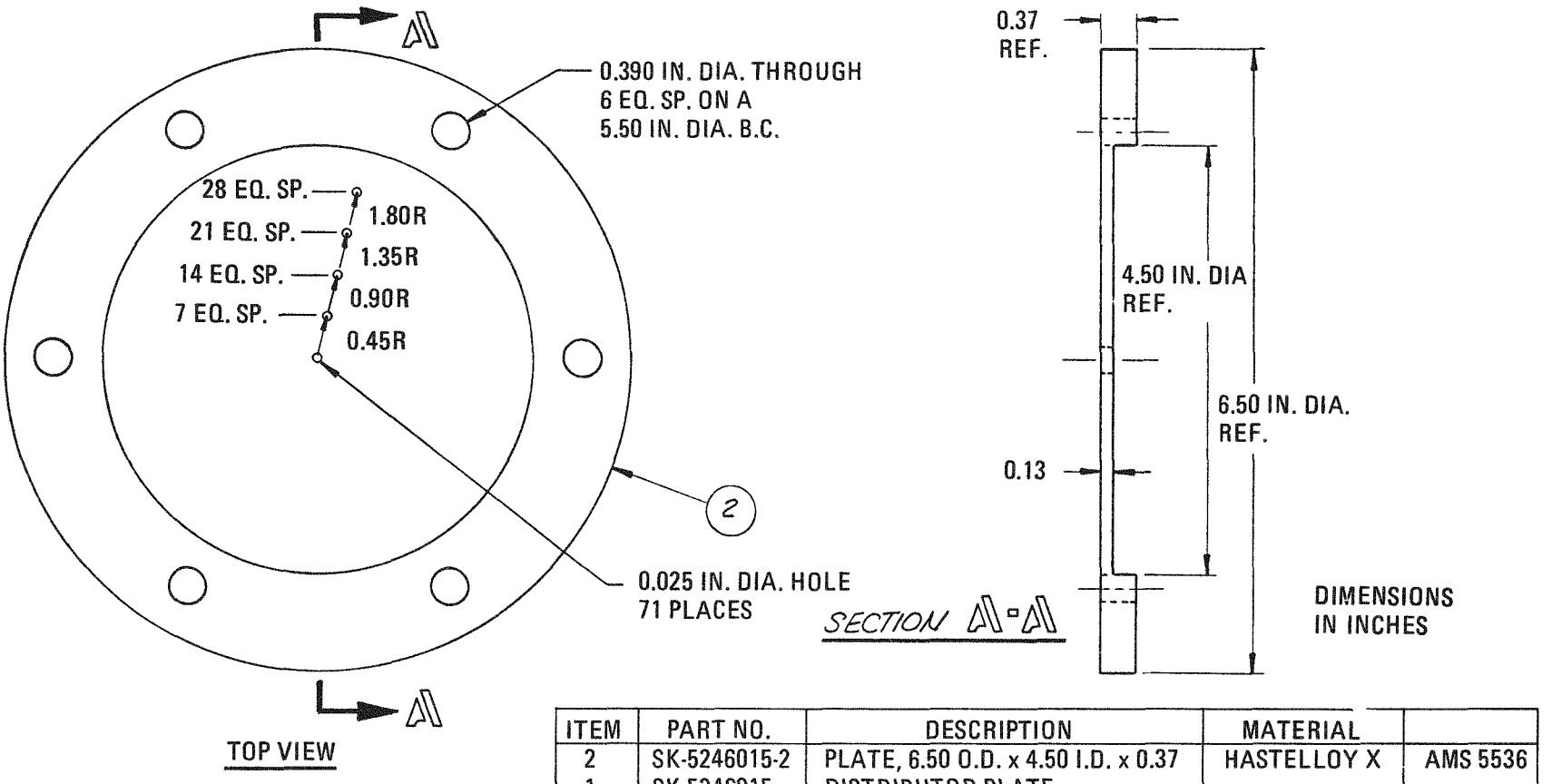

ITEM	PART NO.	DESCRIPTION	MATERIAL	
2	SK-5246015-2	PLATE, 6.50 O.D. x 4.50 I.D. x 0.37	HASTELLOY X	AMS 5536
1	SK-5246015	DISTRIBUTOR PLATE		

Fig. 4-17. 10-cm secondary burner distributor plate

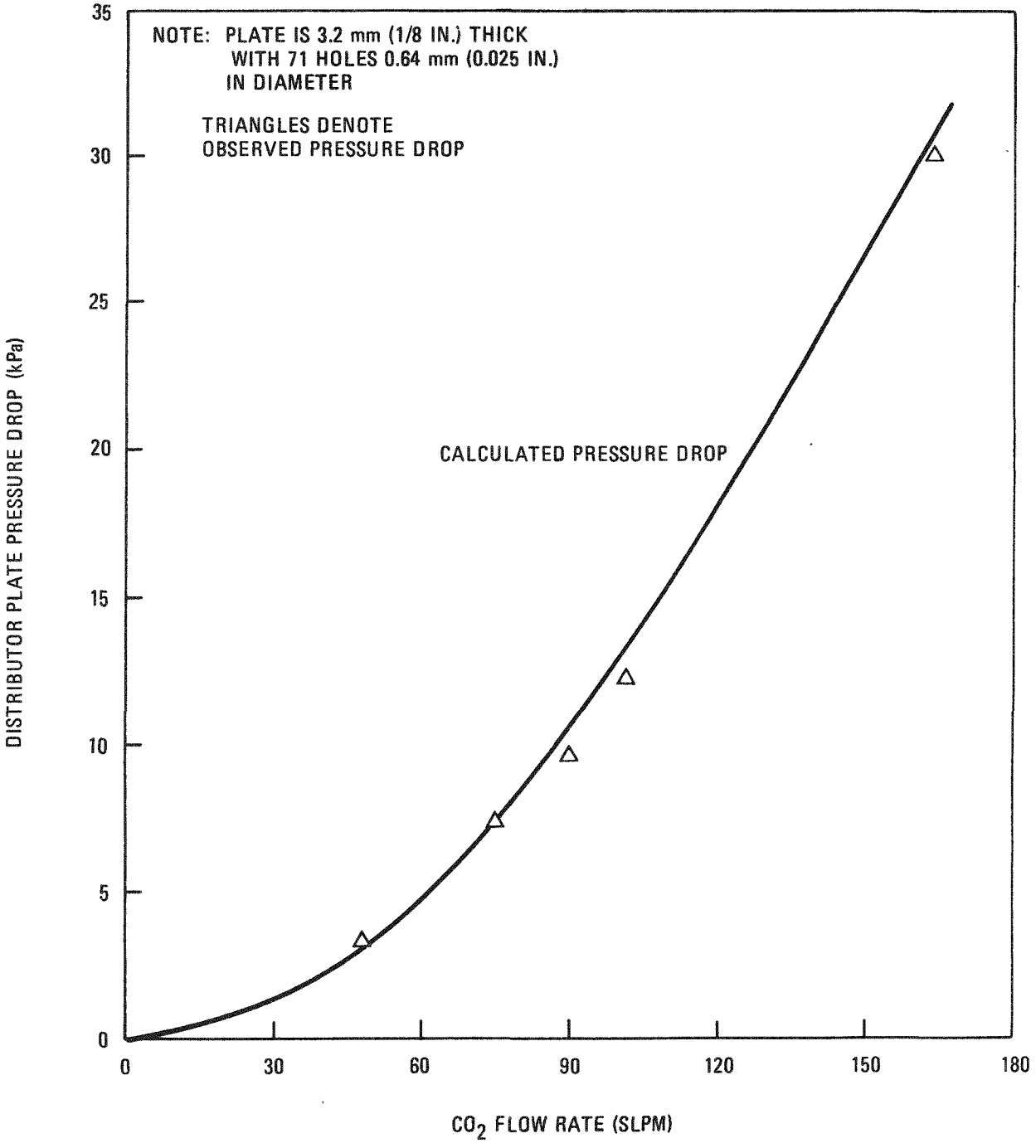

Fig. 4-18. Flow-pressure drop characteristics of 10-cm secondary burner distributor plate

A pneumatic transport system was added later. This system, coupled with a distributor plate sweep tube (a series of gas jets aimed downward at the distributor plate), resulted in complete burner cleanout. A total of eight burner runs have been made since then, with burner cleanout resulting in each run. With the 0.64-mm (0.025-in.) hole diameter, the material which drained back through the plate never amounted to more than a few grams.

4.2.5.3. Analysis and Redesign of 20-cm Secondary Burner Distributor Plate

Experiences with both burners indicate that gas jetting must be minimized. The BISO particle bed was not subject to jetting owing to the size and weight of these spheres; they rolled down over the jetted hole and eliminated the jet. These particles are too heavy to be blown aside by the jet. Secondary burner feed and ash have a steep angle of repose (29° to 36°) that allows them to be lanced by the gas jet and not flow back. A reduction in hole size is necessary for this finer material, with an attendant increase in the number of holes.

Backflow of material into the plenum is another problem that is most likely caused by two factors:

1. The hole size is too large (relative to particle size), so material has a chance to drop through the plate if the gas velocity is too low.
2. The pressure drop across the plate is insufficient to keep the slugging action of the bed from pushing fine material back through at some short time when the slug falls back hard and back pressures the bed. Typical observed maximum pressure variation during a slug is ∿15 kPa (∿60 in. H_2O). The distributor pressure drop should be of this order to ensure against pressure surges pushing material through the plate.

Both of these factors may be dealt with in a judicious distributor design.

Figure 4-19 shows the relationship between hole size, number of holes, and pressure drop at room temperature. Pressure drop increases with temperature such that room temperature is the worst case (lowest plate pressure drop).

The pressure drop required to equal maximum bed pressure fluctuation is 15 kPa (60 in. H_2O). Hole size should be minimized to reduce jetting and solids backflow, but since experience has shown that 0.64 mm (0.025 in.) is effective, this size is chosen. From Fig. 4-19, it can be seen that ∿260 holes are required. A pure radial layout pattern will be used to simplify the machinist operation.

4.3. 10-CM SECONDARY BURNER

Refurbishing of this burner has been completed. Run 1 of Activity Plan 524601 will now be carried out as a shakedown test prior to fissile particle burning experiments.

4.4. FUEL PARTICLE CRUSHING

4.4.1. Introduction

The fuel particle crusher developed and built by General Atomic to break the silicon carbide (SiC) coating of the Fort St. Vrain (FSV) TRISO fertile fuel particles is shown in Fig. 4-20 mounted on top of the 20-cm secondary burner feed hopper. The 560-W (3/4-hp), variable-speed dc electric motor with a 40:1 reducer which powers the crusher through open drive gears is located behind the particle crusher.

This particle crusher has demonstrated the ability of a double-roll crusher to successfully process FSV fertile fuel particles. It is fully operational and has been used in the preparation of feed material for the secondary burner.

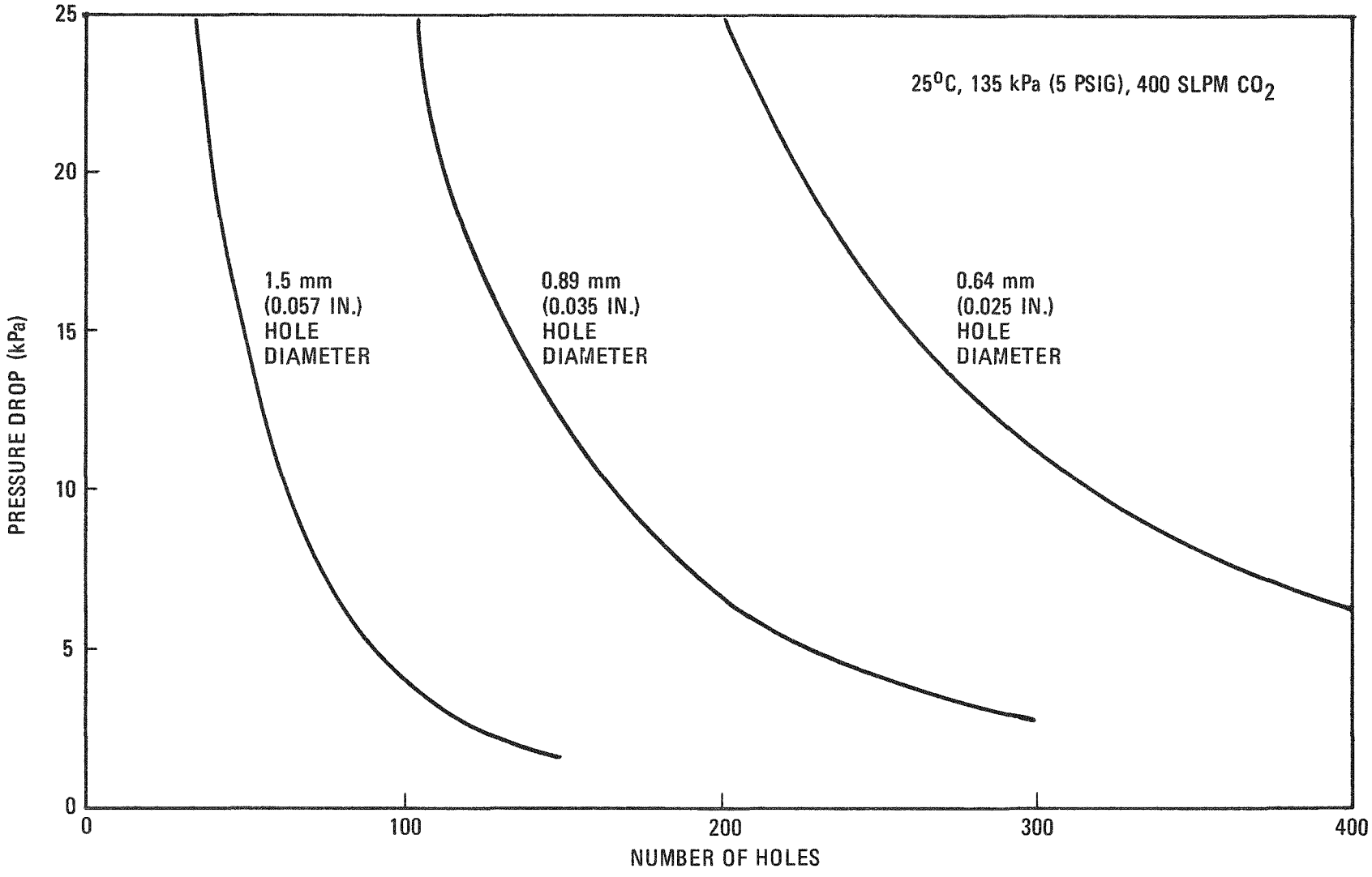

Fig. 4-19. Distributor pressure drop variations

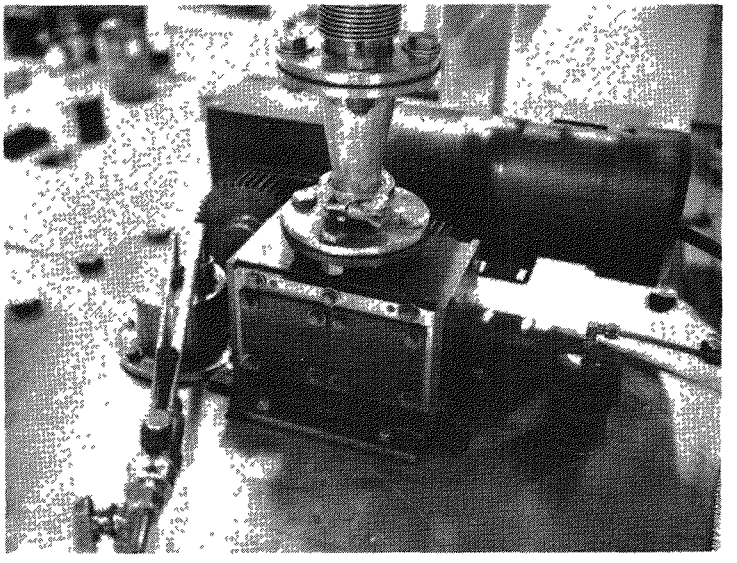

Fig. 4-20. Fuel particle crusher and drive motor (mounted on 20-cm secondary burner hopper)

A second double-roll crusher of similar design, but with different roll diameters, is being built for crushing FSV fissile fuel particles. The delivery of this unit, originally scheduled for October 30, 1976, has been delayed and is now expected in January 1977.

4.4.2. FSV Fertile Particle Crusher

At the completion of the Phase I Activity Plan testing of the fertile particle crusher (and after processing approximately 150 kg of FSV fertile fuel particles), it was found that the amount of unbroken fuel particles had risen from <1% to >2% by weight. The allowance for unbroken particles was established by Design Criteria DC520001 at <1% by weight for secondary burner feed.

The crusher was disassembled to determine the reason for this increase in unbroken fuel particles. No apparent evidence of wear on the roll crushing surfaces or on the roll ends was found, and there was no evidence of spalling, gouging, or galling on any wearing surface. However, each side body plate showed extensive erosive wear in the region opposite the crushing region at the ends of the roll pairs (see Fig. 4-21). The wear pattern was a groove approximately 0.3 mm (0.012 in.) deep by 0.6 mm (0.025 in.) wide by 7.9 mm (0.31 in.) long in each side plate. Two grooves of this size and a roll gap of 0.48 mm (0.019 in.) would be sufficient to pass uncrushed fuel particles 0.51 to 0.56 mm (0.020 to 0.022 in.) in diameter. This would account for ∿2% unbroken particles.

The wear grooves were filled with a ceramic coating material, chromium oxide, which was applied to the wear area by plasma spraying. This material has an equivalent hardness of R_c 74 compared with the side plate hardness of R_c 57 and the roll hardness of R_c 58. There was no local reduction in side plate hardness resulting from the plasma spray coating application.

The crushing surfaces of the hardened 1018 roll and the 4340 roll were very similar in appearance (see Fig. 4-22) after the adherent graphite and carbon coating had been removed with emery paper. Both roll surfaces did

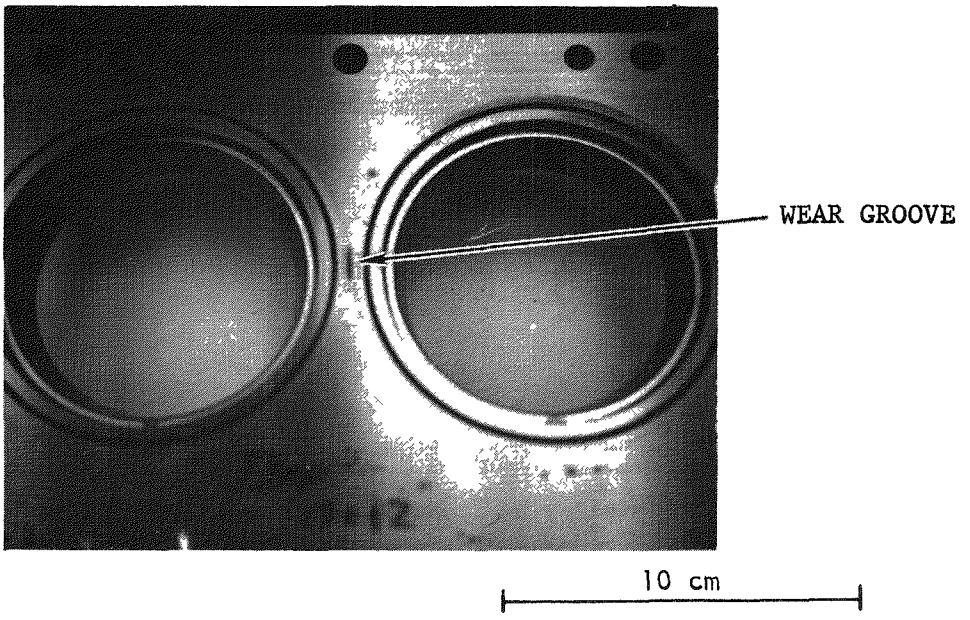

Fig. 4-21. Particle crusher side plate showing wear groove after 150 kg of throughput

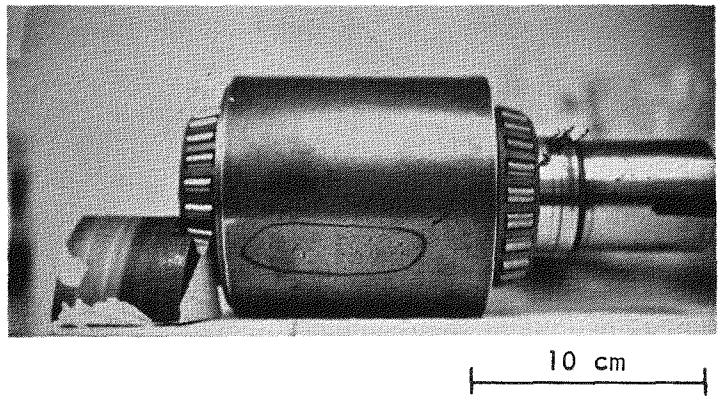

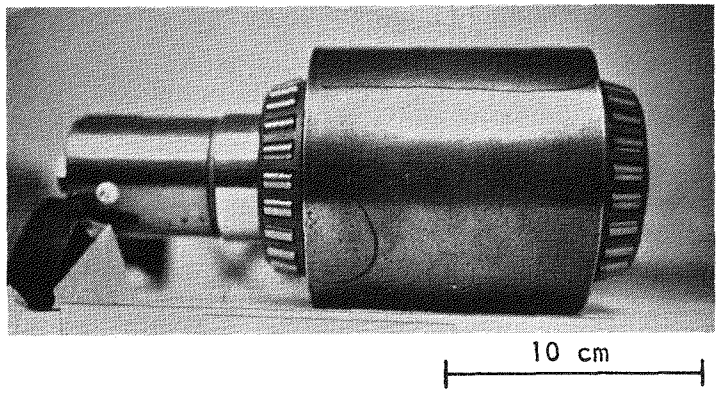

Fig. 4-22. Particle crusher rolls after 150 kg of throughput. Note similarity of surfaces.

contain numerous unidentified anomalies which appeared as clustered pits. These anomalies and the nominal roll surfaces were scanned with a Brush Surface Analyzer for roughness, depth of pits, grooves, etc. Selected pitted areas were explored. The results of the surface scan of both rolls are shown in Table 4-5. From these results it can be seen that the general surface roughness has increased from RMS 16 to a maximum of RMS 28. Some of this increase may have resulted from the hand scouring of the roll o.d.'s with SiC emery paper.

The crushing surfaces of both rolls at the ends had become slightly burnished but still possessed sharp, unbroken edges. The pitted areas were relatively shallow, <0.051 mm (<0.002 in.) deep, although quite wide [5.1 mm (0.20 in.)] and rough (RMS 112). The origin of these pitted regions is unknown, and efforts are continuing to identify their causes and to eliminate them.

4.4.3. FSV Fissile Particle Crusher

The FSV fissile particle crusher is currently under construction, and most critical components are on hand or completed. Principal of these are the roll side bodies made of AISI D2 tool steel. These precision-machined components have been heat treated, finish machined and ground, and accepted by GA quality control inspectors and are ready for final assembly. The four crusher rolls (two spares) have been rough machined and heat treated. Some difficulties have been encountered in flame hardening the crushing surfaces to the desired hardness of R_C 58 to R_C 60. Figure 4-23 shows the results of the flame hardening of the process control and production control specimens. The latter were processed along with the crusher rolls after the correct processing parameters had been verified with the process control specimens. It can be seen from the figure that process specimen A did not possess a satisfactory flame-hardened case and that the situation was corrected and verified by specimen B. The hardness of production control specimens 2 and 6 was at or above the desired minimum hardness of

TABLE 4-5
FERTILE FUEL PARTICLE CRUSHER ROLL SURFACE CONDITION AFTER 150-KG THOUGHPUT

Location	Area	Surface Finish[a] (RMS)	Pitting			Comments
			Width (mm)	Depth (mm)	Finish (RMS)	
Material: 1018						
O.D./end	A1	22	2.39	0.038	--	--
			2.90	0.033/0.038	--	2 local pits
O.D./center	A2	30	5.08	0.020	78	Many local pits
			1.07	0.020	80	
O.D./end	B	14/20	1.71/1.52	0.010	62	2 pits 12.7 mm apart
Material: 4340						
O.D./center	A	20	4.17	>0.023	78	--
			2.03	>0.023	87	--
O.D./center	B	28	1.52	>0.023	110/112	1 of 2 large pits
O.D./center	C-1	18/24	0.51	--	--	Typically many pits
O.D./left center	C-2	--	2.74	>0.015	49	Area photographed

[a] Drawing 5211011 requirement is 16 RMS.

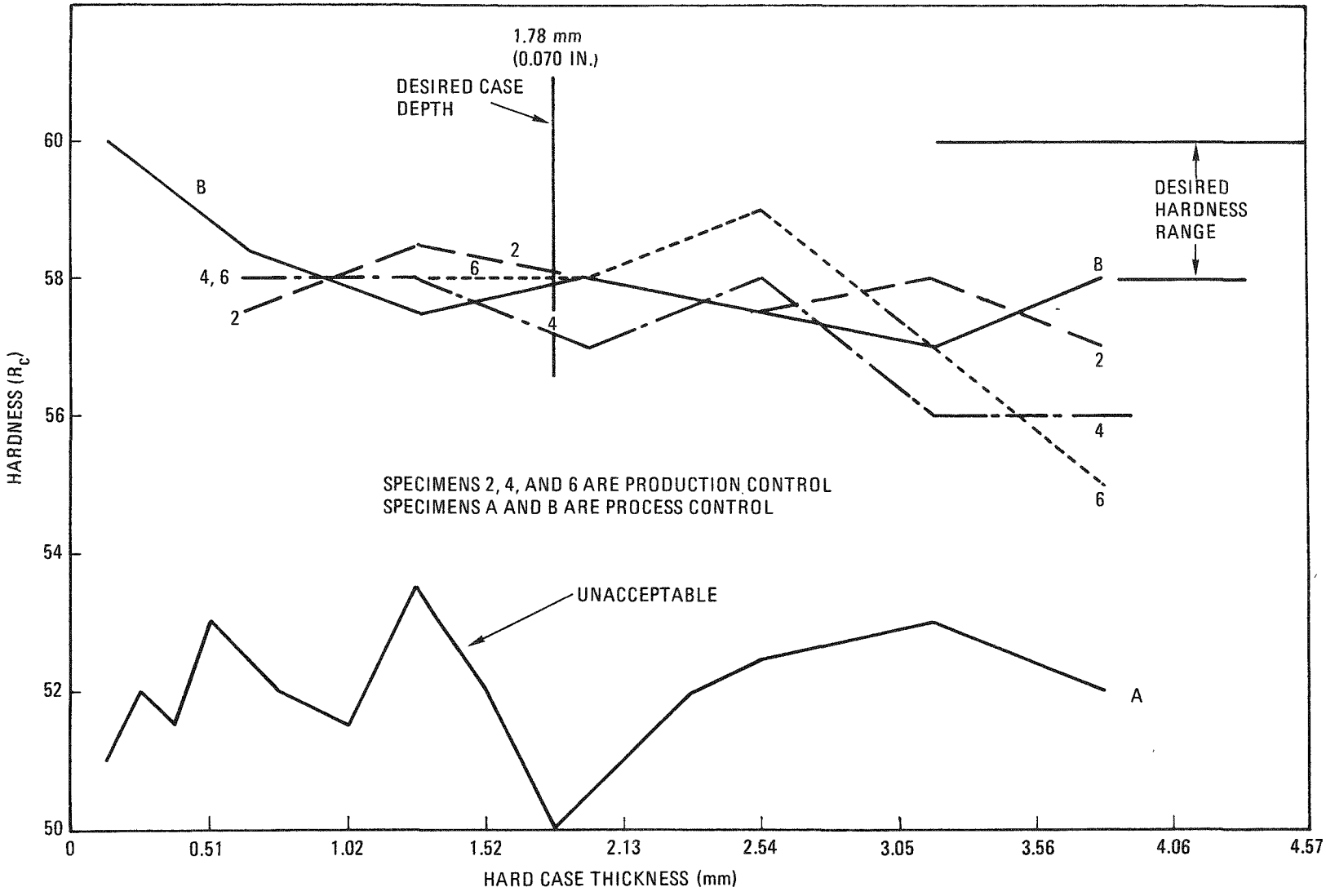

Fig. 4-23. Effect of flame hardening on process control and production control specimens

R_c 58 to the required depth mark of 1.78 mm (0.070 in.). Specimen 4 retained the desired hardness to an acceptable depth of 1.27 mm (0.050 in.).

REFERENCES

4-1. Rickman, W. S., "Evaluation of High Temperature Bed Removal System Integrated with a Penumatic Transport System for Use on Secondary Burners," General Atomic Company, unpublished data.

4-2. Rickman, W. S., "Interim Development Report for Secondary Burning," ERDA Report GA-A13540, General Atomic Company, December 25, 1975.

5. AQUEOUS SEPARATION

5.1. SUMMARY

The design of the engineering-scale dissolver-leacher for incorporation into the engineering-scale head-end line was initiated during the quarter. A review was made of the commercially available centrifuges, and a purchase order was placed for a vertical continuous unit.

A series of bench-scale and pilot plant dissolution runs were made to determine the potential advantage of using a heel operating mode for sol gel ThO_2 kernel dissolution. In the heel mode, excess ThO_2 is charged so that residual ThO_2 remains when the desired terminal solution concentration is attained. After removal of the dissolver solution, fresh ThO_2 is added to the heel. Preliminary results indicate that operating with a 40% heel can reduce the dissolution time by a factor of three.

Bench-scale studies were made on the stripping of macroreticular resin used for solvent cleanup. Prior work indicated 3M HNO_3, 0.05M HF to be an effective stripping agent. Disodium EDTA and oxalic acid were tested as potential alternate stripping agents but were found to be inferior to the nitric acid - hydrofluoric acid mixture.

Previous studies had indicated that the normal paraffin hydrocarbon diluent obtained from South Hampton Company exhibits good stability toward nitration under abnormal operating conditions. Comparable diluents obtained from Conoco and Texaco were tested and found to have comparable stability.

Additional tests were made to determine the effects of SiC and heavy metal carbides in leacher feed on the fission product zirconium decontamination factor during the subsequent solvent extraction processing. The presence of heavy metal carbides was found to have a definite adverse effect, but SiC had no discernible effect.

5.2. DISSOLUTION

5.2.1. Large Engineering-Scale Dissolver-Centrifuge System

5.2.1.1. General

The design documentation requirements for the large engineering-scale dissolver-centrifuge system were established with the release of the Design Document Index for this system (DI526101). The conceptual design for the system (i.e., the design criteria, the PI and the PF drawings) was then initiated.

5.2.1.2. Centrifuge

5.2.1.2.1. Introduction. A centrifuge is needed as an integral part off the dissolver system to be added to the engineering-scale line. The dry head-end portion of the line has been installed and is currently being qualified. Installation of the dissolver-centrifuge will be completed in FY-78, with the qualification testing starting the same year.

Because of the long lead time for centrifuges (12 to 15 months), an RFQ was released in 1975 for the engineering-scale centrifuge. A bid comparison which listed the features of the centrifuges quoted by the manufacturers was made, resulting in the recommendation for the Sharples P850 vertical centrifuge (Fig. 5-1). This recommendation was followed by the issuance of a purchase order in June 1976.

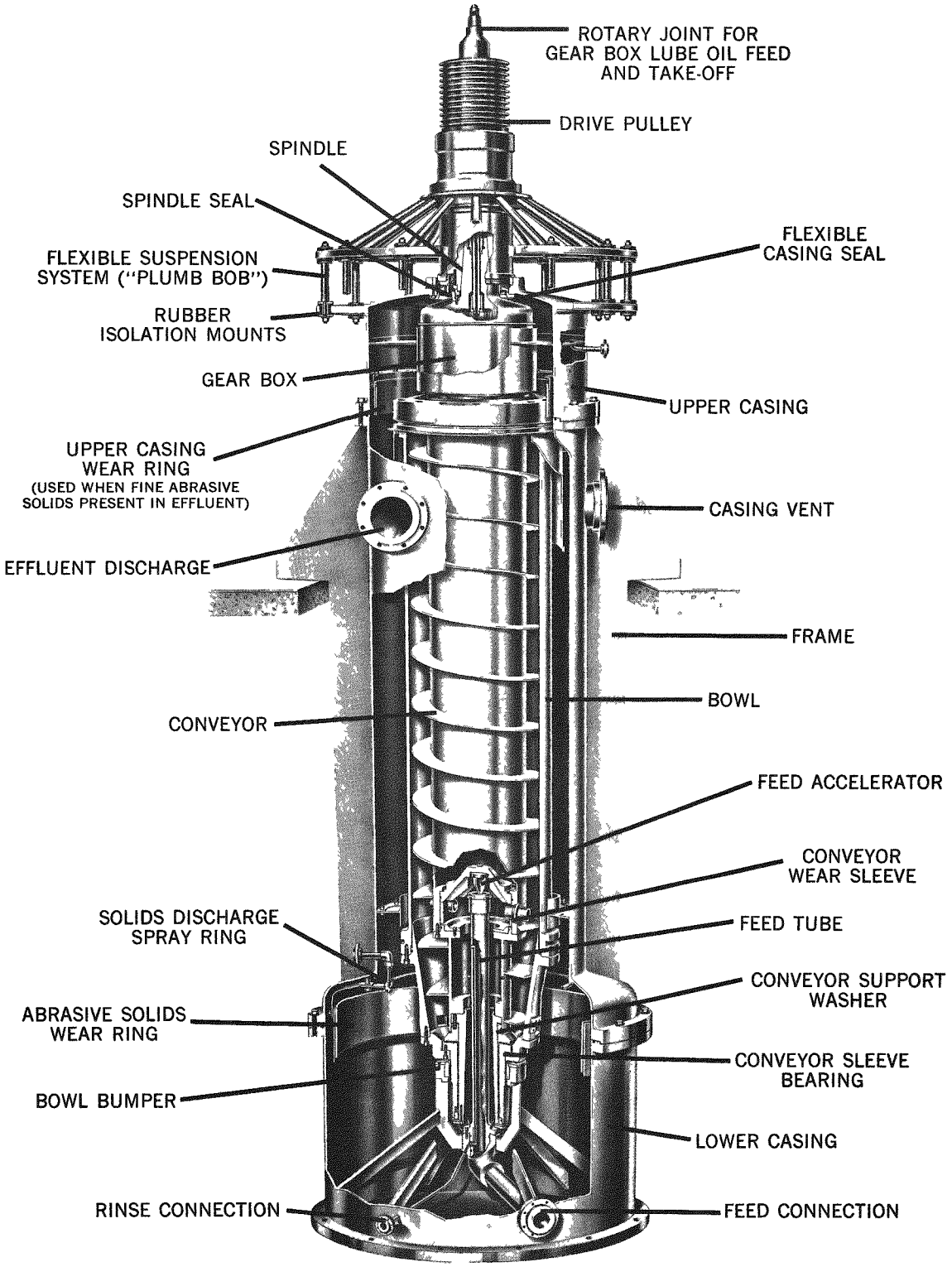

Fig. 5-1. Cutaway view illustrating typical features of vertical models (reprinted by permission of Pennwalt Corporation)

5.2.1.2.2. Discussion. Batch centrifuges have been in use in remotely maintained reprocessing facilities. Unfortunately, in such a machine the solids must be repulped to be removed. In HTGR fuel reprocessing, this is not compatible with the need to dry and package the solids which are the SiC hulls. Also, from a criticality standpoint, a batch centrifuge appears to be harder to adapt than a continuous unit. Therefore, the batch centrifuge is not as desirable as continuous centrifuges for the solid/liquid separation step in the LHTGR reprocessing.

In response to an RFQ, five quotes for continuous centrifuges were received from two manufacturers, Pfaudler and Sharples. These quotes described four horizontal units and one vertical unit. The designs were judged on the basis of their process features and future adaptability to a remotely maintained and highly radioactive environment.

The vertical unit differs in design from the horizontal units in more respects than orientation. In the vertical design the bowl is suspended from the top, where the only seal is located. This "plumb bob" suspension allows the bowl to absorb slight imbalances through shifting the axis of rotation. A horizontal unit is supported at both ends and cannot absorb imbalances, but instead reacts to give increased vibration. The ability of the vertical unit to absorb imbalances also reduces the tolerance required for balancing the bowl.

For remote operation in a hot cell, several features unique to the vertical design give it an advantage over the horizontal unit. First, it requires less floor space. Second, removal and replacement of the internals is simplified in a vertical orientation and the vertical centrifuge is similar in design to the batch centrifuges used in remotely maintained facilities and would be easier to adapt to this service using existing technology. Finally, the seal is not in contact with the process fluids, and the unit self-drains if stopped -- an important feature considering the decay heat generation.

There are also process advantages to the vertical design. It can have a longer bowl than a horizontal unit, which will allow either greater clarity or increased throughput. For pressure or vacuum service, a vertical centrifuge requires only one seal, while there are three seal points for a horizontal design, which results in problems with imbalance and bearing failures.

With respect to reliability and maintainability, the vertical design is favored because of its reduced dependence on balancing (causes less vibration) and its use of one instead of three seal points, which is located away from the process materials. Based on the above features, the vertical centrifuge was chosen over the four horizontal units even though it costs 50% more than a comparable horizontal centrifuge.

5.2.2. Heel Dissolution Investigation

5.2.2.1. Introduction

The previously reported (Ref. 5-1) dissolution method for ThO_2 kernels consisted of batch dissolution whereby the entire charge of ThO_2 kernels was dissolved in sufficient Thorex acid to give a 1M thorium product. Heel dissolution is being investigated to provide an alternative to this method.

Heel operation takes advantage of the rapid dissolution rate during the first portion of leaching of ThO_2 kernels. By interrupting the normal cycle before complete dissolution is achieved, it may be possible to shorten the combined dissolution time for several batches. The point at which the cycle is stopped depends upon the change in dissolution rate and the intercycle time.

For the sol gel ThO_2 kernels, the point of interruption appears to be about 60% to 80% dissolution. To pinpoint the optimum parameters, a series of eight test segments were planned to be carried out in the 13-cm pilot plant leacher and in bench-scale glassware. Segments 1 through 3 will

establish the operating parameters. Segments 4 and 5 will verify these parameters using the centrifuge to separate the heel from the mother liquor. Segments 6 through 8 will investigate the application of steam jet removal for decanting the liquid from the heel.

5.2.2.2. Results

To date, segments 1 and 2 have been completed. Three runs (149, 150, and 151) were conducted in the 13-cm leacher (Fig. 5-2) to satisfy the requirements of segment 1. These runs established the base dissolution curve. Eight bench-scale runs were conducted to satisfy the segment 2 requirements. Comparison of the results for the bench-scale runs and the base dissolution curve yielded the operating parameters to be used for the segment 3 tests.

Table 5-1 gives the operating conditions for runs 149, 150, and 151. Because of analytical delays, misformulated Thorex (normally 13M HNO_3, 0.1M Al^{+3}, 0.05M F^-) was used for run 149. Table 5-2 gives the results of runs 150 and 151, and Fig. 5-3 shows the dissolution curves for these runs. These curves will be used as the baseline for comparison of future runs.

The initial bench-scale tests were made in an Erlenmeyer flask. However, the first two tests yielded rates which were much faster than the engineering-scale test rates (Fig. 5-4). The reason for the difference in rates is believed to be due to the differences in geometry. Better liquid-solid contact is achieved in the flat-bottom glass than in the conical-bottom engineering-scale leacher. To test this hypothesis, a glass dissolver (Fig. 5-5) was fabricated with a 60° conical bottom. Figure 5-6 compares the results of the baseline curve for the conical dissolver, the flask, and the 13-cm leacher. As expected, this change resulted in a reduced rate which is still not as low as that obtained with the engineering-scale equipment.

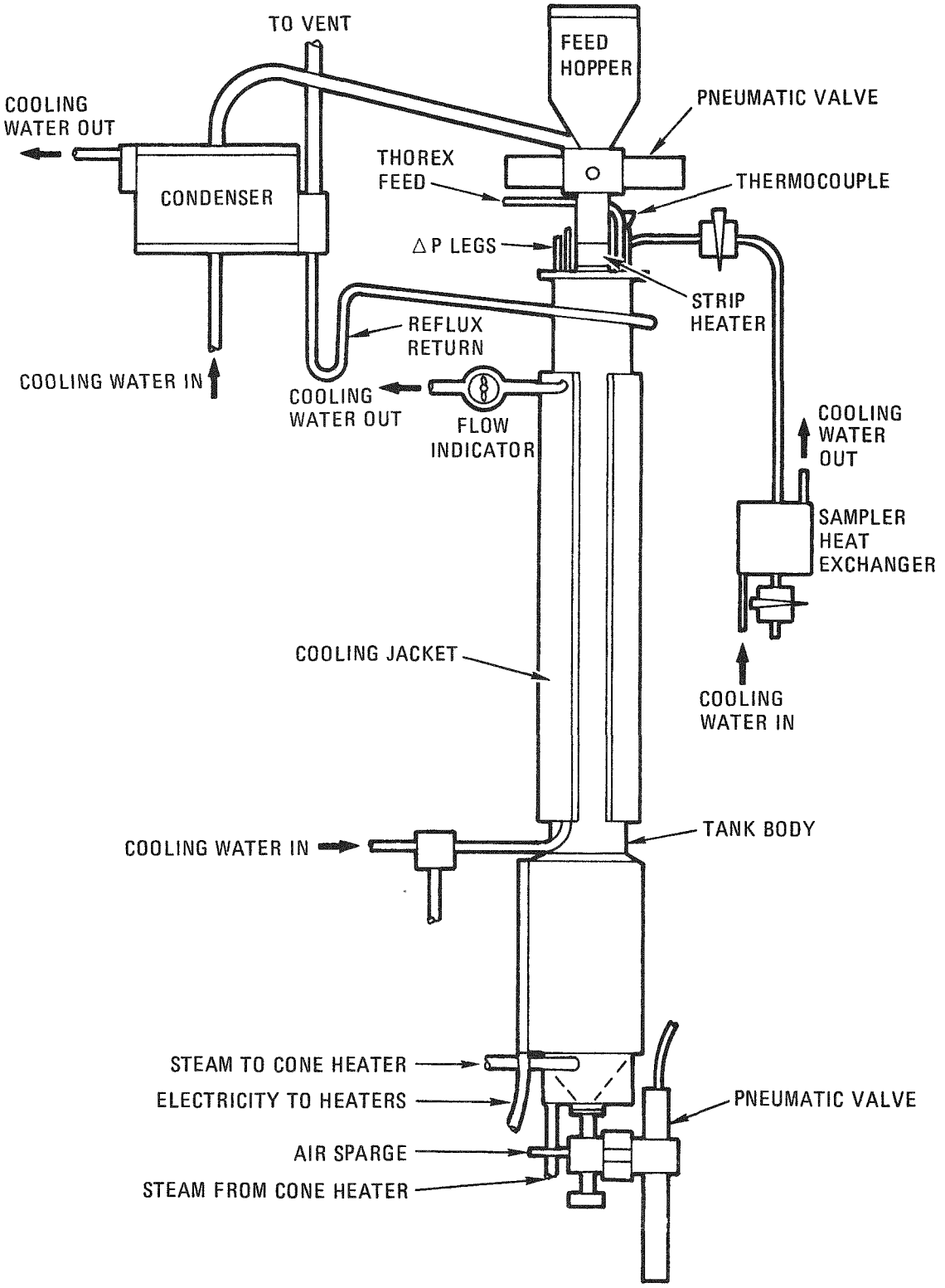

Fig. 5-2. 13-cm-diameter leacher arrangement

TABLE 5-1
OPERATING DATA FOR DISSOLUTION RUNS 149, 150, AND 151

	Run 149	Run 150	Run 151
Dissolver diameter (cm)	13	13	13
Feed material (g)[a]	3040	3026	3005
Thorex[b] (ℓ)	11.86	11.46	11.38
Air sparge rate (ℓ/min)	8.5	8.5	8.5
Dissolution time at boiling point (hr)	4.5	4.5	4.5
Undissolved heel (g)	634	737	721
Heat input (joules/hr x 10^{-6})	9.5	9.5	9.5

[a] ThO_2 sol gel kernels.

[b] 13.46M HNO_3, 0.12M KF, 0.104M $Al(NO_3)_3$ for run 149; 13.0M HNO_3, 0.05M KF; 0.10M $Al(NO_3)_3$ for runs 150 and 151.

TABLE 5-2
OVERALL THORIUM BALANCES FOR DISSOLUTION RUNS 150 AND 151

	Run 150	Run 151
ThO_2 input (g)	3026	3005
ThO_2 output (g)		
Samples	634	249
Mother liquor[a]	1990	1731
Heel	737	721
Total	3361	2701
Material balance (%)[b]	111.0	89.8
Percent dissolution (mother liquor)[c]	79.7	69.0
Percent dissolution (heel)[d]	75.7	76.1

[a] Based on last mother liquor sample taken.

[b] (Output/Input) x 100.

[c] (Output in Mother Liquor/Input) x 100.

[d] [(Input - Heel)/Input] x 100.

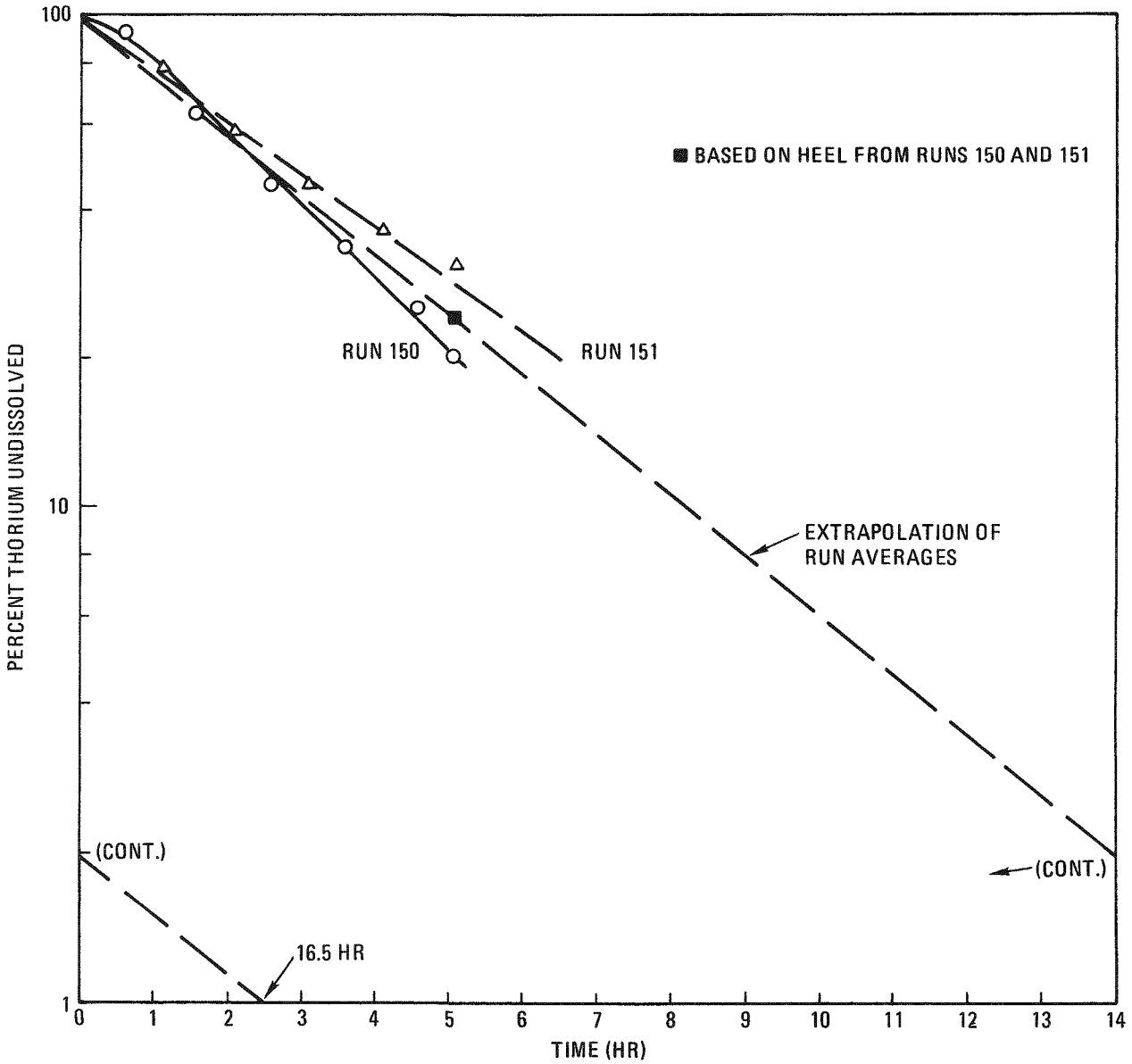

Fig. 5-3. Dissolution curves for Runs 150 and 151

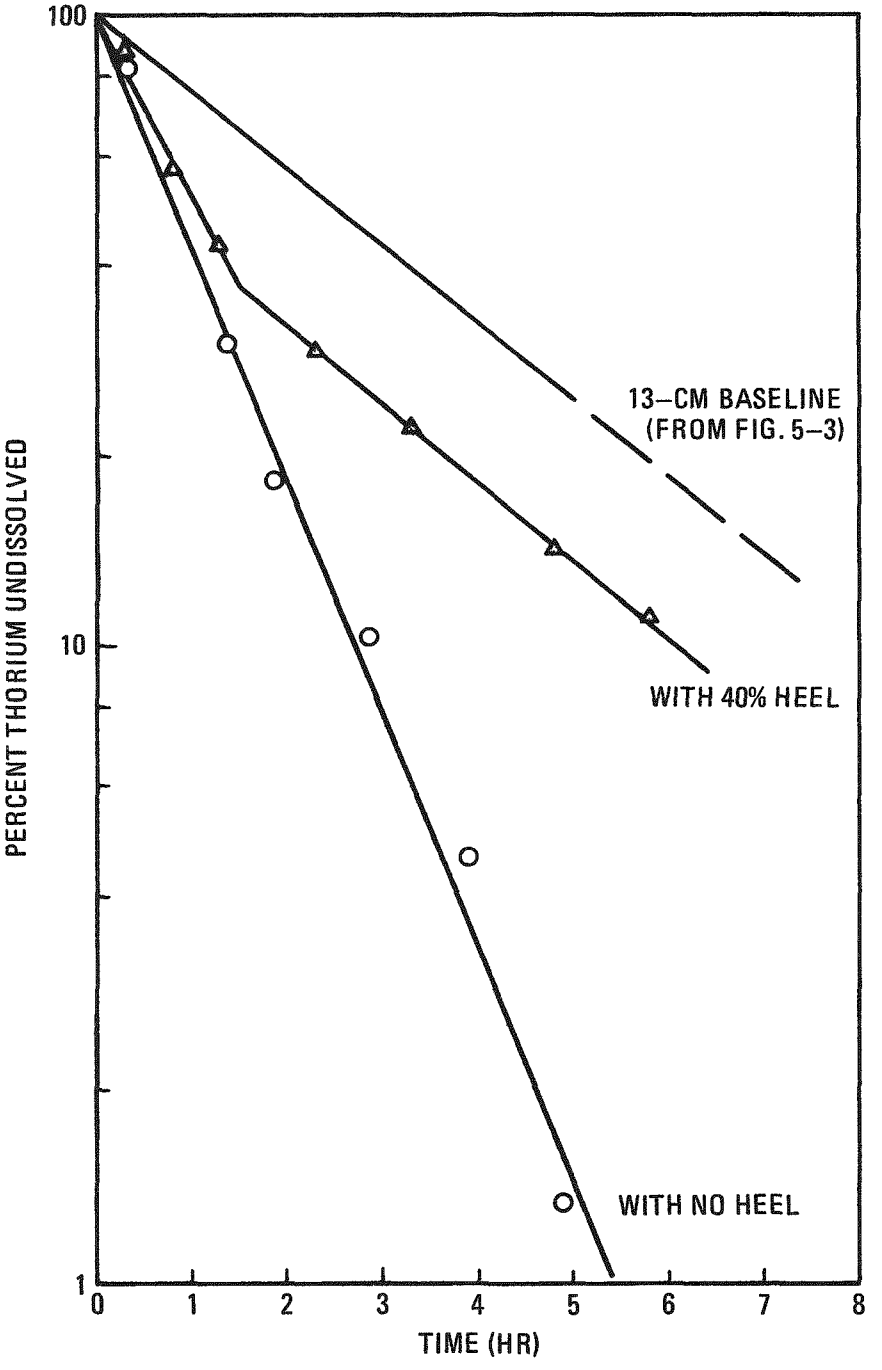

Fig. 5-4. Bench-scale dissolution - Erlenmeyer flask

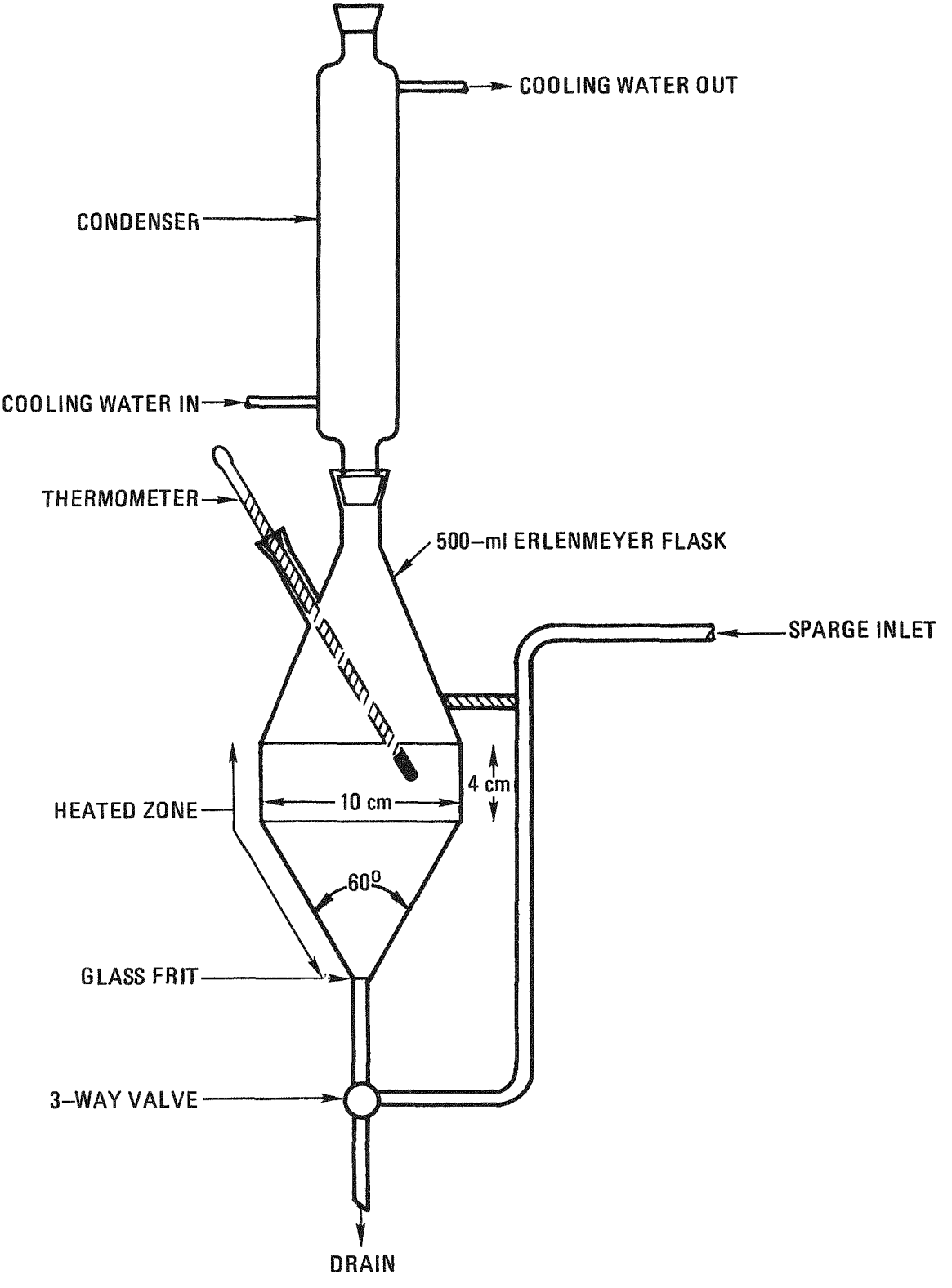

Fig. 5-5. Bench-scale conical dissolver

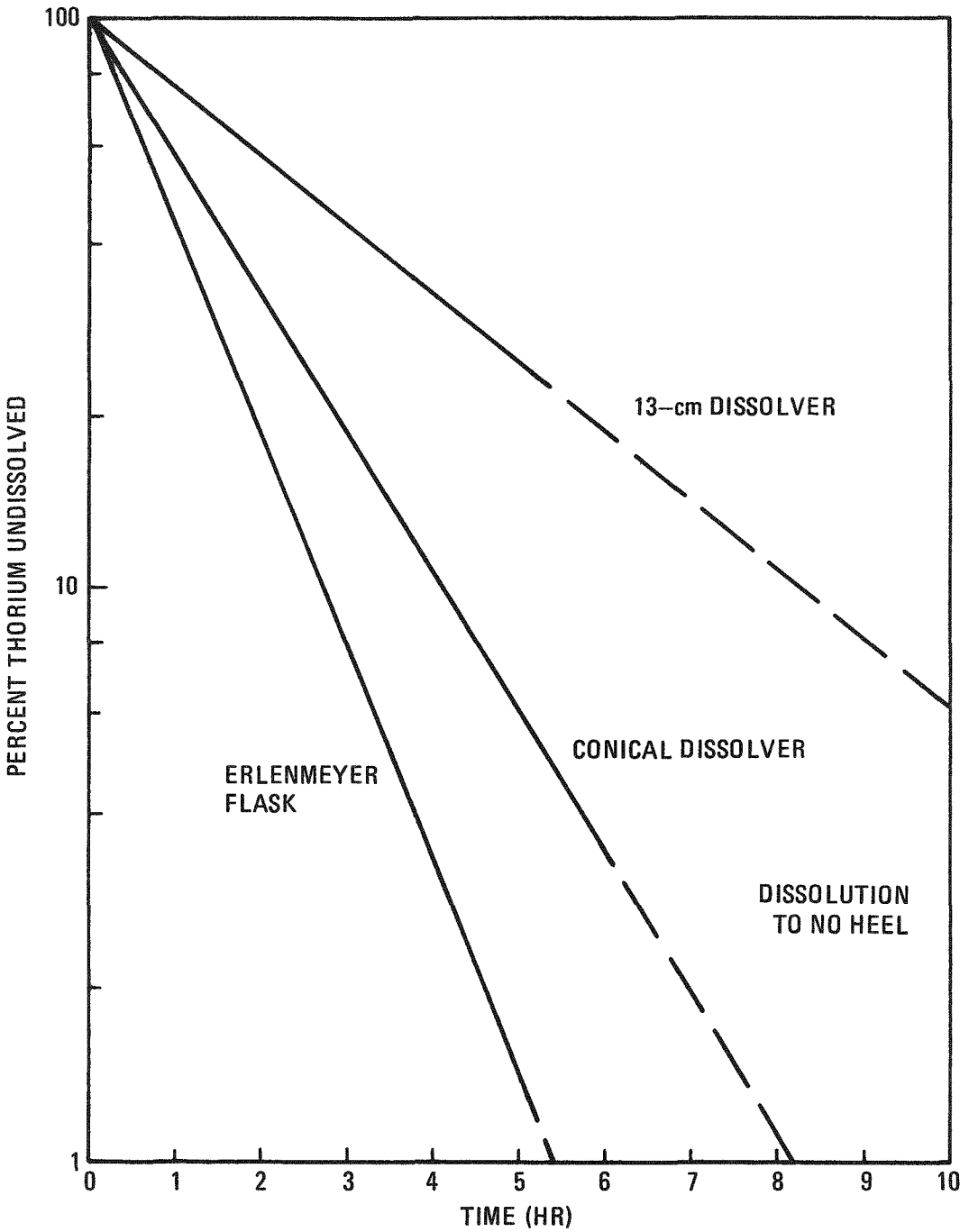

Fig. 5-6. Comparison of dissolution rates in the flask, conical dissolver, and 13-cm dissolver

Based on the above results, the bench-scale work was conducted on the conical dissolver. Figures 5-7 through 5-11 give the results of these tests. Examination of these curves reveals a distinct break in the dissolution rate at 1M thorium concentration.

To extrapolate these results to the engineering-scale test (segment 3), the time to reach 1M thorium concentration was plotted against the percent heel for the flask and conical dissolver tests (Fig. 5-12). The curve for the 13-cm leacher was added by using the estimated time to reach 99% dissolution (from Fig. 5-3) and the intercept of the ordinate from the first two curves. For a 5-hr run, a 38% heel is predicted.

Using the conical dissolver, a three-cycle run was made using a 40% heel. Figure 5-13 presents the results of this run. The dissolution time stabilizes after the first cycle to 91% of the initial dissolution time. Comparing this run with the baseline reveals that a factor of three improvement in the amount dissolved per unit time is obtained.

5.2.2.3. Conclusions and Recommendations

Based on the results of test segments 1 and 2, a threefold increase in the rate of dissolution from heel operation over batch dissolution can be estimated.

A 40% heel with a 5-hr dissolution time is recommended for segment 3 tests.

The rate controlling step or a major contributor for the dissolution of ThO_2 kernels may be the diffusion rate of concentrated thorium nitrate Thorex from the solids bed.

5.3. FEED ADJUSTMENT

Studies of continuous feed adjustment were resumed during the quarter. However, no reportable results have yet been obtained.

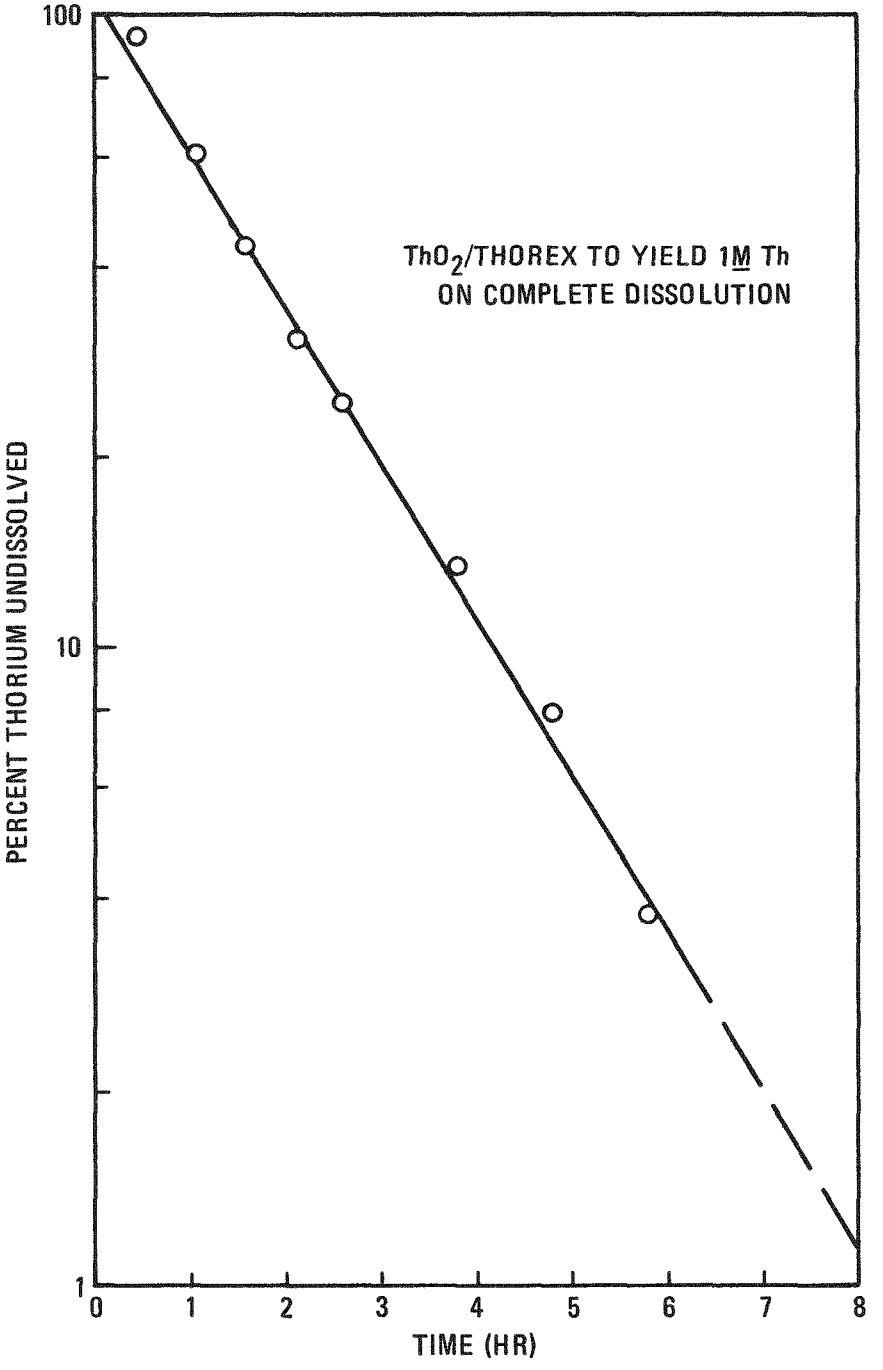

Fig. 5-7. Bench-scale conical dissolver test with 0% heel

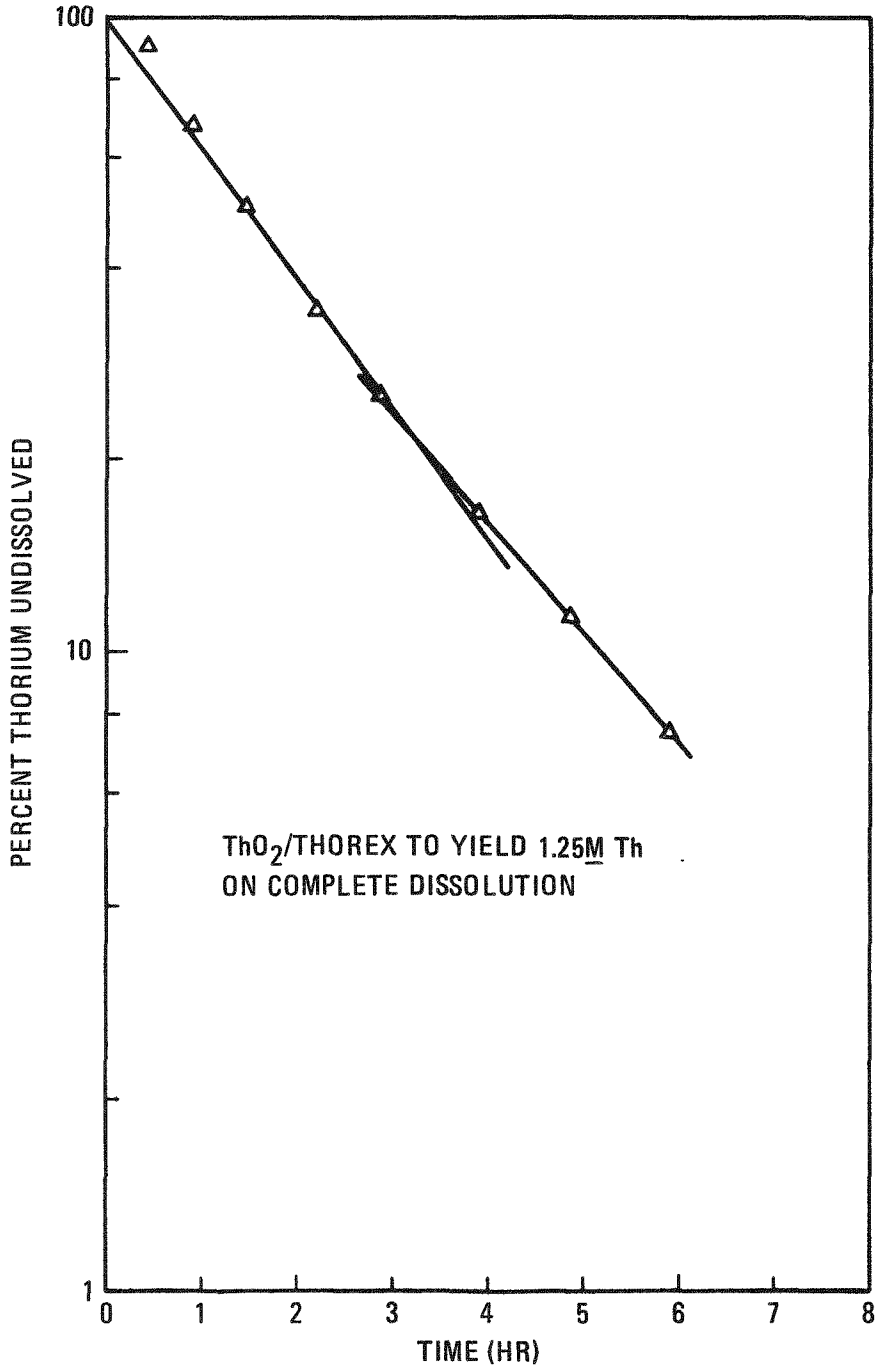

Fig. 5-8. Bench-scale conical dissolver test with 20% heel

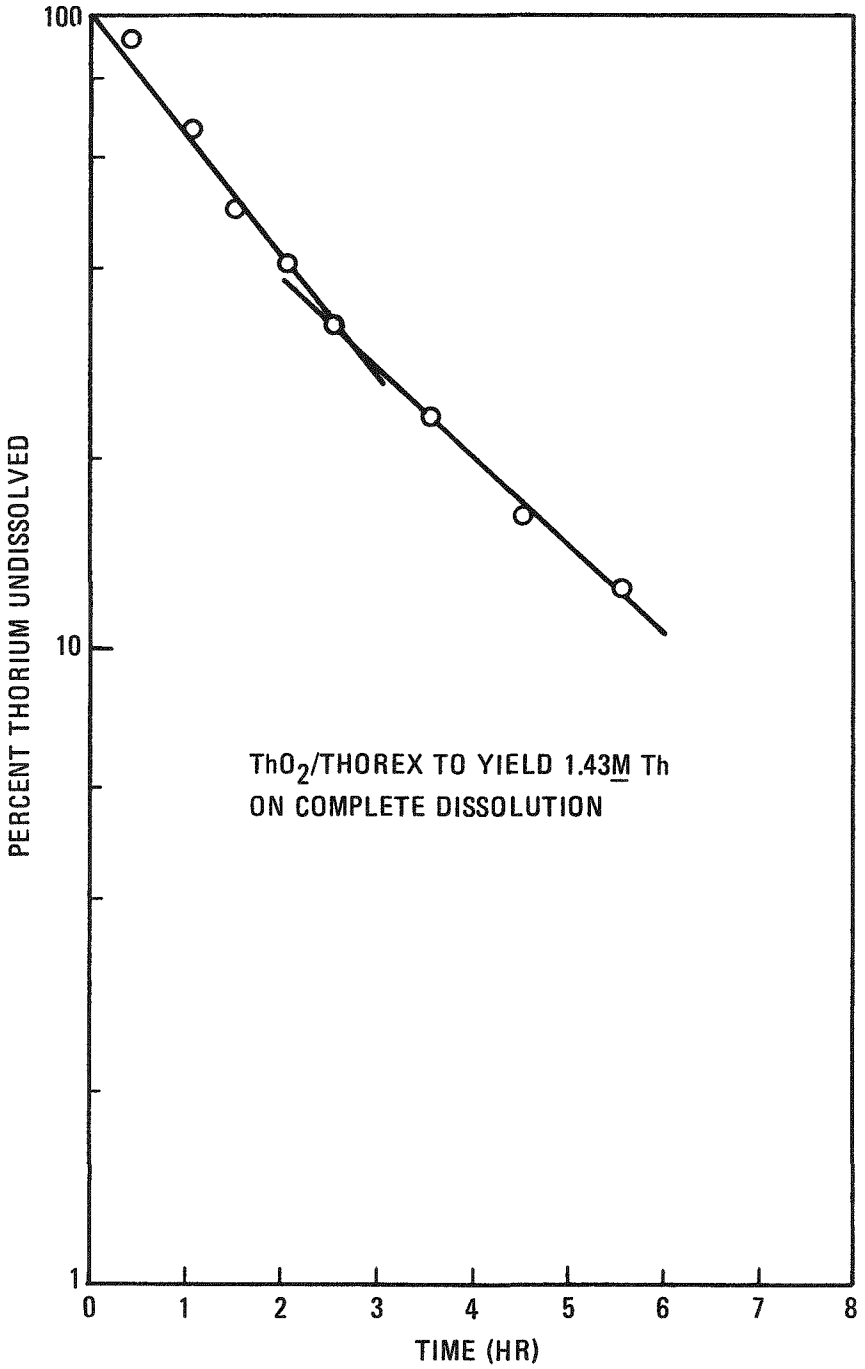

Fig. 5-9. Bench-scale conical dissolver test with 30% heel

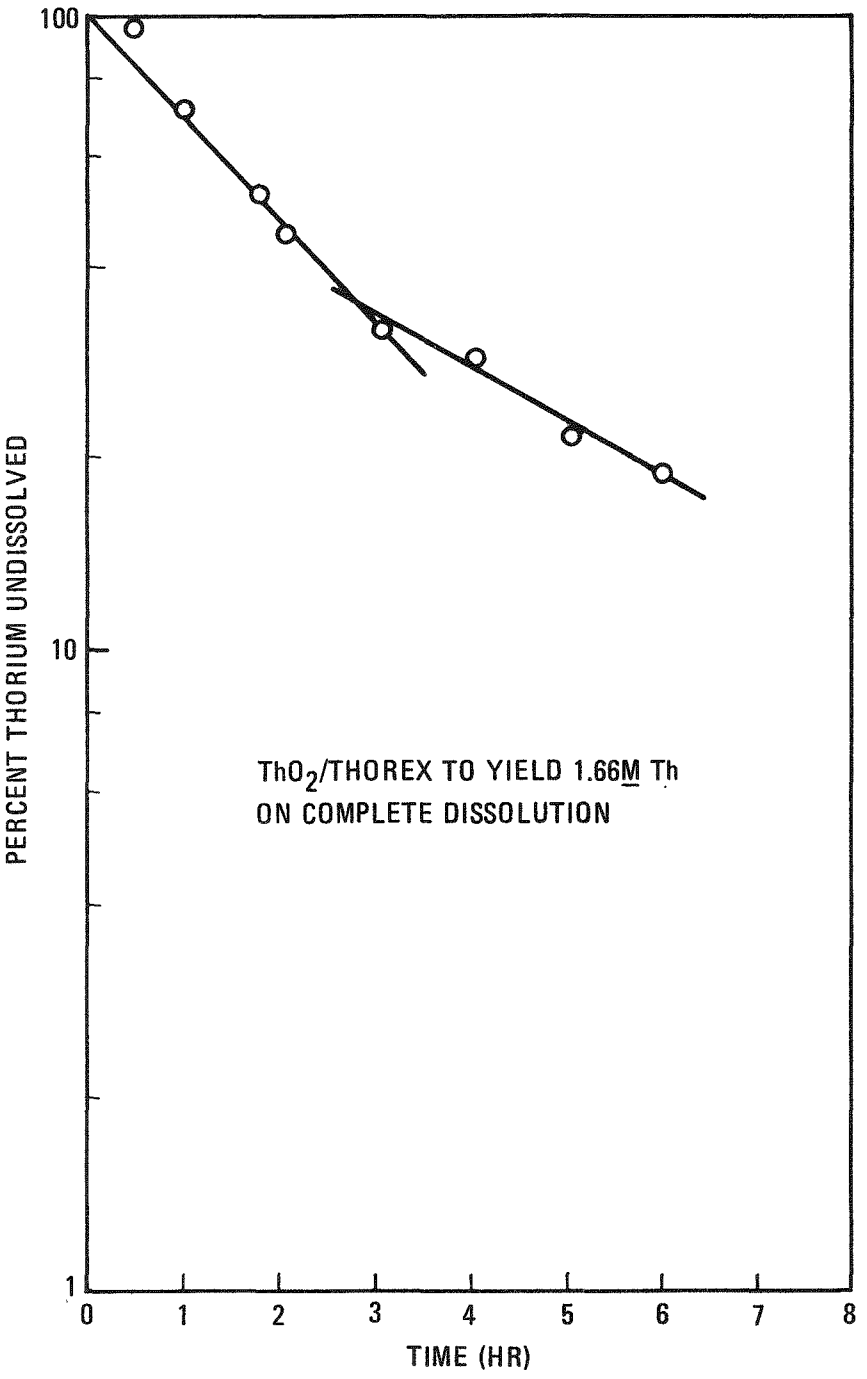

Fig. 5-10. Bench-scale conical dissolver test with 40% heel

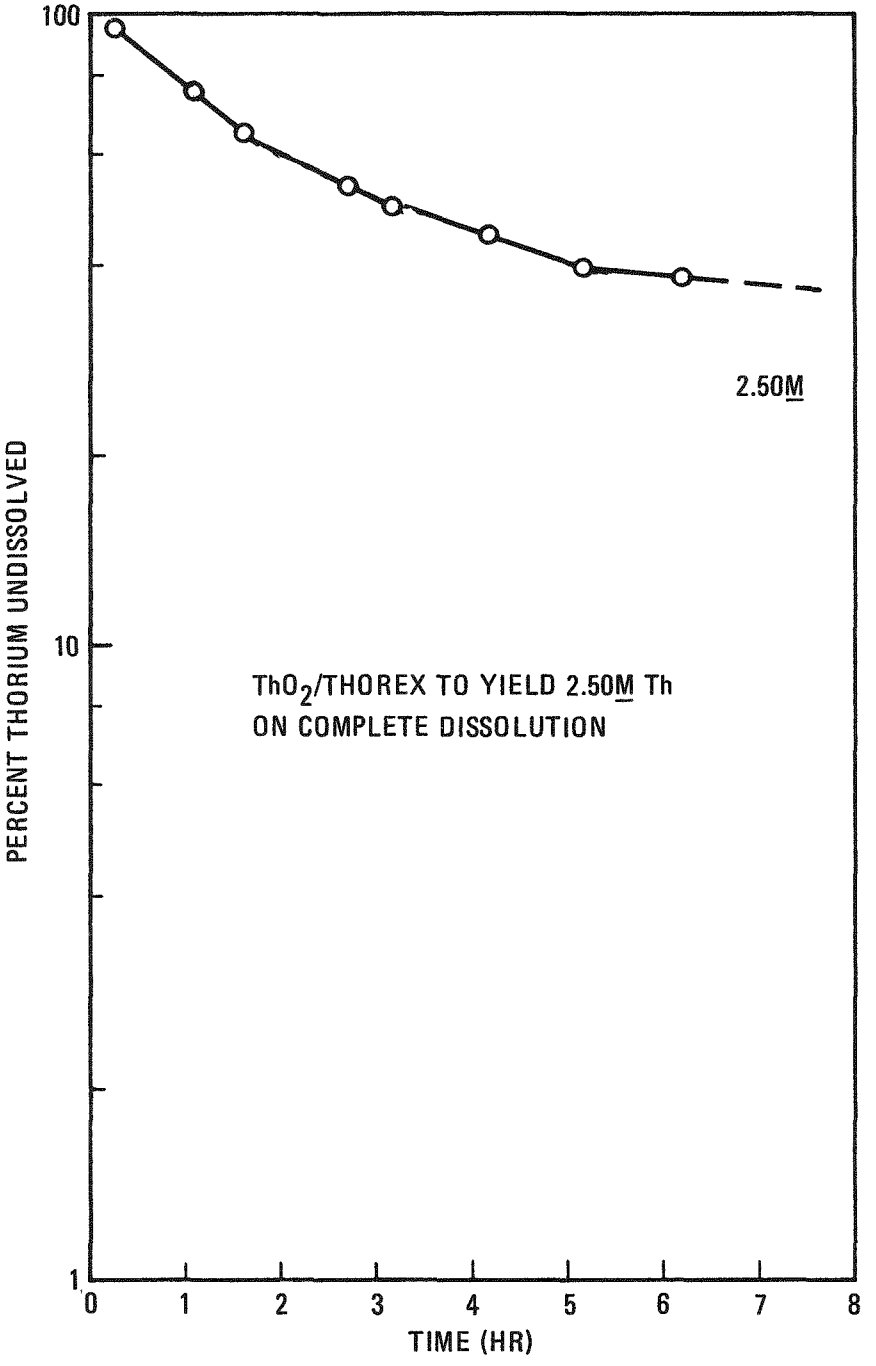

Fig. 5-11. Bench-scale conical dissolver test with 60% heel

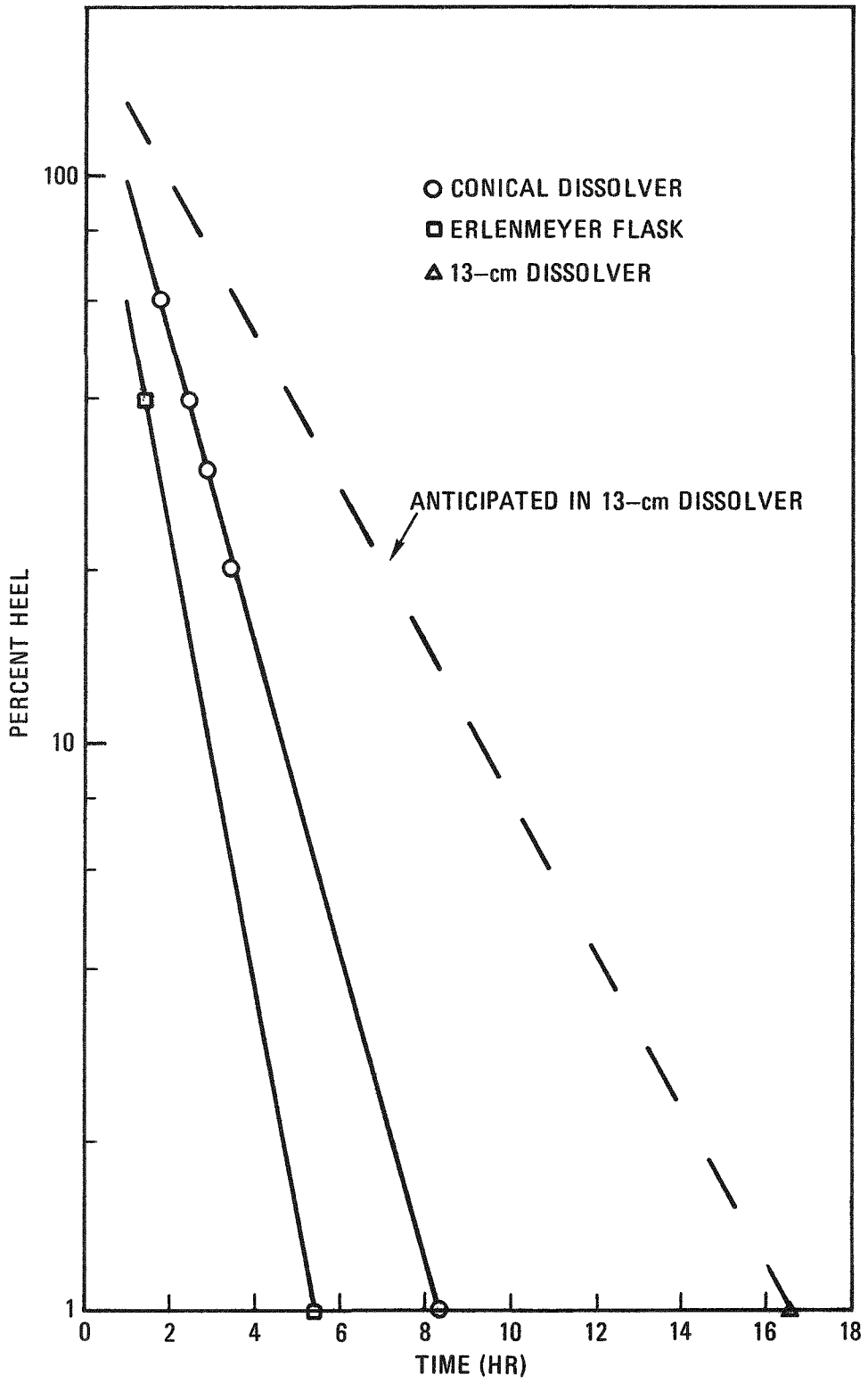

Fig. 5-12. Time to reach 1M Th versus percent heel

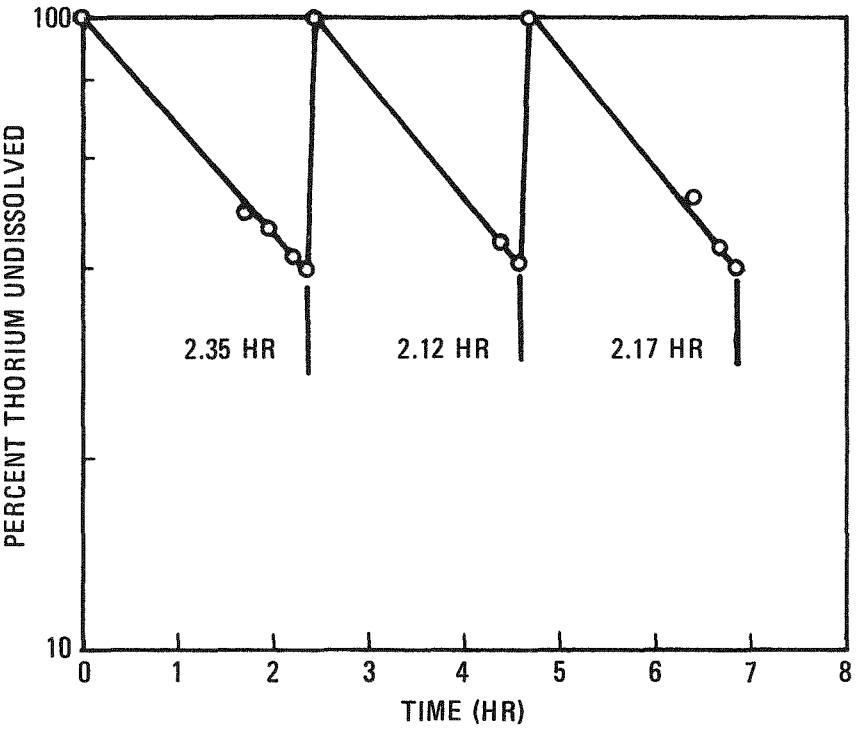

Fig. 5-13. Bench-scale conical dissolver three-cycle dissolution test with 40% heel

5.4. BENCH-SCALE INVESTIGATIONS

5.4.1. Characterization and Stripping Behavior of Solvent Extraction Process-Loaded Macroreticular Resin

Rohm and Haas Company macroreticular (Amberlyst-26) strong base anion exchange resin is currently being used in the solvent extraction pilot plant for the removal of uranium, thorium, zirconium, and solvent degradation products from process solvent. Bench-scale tests have been performed with resin samples obtained following solvent "cleanup" to (1) determine loaded resin uranium, zirconium and thorium content, (2) assess the efficiency of the recommended stripping agent, i.e., 3M HNO_3, 0.05M HF (Ref. 5-2), for the elution of heavy metals and zirconium from loaded macroreticular resins, (3) estimate the maximum capacity of the pilot plant ion exchange bed for removal of heavy metals and zirconium from process solvent, and (4) evaluate disodium EDTA and oxalic acid as stripping agents for resin regeneration.

The uranium, zirconium, and thorium contents of a loaded, wet portion of Amberlyst-26 macroreticular resin following solvent "cleanup" were found to be 1.34, 0.68, and 1.85 mg/ml, respectively. The relative rate of removal during stripping with 3M HNO_3, 0.05M HF was found to be uranium > zirconium > thorium. The total maximum loading for the pilot plant ion exchange bed was calculated to be 5.26 g uranium, 2.67 g zirconium, and 7.27 g thorium, if these materials are in the ratio present in the spent solvent. Assuming maximum resin loading is achievable, 500 liters of the 100 stream (solvent following carbonate washing) containing 10.5 ppm uranium, 5.4 ppm zirconium, and 14.5 ppm thorium could be processed through the pilot plant ion exchange resin bed with complete metal removal.

Samples were prepared for analysis by resin pyrolysis (qualitative elemental analysis) and aqueous stripping of resin beds prepared from process-loaded material. Data obtained from spectrographic analysis of

resin pyrolysis residues were useful in identifying the major elements present on macroreticular resin following process operations. X-ray fluroescence examination of stripped resins and eluate samples provided quantitative information.

Data contained in Tables 5-3 and 5-4 indicate that the relative rate of metal removal during stripping with 3M HNO_3, 0.05M HF is uranium > zirconium > thorium. Further, the data show that stripping with 30 bed volumes of 3M HNO_3, 0.05M HF elutes 93% of resin uranium, 78% of resin zirconium, and 62% of resin thorium for the noted elution rates.

As shown in Table 5-5, essentially all of the resin uranium, zirconium, and thorium was removed during stripping with 70 bed volumes of 3M HNO_3, 0.05M HF. Additionally, a comparison of Zr-95 tracer gamma activity in resin samples contained in equivalent geometry (GeLi detection) revealed a net reduction of $\sim 5 \times 10^3$ following stripping with 70 bed volumes of stripping agent.

The stripping efficiencies of 0.1M disodium EDTA and 10% oxalic acid for resin zirconium, uranium, and thorium removal were found to be less than that observed for 3M HNO_3, 0.05M HF. Comparative data are given in Table 5-6 for resin samples stripped with the three test agents under identical elution rates.

Under test conditions, none of the stripping agents were found to yield rapid regeneration with sufficiently small effluent volumes to permit consideration of the use of macroreticular resins as a viable alternative to carbonate washing of the entire HRDF solvent inventory. However, the macroreticular resin may still be used on selected solvent feeds where high-quality solvent is required.

TABLE 5-3
X-RAY ANALYSIS OF MACRORETICULAR RESIN ELUATE SAMPLES

Solution	Total Volume (ml)	No. of Bed Volumes	Elution Rate (ml/min/cm^2)	Solution (mg/ℓ)		
				Zr	U	Th
H_2O	65	6.5[a]	0.55	1.6	7	4
1st strip[b]	100	10	1.0	33	87	32
2nd strip	100	10	1.15	11	35	42
3rd strip	100	10	2.8	9	3	40
4th strip	400	40	2.5	3.5	1	17

[a] Volume of wet resin = 10.0 ml. Column diameter = 1 cm.

[b] Stripping agent composed of 3M HNO_3 0.05M HF.

TABLE 5-4
MACRORETICULAR RESIN ELUATE SAMPLES - DATA REDUCTION

Solution	Total Volume (ml)	Number of Bed Volumes	Total Solution Metal Content (mg)			Percent of Total Metal in Soln			Percent of Total Metal/Avg Bed Volume		
			Zr	U	Th	Zr	U	Th	Zr	U	Th
H_2O	65	6.5[a]	0.1	0.46	0.26	2	3	1	0.3	0.5	0.2
1st Strip[b]	100	10	3.3	8.7	3.2	49	65	17	4.9	6.5	1.7
2nd Strip	100	10	1.1	3.5	4.2	16	26	23	1.6	2.6	2.3
3rd Strip	100	10	0.9	0.3	4.0	13	2	22	1.3	0.2	2.2
4th Strip	400	40	1.4	0.4	6.8	21	3	37	0.5	0.1	0.9
TOTAL	765	76.5	6.8	13.4	18.5	100	100	100	--	--	--

[a] Volume of wet resin = 10.0 ml

[b] Stripping agent composed of 3M HNO_3, 0.05M HF.

TABLE 5-5
DATA SUMMARY - DIRECT X-RAY ANALYSIS OF MACRORETICULAR RESIN BEADS

Sample	Metal Content (mg/10 ml wet resin)		
	Zr	U	Th
Loaded resin	6.24	11.76	21.14
Stripped resin[(a)]	-0.01	0	0.07
Apparent % Element Removed	100	100	99.7

[(a)] Stripped with 70 bed volumes of 3M HNO_3 0.05M HF.

Note: Material Balance calculated as:

$$\frac{10^2 \times \text{effluent total mg (from Table 5-4)}}{\text{Loaded resin total mg (from above)}}$$

	Zr	U	Th
=	109%	115%	88%

TABLE 5-6
RESIDUAL MACRORETICULAR RESIN METAL CONTENT - ALTERNATE STRIPPING AGENT DATA SUMMARY

Stripping Medium (30 Bed Volumes)[a]	Residual Metal			Total Percent Removed		
	Zr (g/ℓ)	U (g/ℓ)	Th (g/ℓ)	Zr	U	Th
None	0.624	1.18	2.11	--	--	--
3M HNO_3 - 0.05M HF	0.011	0.00	0.19	98.2	100	90.5
0.1M EDTA	0.15	0.97	0.60	76.0	17.7	71.6
10% oxalic acid	0.60	1.14	1.84	3.8	3.4	12.8

[a] Flow rate = 4 bed volumes/hr.

5.4.2. Nitration Stability of Commercial Diluents

Samples of two commercial normal paraffin hydrocarbon diluents (Conoco and Texaco) obtained from AGNS were subjected to tests to determine their stability toward nitration. Analyses of the diluents are presented in Table 5-7. The tests consisted of heating 2.0-ml aliquots of 1M thorium-Thorex solution with 1.0-ml aliquots of TBP dissolved in the respective diluent. No "red-oil" formation or vigorous reaction was observed with either diluent.

Additional testing consisted of heating samples of diluent with equal volumes of 4.0M HNO_3 containing 0.1M HNO_2 (Ref. 5-3). The performance of the two diluents was judged similar to that of previously studied NPH (South Hampton Company, Ref. 5-4).

5.4.3. Effects of Carbide Carbon and Silicon Carbide Feed Content on Zr-95 Distribution in the Acid-Thorex Process

Bench-scale experiments were conducted during this reporting period to assess the effects of feed carbide carbon from heavy metal carbides and silicon carbide content on resultant Zr-95 distribution during batch solvent extraction. The efficiency of the feed adjustment step as a method for the destruction of any extractable zirconium complexes formed was also evaluated. The experimental design used in these studies is given in Fig. 5-14.

Solvent extraction feed samples were prepared for study by the addition of carbide carbon or SiC (0.03 wt % or 0.1 wt % final concentration, respectively) to ^{95}Zr - ^{95}Nb spiked 1M thorium-Thorex solutions. The 0.03 wt % carbide would result from a 10% fissile particle crossover into the fertile stream and subsequent breakage. The samples were then subjected to feed adjustment by evaporation to 135°C or evaporation to 135°C with subsequent steam sparging. Following adjustment of the boiler pot products to give the flowsheet feed point conditions (0.4M Th^{+4} and

TABLE 5-7
NORMAL PARAFFIN HYDROCARBON ANALYSES
(WT %)

	Conoco $C_{12}C_{14}$		Texaco P-4	
	Specification	AGNS Analysis	Specification	AGNS Analysis
C_{10} and lighter	--	<0.2	--	<0.1
C_{11} and lighter	2.0 max.	0.8	--	0.5
C_{12}	10 ± 5	8.5	8-15	8.5
C_{13}	50 min	58.1	45-50	48.5
C_{14}	30-45	32.4	30-45	40.9
C_{15} and higher	2.0 max.	<0.2	--	1.5
C_{16}	--	--	--	0.2
C_{17} or greater	--	--	--	<0.1
Total N-paraffin	97.5 min.	--	98 min.	--
Aromatics	0.6 max.	0.27	0.5 max.	0.42
Bromine index	200 max.	<20 (mg/100 g)	100 max.	<20 (mg/100 g)
Sulfur	10 ppm max.	--	5 ppm max.	--

Specific gravity, 60°F: 0.763
Flash point (Pensky-Martens): 205°F

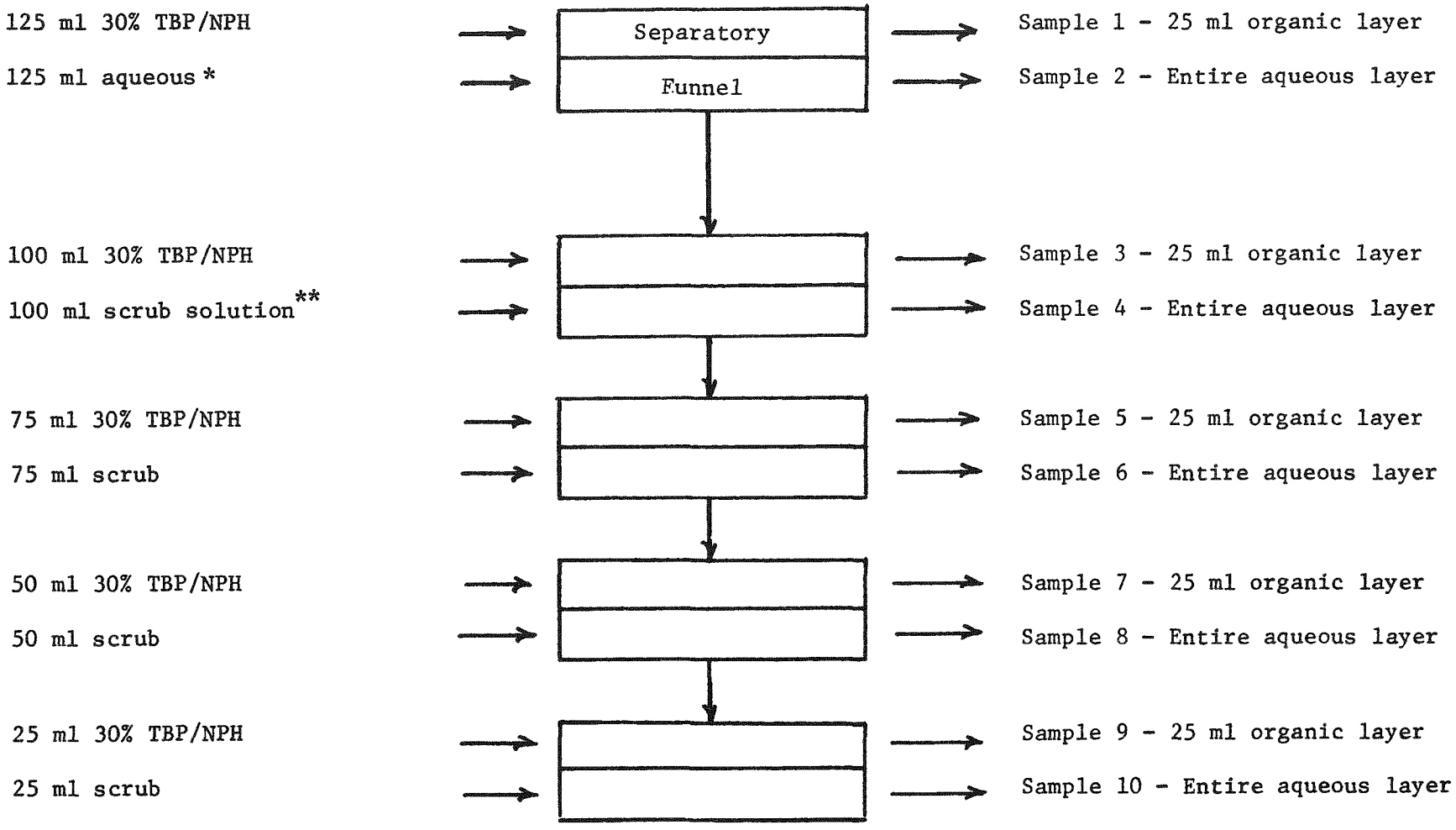

*0.4M Th^{+4} 1.0M H^{+} - feed solution.

**0.25M Th^{+4} 1.0M H^{+} - scrub solution.

Fig. 5-14. Experimental design for carbide studies of ^{95}Zr-^{95}Nb distribution coefficient

1M H^+), an initial extraction was performed with 30% TBP/NPH in a separatory funnel. The solids were allowed to remain through the first solvent contact and were then removed by centrifugation. A scrub solution containing 0.25M Th^{+4} and 1M H^+ was used for all subsequent contacts. Gamma-ray spectrometry with GeLi detection was utilized for measurement of ^{95}Zr - ^{95}Nb tracer activity in organic and aqueous phases following phase separation by centrifugation. Table 5-8 contains ^{95}Zr - ^{95}Nb distribution data from gamma spectrometric analysis of carbide and control solutions. Distribution data for the SiC system are presented in Tables 5-9 and 5-10.

The solvent extraction distribution coefficient for a given element remains constant over a wide concentration range in the absence of side effects. The large variation in calculated K values given in Table 5-8 suggests a marked effect for carbide carbon. This effect is not removed during feed adjustment, and the results emphasize the importance of low crossover of fissile particles (potential source of carbide carbon) into the fertile stream, complete particle crushing, complete combustion in burning operations, and minimum particle breakage in the subsequent dissolution step.

Carbide carbon was also found to have an adverse effect on zirconium-uranium separation in Purex process studies (Ref. 5-5). The lower zirconium decontamination factors found in the Purex studies were apparently the result of the formation of zirconium complexes with ligands formed from the reaction of heavy metal carbides and nitric acid. The present work indicates an analogous effect exists for the Thorex process.

Data contained in Tables 5-9 and 5-10 indicate little variation in calculated Zr-95 distribution coefficients with and without SiC present. Apparently, if nitric acid - SiC reaction products are formed during leaching of secondary burner ash (considered unlikely due to the inertness of SiC), they are effectively destroyed during feed adjustment.

TABLE 5-8

EFFECT OF CARBIDE CARBON ON ^{95}Zr-^{95}Nb DISTRIBUTION COEFFICIENT - DATA SUMMARY

Sample No.[a]	$\left(\frac{\text{Counts}}{\text{Unit Time}} \times \text{Dilution Factor}\right)$ Carbide Present		Calculated K Value In Presence of Carbide[b]		Calculated K Value Control Samples - No Carbide[b,c]	
	^{95}Zr	^{95}Nb	^{95}Zr	^{95}Nb	^{95}Zr	^{95}Nb
1	2872	8573	0.008	0.02	0.042	0.002
2	358,615	431,982				
3	7165	6337	20.62	1.09	0.035	0.051
4	348	5794				
5	395	3619	3.62	0.76	0.062	0.123
6	109	4744				
7	124	1581	1.35	0.38	0.029	0.395
8	92	4193				
9	71	1196	0.91	0.32	0.110	0.049
10	78	3761				
A	3035	8764	0.17	0.03	0.037	0.002
B	175,018	268,874				
C	3699	4306	12.20	1.35	0.035	0.064
D	303	3193				
E	245	1127	1.61	0.44	0.052	0.105
F	152	2569				
G	79	613	0.67	0.29	0.040	0.257
H	118	2138				
I	206	3057	1.76	1.64	0.061	0.038
J	117	1865				

(a) Numbers designate samples prepared by evaporation to 135°C only.
Letters designate samples prepared by evaporation to 135°C with subsequent steam sparging.

(b) $K = \frac{\text{Conc. Isotope Organic Layer}}{\text{Conc. Isotope Aqueous Layer}}$ = Distribution Coefficient.

(c) Typical values obtained for control samples given for comparison.

TABLE 5-9

EFFECT OF SILICON CARBIDE ON ^{95}Zr-^{95}Nb DISTRIBUTION COEFFICIENT - EVAPORATION TO 135° ONLY

Sample No.[a]	Dilution Factor	$\left(\frac{\text{Counts}}{\text{Unit Time}} \times \frac{\text{Dilution}}{\text{Factor}}\right)$		Calculated K Value[b]	
		^{95}Zr	^{95}Nb	^{95}Zr	^{95}Nb
1	None	1039	252	0.042	0.002
2	1/50	24,851	105,981		
3	None	37	43	0.035	0.051
4	None	1044	848		
5	None	3.4	39.8	0.062	0.123
6	None	54.7	323		
7	None	0.46	32.1	0.029	0.395
8	None	15.9	81.2		
9	None	2.8	20.9	0.110	0.049
10	None	25.5	423		
A	None	1088	237	0.042	0.006
B	1/50	25,854	41,582		
C	None	47.4	40.1	0.044	0.014
D	None	1089	2852		
E	None	5.1	24.6	0.088	0.035
F	None	58.2	711		
G	None	0.7	22.6	0.045	0.035
H	None	15.7	642		
I	None	3.4	20.9	0.173	0.027
J	None	19.6	771		

[a] Letters designate samples containing silicon carbide.

[b] $K = \frac{\text{Conc. Isotope Organic Layer}}{\text{Conc. Isotope Aqueous Layer}}$ = Distribution Coefficient.

TABLE 5-10

EFFECT OF SILICON CARBIDE DISTRIBUTION COEFFICIENT - EVAPORATION TO 135°C WITH STEAM STRIPPING

Sample No.[a]	Dilution Factor	$\left(\frac{\text{Counts}}{\text{Unit Time}} \times \frac{\text{Dilution}}{\text{Factor}}\right)$		Calculated K Value[b]	
		^{95}Zr	^{95}Nb	^{95}Zr	^{95}Nb
1	None	856	185	0.037	0.002
2	1/50	23,401	107,667		
3	None	32.8	44.6	0.035	0.064
4	None	942	692		
5	None	3.1	29.8	0.052	0.105
6	None	59.2	284		
7	None	1.4	26.5	0.040	0.257
8	None	35.0	103		
9	None	2.1	17.7	0.061	0.038
10	None	34.7	472		
A	None	866	162	0.034	0.004
B	1/50	25,837	38,998		
C	None	36.1	30.1	0.039	0.021
D	None	918	1406		
E	None	7.1	12.3	0.113	0.007
F	None	63	1732		
G	None	1.2	17.9	0.167	0.008
H	None	7.2	2291		
I	None	3.6	13.9	0.037	0.004
J	None	98.2	3586		

[a] Letters designate samples containing silicon carbide.

[b] $K = \frac{\text{Conc. Isotope Organic Layer}}{\text{Conc. Isotope Aqueous Layer}}$ = Distribution Coefficient.

Additional effort to identify possible conditions for zirconium-ligand destruction, e.g., treatment of the thorium nitrate denitrator pot product with strong oxidants such as permanganate or dichromate, is being considered. Such effort would necessarily include a ruthenium volatilization study.

5.4.4. Estimation of Nitric Acid Concentration in Feed Adjustment Distillates by Conductance Measurement

The feasibility of estimating the nitric acid concentration overhead during feed adjustment by measurement of distillate conductance was assessed during the quarter. The conductance method was found suitable for distillate nitric acid concentrations over a range of 10^{-3}M to 1.0M. This spans the equilibrium distillate nitric acid concentration range required for continuous production of acid-deficient denitrator pot products, as shown in Fig. 5-15 (Ref. 5-1). The conductance of nitric acid solutions does not pass through a maximum over a range of 10^{-4}% to 30% by weight. Therefore, interpretation of conductance versus nitric acid concentration is straightforward.

All conductance measurements reported herein were made with a conductivity bridge and cell (YSI Model 31 and 3401, respectively). Standard nitric acid solutions were prepared and used to calibrate the instrumentation. In order to determine the $[H^+]$ of samples from an actual feed adjustment run, the conductance of overhead samples taken from run SX-25 was measured prior to submission to the GA Analytical Chemistry Department. A calibration data plot of conductance versus HNO_3 molarity was constructed and is shown in Fig. 5-16.

Nitric acid molarity values obtained for feed adjustment run SX-25 from conductance measurements and thermometric titration (Analytical Chemistry Department) are plotted in Fig. 5-17. The agreement between the two methods, i.e., conductance and analytical, is generally within 10%, and is considered acceptable since no attempt was made to flush the denitrator pot product sampling valve between samples.

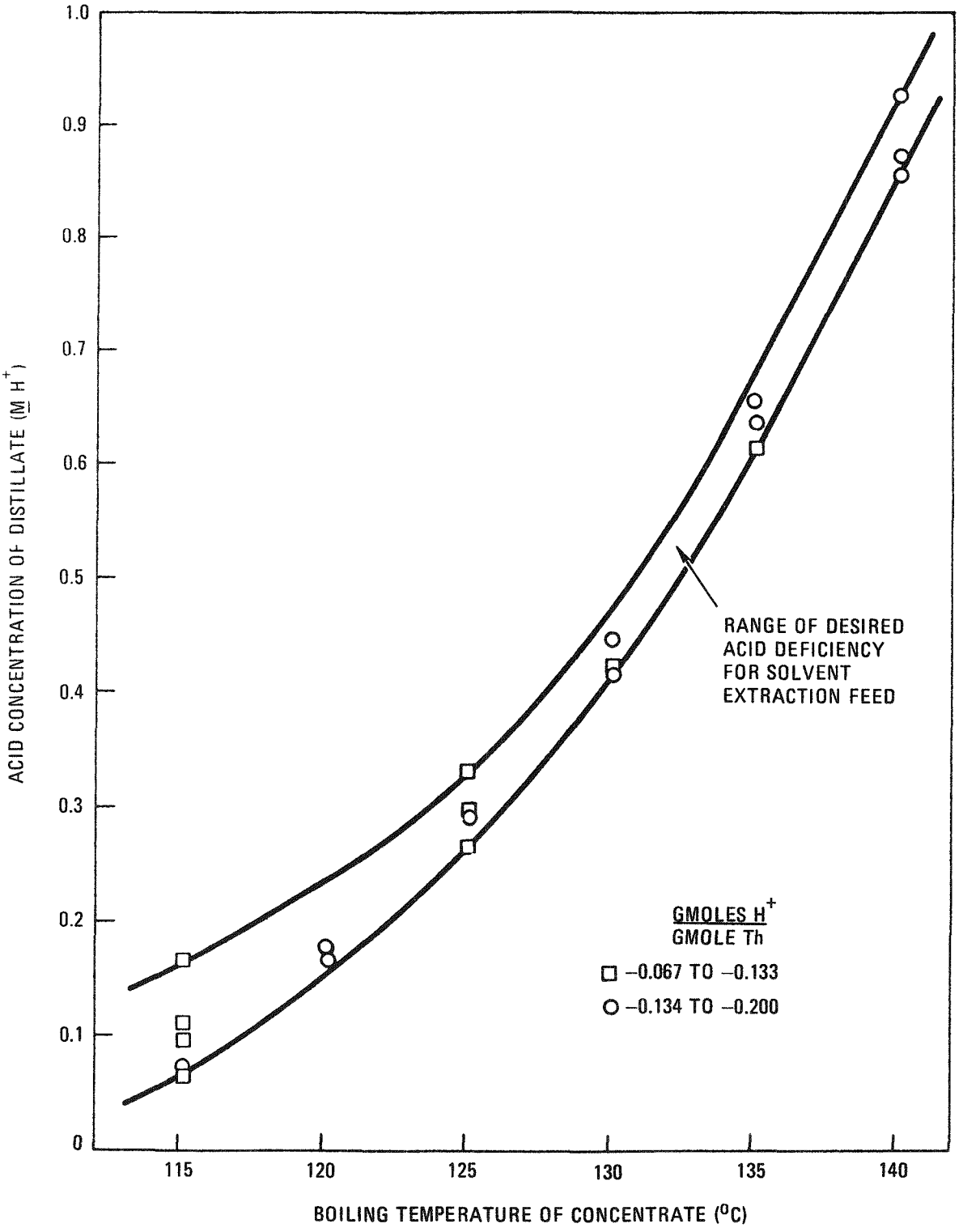

Fig. 5-15. Equilibrium data for determining continuous feed adjustment stripping water requirements (Ref. 5-1)

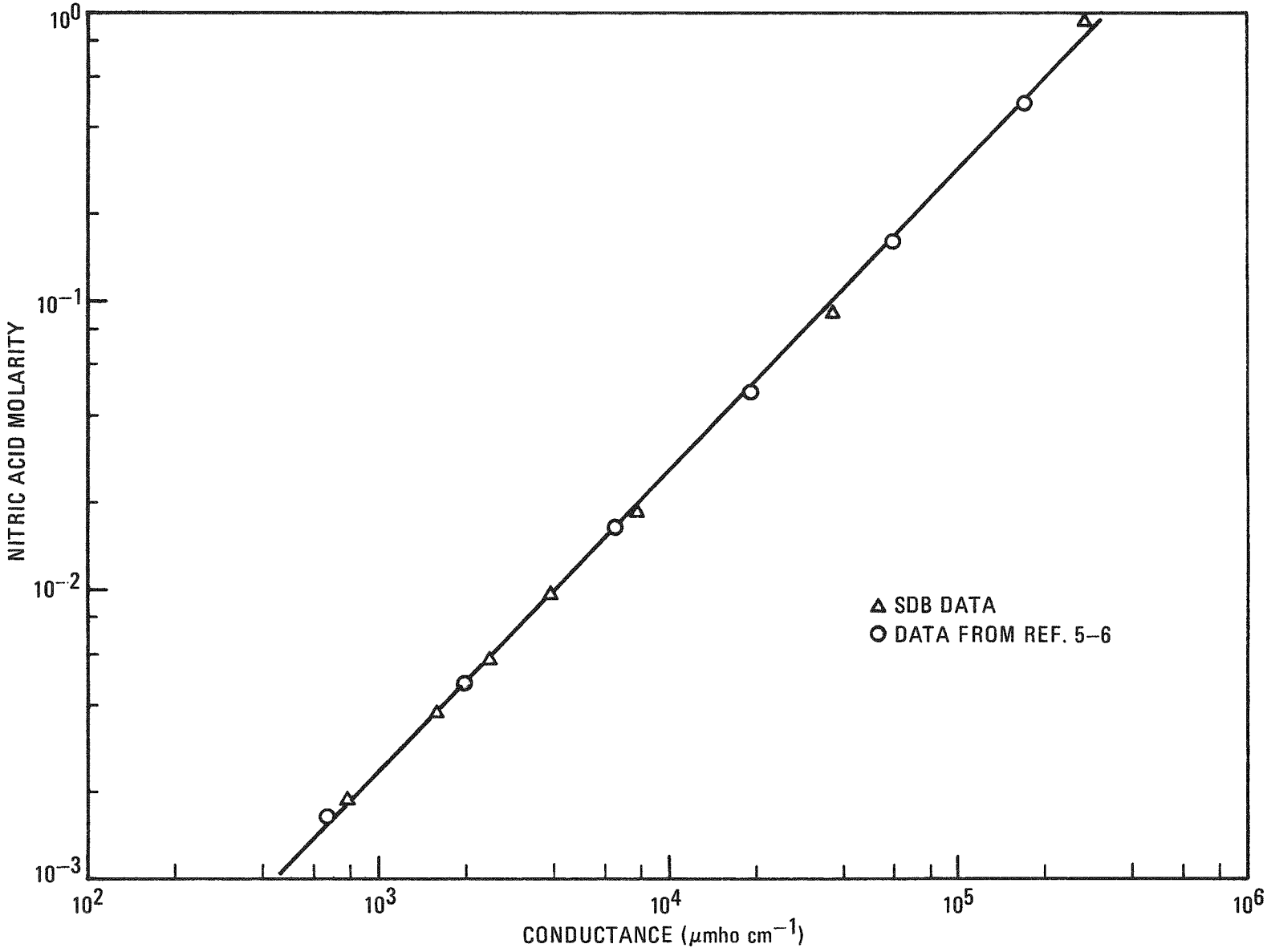

Fig. 5-16. HNO_3 molarity versus conductance

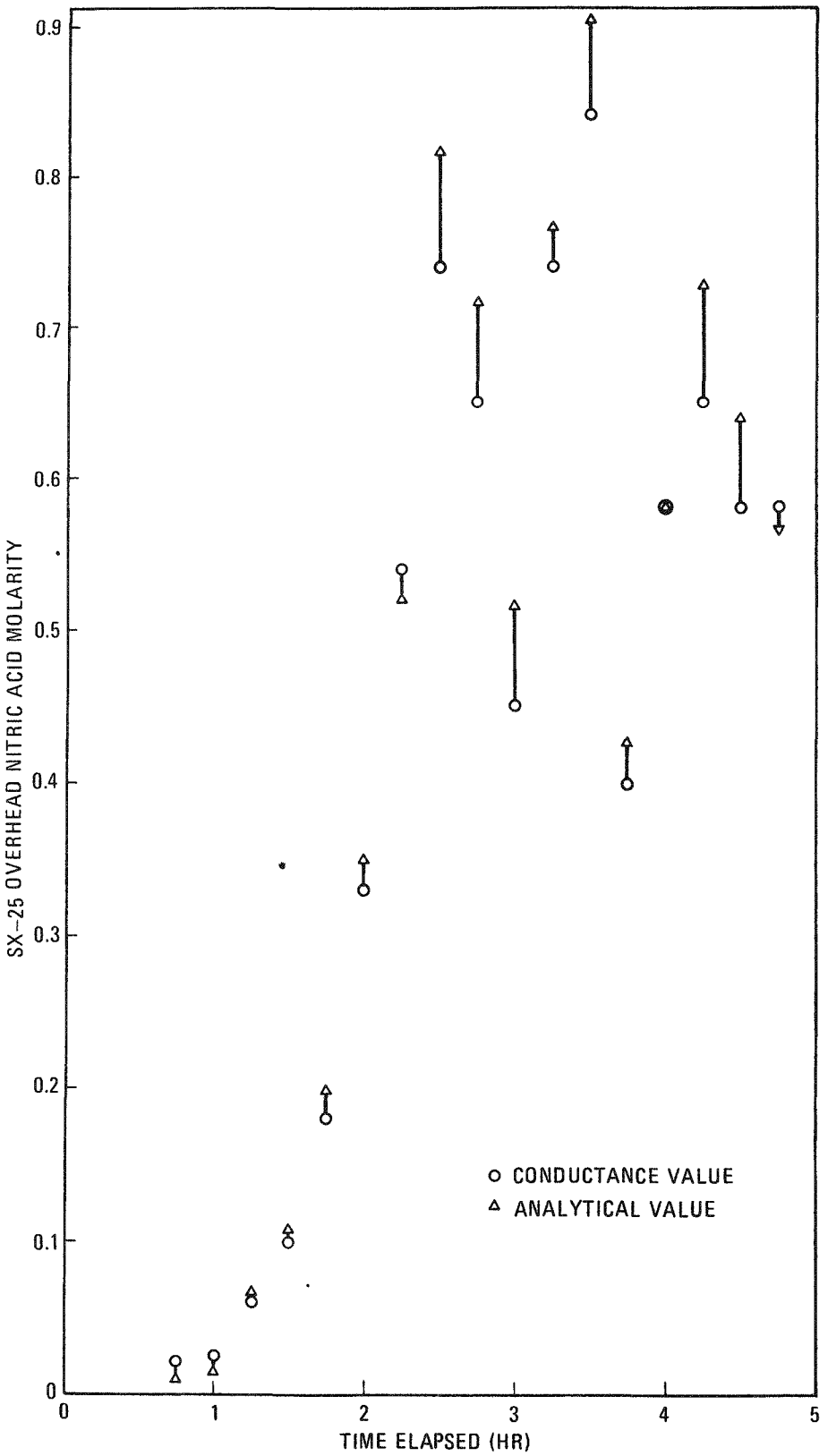

Fig. 5-17. Comparison of conductance and analytical values for HNO_3 molarity - SX Run 25

Based on the above, it is possible to use an in-line conductivity cell in the feed adjustment distillate stream to monitor the performance of a continuous feed adjustment system.

REFERENCES

5-1. "Thorium Utilization Program Quarterly Progress Report for the Period Ending May 31, 1976," ERDA Report GA-A13949, General Atomic Company, June 30, 1976.

5-2. Schulz, W. W., "Macroreticular Ion Exchange Resin Cleanup of Purex Process TBP Solvent," Atlantic Richfield Hanford Company Report ARH-SA-58, August 1, 1970.

5-3. Pollock, H., "A Stable Diluent for Purex Process Extractants," E. I. duPont deNemours & Company (Savannah River) Report DP-294, June 1958.

5-4. "Thorium Utilization Program Quarterly Progress Report for the Period Ending August 31, 1976," ERDA Report GA-A14085, General Atomic Company, September 30, 1976.

5-5. Swanson, J. L., "Improved Zirconium Decontamination in Purex Process," ERDA Report BNWL-1573, Battelle Northwest Laboratory, May 1971.

5-6. Backman Instrument Company Bulletin 4090.

6. SOLVENT EXTRACTION

6.1. SUMMARY

Two solvent extraction runs were completed during the quarter. Run 56 was used to test the operability of the intertie between the 1A centrifugal contactor and the 1S pulsed column. The first cycle of the coextraction-costrip flowsheet (Fig. 6-1) was used for this operation. Run 57 represented the first cycle of the Acid-Thorex flowsheet (Fig. 6-2). These runs utilized the facilities in the solvent extraction pilot plant. The Robatel centrifugal contactor and three pulsed columns were used for run 56, and the Robatel contactor and four pulsed columns were used for run 57.

In both runs, the uranium and thorium losses to the waste streams were typically less than 0.1%. The centrifugal contactor performed satisfactorily even with a second organic phase present. The second organic phase at the bottom of the 1S column complicates interface control. In the pilot plant unit, agitation of the solvent above the centerface was required for interface control as well as the continual reset of the controller as determined by visual observation. If a separate 1S column is used in the HRDF, a different approach to interface detection would be required.

6.2. PROCESS MODIFICATIONS

The 1AP stream from the 1A contactor was allowed to freely drain into a catch tank from which the solution was pumped to the 1S column (Fig. 6-3). This modification was made to eliminate the airlift system which had been used in runs 54 and 55. With this system no backup of the 1AP stream into the 1A contactor occurred, and thus the losses of liquid via the overflow drain which had occurred in runs 54 and 55 (Ref. 6-1) were eliminated.

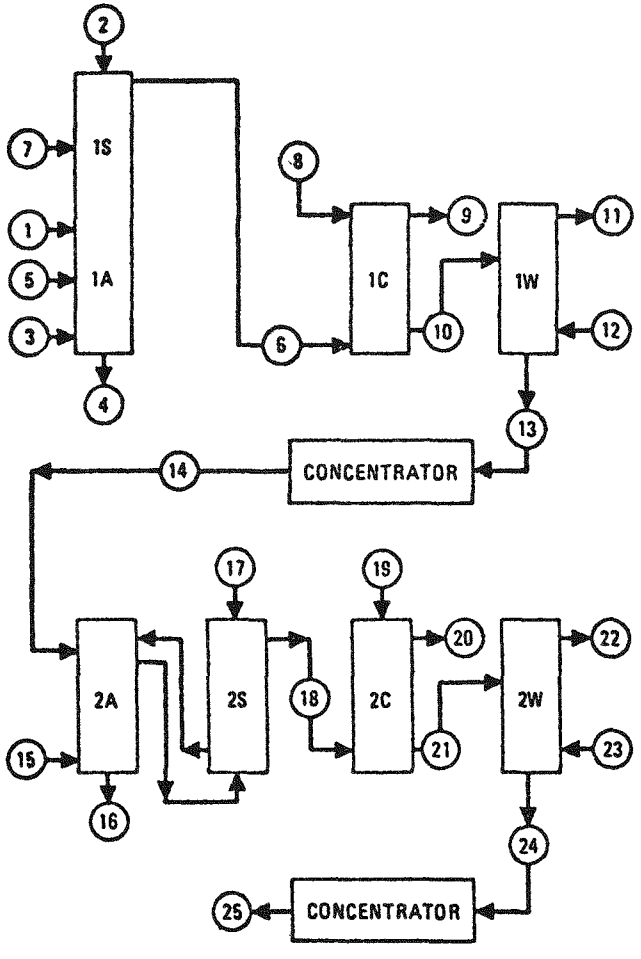

STREAM	STREAM NO.	RELATIVE FLOW	COMPOSITION U (G/L)	Th (G/L)	HNO_3 (M)
1AF	1	100	14	348	<1.0
1AS	2	104			0.01
1AX	3	1000		(30% TBP)	
1AW	4	262		(FISSION PRODUCTS)	
1AA	5	32			13.0
1SP	6	1000	1.4	35	
1AIS	7	26			5.0
1CX	8	1000			0.01
1CW	9	1000		(ORGANIC)	
1CP	10	1000	1.4	35	
1WW	11	100		(NPH)	
1WS	12	100		(NPH)	
1WP	13	1000	1.4	35	
2AF	14	100	14	348	
2AX	15	130		(5% TBP)	
2AW	16	139		255	
2AS	17	39			2.0
2AP	18	130	10.8		
2CX	19	65			0.01
2CW	20	130		(ORGANIC)	
2CU	21	65	21.6		
2WW	22	6		(NPH)	
2WS	23	6		(NPH)	
2WU	24	65	21.6		
U PRODUCT	25	6	233		

Fig. 6-1. Costrip flowsheet

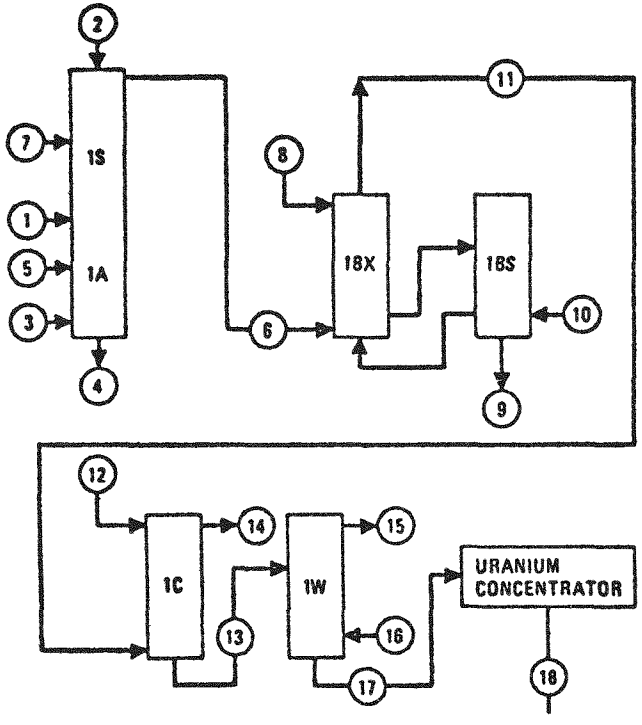

STREAM	STREAM NO.	RELATIVE FLOW	COMPOSITION U (G/L)	COMPOSITION Th (G/L)	COMPOSITION HNO_3 (M)
1AF	1	100	35	348	1.0
1AS	2	104			0.01
1AX	3	1000		(30% TBP)	
1AW	4	262		(FISSION PRODUCTS)	
1AA	5	32			13.0
1SP	6	1000	3.5	35	
1AIS	7	26			5.0
1BX	8	600			0.2
1BT	9	600	Trace	102	
1BS	10	179		(30% TBP)	
1BU	11	1180	2.98		
1CX	12	593			0.01
1CU	13	593	5.93		
1CW	14	1180		(30% TBP)	
1WW	15	59		(NPH)	
1WS	16	59		(NPH)	
1WU	17	593	5.93		
2AF	18	6	233		

Fig. 6-2. Partition flowsheet

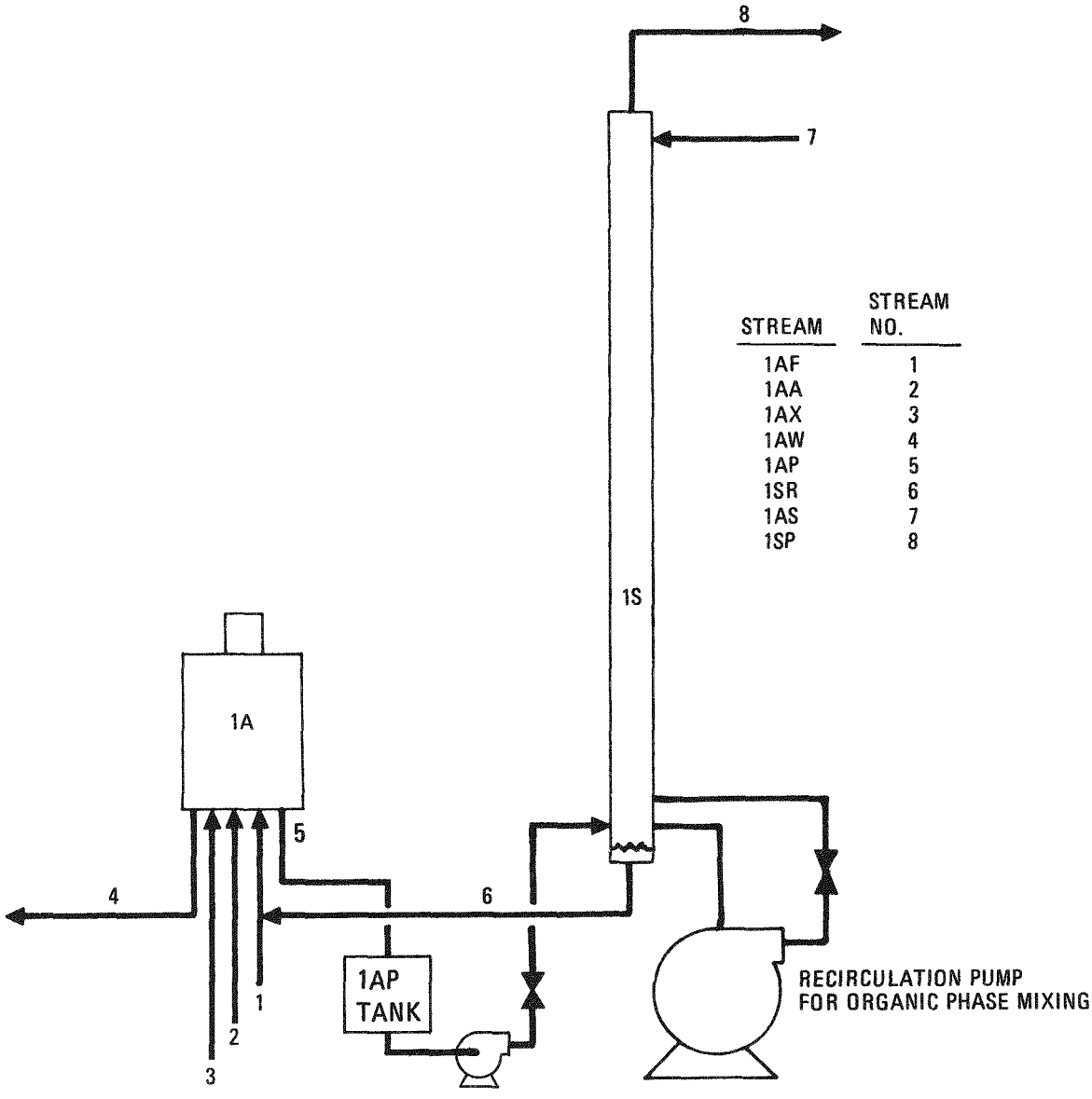

Fig. 6-3. 1A centrifugal contactor and 1S column with 1AP pump system

In the 1S column, the mixer above the interface in the bottom disengaging section (Fig. 6-3) was modified to change the mixing action from vertical to horizontal. This modification appeared to produce a more stable disengaging section by reducing the effects of the third phase (second organic phase).

6.3 RESULTS AND DISCUSSION - RUN 56

Table 6-1 contains the stream analyses and flow rate data for run 56. Table 6-2 contains the loss data and the operating conditions. Table 6-3 contains descriptions of the contactor, columns, and column cartridges.

The operation of run 56 was satisfactory. Operation of the 1A-1S system was greatly improved over runs 54 and 55. Some flooding occurred in the 1S column which may have been associated with the operation of the pump on the 1AP stream. However, since the flooding occurred in the top of the 1S column, the cause was more likely associated with the presence of the third phase (second organic phase) near the top of the column.

Losses via the 1AW stream were low throughout the run. Losses from the stripping column via the 1CW stream were also controlled at a low level.

The 1S column interface control was affected by the buildup of the heavy third phase (second organic phase) above the interface in the bottom disengaging section. The interface is controlled by the differential pressure (density) measured across the disengaging section. However, the density in the disengaging section increased through most of the run as the amount of the heavy third phase increased. As the density increased, the interface controller allowed the interface to drop. The interface was visually checked and the setting on the interface controller was increased as the interface began to drop. This method permitted the interface to be maintained near the same location throughout the run. If a system with a split at the feed point were to be used in HRDF, however, some design

TABLE 6-1
STREAM ANALYSES AND FLOW RATES FOR SOLVENT EXTRACTION RUN 56

Stream	U (g/ℓ)	Th (g/ℓ)	HNO_3 (M)	Flow (ml/min)	Relative Flow
1AF	35.3	368	0.752	84 (86) (92)	100 (100) (100)
1AS	-	-	1.042	177 (179) (170)	211 (208) (185)
1AA	-	-	12.98	26 (28) (29)	31 (33) (32)
1CX	-	-	0.015	962 (960) (1129)	1145 (1116) (1227)
1OS	-	-	-	146 (123) (114.7)	174 (143) (125)
1AW	1.3×10^{-3} (1.5×10^{-3}) (1.7×10^{-3})	4.8×10^{-3} (5.4×10^{-3}) (5.0×10^{-3})	1.538 (1.623) (1.709)	-	-
1AP	2.60 (2.30) (2.68)	38.84 (29.36) (44.2)	0.0869 (0.0695) (0.0730)	-	-
1SR	0.41 (0.51) (0.55)	69.6 (93.2) (101.9)	1.367 (1.435) (1.709)	-	-
1SP	2.68 (3.01)	24.3 (34.4)	0.133 (0.139)	-	-
1CP	2.83 (2.64) (2.76)	23.9 (24.4) (27.9)	0.137 (0.137) (0.137)	-	-
1CW	0.9×10^{-3} (1.0×10^{-3}) (1.3×10^{-3})	0.8×10^{-3} (1.0×10^{-2}) (1.0×10^{-3})	0.0173 (0.0104) (0.0173)	-	-
1OW	- (1.0×10^{-2}) (0.9×10^{-2})	- (1.1×10^{-2}) (1.1×10^{-2})	-	-	-
1OO	-	-	[30%TBP]	-	-
1AX	-	-	[30%TBP]	852 (874) (955)	1014 (1016) (1038)

Note: The data in parentheses correspond to a second and third set of operating conditions.

TABLE 6-2
LOSS DATA AND OPERATING CONDITIONS FOR SOLVENT EXTRACTION RUN 56

Contactor	Purpose	Vol Velocity (gal/hr/ft^2)	$\overline{V}_a$ (cm/sec) (a)	$\overline{V}_o$ (cm/sec) (a)	Flooding Freq (cpm)	Continuous Phase	Aqueous to Organic Ratio	Percent Loss		% Flooding Frequency	Temp. (°C)
								U	Th		
1A Centrifugal	Extraction				<500 rpm		0.337 (0.335) (0.305)	0.01 (0.01) (0.02)	0.005 (0.005) (0.004)	1200 rpm - (2300 rpm)	Ambient
1S Pulse Column	Scrub	748 (765) (818)	0.146 (0.147) (0.140)	0.700 (0.717) (0.785)	109 (106) (102)	Organic	0.208 (0.205) (0.178)			62 (64) (59)	Ambient
1C Pulse Column	Strip	586 (593) (673)	0.351 (0.351) (0.412)	0.311 (0.319) (0.349)	95 (95) (90)	Aqueous	1.13 (1.10) (1.18)	0.03 (0.03) (0.04)	0.002 (0.03) (0.003)	74 (74) (78)	47
1O Pulse Column	Solvent Wash	726 (725) (778)	0.120 (0.101) (0.107)	0.700 (0.718) (0.772)	∿100	Organic	0.171 (0.140) (0.120)			75 (70) (70)	32

Note: The data in parentheses correspond to a second and third set of operating conditions.

(a) V_a is aqueous phase superficial velocity and V_o is organic phase superficial velocity.

TABLE 6-3
SOLVENT EXTRACTION RUN 56: CENTRIFUGAL CONTACTOR AND COLUMN CARTRIDGE DESCRIPTION

Unit	Purpose	Diameter (mm)	Total Height of Mixing Area (m)	Other			
				8 stages with 0.4 liters total holdup per stage			
				Plates			Plate Spacing (mm)
1A contactor	Extraction	180	0.32	Nozzle Direction	Hole Size (mm)	% Free Area	
1S column	Scrub	51	6.7	Down	3.2	23	51
1C column	Strip	76	4.6	Up	4.8	23	Graded[a]
1O column	Solvent wash	51	5.5	Down	3.2	23	51

[a] Graded cartridge is, from the bottom, 2.6 m with 100-mm spacing, 0.5 m with 76-mm spacing, and 1.5 m with 51-mm spacing.

compensation for this wide density change would be needed. The second organic phase had no discernible effect on the mechanical operation of the centrifugal contactor.

The 10 column flooded soon after startup. The temperature in the column had not increased to the nominal level. After recovery from the flooded condition, no additional operating problems occurred with the 10 column at the increased temperature.

6.4. RESULTS AND DISCUSSION - RUN 57

Run 57 was designed to be used as the benchmark run for the partition flowsheet with the centrifugal contactor used as the extraction section. The equipment operated very well throughout the run. The 10 column was not used for solvent washing owing to failure of the electrical controls for the column pulser.

Table 6-4 contains the stream analyses and flow rate data for run 57. Table 6-5 contains the loss data and the operating conditions. Table 6-6 contains descriptions of the contactor, columns, and column cartridges.

As in run 56, the 1AP pump system worked well. No loss of liquid occurred via the overflow drain from the centrifugal contactor. A loss of liquid via the overflow drain had been observed with the airlift system used in runs 54 and 55 (Ref. 6-1). The centrifugal contactor functioned satisfactorily with a second organic phase present.

A gradual temperature increase in the effluent streams from the 1A centrifugal contactor occurred during the run. Early in the run, the temperatures of the 1AW and 1AP streams averaged about 24°C. Later in the run, the temperatures had increased to 28°C. Near the end of the run, the temperatures averaged 28.3°C.

From this operation it was concluded that the contactor can be coupled to a separated organic continuous pulse column scrub section as long as the

TABLE 6-4
STREAM ANALYSES AND FLOW RATES FOR SOLVENT EXTRACTION RUN 57

Stream	Stream No.	U (g/ℓ)	Th (g/ℓ)	HNO_3 (M)	Flow (ml/min)	Relative Flow
1AF	1	33.1	335	0.869	103 (94) (100)	100 (100) (100)
1AS	2			1.025	180 (175) (174)	175 (186) (174)
1AA	5			∿13	25 (25) (24)	24 (27) (24)
1AX	3			[30%TBP]	934 (965) (962)	907 (1027) (962)
1BX	8			0.184	700 (691) (679)	680 (735) (679)
1CX	12			0.042	588 (581) (606)	571 (618) (606)
1BS	10			[30%TBP]	153 (169) (187)	149 (180) (187)
1AW	4	1.22×10^{-2} (1.26×10^{-2}) (9.6×10^{-3})	2.3×10^{-2} (2.3×10^{-2}) (2.3×10^{-2})	1.824 (1.824) (1.824)		
1AP	-	1.22 (1.21) (1.40)	21.8 (23.1) (21.6)	0.261 (0.226) (0.243)		
1SR	-	0.43 (0.43) (0.58)	75.4 (84.1) (99.0)	1.738 (1.738) (1.738)		
1SP	6	3.43 (2.87) (2.78)	26.1 (27.1) (27.0)	0.156 (0.139) (0.191)		

TABLE 6-4 (Continued)

Stream	Stream No.	U (g/ℓ)	Th (g/ℓ)	HNO_3 (M)	Flow (ml/min)	Relative Flow
1BXT	-	0.75 (0.79) (0.68)	38.8 (46.8) (47.1)	0.423 (0.399) (0.394)		
1BU	11	2.63 (3.42) (2.06)	0.5×10^{-3} (0.5×10^{-3}) (0.5×10^{-3})	0.017 (0.035) (0.017)		
1BT	9	1.16×10^{-2} (1.14×10^{-2}) (9.2×10^{-3})	33.1 (25.3) (45.0)	0.423 (0.388) (0.388)		
1BSU	-	3.43 (4.43) (2.09)	13.97 (10.99) (19.69)	0.111 (0.087) (0.104)		
1CU	13	4.33 (5.44) (4.68)	9.3×10^{-3} (8.2×10^{-3}) (3.7×10^{-3})	0.111 (0.122) (0.104)		
1CW	14	1.8×10^{-3} ($<0.5\times10^{-3}$) ($<0.5\times10^{-3}$)	$<0.5\times10^{-3}$ (2.0×10^{-3}) (1.2×10^{-3})	0.007 (0.010) (0.010)		

Note: The values in parentheses correspond to a second and third set of operating conditions.

TABLE 6-5
LOSS DATA AND OPERATING CONDITIONS FOR SOLVENT EXTRACTION RUN 57

Contactor	Purpose	Vol Velocity (gal/hr/ft^2)	$\overline{V}_a$ (cm/sec) (a)	$\overline{V}_o$ (cm/sec) (a)	Flooding Freq (cpm)	Continuous Phase	Aqueous to Organic Ratio	Percent Loss		% Flooding Frequency	Temp. (°C)
								U	Th		
1A Centrifugal	Extraction				<500 rpm		0.330 (0.305) (0.310)	0.11 (0.12) (0.09)	0.02 (0.02) (0.02)	1200 RMP	24(b) (28) (28)
1S Pulse Column	Scrub	810 (829) (826)	0.148 (0.144) (0.143)	0.767 (0.793) (0.790)	101 (100) (101)	Organic	0.193 (0.181) (0.181)	- - -	- - -	79 (72) (71)	Ambient
1BX Pulse Column	Partition	577 (590) (591)	0.255 (0.252) (0.248)	0.397 (0.415) (0.420)	84 (83) (83)	Aqueous	0.644 (0.609) (0.591)	- - -	<0.01 (<0.01) (<0.01)	67 (67) (67)	Ambient
1BS Pulse Column	Partition-Scrub	620 (625) (630)	0.575 (0.567) (0.558)	0.126 (0.139) (0.154)	86 (85) (85)	Aqueous	4.58 (4.09) (3.63)	0.24 (0.25) (0.19)	- - -	70 (71) (71)	Ambient
1C Pulse Column	U Strip	541 (554) (567)	0.215 (0.212) (0.211)	0.396) (0.414) (0.430)	98 (97) (96)	Aqueous	0.541 (0.512) (0.527)	0.06 (<0.02) (<0.02)	- - -	66 (67) (68)	53

(a) $\overline{V}_a$ is aqueous phase superficial velocity; $\overline{V}_o$ is organic phase superficial velocity.

(b) Temperatures for the 1A contactor are the average temperatures of the two effluent streams.

Note: The data in parentheses correspond to a second and third set of operating conditions.

TABLE 6-6
SOLVENT EXTRACTION RUN 57: CENTRIFUGAL CONTACTOR AND COLUMN CARTRIDGE DESCRIPTION

Unit	Purpose	Diameter (mm)	Total Height of Mixing Area (m)	Other			
1A contactor	Extraction	180	0.32	8 stages with 0.4 liters total holdup per stage			
				Plates			Plate Spacing (mm)
				Nozzle Direction	Hole Size (mm)	% Free Area	
1S column	Scrub	51	6.7	Down	3.2	23	51
1BX column	Partition	76	5.8	Up	4.8	23	Graded[a]
1BS column	Partition-scrub	51	5.2	Up	4.8	23	51
1C column	U strip	76	4.6	Up	4.8	23	Graded[a]

[a] Graded cartridge is, from the bottom, 2.6 m with 100-mm spacing, 0.5 m with 76-mm spacing, and the remainder with 51-mm spacing.

contactor organic outflow is not restricted and the pulse column has some method of mechanical mixing above the interface to prevent the second organic phase from separating. If this complicated contactor is used for extraction, two additional pumps are required to couple the contactor to a pulse column scrub section.

A cyclic flood developed in the 1BS column in the early part of run 57. The flood was stopped by a reduction in the frequency of the column pulse rate.

REFERENCE

6-1. "Thorium Utilization Program Quarterly Progress Report for the Period Ending August 31, 1976," ERDA Report GA-A14085, General Atomic Company, September 30, 1976.

7. DRY SOLIDS HANDLING

7.1. SUMMARY

Since the completion of the installation and checkout of the solids handling system, progress has been made with both component and system qualification testing.

Work involving inlet filters, conveying lines, in-bunker filters, blowers, bunkers, level sensors, feeders, and weigh cells is described in this section. The inlet filter on the secondary burner product removal system successfully contained material when the line flooded. Steps are being taken to monitor erosion of bends in conveying lines. Five of the six in-bunker multitube metal filters have been pre-loaded. These filters have proven to be efficient. The effective volumes of two of the bunkers have been measured using level sensors. The primary burner feeder has been calibrated for the feed materials used so far. The calibration of the weigh cells is progressing.

Two of the six pneumatic transfer subsystems have been tested. The primary burner product removal system has successfully transported crushed graphite, simulated crushed fuel elements, and fuel particles. The transport of particles has been tested at 700°C. The secondary burner product removal system plugged during both trials to date. This is apparently caused by the initial surge of material from the burner.

Progress is being made toward obtaining similar results with shear cells at GA and ORNL.

7.2. INTRODUCTION

The development work, as described in the Experimental Plan, is divided into several development stages:

1. Cold laboratory development.
2. Hot laboratory development.
3. Cold engineering development.
4. Hot engineering development.
5. Cold prototype development.
6. Procedure development.

During this quarter, progress was made in development stages 1 and 3.

7.3. COLD LABORATORY DEVELOPMENT (DEVELOPMENT STAGE 1)

7.3.1. Effect of Irradiation on Flow Properties

The behavior of particulate solids in gravity flow equipment depends on material properties such as internal friction, cohesive strength, wall friction, and density. In order to establish the effect of irradiation on cohesive strength and internal friction, ORNL and GA are conducting a joint investigation using crushed graphite. The flow properties of particulate solids are measured on a laboratory scale in a shear cell. For this investigation Jenike shear cells are used. A cylindrical top, filled with material, is loaded with weights and pushed across a filled cylindrical base at a constant speed. The force required to overcome friction in the shear plane between the top and the base is recorded. Discussions between personnel from both locations in August resulted in standardizing the operating procedures. More recently, a sample of unirradiated graphite was crushed and tested at ORNL and then was sent to GA, where it was tested under the same applied loads. The two sets of results showed significant differences. Further discussions in November at ORNL resulted in the identification of small, but possibly significant, differences in the two shear cells, particularly in the alignment, speed, and shape of the pushing mechanism which applies a shear force to the cell.

7.3.2. Effect of Temperature on Flow Properties

Commercial reprocessing facilities will be dealing with irradiated material which will be at temperatures above ambient owing to fission product decay heat. It would be preferable to measure the effect of irradiation and temperature simultaneously, but hot cell operating constraints limit flow property measurements with irradiated material to ambient temperatures. Therefore, these two effects must be determined separately. A heated consolidation bench, in which unirradiated samples can be consolidated at elevated temperatures, has been purchased and installed.

7.4. COLD ENGINEERING DEVELOPMENT (DEVELOPMENT STAGE 3)

7.4.1. Procurement, Installation, and Checkout

Procurement, installation, and checkout are complete for the solids handling system (see Fig. 7-1). The system is divided into six subsystems (see Fig. 7-2):

Subsystem No. 1. Crusher product removal system.
Subsystem No. 2. Primary burner feed system.
Subsystem No. 3. Primary burner product removal system.
Subsystem No. 4. Particle classifier feed system.
Subsystem No. 5. Particle crusher feed system.
Subsystem No. 6. Secondary burner product removal system.

The engineering detail drawings have been revised to incorporate minor design changes made to reduce manufacturing costs.

The pilot plant documentation is now complete except for the maintenance manual (MM520101), which is being drafted, and the design report (DR520101), which is scheduled for FY-78.

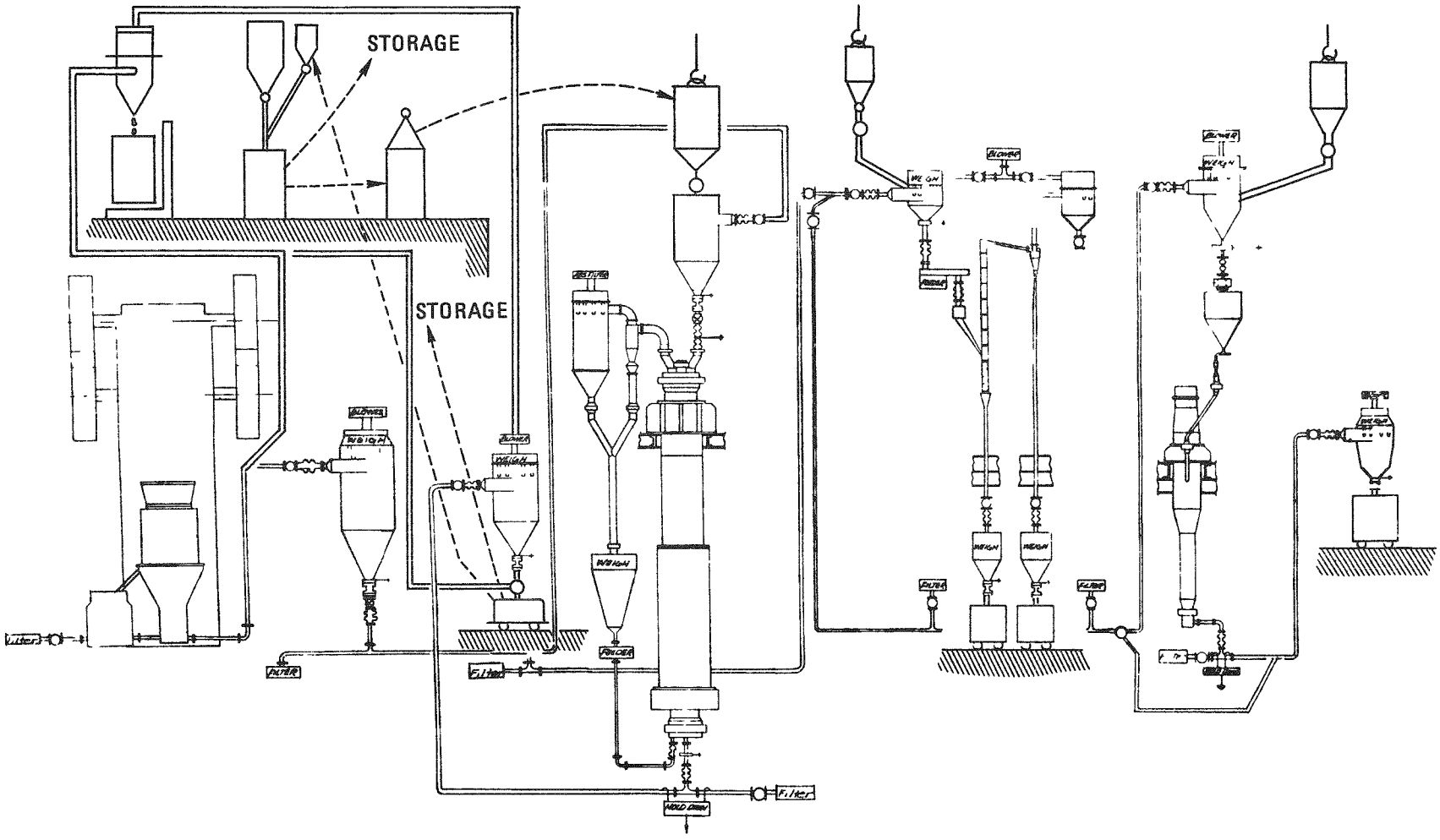

Fig. 7-1. Solids handling system

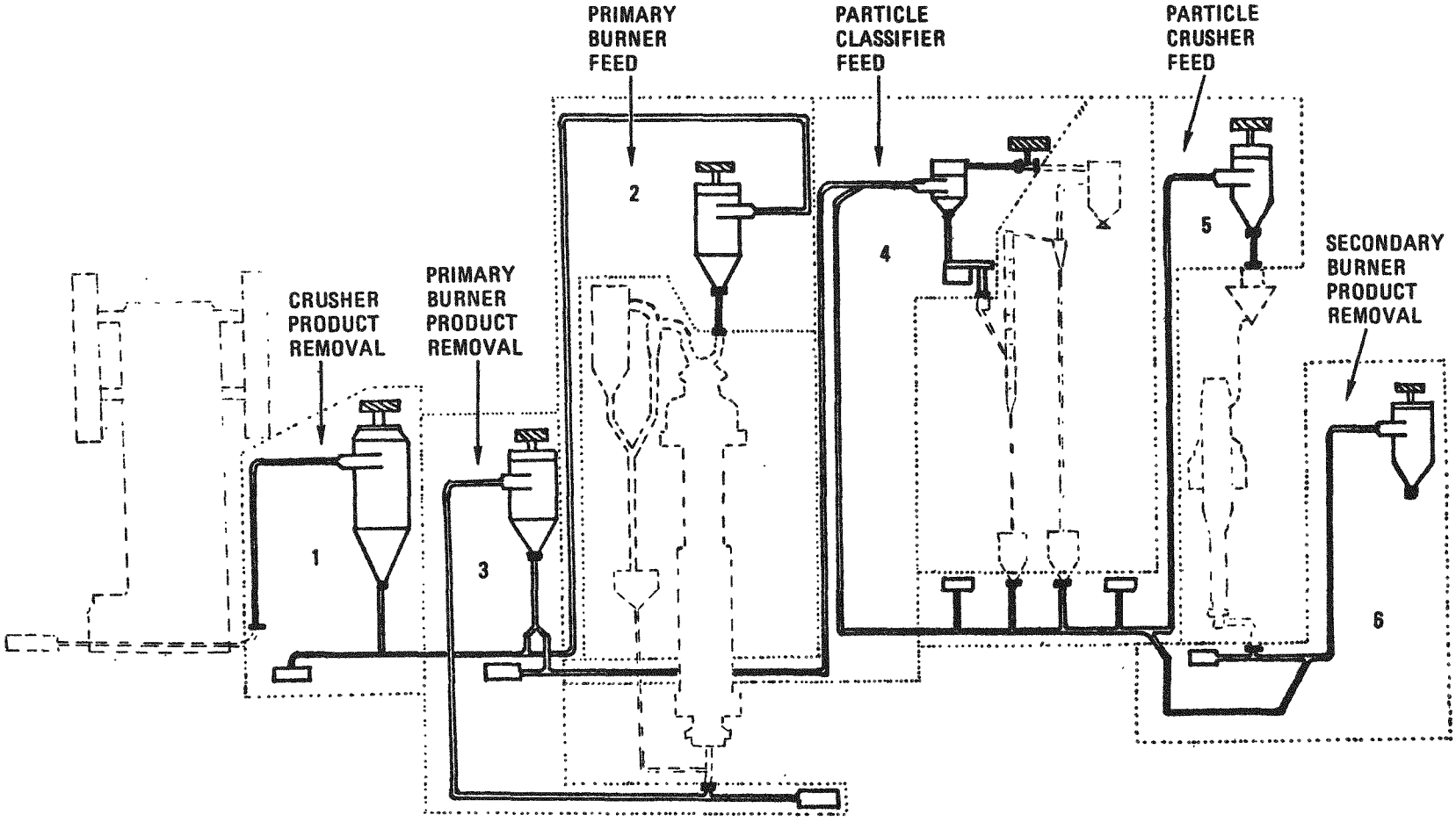

Fig. 7-2. Solids handling subsystems

7.4.2. Qualification Testing

The activities in the coming months will be concerned with qualification testing, which can be defined as partial verification of the design under simulated conditions prior to sequential operation. The qualification testing of each subsystem is divided into two phases. Phase I is concerned with component testing and Phase II with system testing.

7.4.2.1. Component Qualification

7.4.2.1.1. Description of Components.

Inlet Filters. At the beginning of each pneumatic transport line, there is a HEPA filter (see Fig. 7-3). In order to prevent damage from above, a protective plate is placed over the inlet to the filter. These filters serve two purposes: to prevent stray particulates from entering the line and, in the event of a mishap, to prevent particulate material from leaving the line. It is important to verify the latter capability.

Conveying Lines. The conveying lines are 2-in. and 1-1/2-in. o.d. stainless steel tubing. The lines are in manageable sections, which are clamped together. Bends are gradual (bend radius to pipe diameter = $\sim$12), and the first bend in each subsystem is placed as far away from the solids inlet as possible, in order to allow the conveying mixture to accelerate prior to the deceleration in the bend. As a conveying line erodes, bends usually suffer the worst effects. The rate of erosion is of interest. Just before the end of each conveying line there is a bunker inlet valve, which isolates the bunker, a bellows, needed for weigh cell accuracy, and an expansion in the line diameter. This expansion is intended to begin slowing down the conveyed particles. The tangential entry to the bunker prevents perpendicular impingement of particulates on metal walls or filter surfaces (see Fig. 7-4).

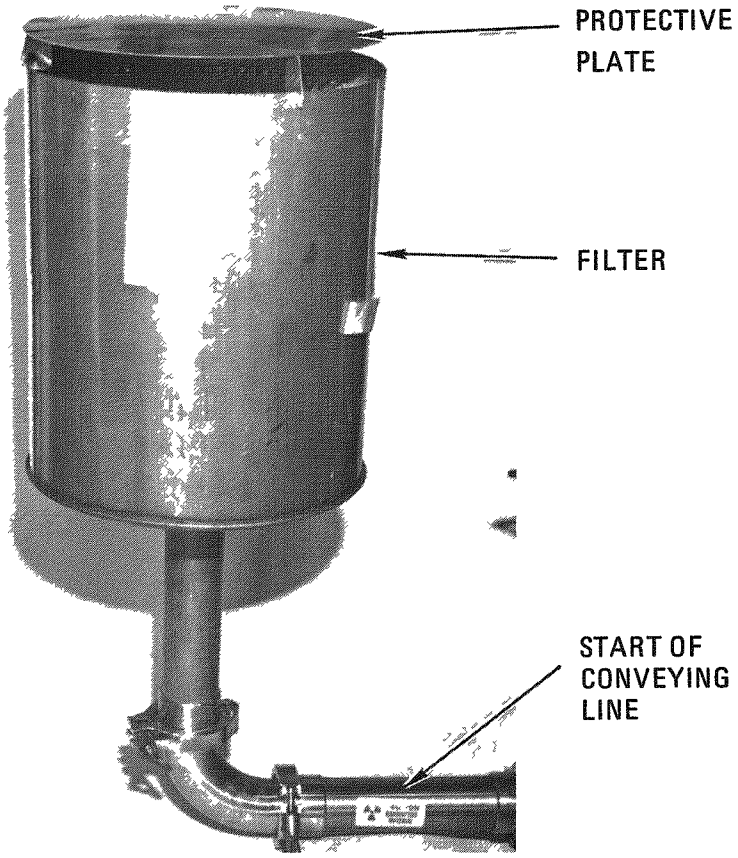

Fig. 7-3. Conveying line inlet filter [line diameter 5.08 cm (2 in.)]

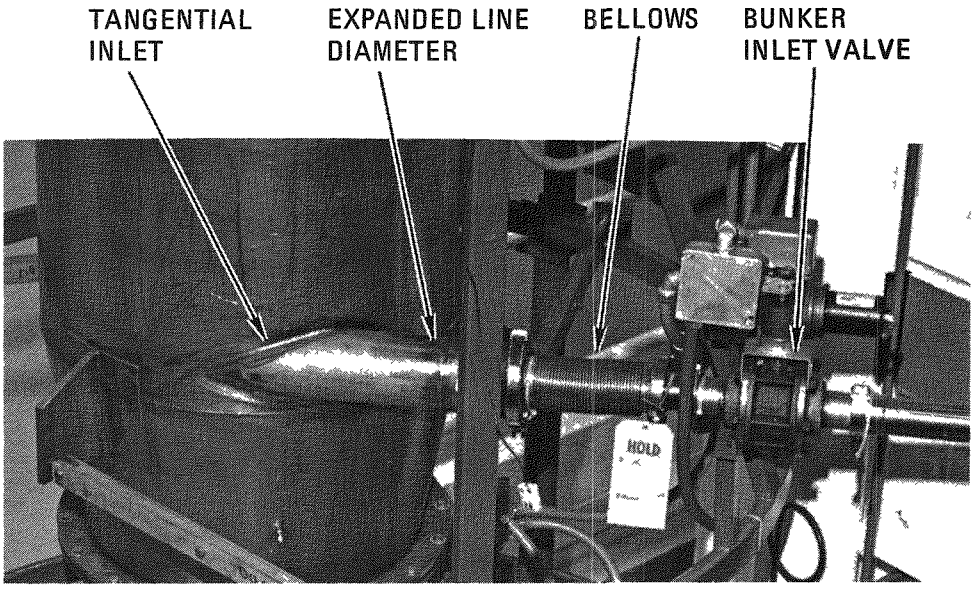

Fig. 7-4. End of a pneumatic conveying line [5.08 cm (2 in.) conveying line expanding to 10.16 cm (4 in.); 63.50 cm (25 in.) diameter bunker]

Bunkers. The bunkers perform storage, weighing, dosing, and pneumatic transfer receiving functions. They were sized conservatively; i.e., the top surface of the bed was assumed to be concave. They are designed to discharge the entire contents and to withstand 107 kPa and 59 kPa. A pressure relief valve opens at 107 kPa, and in the event that the valve fails, a bursting disk is available. The 59 kPa pressure is relieved at the blower. Three bunkers, the crusher product, the primary burner feed, and the secondary burner product bunkers, are equipped with aerated bottoms (see Fig. 7-5). Gas flows via a flowmeter through a woven steel mesh cone, so that the bunker contents are loosened and can flow easily.

In-Bunker Filters. Inside the bunkers are porous stainless steel filter pipes (see Fig. 7-6) to separate the gas and solids received from the pneumatic conveying lines. They have a mean pore size of 5 μm and are intended to prevent particles larger than 5 μm from entering the blowers, where they could damage the rotors. The filters are cleaned by a reverse flow of high-pressure CO_2, which is distributed through a manifold and solenoid valves (see Fig. 7-7), which are controlled by a cam-timer. Both the CO_2 supply line and filter exhaust line have bellows connections, as required by the load cells. In order to observe the pressure drop across the filters, a differential pressure gauge is installed on each bunker. The pressure tap on the bunker also serves as an inlet for argon from the argon-dump system, described in the last quarterly report (Ref. 7-1) (see Fig. 7-8).

Blowers. The rotary blowers are mounted in frames (see Fig. 7-9), together with an electric motor, an inlet filter, an outlet filter, an underpressure relief valve set at 40 kPa (12 in. Hg), and a pressure gauge, which also registers in the control room. Except for the variable-speed classifier blower, the blowers are fixed-speed units. The major goal of the system testing is to establish a suitable speed for permanent operation. The gas, after compression, goes to a central vent system.

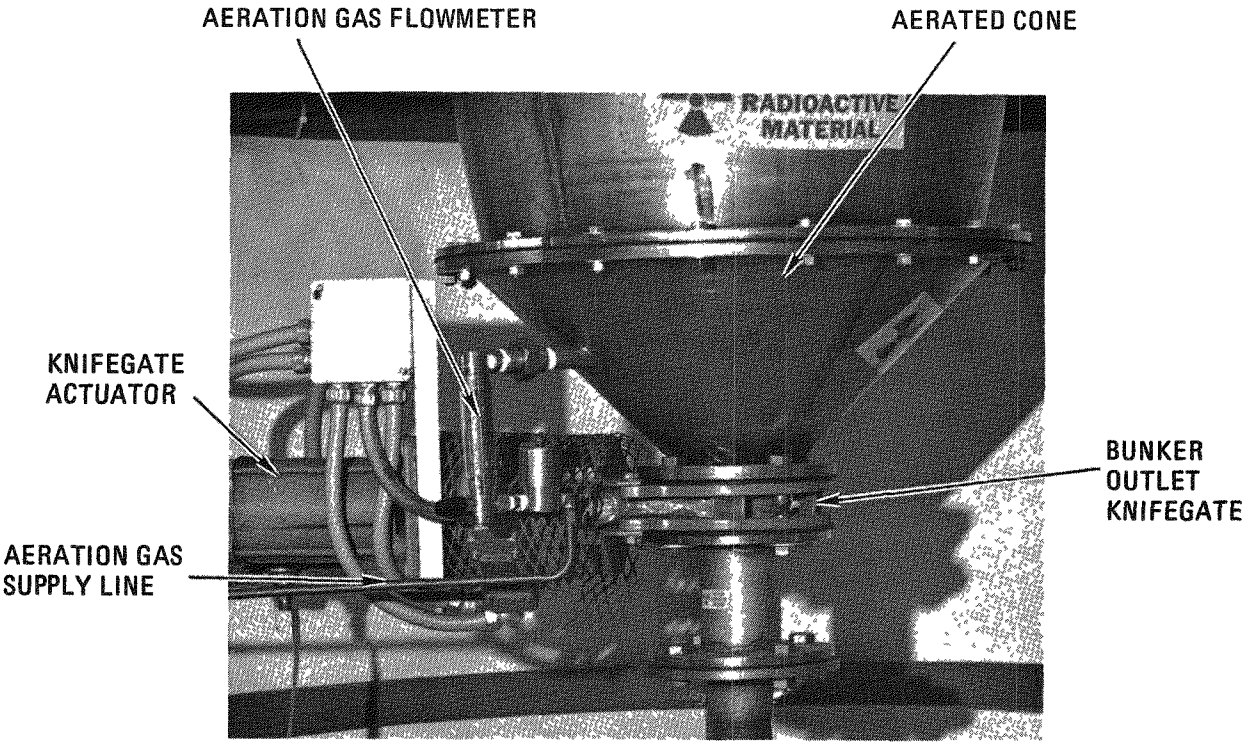

Fig. 7-5. Aerated cone and bunker outlet [5.08 cm (2 in.) diameter]

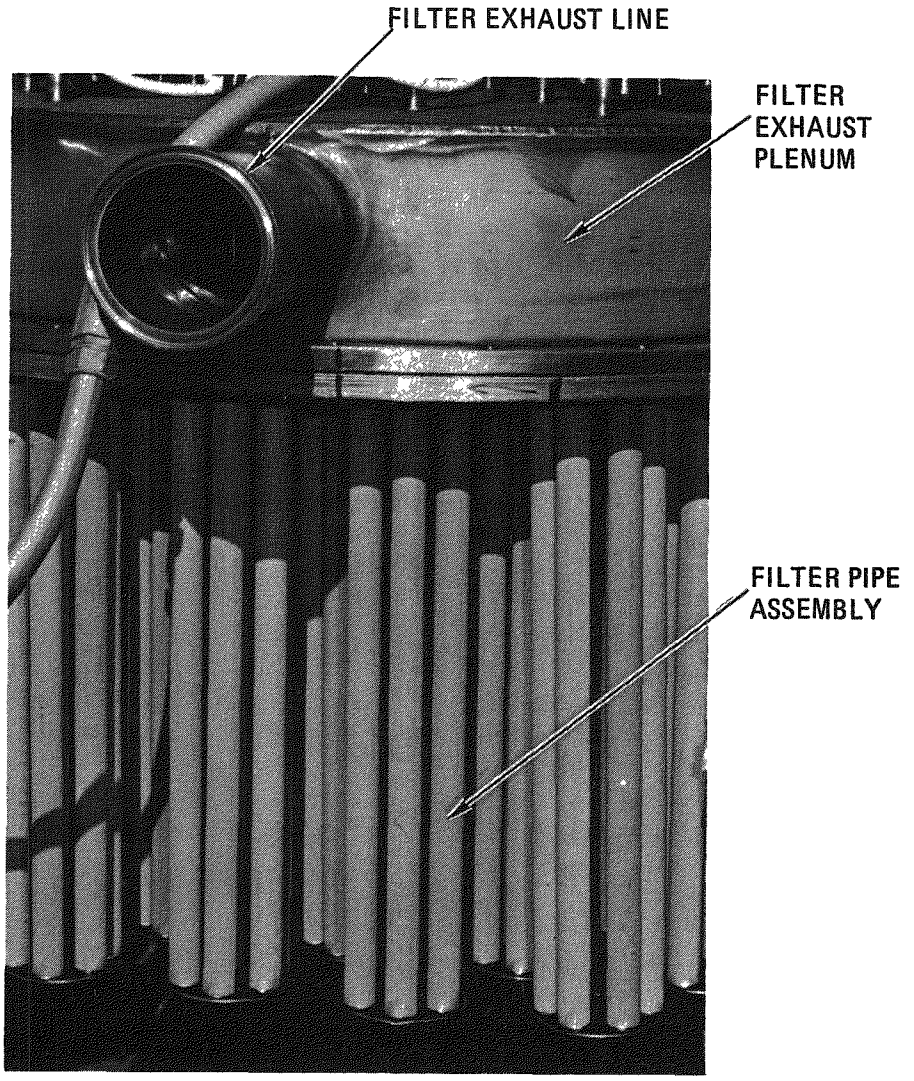

Fig. 7-6. Porous stainless steel in-bunker filter pipes [2.54 cm (1 in.) diameter pipes in groups of six]

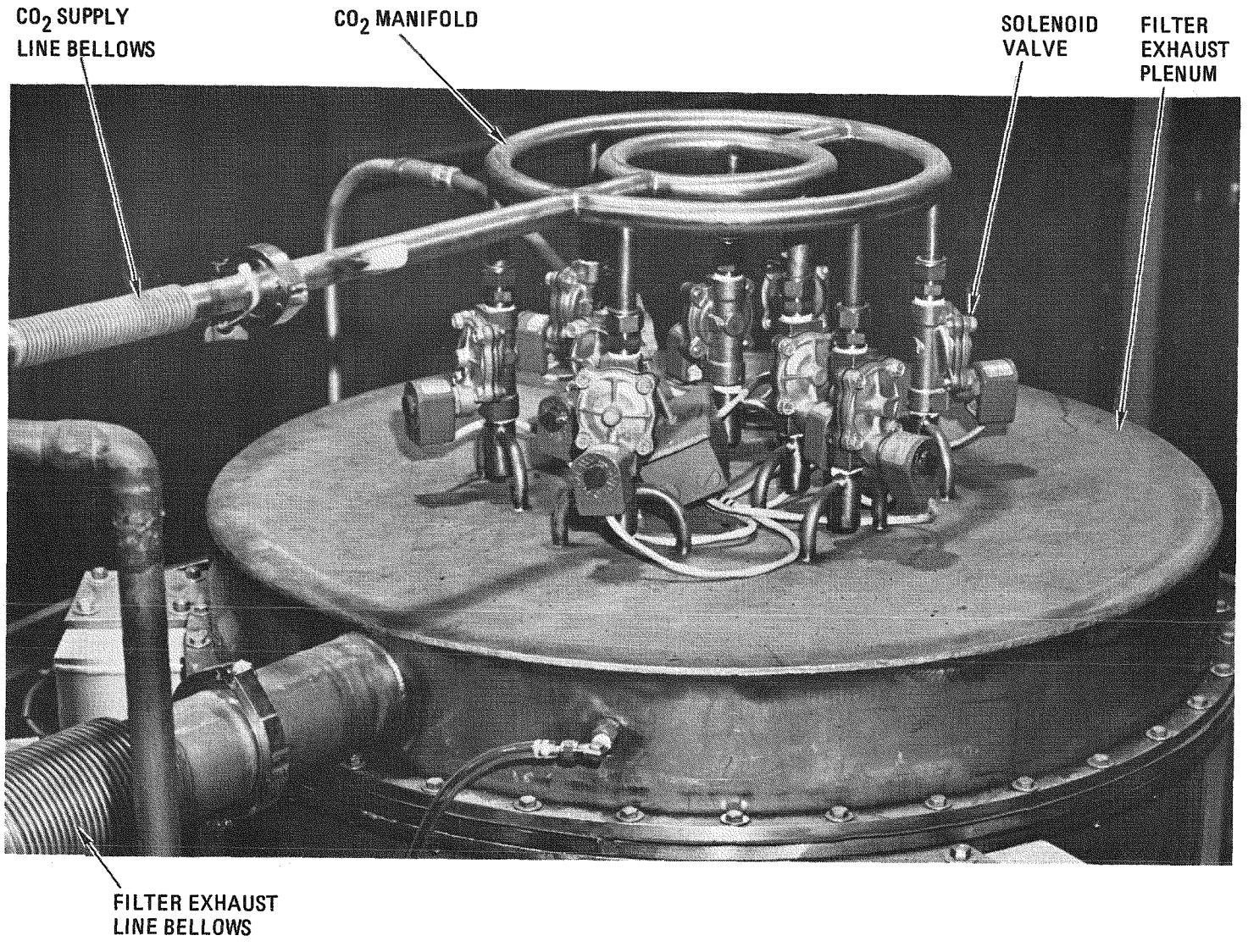

Fig. 7-7. In-bunker filter blow-back assembly [91.44 cm (36 in.) diameter bunker]

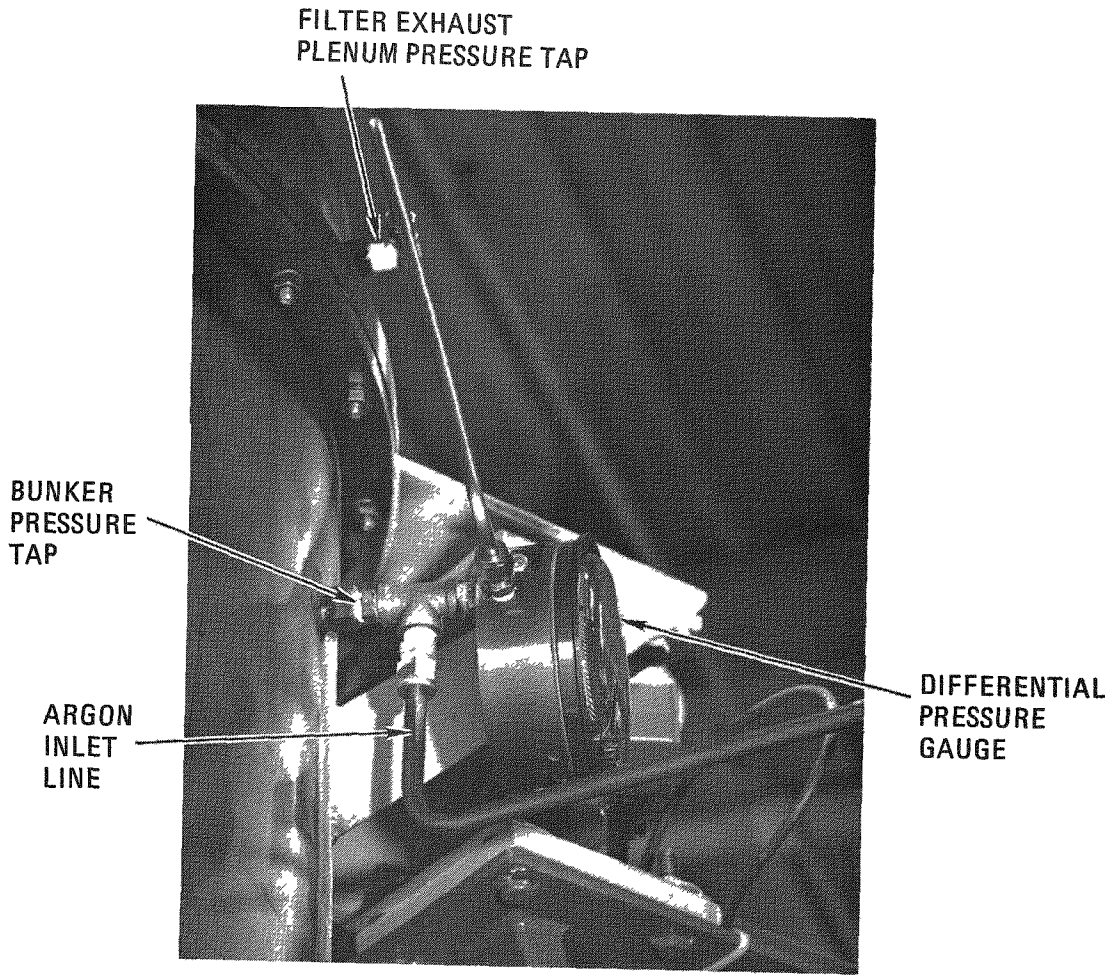

Fig. 7-8. In-bunker filter pressure drop measurement arrangement and argon inlet line

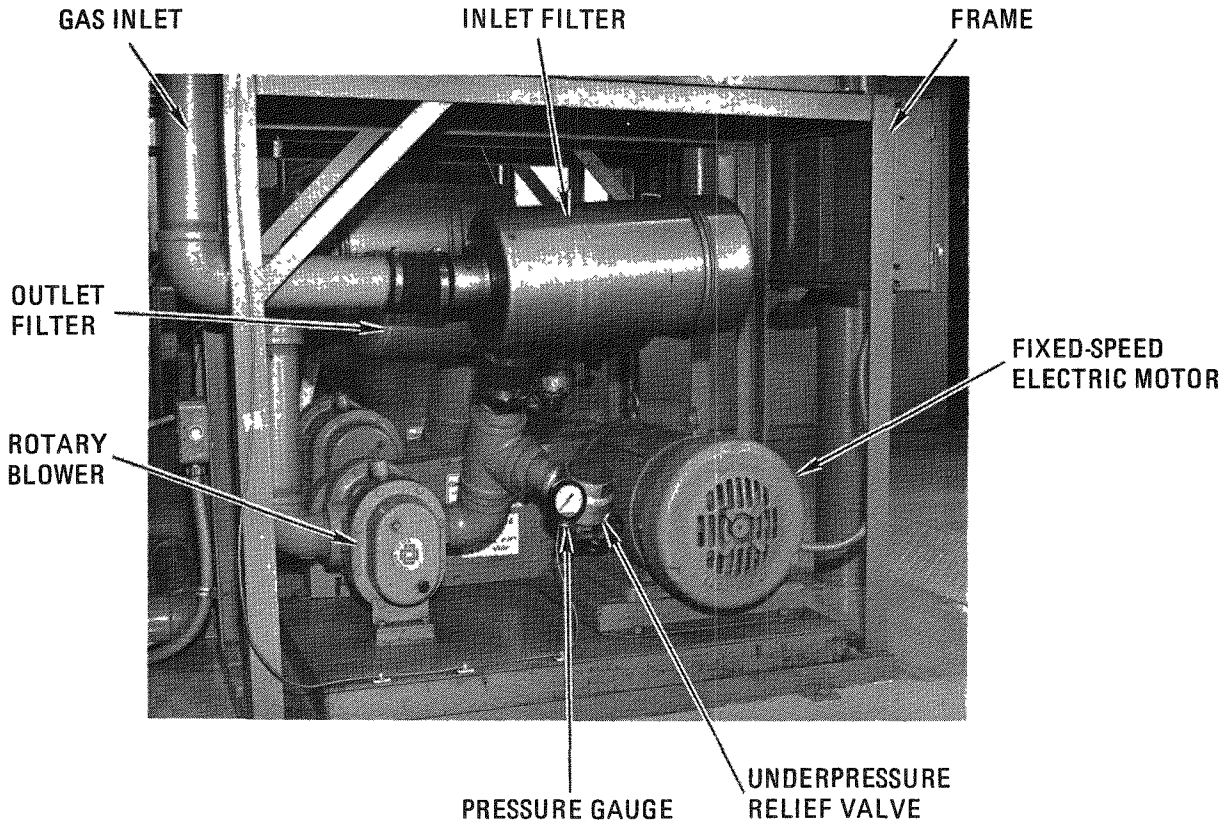

Fig. 7-9. Rotary blower used to provide moving air for pneumatic conveying

Level Sensors. In order to prevent the overfilling of bunkers, level sensors are used. The principle involved is the interruption of an ultrasonic beam, which is propagated between two sensors. These sensors are placed just below the level at which the conveying line enters (see Fig. 7-10). An alarm in the control room is activated when this level is reached, and the feeding of solids to the conveying line can be stopped automatically. Experimental determination of the capacity of the bunkers fitted with these devices (subsystems No. 1 through 5) is required.

Feeders. A feeder is defined as a device which controls the rate at which material leaves a bunker or some other form of storage. The only mechanical feeders in the system are a star valve, which meters crushed fuel elements to the primary burner, and a vibrating feeder, which meters burned-back fuel particles to the classifier. The flow rate out of the other bunkers is controlled by the size of the outlet. It is important to verify that the flow rate is consistent with the capacity of the conveying system and that the orifice required for such a flow rate is not too small for steady flow. The bunker outlets are gate valves (see Fig. 7-5).

Weigh Cells. The bunkers rest on load cells (see Fig. 7-11) which record the material weight continuously. Upon command, a value of the weight, averaged over 10 sec, is printed out. Several special provisions have been made to ensure that accurate readings are obtained. The bunker assemblies themselves are supported on three load cells which are mounted on a cage (see Fig. 7-12). All connecting lines either contain metal bellows or, if they are narrow, are unsupported over at least two horizontal feet. In order to prevent rotation of the bunkers, tie bars are attached to the bunker and the support cage (see Fig. 7-13). Calibration of the load cells is required to verify the adequacy of these precautions.

7.4.2.1.2. Component Testing.

Inlet Filters. During the first dump of product from the secondary burner into the secondary burner product removal system (subsystem No. 6,

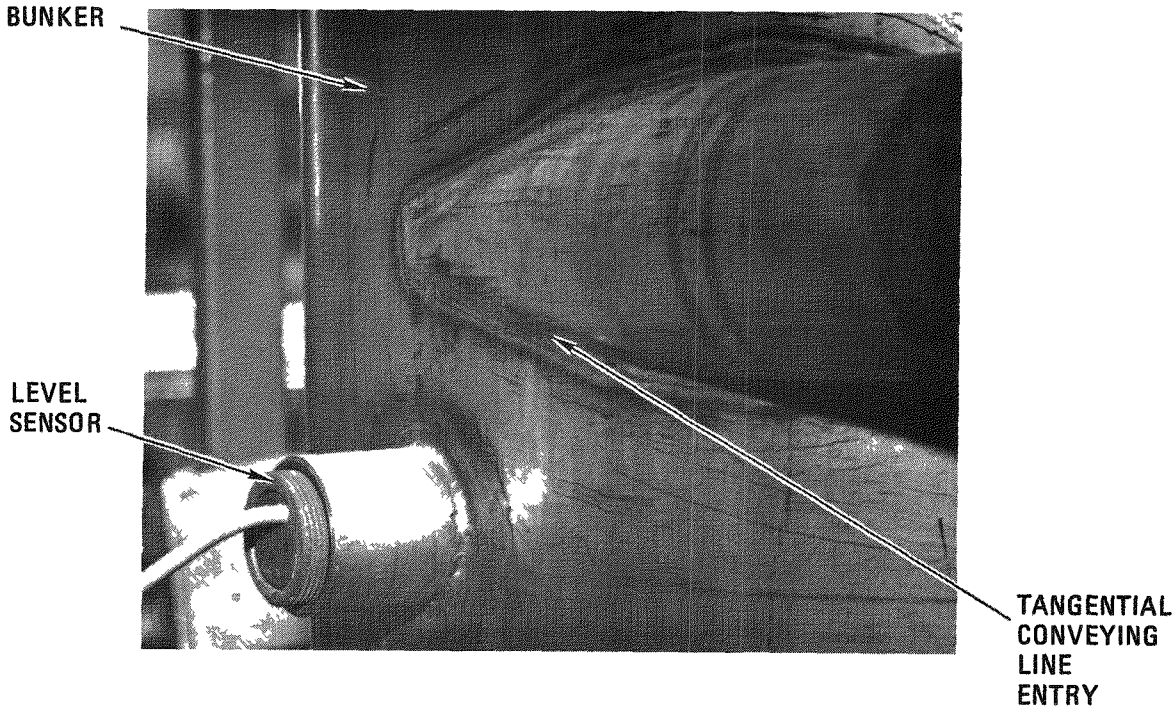

Fig. 7-10. Ultrasonic level sensor [5.08 cm (2 in.) diameter] used for indicating a maximum safe level in a storage bunker

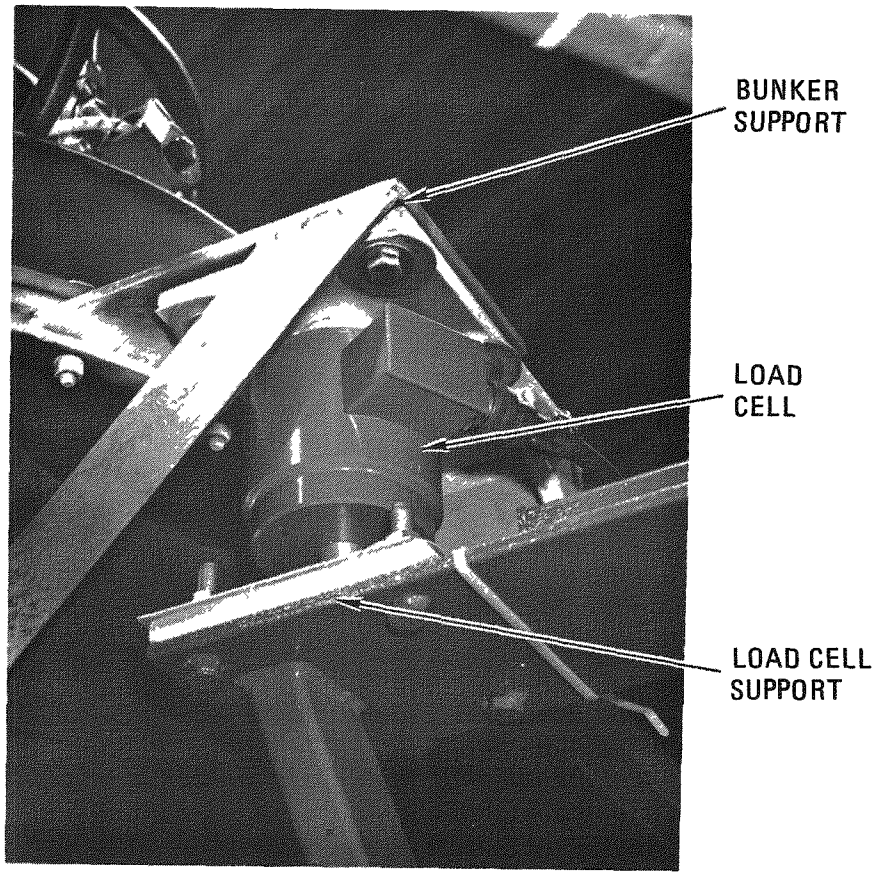

Fig. 7-11. Bunker load cell used for monitoring the weight of material within

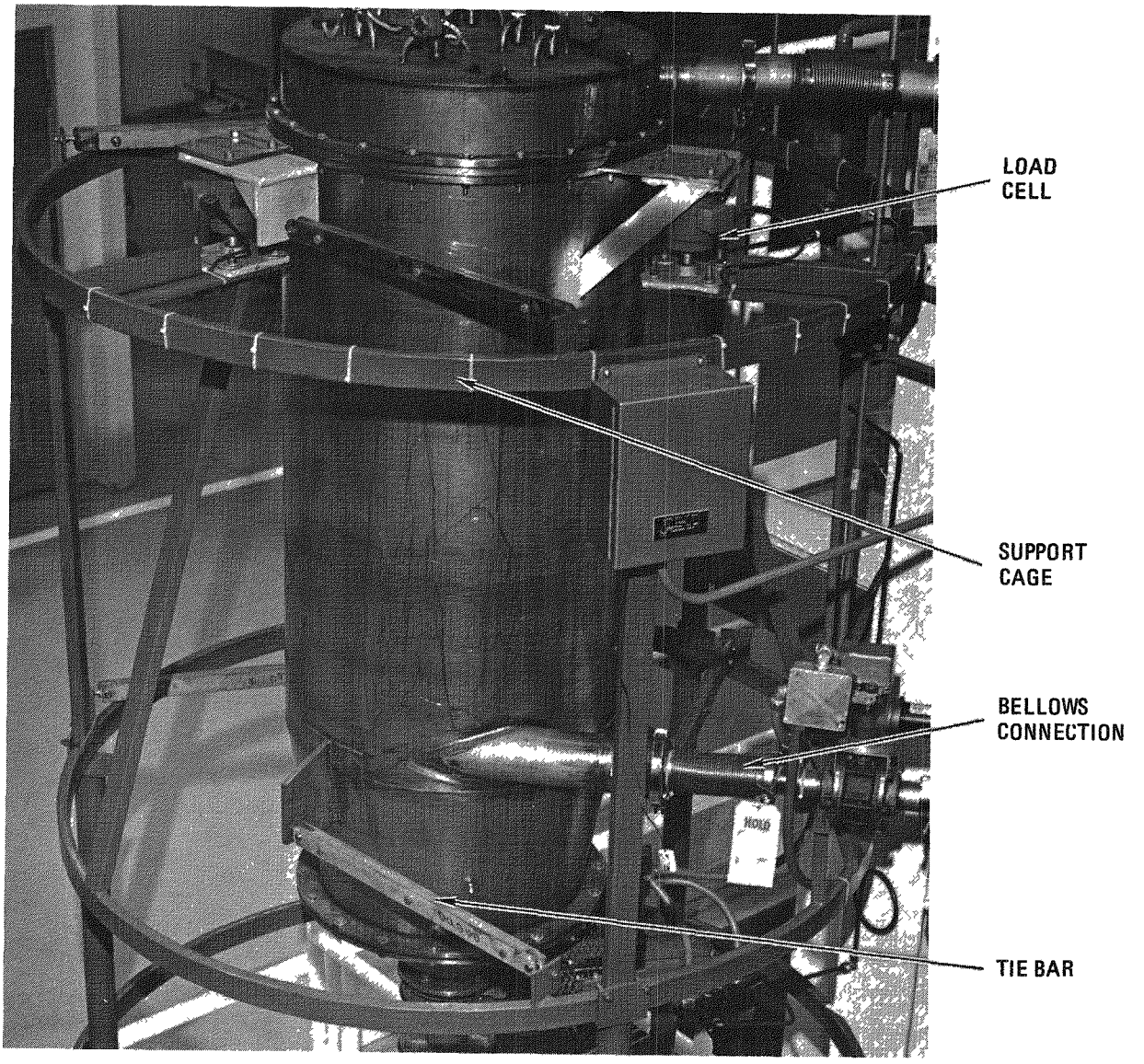

Fig. 7-12. Bunker and support cage [63.50 cm (25 in.) diameter bunker]

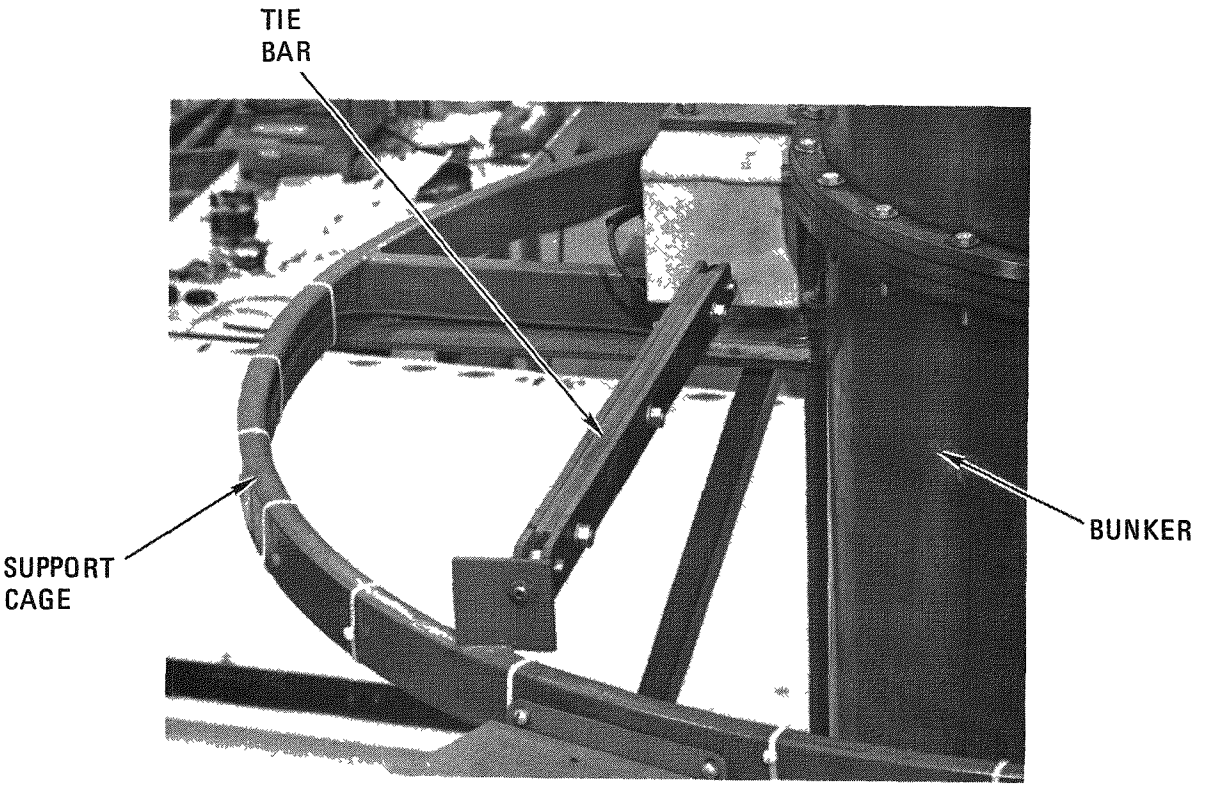

Fig. 7-13. Bunker tie bar used to prevent rotation of the bunker on its load cells

see Section 7.4.2.2.7), material flowed backwards, against the gas flow, and down into the inlet filter, which was below the level of the burner outlet and pointing downward. The outside of the filter was subsequently examined for evidence of radioactivity. None was observed. Since secondary burner product is the finest material the solids handling system needs to convey (mean size ≃ 50 μm), it may be concluded that the inlet filters adequately perform the function of containing material. In subsequent secondary burner product removals, the filter was installed pointing upward and at a height close to the level of the fluid bed. This is intended to prevent fluidized material from entering the filter under "hydrostatic" pressure. As part of the testing of the primary burner product removal system (subsystem No. 3, see Section 7.4.2.2.4), the pressure across the inlet filter was measured over a range of gas velocities. A Magnahelic gauge, mounted on a short length of pipe, was installed just past the filter. This will be repeated during testing of other subsystems.

Conveying Lines. Ultrasonic measurement techniques are currently under study for use in monitoring possible bend erosion of the pneumatic transport tubing. A simple, hand-held device, a Branson Caliper 101 Ultrasonic Transceiver, has been tested with calibration blocks and with transport tubing sections. Results thus far have been erratic. A larger, more sophisticated machine, the Sperry UM 771 Reflectoscope, is currently being tested. The Sperry device, which has a wide adjustment capability and a highly accurate oscilloscope display, is expected to prove satisfactory.

In-Bunker Filters. The test procedure is intended to verify that the filters prevent particles greater than 5 μm from leaving the bunker, to verify that the pressure drop is acceptable, and to pre-load the filters so that material entering the bunker can be recovered. The steps involved are:

1. Using the test-rig variable speed blower, the pressure drop across the filters is measured at 30%, 60%, and 90% power.

2. With the gas flow at 90% power, approximately 3 kg of graphite fines are introduced into the conveying line. The weight added is noted. For the secondary burner product bunker, fine silicon carbide was used.

3. With the blower off, one complete blowback cycle is actuated. The blower is restarted and the pressure drop is measured. This is repeated with 10 complete blowback cycles. Blown-back fines are then removed and the weight on the filters is calculated.

4. Steps 2 and 3 are repeated until 95% of the fines going in are recovered.

5. Before and after the tests, a sample wipe is taken from the inside of the filter exhaust line and is analyzed for particle size distribution.

The pressure drop and holdup results are given in Table 7-1. Only five of the systems have been tested so far, the No. 2 (primary burner feed system) having been partially dismantled for nonsequential operation. No more than one repeat test was required to bring the holdup down to acceptable levels.

The sample wipes, taken before and after testing, were examined by photographing a strip of the wipe at 120X. The particles on the photographs were counted according to size. Two sizes were used (greater than and less than 1/2 mm, which corresponds to 4.2 μm). The results of eight of the 10 wipes are shown in Table 7-2. Application of the "t-test" shows that the percentages of particles below 4.2 μm before and after loading the filters are not significantly different. Since particles coming through the filters can be expected to be deposited to some extent, and since the deposited particles present before the filter loading can be assumed to be sufficiently strongly adhering not to have been lifted off during the testing, it may be concluded that no significant quantities of particles are passing through the filters.

TABLE 7-1
IN-BUNKER FILTER LOADING TEST RESULTS

Subsystem	No. 1		No. 3		No. 4		No. 5		No. 6	
Test Number	1	2	1	2	1	2	1	2	1	2
ΔP (clean filter, 30% power), Pa	150		250		200		120		120	
ΔP (clean filter, 60% power), Pa	450		450		470		500		430	
ΔP (clean filter, 90% power), Pa	720		620		700		720		620	
ΔP (loaded filter, 90% power), Pa	770		700		820		750		620	
ΔP after 1 blow-back cycle, Pa	720		620		820		620		620	620
ΔP after 10 blow-back cycles, Pa	720		620		700	700	620	620	620	620
Weight of fines added, g	2725	3116	2997	2757	2315	2140	2589	2401	3077	2950
Weight of fines recovered, g	2595	3129	2765	2736	2140	2120	2401	2310	2950	2936
Holdup, g	130	-13	232	21	175	20	188[(a)]	91[(a)]	112	14

[(a)] Includes spillage.

TABLE 7-2
SIZE DISTRIBUTION OF SAMPLE WIPES TAKEN FROM FILTER EXHAUST LINES

	Total Number of Particles on Photographs	Percentage Above 4.2 μm
Subsystem No. 3		
Before testing	344	58.2
After testing	709	58.0
Subsystem No. 4		
Before testing	1204	60.2
After testing	648	32.3
Subsystem No. 5		
Before testing	1563	48.6
After testing	1687	50.1
Subystem No. 6		
Before testing	962	59.1
After testing	247	55.5

Notes:

1. Mean percentage above 4.2 μm before testing = 56.5%
   Mean percentage above 4.2 μm after testing = 49.0%
   Difference in the means = 7.5%
2. Joint estimate of the standard deviation = 9.0%

More definite verification of filter performance could be obtained by installing a sampling/filtering system in the off-gas line of one of the more frequently used systems.

Blowers. No separate tests are required.

Bunkers. The specific test for each of the bunkers is the experimental determination of the volume of material required to activate the high-level alarm. In the case of the secondary burner product bunker, which has no level sensors, the volume will be calculated based on results from other bunkers.

The primary burner product bunker and the crusher product bunker have both been filled through their pneumatic conveying systems with crushed graphite until the alarms were activated. The shape of the top surface of the material was nearly flat, so that the volume of solids was substantially larger than the conservative design value; see Table 7-3, which also gives the implied volume of the secondary burner product bunker.

Level Sensors. During the filling of the crusher product and primary burner product bunkers, the level sensors were activated, and during emptying they were de-activated satisfactorily. During the discharge of fuel particles at 700°C from the primary burner, however, the high-level alarm in the primary burner product bunker was activated. Subsequent examination showed the faces of the sensors to be coated with a layer of very fine particles. When the faces were cleaned, the alarm was de-activated. The general phenomenon of powder deposition on the sensors will be followed closely.

Feeders.

Primary Burner Feed Star Valve. The primary burner feed bunker load cells have been used to measure the capacity of the star valve at different speed settings for crushed graphite and for simulated fresh

TABLE 7-3
EFFECTIVE BUNKER VOLUMES

Bunker	Design Volume (m^3)	Experimentally Determined Volume (m^3)	Volume Below Top of Sensor (m^3)
Crusher product	0.550	0.736	0.790
Primary burner product	0.136	0.283	0.252
Secondary burner product	0.028	Has no level sensors	0.110 (to top of cone)

feed (83 wt % graphite, 17 wt % fertile TRISO "A" particles). The results are given in Fig. 7-14. Figure 7-15 shows the variation with time in the flow rate of simulated feed when beginning with a full bunker. The reason for this variation is most probably the tendency of fuel particles to percolate down through the crushed graphite, filling the interstices near the bunker outlet. As the bunker becomes empty, the flow rate of simulated fresh feed tends to approach that of crushed graphite.

Feeding Through Orifices - General Comments. With the exception of the primary burner and classifier feed bunkers, the flow rate out of the bunkers is controlled by an orifice. Johanson (Ref. 7-2) derives a simple expression for the flow rate using a force balance on an arch:

$$F = \gamma \frac{\pi}{4} D^2 \sqrt{\frac{D\,g}{4 \tan \theta}} \sqrt{\left(1 - \frac{ff}{FF}\right)} = F_i \sqrt{\left(1 - \frac{ff}{FF}\right)} \quad ,$$

where F = flow rate, kg/sec,

γ = bulk density, kg/m^3,

D = diameter of outlet, m (for coarse particles, D should be reduced by a particle diameter),

θ = angle of approach of solids (hopper slope in a mass flow bunker),

ff = flow factor of the bunker,

FF = flow function of the solid,

F_i = flow rate of an ideal solid, kg/sec.

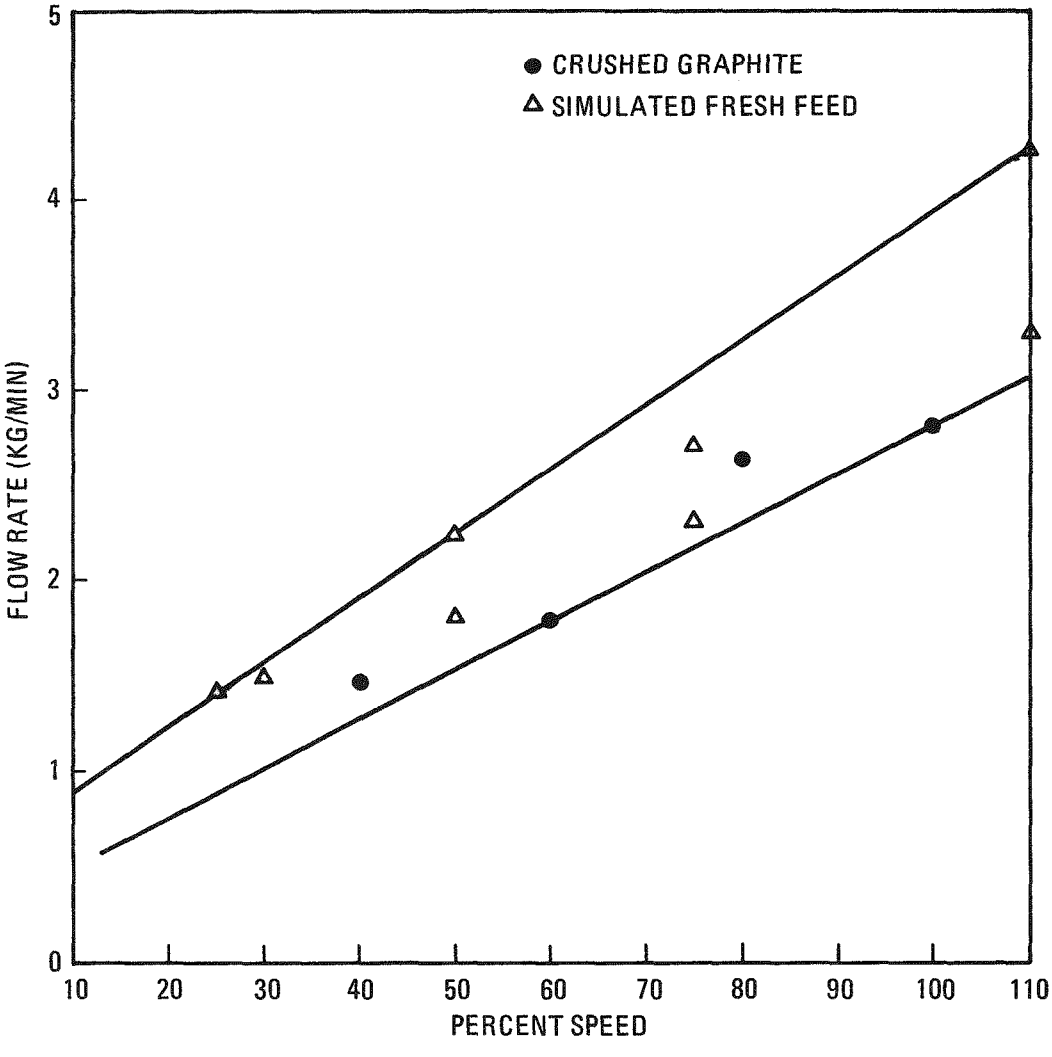

Fig. 7-14. Flow rate into primary burner versus star valve speed setting

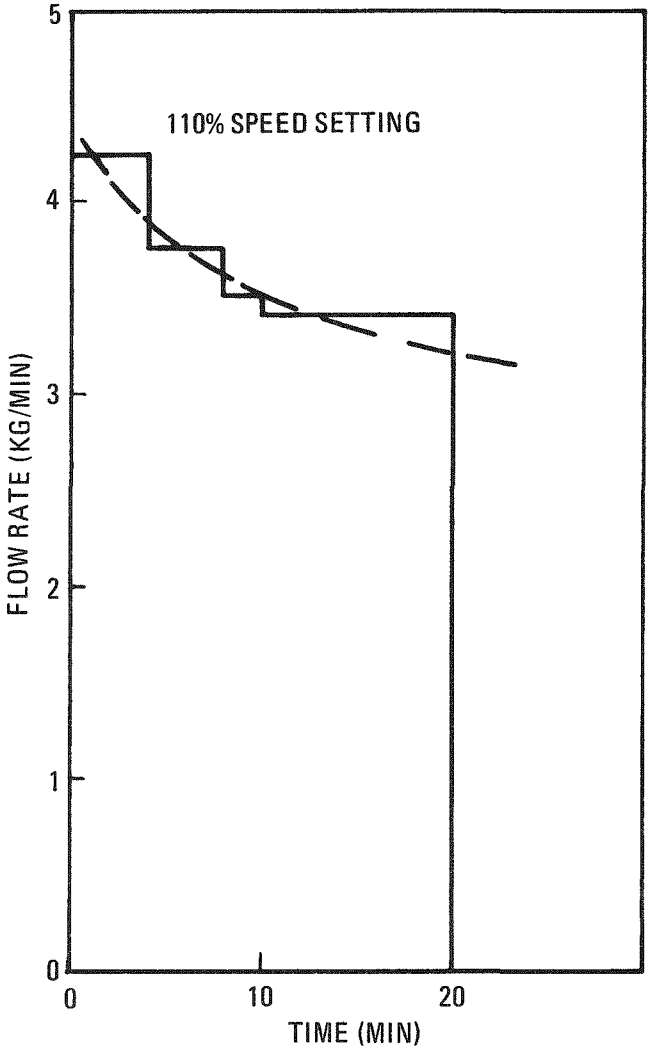

Fig. 7-15. Variation of flow rate of simulated fresh feed with time

A simple extension of the force balance to include a pressure gradient due to flow of gas through the particulate solids yields

$$F = F_i \sqrt{\left(1 \pm \frac{1}{\gamma g} \frac{dp}{dz} - \frac{ff}{FF}\right)} \quad ,$$

where + (dp/dz) = pressure gradient in the same direction as the flow, Pa/m,

- (dp/dz) = pressure gradient against the flow.

The last equation shows how a downflow of gas can be used to overcome the effect of cohesion and to increase the natural gravity flow rate. This latter effect is particularly marked when discharging from the burners. A negative pressure gradient can be created by upward leakage from a pneumatic conveying system which is at a higher pressure or from an upflow of gas needed to replace the volume vacated by solids flowing out of a bunker with a sealed top. Another phenomenon is an increase in the porosity in a flowing solid just above the bunker outlet. This results in an underpressure just above the outlet, the magnitude of which depends on the permeability of the material. The underpressure causes a negative pressure gradient, which tends to retard the flow, particularly of fine materials.

The minimum outlet size for a cohesive material can be estimated from flow property measurements using Jenike and Johanson's flow model (Ref. 7-3). There is also a minimum outlet size for a free-flowing solid, based on the diameter needed to avoid mechanical interlocking. Normally, an outlet with a diameter nine times the average particle size is required.

All these factors must be taken into consideration when a bunker must handle different solids which are to be conveyed pneumatically. The capacity of a conveying system is fixed by the maximum allowable pressure drop. The orifice size which gives the maximum conveyable flow rate for one material must be compatible with the minimum flow requirements of the other materials. If it is not, the orifice size must be changed, depending on which material is present.

Weigh Cells. Considerable debugging was required on the Orbitron weigh cell system. The calibration results to date are:

System	Accuracy of Calibration
Primary burner feed bunker	<±0.5% of design load
Primary burner product bunker	<±0.5% of design load
Particle crusher feed bunker	<±0.5% of design load
Secondary burner product bunker	<±0.5% of design load

These accuracies are satisfactory; however, they are sensitive to outside influences. Any blowback systems, blowers, and burner systems related to a bunker must be turned off prior to taking weight readings. People must be cleared from the vicinity of the bunker platform and nearby elevated walkways for maximum accuracy.

7.4.2.2. System Qualification

7.4.2.2.1. Introduction. The goal of system qualification is to ensure that each subsystem can convey material at a rate compatible with upstream and downstream operations so that particle breakage is minimal. This involves establishing the conveying characteristics of each system by measuring pressure drops at different solids flow rates over a range of gas velocities. The determination of the saltation point, i.e., where the suspension collapses and particles fill up the line, is also required. The ability to restart, after plugging the line, by use of the blower only should also be investigated.

The solids handling test rig, described in previous quarterly reports, is equipped with a variable-speed blower, which is being used for system qualification. Once the optimal conditions for a given system have been determined, a fixed-speed blower, suitably set, can be used.

The gas flow is measured with an orifice plate, which had been calibrated previously with a rotameter. It is mounted on the discharge side of the variable-speed blower. The solids flow rate is measured using the load cells on the receiving bunker. An accurate total weight change measurement is taken before and after each run, with the blower off. During transport, the instantaneous weight is noted every 10 sec or so in order to check the linearity. Pressures throughout the system are measured with Magnahelic gauges.

The data are needed not only for setting a fixed blower speed but also for future designs. Full analysis and modelling will be performed later.

Some subsystems have been temporarily modified for the purposes of nonsequential operation, and thus they cannot be fully qualified at this time. Partial qualification is possible, however, and results of interest are given below.

7.4.2.2.2. Crusher Product Removal System (Subsystem No. 1). During testing of the vibrating screener, which is part of the UNIFRAME, graphite passing through the screen was conveyed to the crusher product bunker. At one point, the blower was turned off, and the screener hopper was allowed to fill up. Graphite flowed into the line. Attempts to start conveying resulted in a rapid pressure buildup and activation of the underpressure relief valve. Similar experiments with a small bunker in the solids handling test rig (Ref. 7-4) had shown that transport could be readily achieved. The reason for this difference in behavior will be investigated.

7.4.2.2.3. Primary Burner Feed System (Subsystem No. 2). Simulated fresh feed has been prepared by allowing crushed graphite and fuel particles to flow simultaneously into a barrel. In order to ensure the correct flow rate of fuel particles, measurements with different sized orifices had been made.

7.4.2.2.4. Primary Burner Product Removal System (Subsystem No. 3). A diagram of the piping for subsystem No. 3 is shown in Fig. 7-16. Pressures and pressure drops were measured past the inlet filter (P_1), at the bunker (P_2), across the in-bunker filters (ΔP_3), at the end of the system (P_4), at the inlet to the variable-speed blower (P_5), in front of the orifice plate (P_6), and across the orifice plate (ΔP_7). The temperature at the exit from the variable-speed blower was also measured.

The inlet gas velocity is related to the orifice plate measurements by

$$V = 4.57 \sqrt{\Delta P_7} \sqrt{\frac{(T + 273)}{300} \cdot \frac{100}{(100 + P_6)}} \quad ,$$

where V is in m/sec, T is in °C, and P is in kPa.

Gas Flow. The pressure drops for gas only are shown in Fig. 7-17. The pressure drop in the conveying line, which is assumed to be hydrodynamically smooth, can be calculated using the Blasius expression. For gas flow, no account is taken of bends, which are assumed to be so gradual that there is no additional pressure drop. Table 7-4 gives a comparison between measured and predicted values for the conveying line pressure drop ($P_2 - P_1$). Bearing in mind the error inherent in subtracting two pressure readings and calculating the gas flow from an orifice plate, the agreement is satisfactory and validates the instrumentation.

Gas and Solids. The experiments in the primary burner product removal system are limited to the experiments done in the burner.

Previous calculations have shown that the removal of burner product is complex. The rate at which material can be conveyed is limited by the allowable pressure drop (40.6 kPa). Under ambient conditions, once a safe conveying velocity has been established, the flow rate of solids can be set at any value short of overloading. With fuel particles it is best to keep

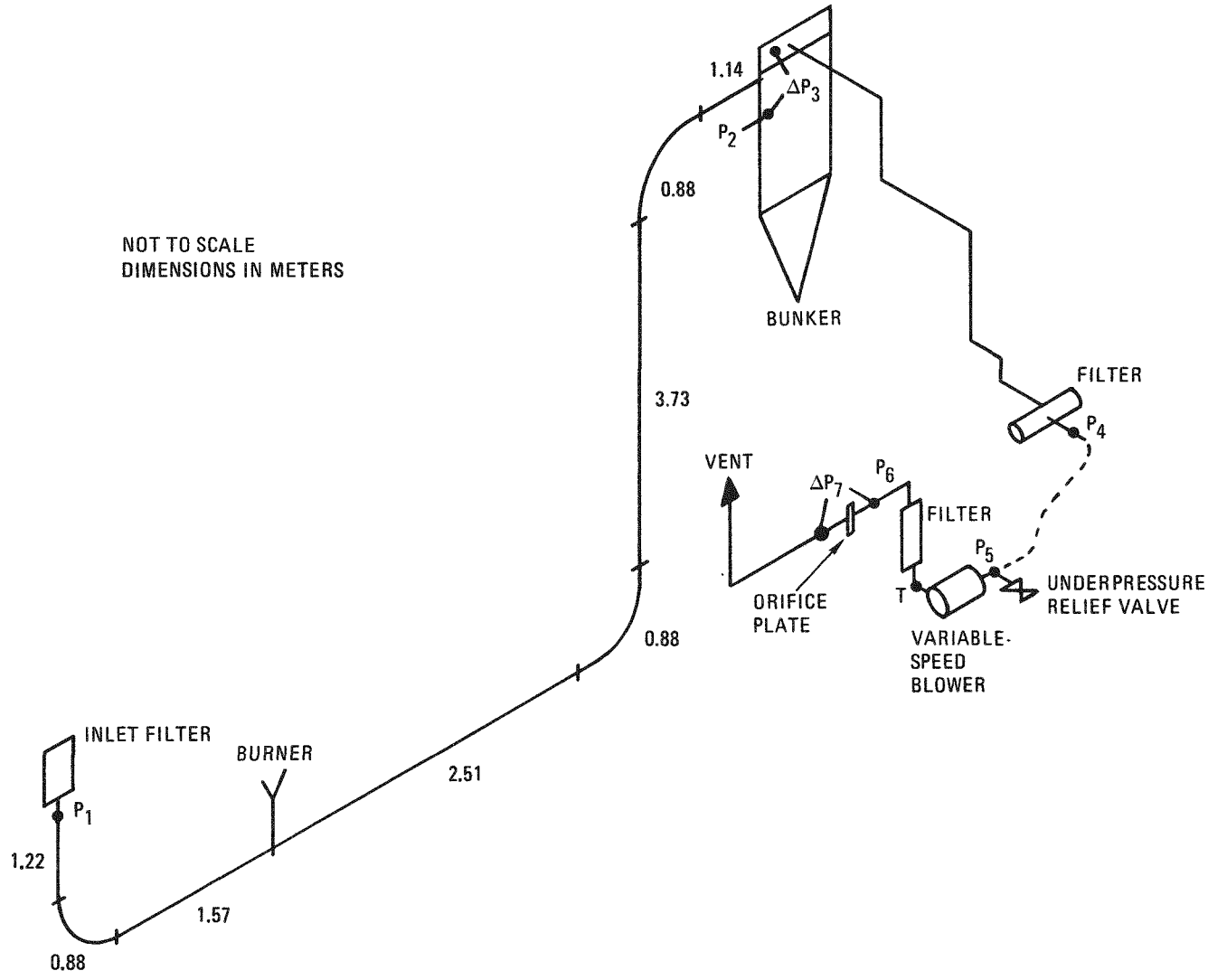

Fig. 7-16. Primary burner product removal system

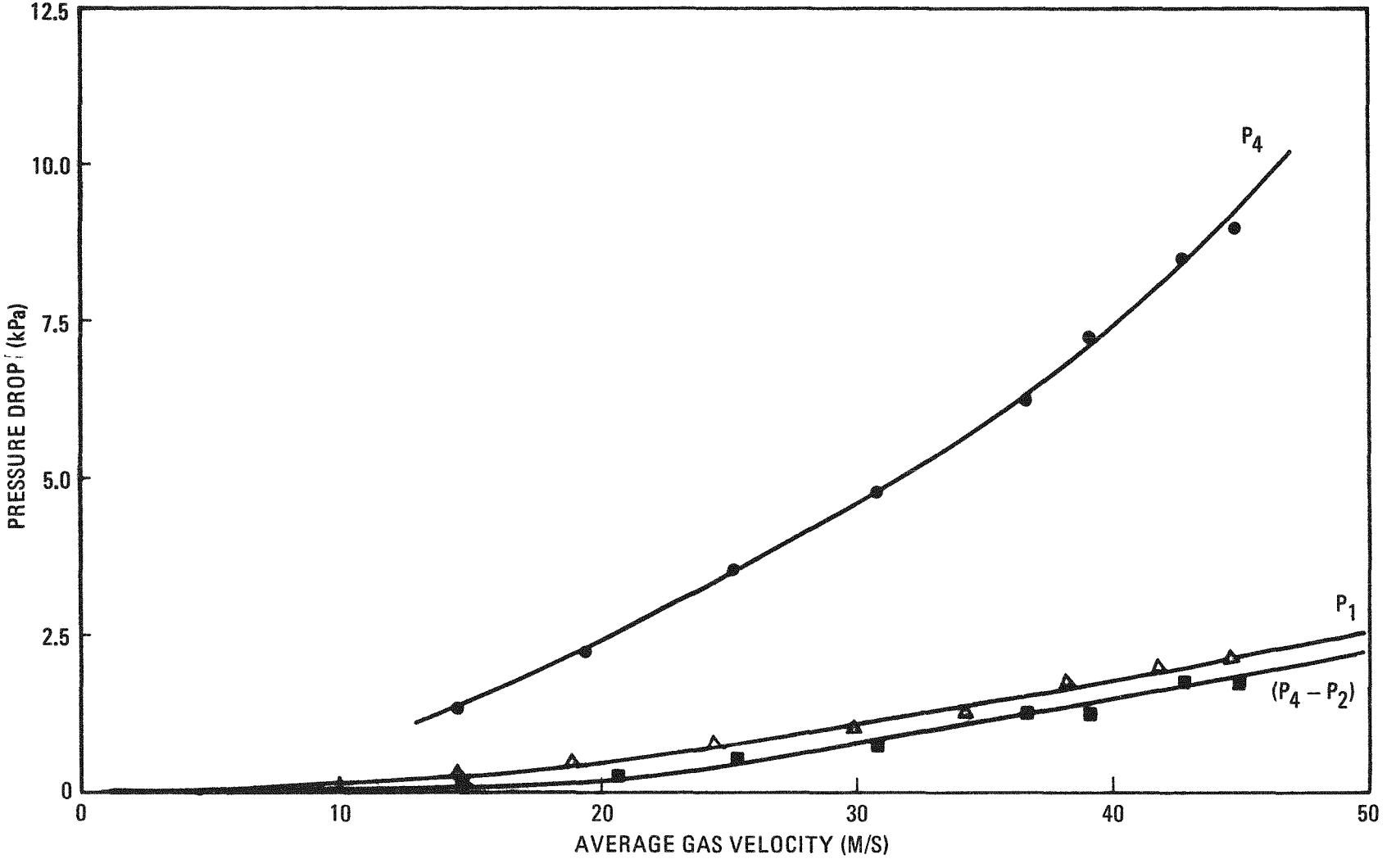

Fig. 7-17. Pressure drops for gas in primary burner product removal system

TABLE 7-4
PRESSURE DROPS FOR GAS ONLY IN THE
PRIMARY BURNER PRODUCT REMOVAL SYSTEM

Mean Gas Velocity (m/s)	Calculated ($P_2 - P_1$) (kPa)	Observed ($P_2 - P_1$) (kPa)	Difference (Calc. - Obs.) (kPa)
44.8	5.30	5.10	+0.20
42.7	4.86	4.81	+0.05
39.0	4.21	4.23	-0.02
36.6	3.76	3.44	+0.32
30.8	2.79	2.81	-0.02
25.3	1.97	2.12	-0.15
19.5	1.27	1.57	-0.30
14.6	0.75	1.00	-0.25

the loading high, since this reduces the breakage. When conveying heated particles, heat is transferred to the gas, which expands and accelerates the particles, thereby increasing the risk of particle breakage.

The flow rate of solids from a bunker is independent of the height of material. This is not the case for a fluidized bed. If fluidization is lost, one can get aerated flow, at rates higher than gravity flow but less than fluidized flow. As solids are discharged from the vertex of the burner, the gas entering the burner through the plenum will go up through the bed, possibly maintaining fluidization, and down through the discharge line. The relative quantities will depend on the height of the bed and the resistance caused by the column of discharging particles. As discussed in Section 7.4.2.1.2, this resistance, in turn, determines the rate of discharge through the pressure gradient at the choking orifice. Calculation of this pressure gradient requires a knowledge of the porosity, which is unknown.

Large HTGR fuel particles, when burned back, have a difference in density of a factor 4. Thus, if there were to be complete segregation, the flow rate could vary by the same ratio. This and the added factor of an unknown but potentially significant increase in flow rate caused by the pressure gradient due to the downward flow of fluidizing gas make it clear that experimentation is required.

The strategy is to use a small orifice below the burner and to reduce the conveying gas velocity, using the variable-speed blower, as the discharge of a batch proceeds. This reduction is required to prevent excessive gas velocities in the line, which steadily heats up as conveying proceeds. The extent to which the velocity can be reduced without saltation remains to be seen. Similarly, the particle breakage will have to be measured.

The following experiments, in conjunction with burner runs, have been conducted:

1. Crushed graphite (cold).
2. FSV TRISO fertile "A" particles (cold).
3. FSV TRISO fertile "A" particles (hot).
4. Simulated fuel (18 wt % particles) (cold).

Cold Conveying. The conveying lines pressure drops, $P_2 - P_1$, for the cold conveying experiments are shown as a function of mean gas velocity and solids flow rate in Fig. 7-18. The typical course of events during a run was to start at a fairly high velocity and then slowly reduce the power setting on the variable-speed blower, pausing to wait for pressure readings to become steady after each variation. When conveying crushed graphite, the velocity was deliberately reduced until the pressure drop began to increase, the underpressure relief valve opened, and the suspension in the line collapsed, plugging it. After closing the burner outlet valve, repeated attempts to restart using the blower were unsuccessful. The line had to be dismantled and cleaned out. When conveying FSV fertile TRISO "A" fuel particles, the velocity was reduced very gradually. Below a mean gas velocity of 20 m/s, the pressure drop began to increase slightly. Saltation was not allowed to occur. When conveying simulated fuel, the initial flow rate was so high that the relief valve opened and the line plugged. The burner outlet valve was closed almost immediately, thereby avoiding complete packing of the line. The line was cleared out using the blower. Thereafter the flow rate, while high, could be handled. It would appear that some segregation had taken place, and an initial surge of predominantly fuel particles had overloaded the system.

Pressure drops obtained with crushed graphite in the solids test rig (Ref. 7-4) were predicted quite well by using half the value of the Engineering Equipment Users Association (EEUA) formula (Ref. 7-5). Figure 7-19 shows a satisfactory agreement for all three types of solid using the same method.

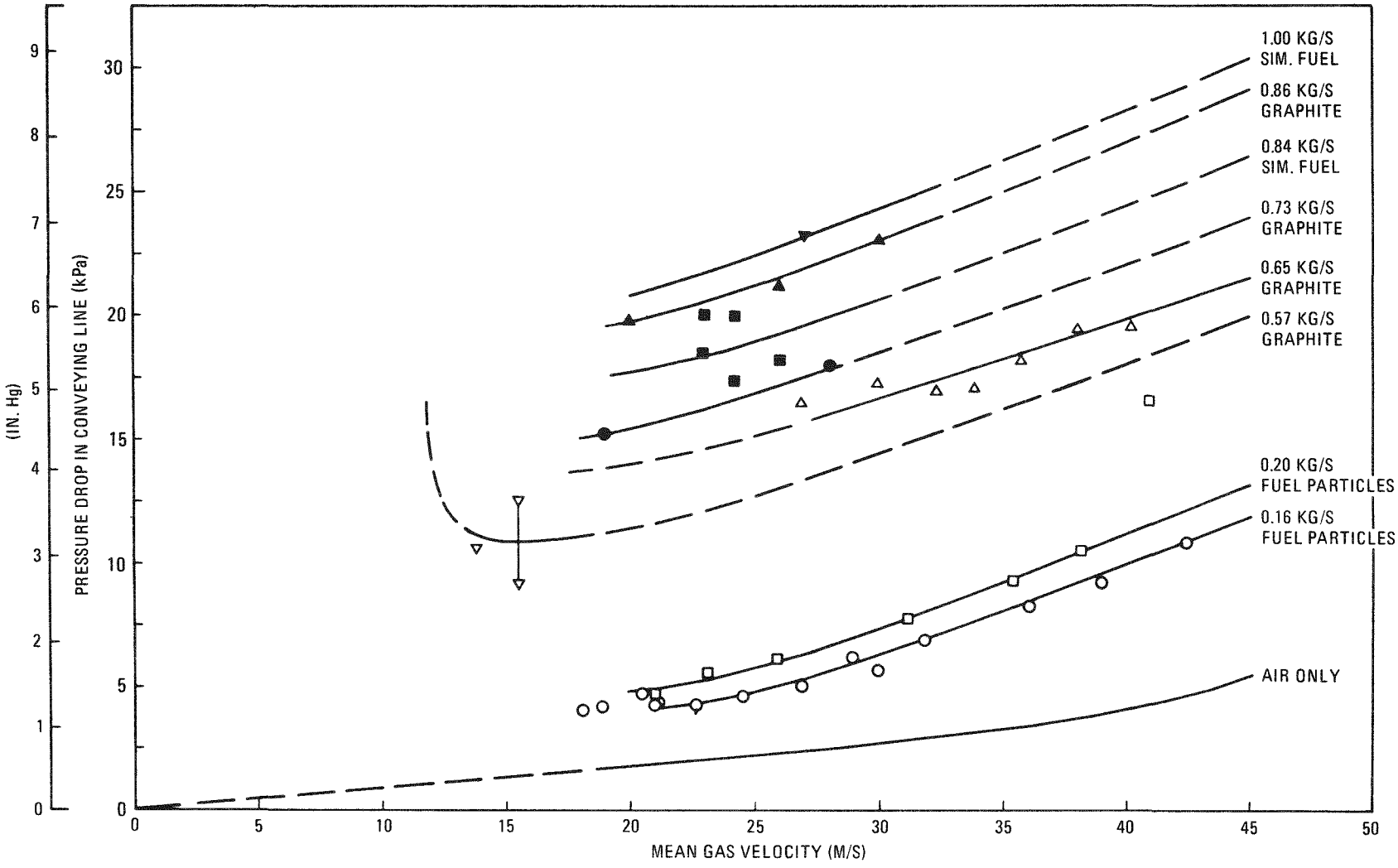

Fig. 7-18. Pressure drops in cold conveying in the primary burner product removal system

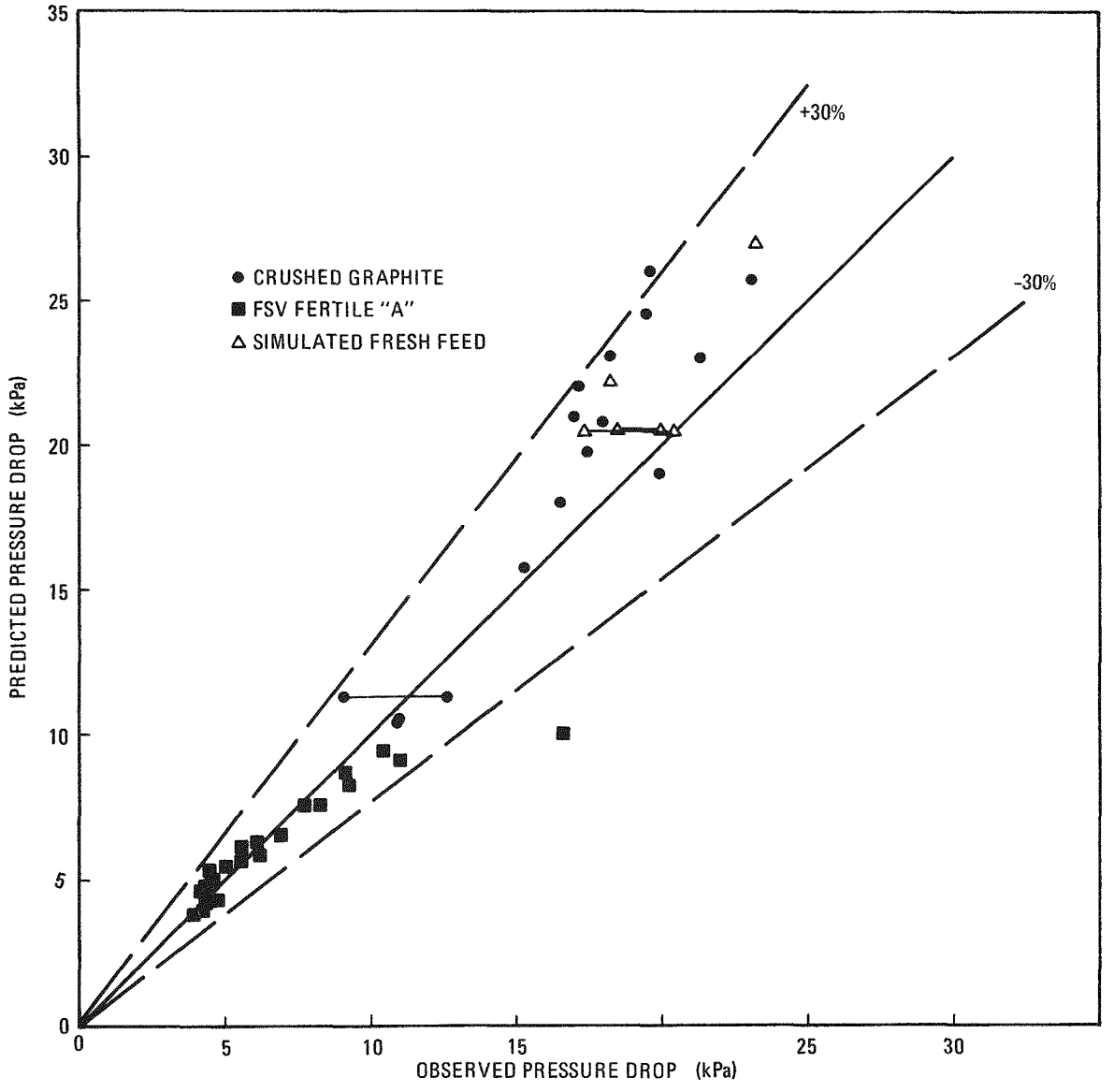

Fig. 7-19. Predicted versus observed pressure drops for pneumatic conveying of cold material (predicted value is half the EEUA prediction, Ref. 7-5) in the primary burner product removal system

The plenum of the 40-cm primary burner has an included angle of 90°, with a 0.0254-m outlet. The gravity flow rate of crushed graphite, if there were no mechanical interlocking, would be 0.09 kg/s. During the crushed graphite discharge, below the outlet ball valve there was a reducing cone (included angle = 15°, outlet = 0.0475 m). The gravity flow rate of graphite would be 1.33 kg/s. Flow rates from 0.65 to 0.86 kg/s were observed for graphite which had been fluidized during burner heatup tests and which had lost considerable amounts of fines. The crushed graphite left in the feed hopper was then fed to the burner and discharged straight away. Flow was somewhat erratic and stopped altogether on occasion owing to the presence of fines. Rates of 0.73 to 0.57 kg/s were observed, depending on the amount of gas passing through the plenum. It can be concluded that flow through the vertex of the burner plenum was limiting.

For the discharge of fuel particles, the original 2-in. gate valve was installed, with a small [0.75-in. (0.0191 m) diameter] orifice immediately below it. The flow rate of 0.16 kg/s obtained with no gas flow to the burner represents an angle of approach (see Section 7.4.2.1.2) of 27°, for a bulk density of 2000 kg/m^3. When gas flowed into the burner through the plenum, the rate increased to 0.20 kg/s. This small increase indicates some aeration, but no fluidization.

The flow rates of simulated fuel (1.0 kg/s for the material used for heatup tests, 0.84 kg/s for material in the feed hopper which went straight through the burner) followed the same pattern as those of crushed graphite. Although the flow rate of the feed still containing fines fluctuated, no blockages occurred.

At ambient temperatures, there is barely enough gas available to the primary burner to fluidize the bed. When solids are being discharged through the vertex, with the accompanying gas leakage, it is therefore reasonable to assume that the bed is in a quasi-fluidized state.

Fuel particle breakage for the transport of particles only has been measured at less than 1%. It is not known which breakage is due to fluidization and which is due to pneumatic conveying. Similar analysis of the two batches of simulated fresh fuel (both conveyed, only one fluidized) should provide this information.

Hot Conveying. The first attempt at hot fuel particle discharge was made with the original outlet configuration (0.05-m knifegate outlet valve, below which was a reducing cone with an included angle of 25° and a 0.0254-m outlet). The flow rate out of the bed, which was at 700°C, was so large that the blower relief valve opened and the line plugged.

The second attempt was made with an orifice [0.0157-m (0.62 in.) diameter] below the knifegate valve. The bed was initially at ambient temperature and was heated up in stages. Batches of around 85 kg were successfully dumped at 200°, 400°, and 700°C. The pressure drops were observed, as was the temperature of the gas inside the bunker. The balance of material in the bed was discharged at 190°C, and the temperature then decreased to 120°C.

The gravity flow rate through the orifice, using the angle of approach calculated in the cold conveying, is 0.096 kg/s. Rates between 0.16 and 0.23 kg/s were observed. The elevated temperature of the bed in the burner meant that the fluidizing gas was sufficiently heated to fluidize. The pressure below the bed, which can be measured only before discharge, was 150 kPa with the complete bed, decreasing to 138 kPa prior to the hottest dump.

As expected, the gas temperature in the product bunker increased steadily throughout each dump (see Fig. 7-20). The increase in gas temperature caused an increase in velocity and consequently in pressure drop. The power setting on the variable-speed blower was steadily reduced so that the pressure drop did not increase inordinately.

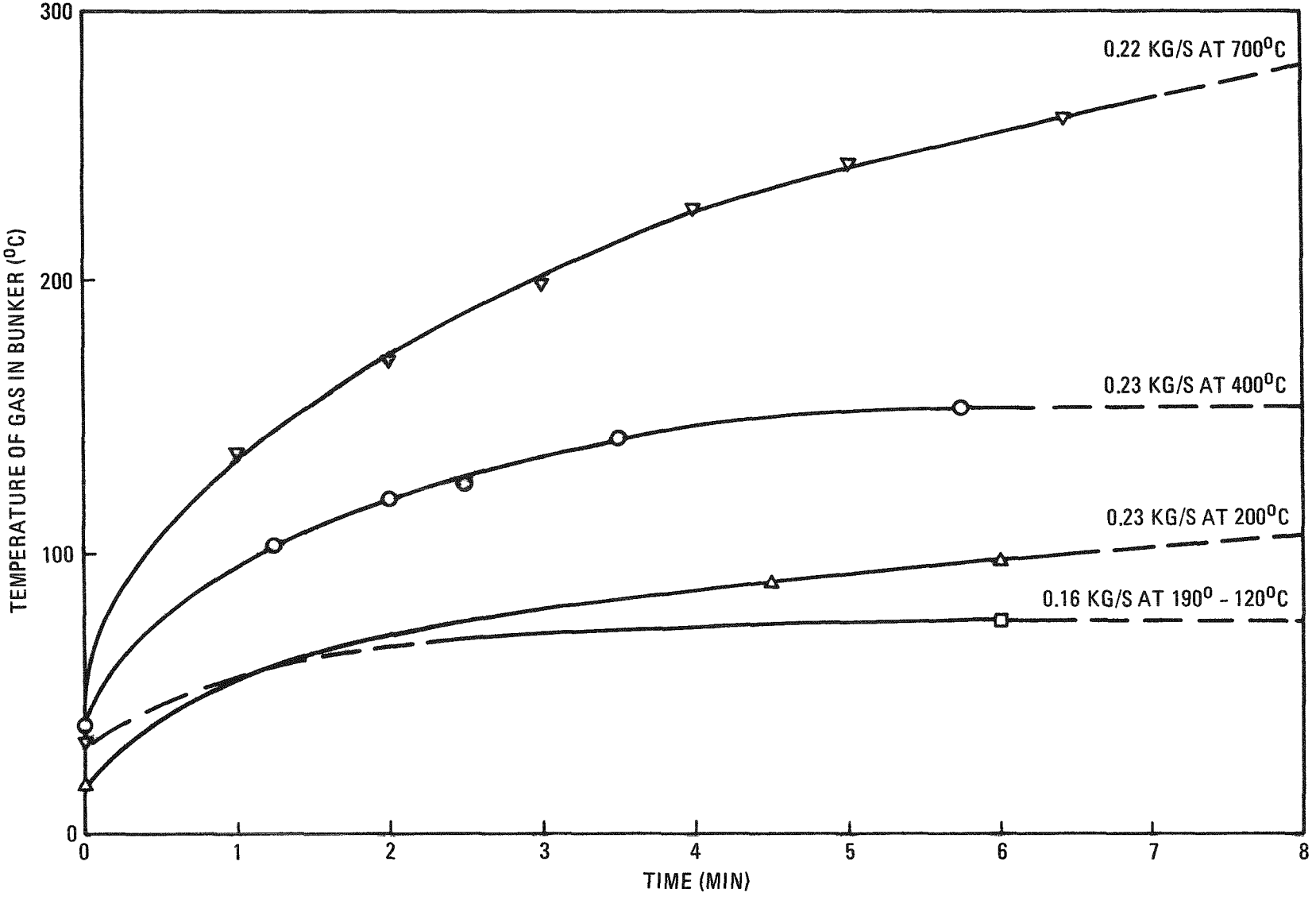

Fig. 7-20. Temperature of gas in product bunker throughout each dump

At the beginning of each dump, there was an initial surge of material, as reflected by the pressure drop. However, the pressure drop soon became steady, and then began to increase again.

After passing through the in-bunker filters, which act as a heat sink, the conveying gas did not get hot during the dump. Following a dump, however, after the filters had warmed up, the gas did get hot.

During and after the dump at 700°C, the side of the bunker in the neighborhood of the level sensors deflected inward somewhat. When this area cooled down, much of the deformation disappeared.

The flow rate was followed throughout each dump (see Fig. 7-21). There was a steady decrease during each discharge as the height of the fluidized bed decreased.

The system pressure drop, inlet velocity, outlet velocity, and blower power setting for the different batch discharges are given in Table 7-5.

All the material in the bunker was allowed to cool before removal and sampling. Particle breakage, measured in duplicate samples, was approximately 1.5%. As with the cold tests, the amount of broken particles leaving the burner is not known.

7.4.2.2.5. Classifier Feed System (Subsystem No. 4). There was no activity on this subsystem.

7.4.2.2.6. Particle Crusher Feed System (Subsystem No. 5). The particle transfer can (Ref. 7-1) has been used to feed fuel particles, with air assist, to the particle crusher feed bunker through the bunker penetration intended for a level sensor.

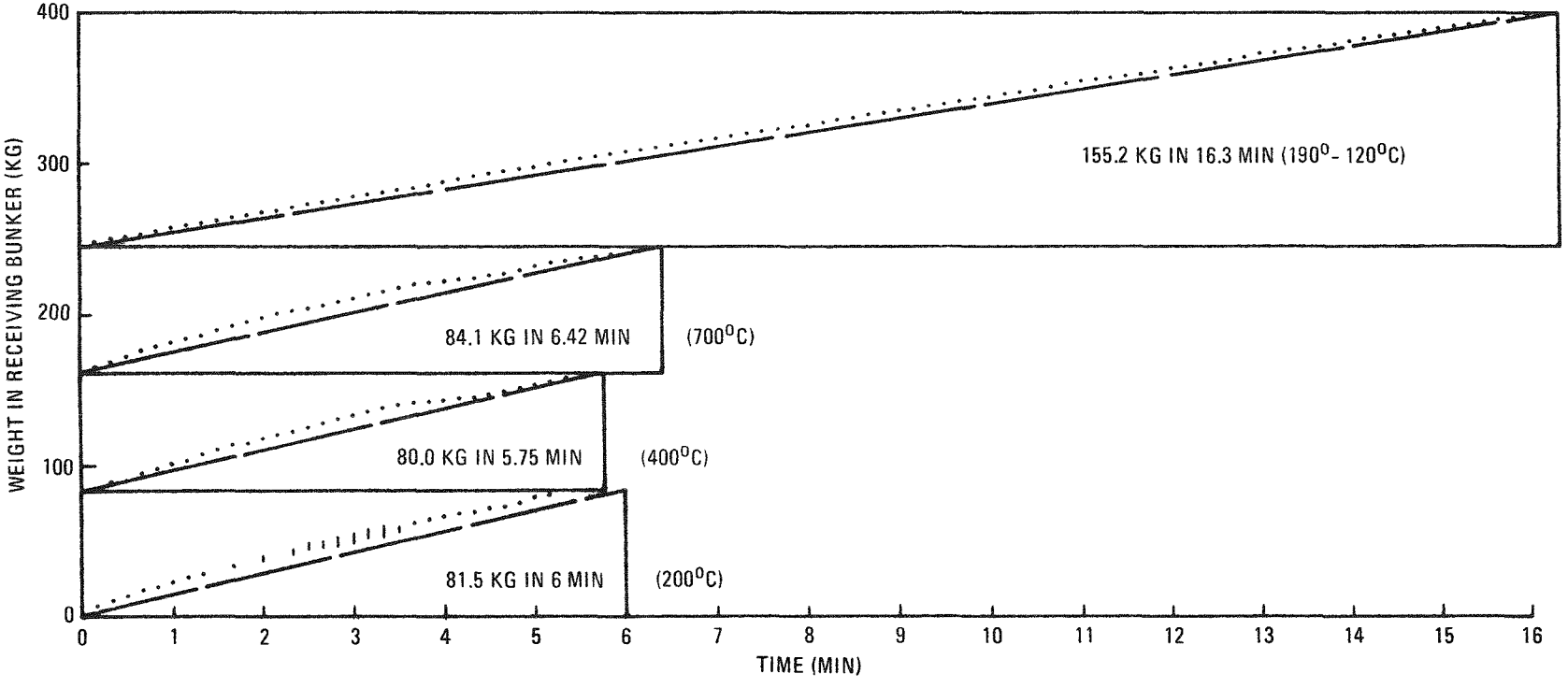

Fig. 7-21. Variations in flow rate during batch discharge from the primary burner

TABLE 7-5
RANGE OF PRESSURES, VELOCITIES, AND POWER SETTINGS DURING BATCH DISCHARGES FROM THE PRIMARY BURNER

Burner Bed Temperature (°C)	Initial Surge Pressure, P_4 (kPa)	Initial Conditions				Final Conditions			
		P_4 (kPa)	Inlet Gas Velocity (m/s)	Outlet Gas Velocity (m/s)	Blower Power (%)	P_4 (kPa)	Inlet Gas Velocity (m/s)	Outlet Gas Velocity (m/s)	Blower Power (%)
200	18.4	14.9	27	33	65	12.5	19	29	46
400	17.9	15.9	22	26	55	12.7	17	31	45
700	19.9	17.4	21	25	55	13.4	17	38	45
190 - 120	12.0	9.0	26	29	55	8.5	20	28	45

7.4.2.2.7. Secondary Burner Product Removal System (Subsystem No. 6). Two attempts have been made to remove secondary burner product using the pneumatic conveying system. Neither was successful. This system is not concerned with particle breakage, so there is no reason to stay close to the saltation point. The only limit is the 40-kPa pressure drop. During the shakedown testing of the secondary burner, a batch of coated BISO fertile particles was heated, cooled, and then dumped into the system. The fixed-speed blower, which draws approximately 0.054 Nm^3/s at the observed pressure drop (37 kPa), was used. The inlet velocity was 31 m/s. Bearing in mind the requirement to be able to remove product at 800°C, and also the subsequent gas heating and pressure drop increase, it was decided to use the variable-speed blower to establish a lower conveying velocity.

The first trial was made with a power setting of 65%. The bed was cold. The minimum pickup velocity, at a blower inlet underpressure of 40 kPa, was approximately 20 m/s. As soon as the burner outlet valve was actuated, the pressure rose very rapidly and the blower underpressure relief valve was actuated. The suspension in the line collapsed, and transport could not be restarted. Some 30 kg of secondary burner product was removed from the line. The material remaining in the burner was removed at 100% power. The pressure drop across the system fluctuated, with a maximum of about 25 kPa. The flow rate of solids fluctuated substantially.

The second trial was made with a power setting of 100% (minimum inlet velocity of approximately 32 m/s). The bed temperature was approximately 100°C. The system plugged after activation of the underpressure relief valve. The 23 kg remaining in the burner were removed using the fixed-speed blower. The flow rate was steady at 0.5 kg/s, and the pressure drop was 37 kPa. The steadiness of the flow rate indicates that the bed was no longer completely fluidized. Presumably, a considerable quantity of the gas leaves through the outlet valve, which is in the side of the burner. It is reasonable to assume that there is an initial surge. The results to date indicate that it is considerable. The next trial will be using the

fixed-speed blower. In order to increase the chances of accommodating the initial surge, the underpressure relief valve will be reset to 50 kPa. The product bunker has been strengthened appropriately.

REFERENCES

7-1. "Throium Utilization Program Quarterly Progress Report for the Period Ending August 31, 1976," ERDA Report GA-A14085, General Atomic Company, September 30, 1976.

7-2. Johanson, J. R., "Method of Calculating Rate of Discharge from Hoppers and Bins," Trans. Soc. Mining Engrs. pp. 69-80 (March 1965).

7-3. Jenike, A. W., "Storage and Flow of Solids," Bulletin 123 of the Utah Engineering Experiment Station, University of Utah, 1964.

7-4. "Thorium Utilization Program Quarterly Progress Report for the Period Ending November 30, 1975," ERDA Report GA-A13746, General Atomic Company, December 31, 1975.

7-5. "Pnuematic Handling of Powdered Materials," Engineering Equipment Users Association (EEUA), Constable and Company, Ltd., London, 1963.

8. GASEOUS EFFLUENT TREATMENT

8.1. SUMMARY

The characterization of gaseous fission product release from an HTGR fuel reprocessing plant into off-gas streams and the system development necessary for their treatment have been described in previous reports (Refs. 8-1, 8-2). The proposed treatment scheme (Ref. 8-2) has been reviewed in depth in view of recent developments in off-gas treatment technology. Individual treatment system components and the integrated system development have been reviewed and discussed during visits to Idaho National Engineering Laboratory (INEL) and Oak Ridge National Laboratory (ORNL). From these reviews, it became apparent that a few changes to the proposed treatment scheme are necessary. These changes are discussed in Section 8.2.

Work on the HRDF material balance for the head-end process and the gaseous fission product distribution has been completed based on updated input from the head-end operations. Based on the estimated fission product release to the off-gas streams and the estimated dose rate,* a preliminary effort was made to establish the target decontamination factors (DFs) and design basis for HRDF, which are compatible both with the current EPA proposed standards, i.e., 25 mrem/yr, and with the current development stage of the technology.

---

*Dose rates quoted in this report are for preliminary reference only. Since they are site-specific, the numbers will be updated as more representative information becomes available.

The behavior and the pathway of semivolatile fission products still remain a major uncertainty in the entire off-gas treatment system. The lack of clear understanding of controlling variables for the release of semivolatiles as well as the lack of experimental data made it necessary to initially take a fundamental and academic approach to the problem, namely to attempt to define the chemical and physical forms of the semivolatile fission products and to measure the equilibrium vapor pressures. Since this is a rather tedious process, a near-term solution is desirable. The ORNL hot cell large-scale fluidized-bed burner will provide much useful information in a timely manner by judicious experimental planning. However, in view of the scale of this hot cell work, it is believed that HET is the only system that will provide meaningful data for the large-scale HRDF system design for control of semivolatiles.

The feasibility of each individual treatment step has been established in laboratory-scale equipment. However, the results from a preliminary test of a combined system at INEL show a considerable amount of cross-contamination of the beds, especially by iodine. Studies of the system integration will be continued in an effort to minimize the system cross-contamination. Since the effect of bed contamination on the overall system performance may be greatly influenced by physical factors such as the bed sizes, the geometric configuration, and the operating parameters, it is essential to test the integrated system on an engineering scale. Work on a cold engineering-scale system design will be initiated during the next quarter. The scale-up studies should include packed-bed performance, heat transfer considerations, and measurement and control requirements. The last two areas need special attention since their importance in large equipment is very significant.

8.2. SYSTEM INTEGRATION

The necessity of separately processing the off-gas streams from the primary burner, the secondary burner, and the dissolver has been

established in previous reports (Refs. 8-1, 8-2). However, the proposed treatment scheme utilizes a molecular sieve bed for the secondary burner burner off-gas to separate krypton from the CO_2 stream. The CO_2 flow from the secondary burner, although small compared with the primary burner off-gas flow, is still a substantial quantity. Since CO_2, the major component in the stream, is the absorbate, the amount of heat of adsorption will be significant. The physical size of a molecular sieve bed with both enough adsorption capacity for the secondary burner off-gas batch and enough cooling capacity for heat removal will be prohibitively large. The following changes are recommended:

1. The secondary burner off-gas stream can be recombined with the primary burner off-gas stream at the radon removal bed after the HTO removal. The low flow of secondary burner off-gas in the primary stream radon removal bed and KALC system is believed not be be detrimental. Although the linear velocity will be very low in the radon bed, the long residence time will compensate for the low adsorption coefficient resulting from lack of turbulence. In addition, a true turbulence state never develops in such a granular bed, and the transition from laminar to turbulent regime occurs very gradually to result in a gradual decrease in the adsorption efficiency as the flow rate decreases. An additional long residence time will be provided by the KALC surge tanks, which also will enable the system to handle a low flow from the secondary burner in the absence of the primary burner off-gas stream.

2. The dissolver off-gas stream can still be treated by a molecular sieve bed to effect a CO_2-krypton separation. Since the CO_2 content in this stream will be very low, the CO_2 removal bed can be designed into a small unit without much of a heat removal problem. This flow scheme alleviates the problem of

adding a substantial amount of light gases (air) into the KALC system, which would be encountered if the streams were combined into a single treatment stream. The small amount of CO_2 also allows the use of a separate CO_2 fixation unit for the stream, or it can be released into the stack without fixation.

The potential advantages of this flow scheme are twofold. First, the CO_2-krypton separation system can be reduced to an economical and manageable size. Second, the complete physical separation of the burner and dissolver off-gas treatment trains simplifies the cell arrangement and the design and operation of the integrated off-gas treatment system. A revised flow scheme is shown in Fig. 8-1.

8.3. FISSION PRODUCT DISTRIBUTION

The material balance for the HRDF head-end process has been completed, and the fission product distribution in various off-gas and waste streams has been computed based on updated information from head-end operations. The following assumptions are additions to or revisions of those reported earlier (Ref. 8-1):

1. During primary burning, 10% of the krypton, 20% of the H-3, and 4% of the I_2 are released from the BISO fertile particles to the off-gas.

2. Particle breakages up to and including the primary burner operation have been estimated (see Table 8-1).

3. In the classifier, 1.5% cross-over of unbroken fertile particles into the fissile stream, 2% cross-over of unbroken fissile particles into the fertile stream, and 75% cross-over of broken fertile particles into the fissile stream are assumed.

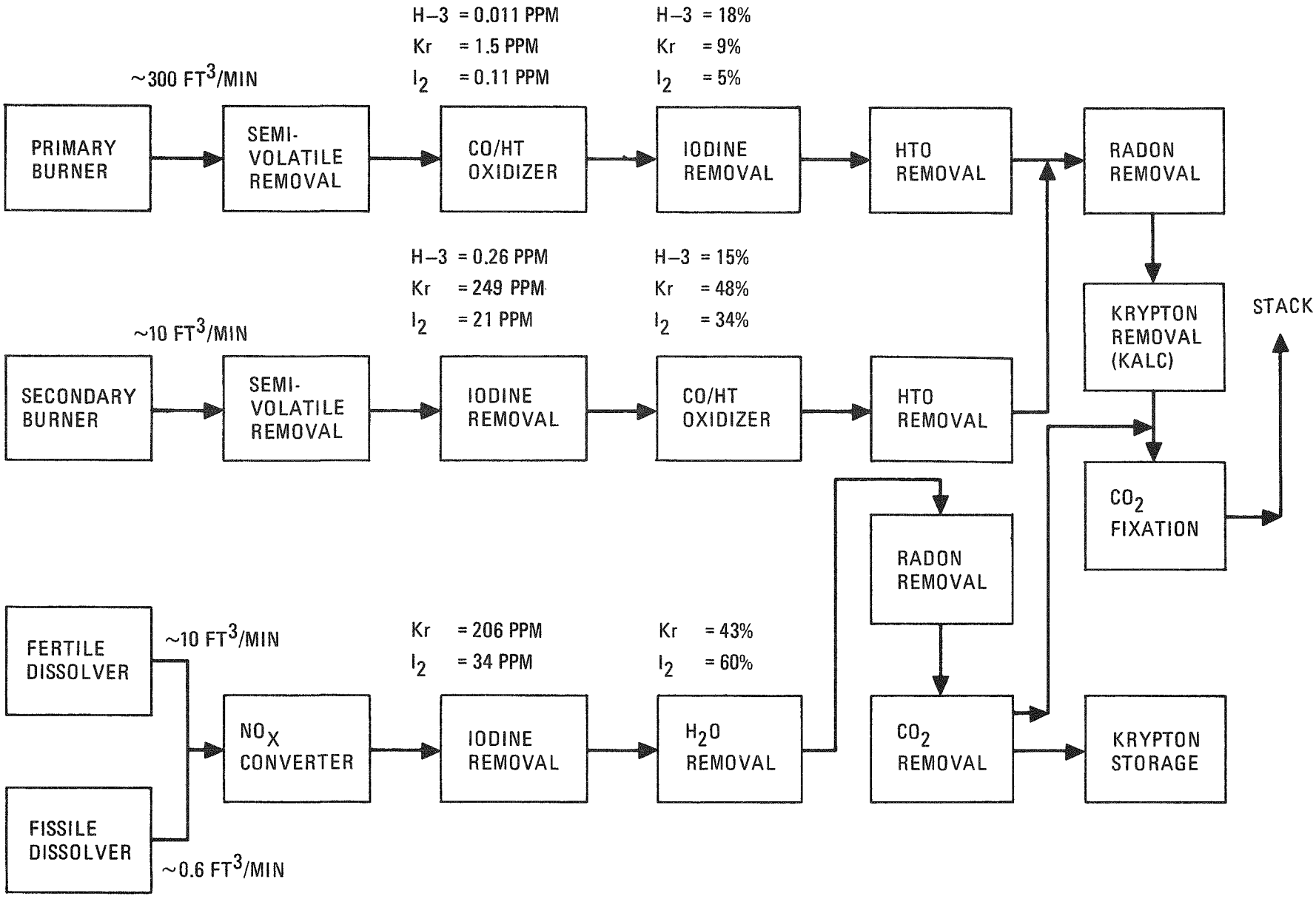

Fig. 8-1. Proposed burner and dissolver off-gas treatment scheme

TABLE 8-1
ESTIMATED PARTICLE BREAKAGE

	Fertile BISO Particles (%)	Fissile TRISO Particles (%)
Irradiation	0.4	0.7
Crushing	1.0	2.6
Pneumatic transport		0.5
Primary burner	~0	2.5
Primary burner fines recycle	~0	1.0
Subtotal to the primary burner	1.4	7.3

4. The secondary burner will operate four instead of two 6-hr batch cycles a day to handle the product from two primary burners.

The resulting fission product distribution is shown in Table 8-2. The concentration levels of these fission products in each treatment stream are also shown in Fig. 8-1.

8.4. TARGET DECONTAMINATION FACTORS

Based on the HRDF material flow and the spent fuel composition (Ref. 8-3), the annual release of major volatile fission products to the off-gas streams has been estimated (Table 8-3). The target DFs are established, which are compatible with the current EPA proposed standard, i.e., 25 mrem/yr, and with the current stage of technology development. In interpreting Table 8-3, the following points should be taken into consideration:

1. The tritium inventory in spent fuels may be as large as 5 to 7 times that shown in the table owing to an uncertainty in ternary fission.

2. The total body dose rates are site-specific. Therefore, the numbers are given only as a preliminary reference, and studies to improve them are under way. The uncertainties in the dose rates, however, may not significantly affect the target DFs, except for the iodine dose rate uncertainty because of high biological impact of this element.

3. Current technology, after verification on an engineering scale, may be sufficient for HRDF. Further development and improved DFs are required for a large-scale commercial reprocessing plant.

TABLE 8-2
VOLATILE FISSION PRODUCT DISTRIBUTION IN OFF-GAS STREAM
(% OF TOTAL)

	Primary Burner Off-Gas[a]	Secondary Burner Off-Gas[b]	Fertile Dissolver Off-Gas	Fissile Dissolver Off-Gas	Aqueous Stream	Solid Waste
H-3	18.0	14.9	-	-	67.1	-
C-14	99.6	0.4	-	-	-	-
Kr	8.6	47.7	41.6	1.1	-	1.0
I_2	5.2	34.1	59.2	0.8	-	0.7
Rn-220	(c)	(c)	(c)	(c)	(c)	(c)

[a] Includes purge gases from the crusher, the pneumatic transport system, and the bunkers.

[b] Includes purge gases from the classifier, the pneumatic transport system, and the bunkers.

[c] Amount depends on the source (Th-288) batch size and the time of exposure to the waste stream.

TABLE 8-3
ANNUAL RELEASE OF MAJOR VOLATILE FISSION PRODUCTS TO OFF-GAS FROM HRDF[a] (WITHOUT TREATMENT)

	Total Release (g/yr)	Total Emission (Ci/yr)	Fractional Release to Off-Gas (%)	Total Dose[b] (mrem/yr)	Target DF
H-3	45.2	4.37×10^{5}	32.9	7.92	1000
C-14	59.6	3.04×10	100	1.30	-
Kr-85	1.87×10^{5}	5.84×10^{6}	100	48.1	100
I-129	4.97×10^{4}	8.61	100	4.2×10^{3}	1000
I-131	2.54×10^{-4}	31.5	100	8.7×10^{2}	1000
Rn-220	(c)	(c)	100	(c)	10^{6}
α-aerosols[b]	-	5.4×10^{6}	10^{-6}	-	(d)
β-aerosols[b]	-	7.5×10^{8}	10^{-6}	-	(d)

[a] HRDF Phase 1: throughput = 10,000 FE/yr; heavy metal = 98 MT/yr.

[b] Ref. 8-4.

[c] Amount depends on the source (Th-228) size and the time of exposure to the off-gas, owing to the short (55.8 sec) half-life of Rn-220.

[d] Nearly complete removal is expected.

4. Although C-14 may not seem to be a serious problem, its release should be carefully limited in order to minimize the global accumulation.

5. Owing to the short half-life (55.8 sec) of Rn-220 and its continuous generation from the source term (Th-228 and Ra-224), the inventory of Rn-220 soon reaches its equilibrium value (99% in ∿370 sec) in the presence of the source. Owing to this high generation and high decay rate, the total amount that has to be treated depends largely on the generation term rather than on the inventory in spent fuel. The size of the radon removal bed, or the necessary DF, therefore depends on the batch size of the source term rather than on the plant throughput. The high particle buildup in the primary burner requires a DF of 10^6 with the current operating cycle. The required DF for dissolver off-gases for Rn-220 will also depend on the batch size as well as on the purge rate due to the high solubility of radon in water. In any case, the batch sizes should be minimized in order to reduce the radon treatment system.

6. The dissolver off-gas contains nitrogen oxides in addition to various fission product gases. The amount of NO_x greatly depends on the system design, which affects the scrubbing efficiency of the condenser. With an assumed 80% scrubbing efficiency, the NO_x does not need any treatment if properly diluted with stack gas.

REFERENCES

8-1. "Thorium Utilization Program Quarterly Progress Report for the Period Ending May 31, 1976," ERDA Report GA-A13949, General Atomic Company, June 30, 1976.

8-2. "Thorium Utilization Program Quarterly Progress Report for the Period Ending August 31, 1976," ERDA Report GA-A14085, General Atomic Company, September 30, 1976.

8-3. Hamilton, C. J., et al., "HTGR Spent Fuel Composition and Fuel Element Block Flow," ERDA Report GA-A13886, General Atomic Company, July 1, 1976.

8-4. Laser, M., et al., "AKUT: A Process for the Separation of Aerosols, Krypton and Tritium from Burner Off-Gas in HTGR Fuel Reprocessing," Kernforschungsanlage Report GERHTR-109, Jülich, Germany, August 1974.

9. PLANT MANAGEMENT

9.1. MAINTAINABILITY AND RELIABILITY

This activity is scheduled to start in January 1977. The objectives of this study will be to establish target reliabilities for HRDF Unit Operations and to provide guidance to the development program through parametric reliability/maintainability tradeoff evaluations.

9.2. HOT ENGINEERING TEST (HET) REPROCESSING PRELIMINARY DESIGN

9.2.1. HET Project

The HET-Reprocessing system design criteria were completed and compiled into the initial draft of the Criteria Document for the HTGR Fuel Recycle Hot Engineering Test. The GA project staff participated with project engineering personnel from UCC-ND and Ralph M. Parsons Company (RMPCo) in the design criteria document review and preparation of the final document, which was approved by the Oak Ridge Operations Office on October 14, 1976.

Conceptual design was initiated on the HET-Reprocessing systems under GA responsibility. These include:

1. Primary Burning (System 1200)
2. Particle Classification and Material Handling (System 1300)
3. Particle Crushing and Secondary Burning (System 1400)
4. Dissolution and Feed Adjustment (System 1500)
5. Solvent Extraction (System 1600)

Draft P&IDs and facility-related system interface data were transmitted to RMPCo to initiate preparation of system P&IDs. RMPCo has

prepared preliminary P&IDs for the following GA reprocessing systems: Primary Burning, Particle Classification and Material Handling, and Particle Crushing and Secondary Burning. The preliminary drawings were reviewed with RMPCo and UCC-ND and the P&IDs are scheduled for final drafting during the next reporting period. Preliminary P&IDs for the following RMPCo reprocessing support systems were reviewed and comments submitted: Product Handling, Burner Off-Gas, Dissolver Off-Gas, and Burner Cooling.

TURF cell arrangement drawings prepared earlier by GA were released to RMPCo by UCC-ND for use as initial reprocessing equipment arrangements in Cells D and E. The GA project staff reviewed the arrangement drawings, incorporating the current system equipment designs, and transmitted comments to RMPCo. An arrangement drawing for the aqueous systems -- System 1500, System 1600, and System 1800 -- was prepared using the TURF Cell G facility and was transmitted to RMPCo.

Members of the GA project participated with UCC-ND in developing HET radioactive feed material and on-site material handling concepts. As a result of several joint meetings, it was decided that radioactive fuel elements would be received, pre-sized, and stored as required, utilizing ORNL facilities.

HET project members attended several meetings during this reporting period, i.e., HET Technical Design Review, Design Criteria Review, HETF Technical Interchange and Site Inspection, and HETF Shipping and Radioactive Material Handling meetings. Draft HRDF/HETF Requirements Documents, Level 0 and Level 1, were reviewed and comments were submitted to UCC-ND. Word documentation input was provided for the HET Reprocessing Facility Conceptual Design Report for the 30% documentation submittal including the GA systems in Section 2.0, "Brief Physical Description of Reprocessing System."

9.2.2. Primary Burning - System 1200

9.2.2.1. Equipment General Arrangement

A conceptual design arrangement for the primary burner system has been prepared and is shown in Fig. 9-1.* The system consists of the following equipment items:

1. Eight-inch-diameter burner with cooling jacket and insulation.
2. Feed hopper.
3. Rotary feed valve.
4. Cyclone for fines removal with cooling jacket.
5. Fines filter vessel.
6. Fines collection hopper.
7. Fines rotary feed valve.
8. Interconnecting piping and expansion joints.
9. Support structure.

The 8-in. burner is suspended vertically and rests on horizontal framing members which are connected to cell wall anchor points and also to the cell floor through column members. In order to permit gravity flow design, the feed and recycle fines feed hoppers are mounted in close proximity to the vessel to minimize head height requirements. The feed hopper, recycle fines hopper, cyclone, and filter vessel are supported on a structural frame which is connected to the cell wall.

A single penetration through the side wall of the burner provides a common feed entry for both crushed fuel and recycle fines. The burner vessel exhausts through a top penetration to the cyclone. A thermowell probe extends down into the bed and can be removed remotely. The distributer cone is attached to the burner by a Gray-Loc remote disconnect. All connections for piping and instrumentation can be remotely disconnected

*Figures appear at the end of Section 9.

to permit equipment removal and maintenance. A special cart fixture located directly under the base of the burner permits removal of the distributer cone for maintenance or replacement.

Connecting piping between the burner vessel and the feed hopper, cyclone, and fines hopper contains expansion joints to compensate for thermal expansion. All connections to the base of the burner are designed to accommodate approximately 38.1 mm (1.5 in.) of downward thermal growth.

The burner vessel contains an integral jacket through which cooling gas circulates to remove process heat. The cyclone is also jacketed with cooling gas to reduce metal temperatures to 650°C. The vessels and hot piping are insulated to accommodate a maximum equipment surface temperature of 140°F.

9.2.2.2. Fines Recycle

The fines recycle loop of the HET primary burner system consists of the equipment necessary to remove elutriated fines from the process off-gas and return them to the combustion zone of the burner. The single-hopper gravity recycle system (Fig. 9-2) is comprised of a cyclone, a pulsed blowback filter system for separation of elutriated fines, a collection hopper, and a rotary feeder for metered transport of fines to the burner.

The majority of elutriated material is removed in the cyclone, with the remaining smaller fines proceeding on to the filter system. The blow-back filters are cylindrical, sintered stainless steel filters capable of 100% removal of all material >1 μm. The material removed by the cyclone and filter system returns by gravity to the recycle hopper. Gravity flow of fines from this hopper is aided by an aerated (CO_2) screen in the hopper bottom above the rotary valve. Discharge of recycle fines is metered by the rotary feeder and reenters the burner by gravity flow. A slide valve located between the hopper outlet and the rotary valve inlet permits system isolation from the burner and rotary valve replacement while the hopper contains fines.

The relatively high temperature of the fines entering the recycle hopper necessitates the use of a rotary valve designed for such extreme conditions. The design and materials of construction must be able to withstand ∿500°C and provide a sufficient seal against ≤10 in. of water backpressure to prevent gas bypassing. Control of the gravity recycle system is achieved by (1) metering aerated CO_2, (2) controlling rotary valve rpm (fines recycle rate), and (3) metering mid-reactor (recycle inlet) O_2/CO_2 flow to the burner to control combustion of fines in the above-bed fines burning zone.

Instrumentation for the gravity recycle system includes various thermocouples and pressure taps throughout the system. Thermocouples are located in the following places:

1. Thermowell in the hopper (2 T/C's).
2. Hopper outlet below rotary valve (1 T/C).
3. Recycle inlet to the burner (1 T/C).
4. Inlet line to the cyclone (1 T/C).
5. Inlet line to the filter chamber (1 T/C).
6. Outlet line from the filter chamber (1 T/C).

Pressure taps are located in the following places:

1. Inlet line to the cyclone.
2. Inlet line to the filter chamber.
3. Outlet line from the filter chamber.
4. Hopper outlet below the rotary valve.

A load cell weigh system permits determination of the fines collection hopper inventory throughout the run campaign.

Finally, a fines sampling system is provided for removal and analysis of recycle material. One of several possible sampling systems is shown in Fig. 9-2 and consists of a dead leg and ball valve at the outlet line below the rotary valve. Sample material is removed by gravity to a standard HET sample container.

9.2.3. Dissolution and Feed Adjustment - System 1500; Solvent Extraction - System 1600

Preliminary piping and instrument diagrams have been prepared for Systems 1500 and 1600. A conceptual Cell G equipment layout for the aqueous processing systems was prepared (Fig. 9-3). Top assembly drawings for the equipment items shown in the System 1500 and System 1600 process flow diagrams (Figs. 9-4 and 9-5) are in drafting.

As a result of HET technical review meetings during this reporting period, the HET aqueous processing requirements were reduced. The following equipment items were deleted from the systems:

1. 1CU tank. The 1CU stream will be fed directly to the uranium concentrator from solvent extraction.

2. HLW tank. The high-level waste will not be stored in Cell G, but will be jetted directly to the TURF waste system from the 1AW collection tank following each solvent extraction run.

3. Thorium storage tank. The thorium product will not be concentrated and stored routinely in Cell G. A normally blanked route will be installed to the System 1800 concentrator to allow recycle of any thorium product that does not meet specifications for waste disposal.

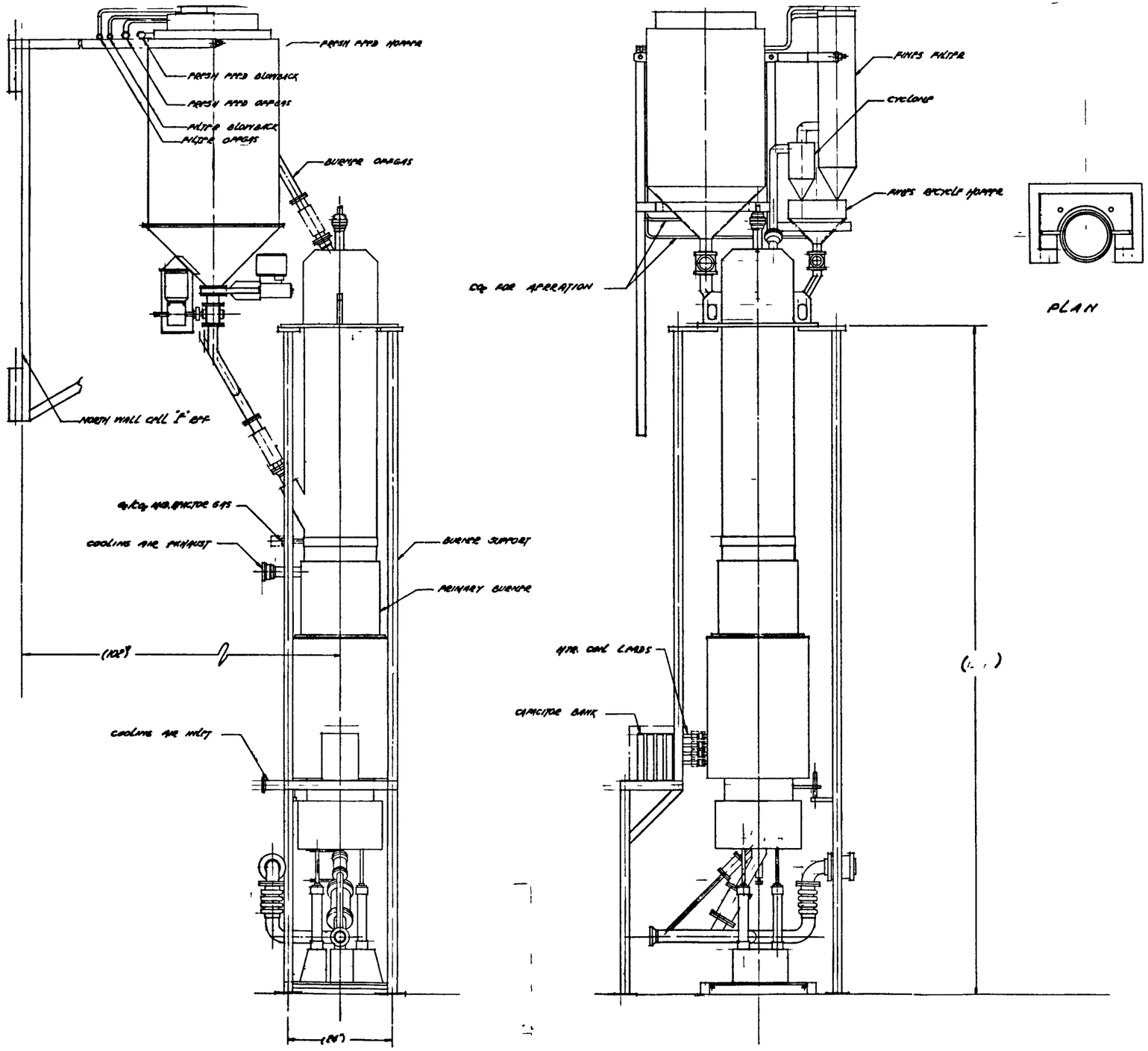

Fig. 9-1. Primary burner arrangement

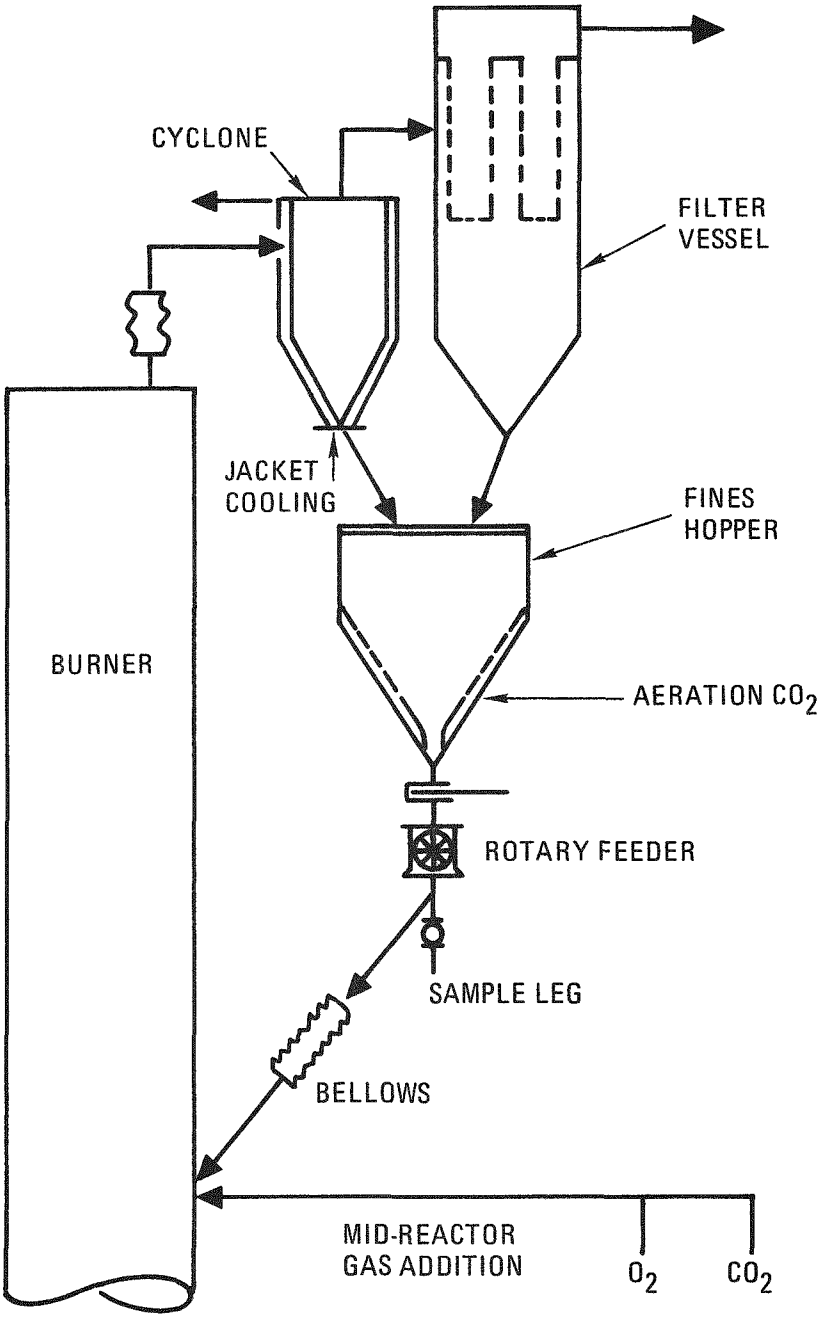

Fig. 9-2. Fines recycle system, HET primary burner

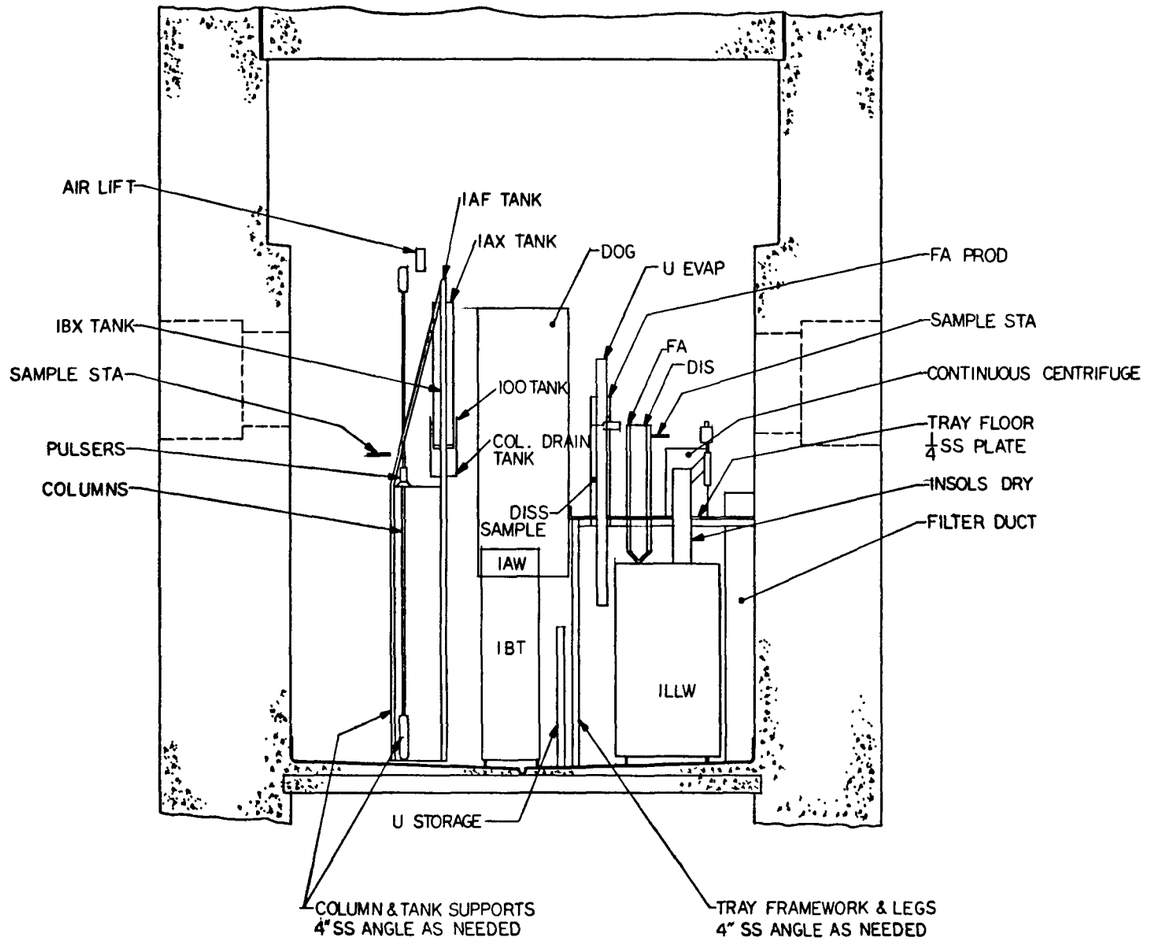

SECTION A-A
ROTATED 90°

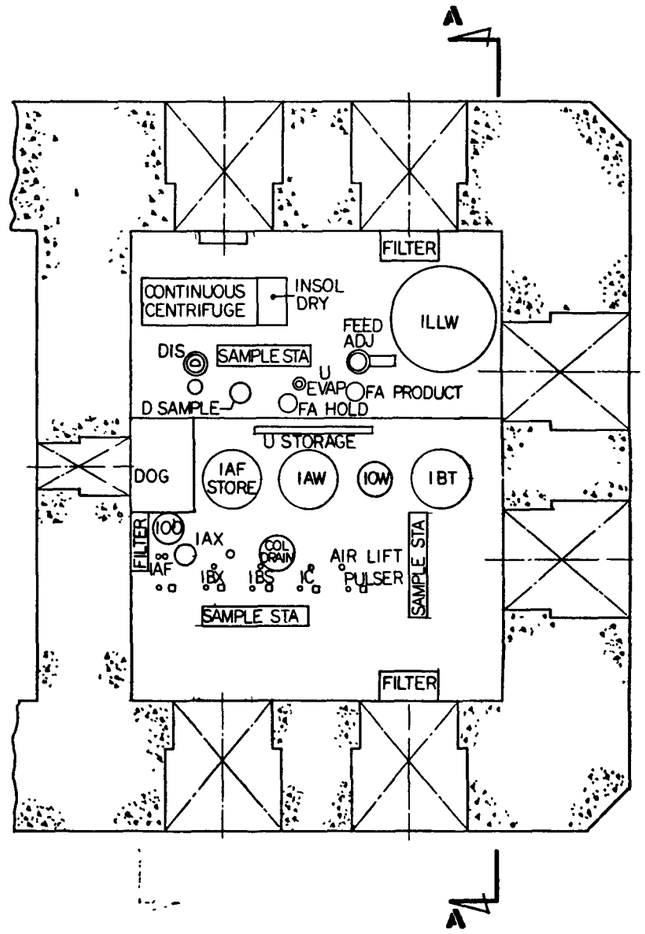

Fig. 9-3. TURF cell G aqueous system arrangement

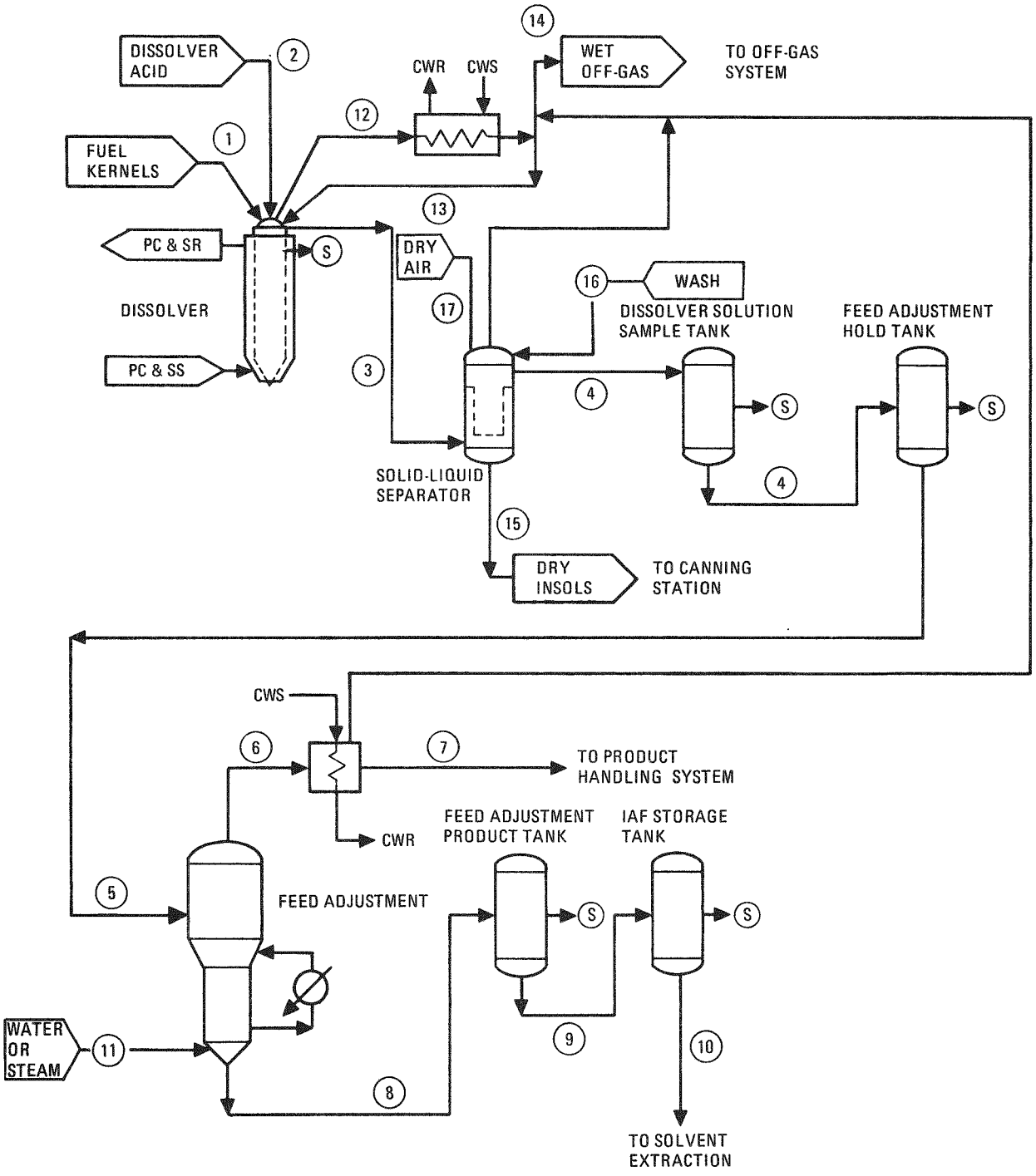

Fig. 9-4. Process flow diagram for HET System 1500 - Dissolution and Feed Adjustment

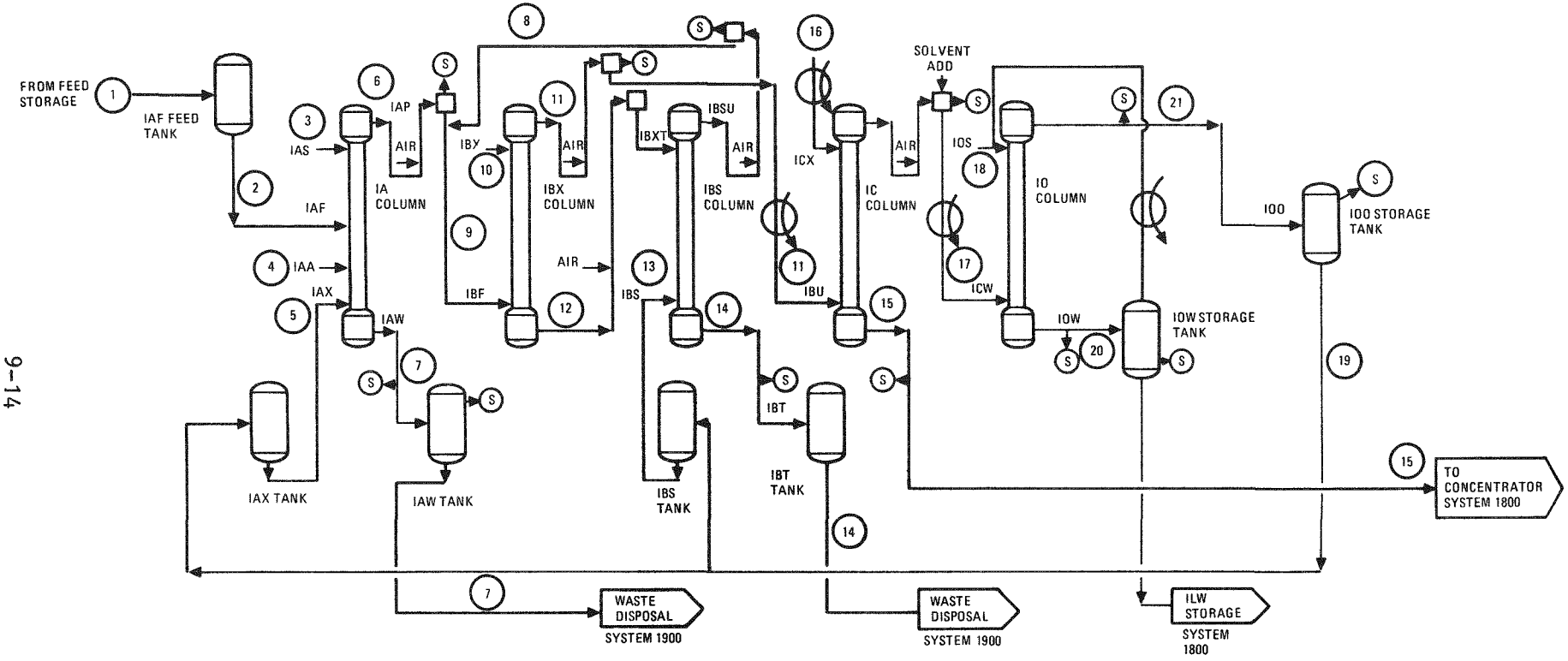

Fig. 9-5. Process flow diagram for HET System 1600 - Solvent Extraction

10. HET FUEL SHIPPING

10.1. SUMMARY

Irradiated Fort St. Vrain fuel will be used as the primary feed material for the HET program. This requires that the irradiated fuel be transported from its storage location at the Irradiated Fuel Storage Facility (IFSF) in Idaho to ORNL. This transport will require the use of a licensed shipping cask.

Shipping studies performed during the past few months have identified two candidate casks which are suitable for this task. These are the FSV-1 cask, which is used to transport the spent fuel from the FSV reactor to the IFSF, and the PB-2 cask, which is used to transport spent fuel from the Peach Bottom reactor to the IFSF. Both casks are owned by GA and are licensed to current federal shipping requirements. The studies also determined that the FSV-1 cask had very limited availability due to its high utilization for FSV irradiated fuel shipments and was therefore not considered a viable candidate for the HET program. Subsequent design activities have been directed toward definition of modifications required to adapt the PB-2 cask for the transport of FSV fuel. The Peach Bottom fuel has a long cylindrical configuration and is carried in an 18-element basket positioned in the cask cavity. The FSV fuel has a short hexagonal configuration and therefore requires special equipment to permit positioning in and transport by the PB-2 cask.

10.2. FUEL HANDLING CANISTER DESIGN FOR FSV SPENT FUEL SHIPMENT

Various design concepts have been considered for shipment of FSV fuel in the PB-2 cask. Schematic drawings for the two candidate designs are shown in Figs. 10-1 and 10-2.

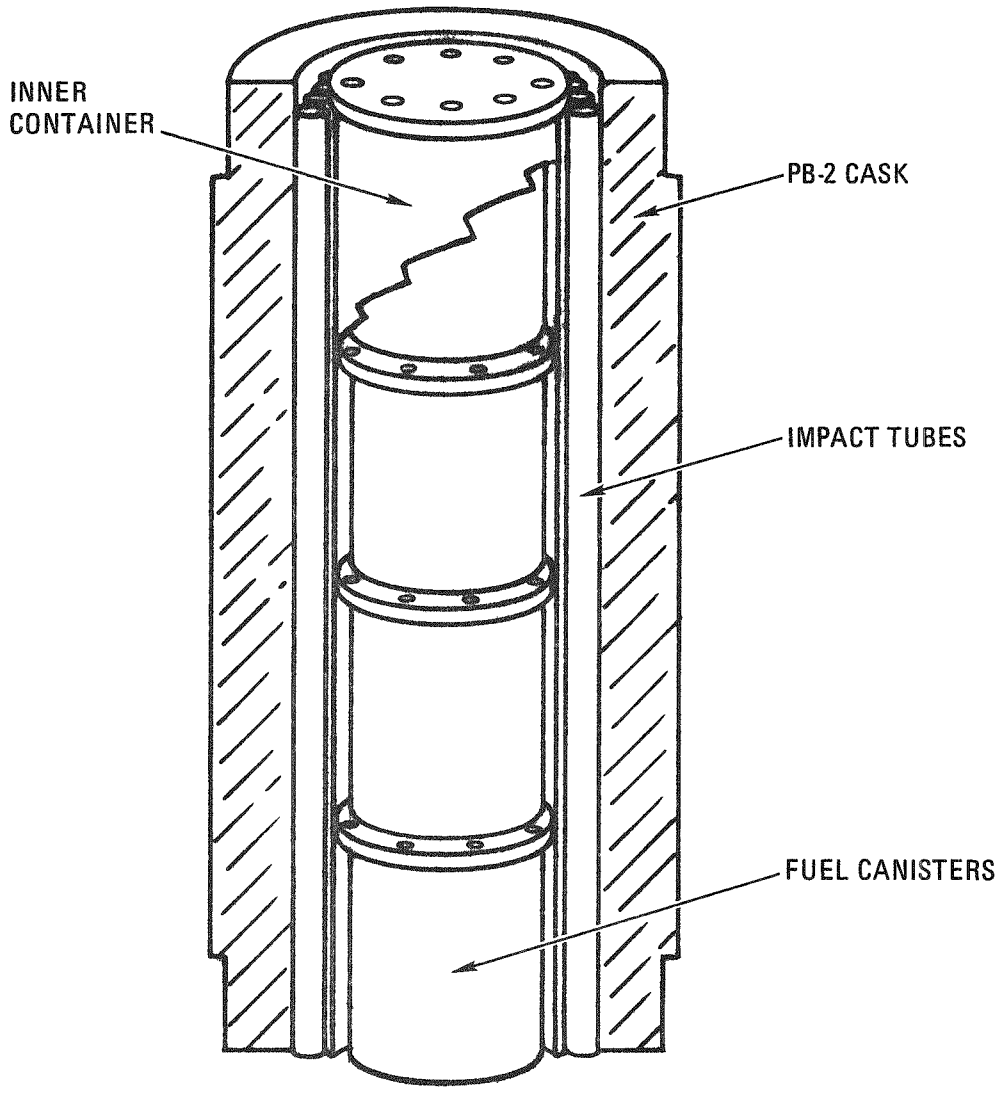

Fig. 10-1. Design 1 for shipping FSV fuel in Peach Bottom cask

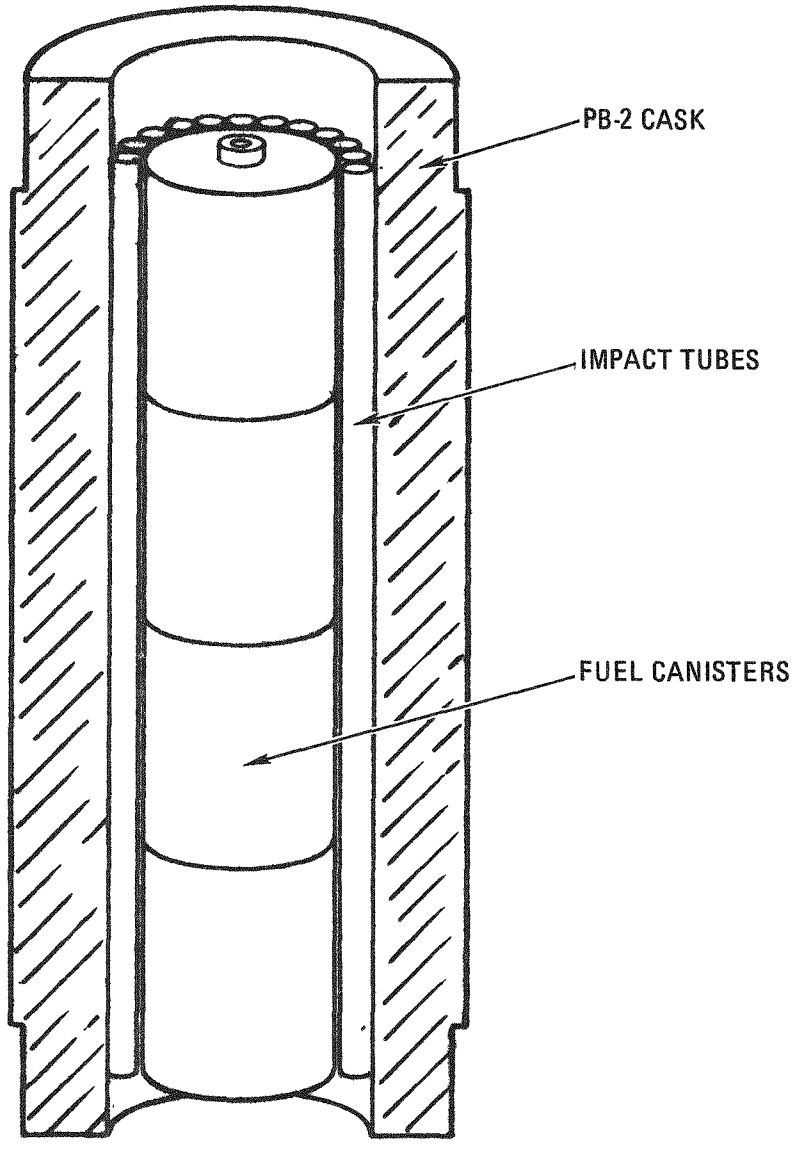

Fig. 10-2. Design 2 for shipping FSV fuel in Peach Bottom cask. This is the currently preferred design.

Design No. 1 has each fuel element stored in a fuel handling canister which has a bolted closure sealed with a gasket or O-ring. Four of these canisters are stacked in a long inner container which has a bolted closure and is the primary containment for the system. The diameter of this inner container is less than that of the cask, and the annular space is taken up by tubes which serve as impact limiters for the side drop accident condition.

Design No. 2 has each element stored in a canister which is sealed by welding the cover, and this canister is the primary containment. Four canisters are stacked in the PB-2 cask and surrounded by an array of aluminum tubes which serve as impact limiters. The stacked height of the canisters is less than the length of the cask cavity; therefore, honeycomb or tubular impact limiters are installed at both ends to take up the axial void space.

When the cask is unloaded at ORNL, the operation must be performed in the fuel storage basin in the TURF facility, and with the first design the inner container lid must be removed under water. If the fuel handling canisters have leaked, gaseous fission products will escape as the container lid is removed and the container flooded. The pool area ventilating system is not presently equipped to handle high levels of airborne contaminants. To circumvent this problem, the inner container must have test ports for sampling and/or purging before the lid is removed, and this must be done under water. Also, after the fuel handling canisters have been removed, the inner container must be lifted to the pool surface and the remaining water pumped out before the container is placed in the decontamination pit.

Design No. 2 eliminates the inner container. The cask inner space can be tested for fission product release before being sent to the pool by using the test ports that are provided in the cask trunnion mounts. The cask can be purged if necessary and then unloaded in the pool.

The PB-2 cask was licensed for Peach Bottom fuel elements, with each element encased in an aluminum tube which had been Magnaform sealed to provide the primary containment. If each FSV fuel element is sealed in a

canister that has been welded to form the primary containments as proposed in design No. 2, the original licensing philosophy is more closely followed.

10.3. WELDED CANISTER DESIGN

The welded canister conceptual design is shown in Fig. 10-3. The 3/8-in.-thick end covers have a maximum stress of 10,200 psi when the external pressure is 25 psi. The maximum expected pressure is 15 psi when the canister is immersed in 30 ft of water in the fuel storage basin pool. Side stresses are accordingly very low (900 psi).

Results of preliminary calculations of the effect of the impact limiter tubes are shown in Fig. 10-4. The side impact load without the limiters would be about 370 G.

The use of a welded canister as the primary containment in the PB-2 shipping system provides handling and licensing advantages over the bolted inner container, as pointed out above, and is therefore the preferred design for use with the PB-2 cask. Welding provides a structural-metallurgical seal that is more reliable than a bolted cover and also eliminates gaskets or O-rings that would be subject to radiation damage. Handling at ORNL and ICPP is simplified and less hazardous (see Figs. 10-5 through 10-7).

The welding machine required at ICPP is a commercially available type automatic welder. The welding operation will likely require less time than handling gaskets and bolting remotely. After welding, the canister is pressurized and the weld is leak checked and the test port plug inserted. The opening device necessary at ORNL is envisioned as a turntable with a small saw or cutting wheel.

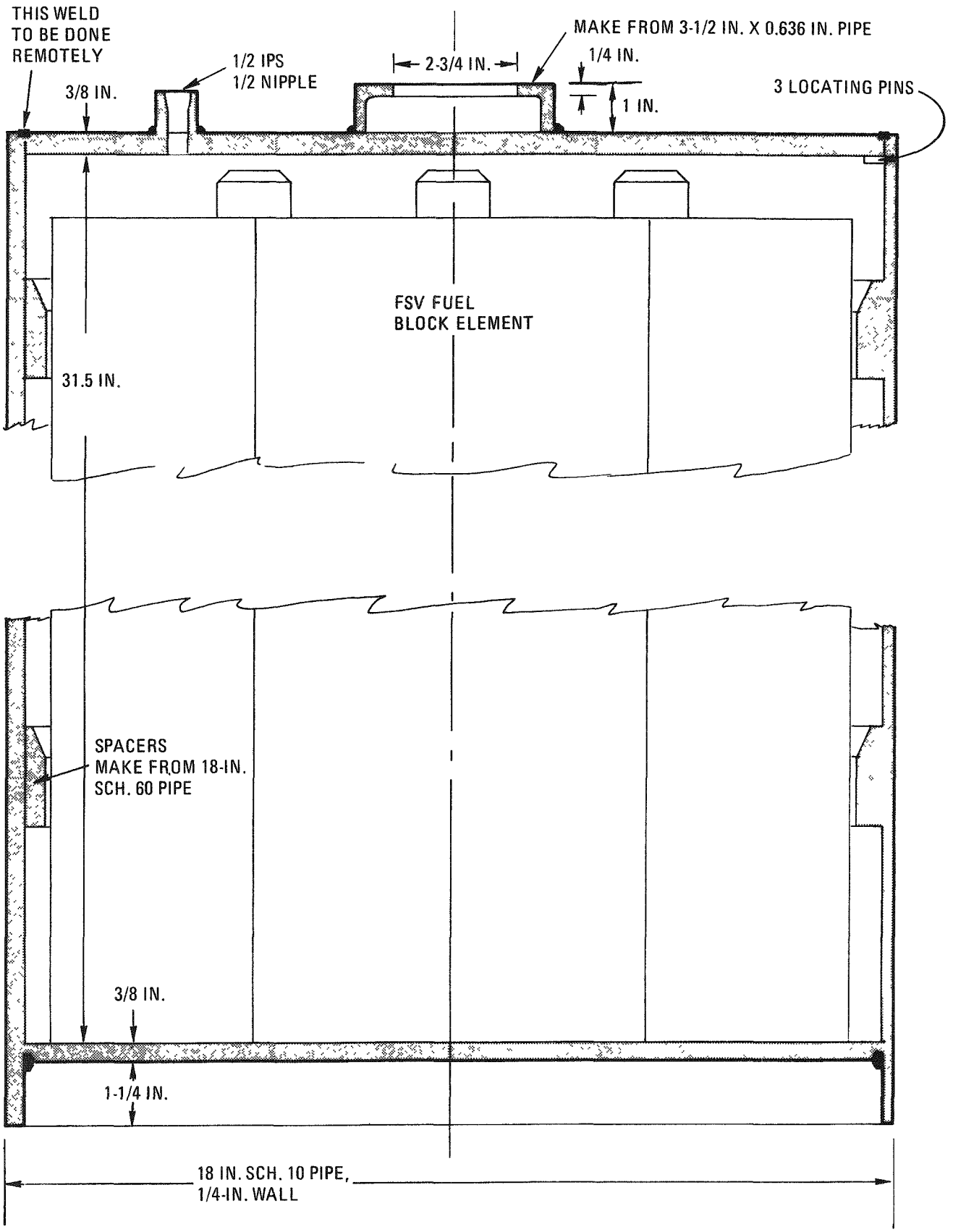

Fig. 10-3. Welded fuel handling canister

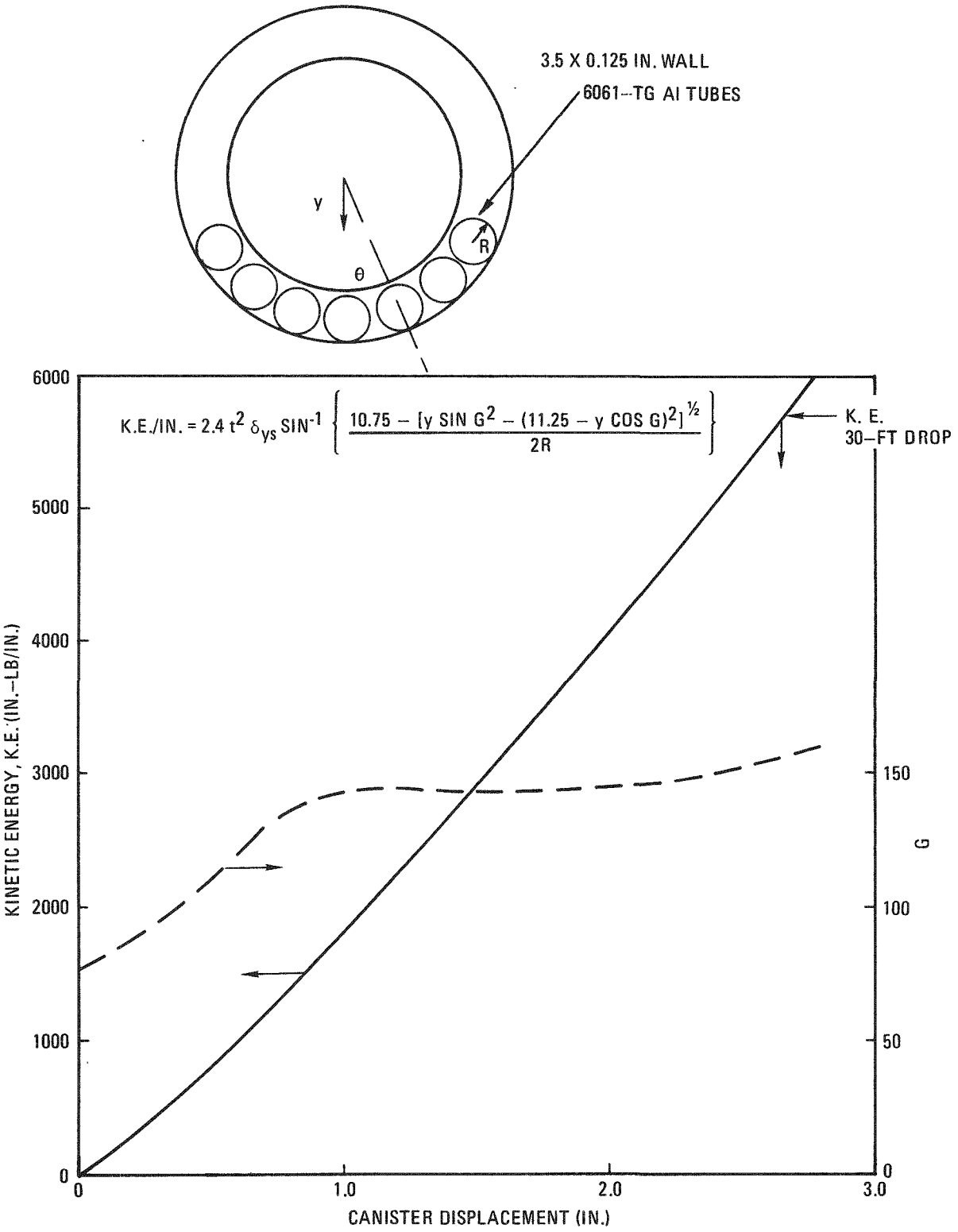

Fig. 10-4. Kinetic energy and "G" load of impact tube assembly versus displacement of fuel canister

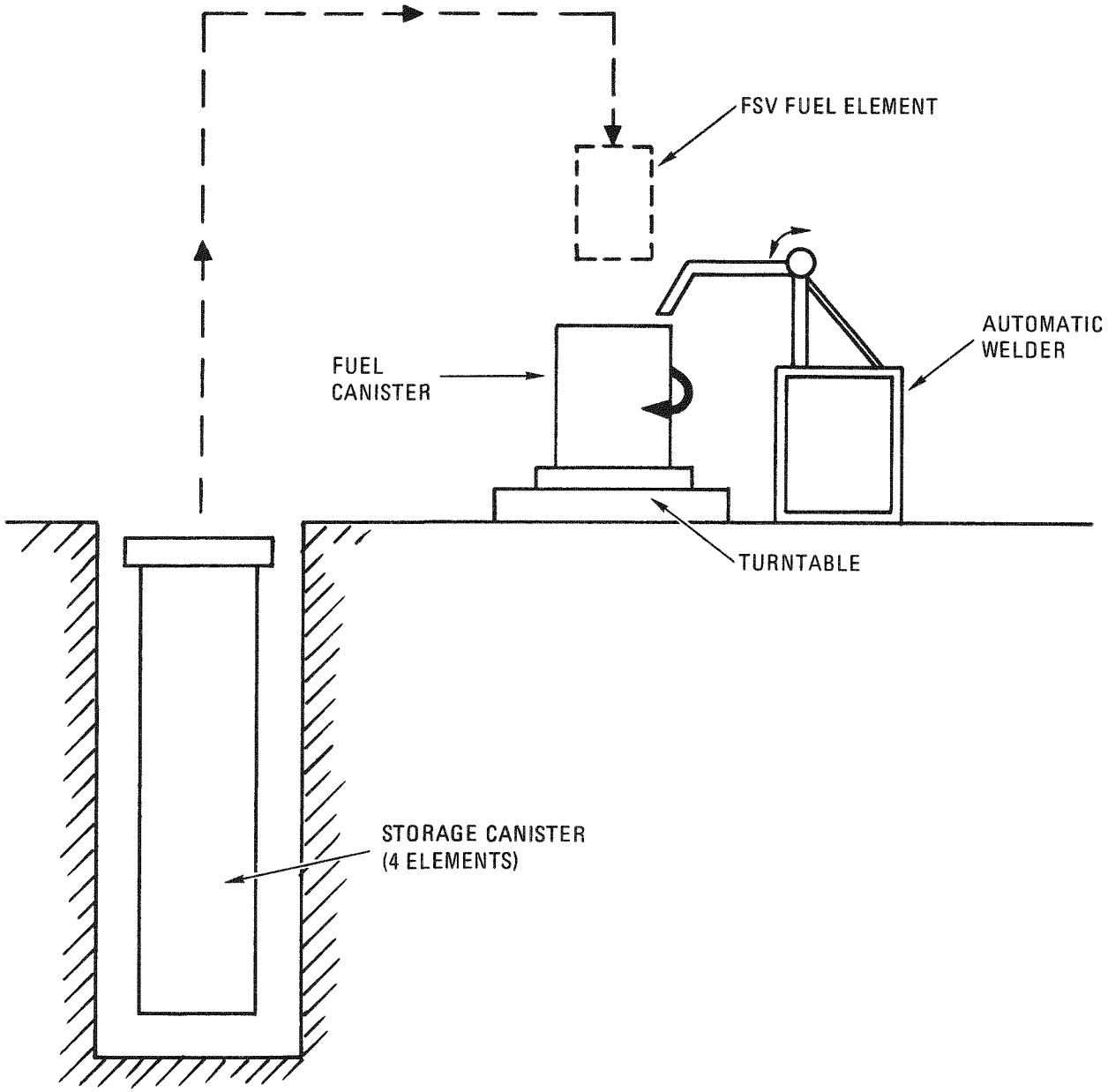

Fig. 10-5. Fuel handling at ORNL

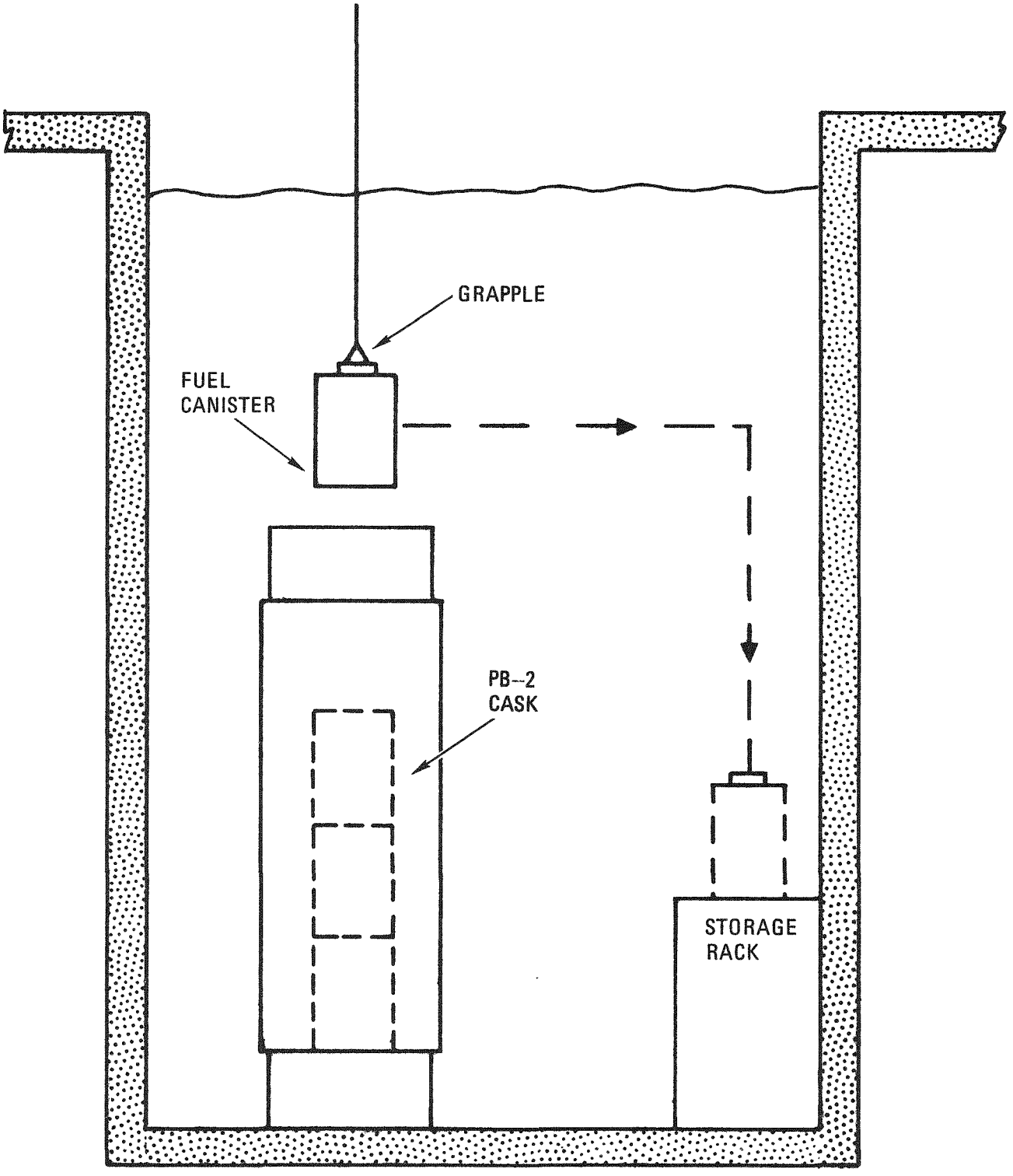

Fig. 10-6. Fuel storage basin at TURF

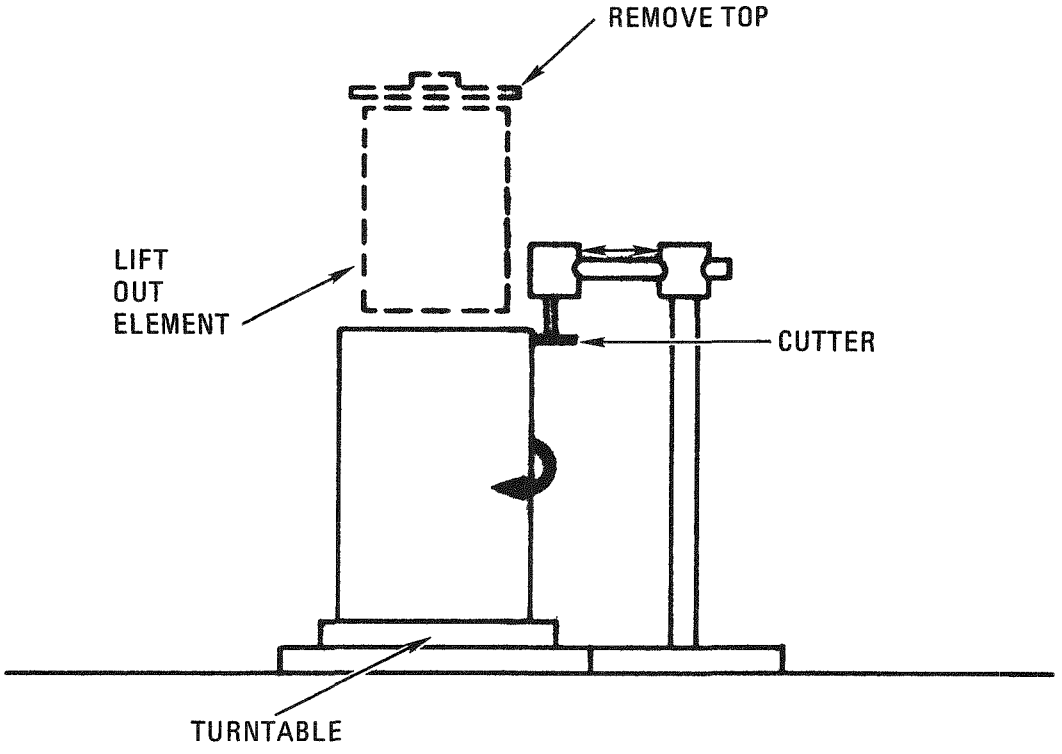

Fig. 10-7. Canister opening at ORNL

11. HTGR RECYCLE DEMONSTRATION FACILITY (HRDF)

11.1. REPROCESSING FLOWSHEET REVIEW AND MATERIAL BALANCE

This study is part of the continuing technology assessment to ensure that (1) the proposed HRDF flowsheet incorporates recent technology development improvements and new design data, and (2) supporting technical programs are apprised of flowsheet design issues requiring resoltuion. The updated reprocessing flowsheet is intended to become an approved baseline document for HRDF design definition and to provide guidance for technical development activities.

During this reporting period, HRDF flowsheets for the reprocessing head-end and off-gas treatment systems were revised to incorporate process and design improvements developed at GA and other sites during the past year. The flowsheet revisions made to date include a number of suggested changes which address specific design issues.

11.1.1. Head-End Process System

The basic function of the head-end process system of the reprocessing plant is to separate the fissile and fertile fuel particles from spent graphite fuel elements and to convert the fuel particles into uranium and thorium nitrate solutions for further processing in the solvent extraction system.

A block flow diagram of the HTGR fuel reprocessing flowsheet currently under development is shown in Fig. 11-1. Separation of the fissile and fertile fuel particles from spent fuel elements is accomplished by the head-end process system, which entails primarily a crush-burn-leach operational sequence. The spent fuel elements are crushed in a three-stage size

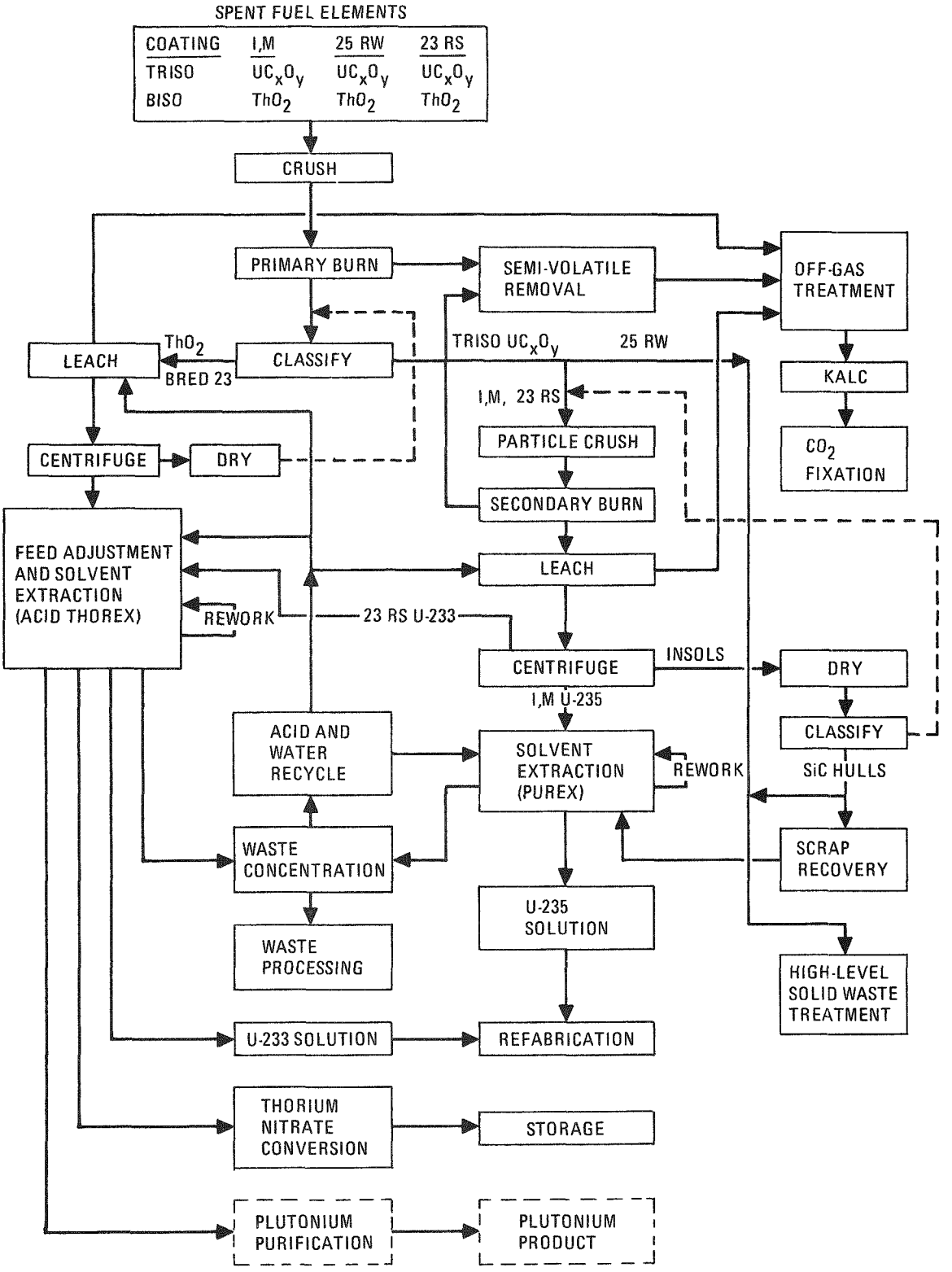

Fig. 11-1. Reprocessing flow diagram

reduction unit to provide feed material for a fluidized-bed primary burner which removes the fuel element graphite moderator and outer carbon coating of the fuel particles by conversion to CO_2. The remaining fuel particles are separated into SiC-coated fissile and burned-back fertile particle fractions by pneumatic classification. The burned-back fertile particle fraction is dissolved in a Thorex - nitric acid solution; the leachate is clarified from insolubles by centrifugation and routed to a feed adjustment step for subsequent solvent extraction processing to remove fission products and to separate fissile and fertile fuel values. The partially burned-back SiC-coated fissile particle fraction is crushed to expose the fuel for completion of the carbon elimination process in a fluidized-bed secondary burner. The fissile ash from the secondary burner is dissolved in nitric acid solution, insolubles are removed by centrifugation, and the clarified leachate is routed to feed adjustment for solvent extraction processing. Appropriate processing variations to the basic flowsheet are employed to reprocess FSV TRISO/TRISO fuel particles.

11.1.1.1. Basis for HRDF Head-End Flowsheet Review

The head-end system in the HRDF will reprocess spent initial and makeup (I,M) U-235-containing fuel elements from the FSV reactor and spent I, M, U-233 recycle (23RS) and U-235 recycle (25RW) fuel elements from other HTGRs. To accommodate differences in fuel particle design between certain FSV reactor core segments and the current reference LHTGR fuel design, the HRDF head-end process system will include processing flexibilities which are not readily apparent from the simplified block flow diagram in Fig. 11-1. However, these processing flexibilities are indicated in process flowsheets to be published in a topical report on this study. The process flowsheets describe the current baseline concept for the HRDF head-end process system.

The HRDF will process a number of HTGR fuel element types, e.g., standard elements, control elements, and half-size elements. Material balance tables which will be associated with each process flowsheet are

based on the reprocessing of standard U-235-containing makeup elements and are representative of typical LHTGR spent fuel compositions and fuel element block flows to be expected for the HRDF. Both the typical material flows and variants thereof, which will be experienced in the HRDF because of the variety of HTGR fuel element designs to be reprocessed in this facility, will be discussed more fully in a topical report (Ref. 11-1).

The HRDF head-end process system will be designed to reprocess 10,000 spent fuel elements annually during Phase I operations, with a design capacity of 43 elements each day, 233 days per year. A second head-end process system of identical capacity will be added for Phase II operations of the HRDF. The material balance tables associated with the process flowsheets will correspond to an annual throughput of 10,000 spent LHTGR standard fuel elements. Head-end system capacity is based on 80% equipment availability, 90% equipment utilization efficiency, and 30 days per year allowance for customer accountability, sweep-down, and sampling operations. Surge capacity will be provided in the HRDF head-end process system to enhance continuous operation of this and related process systems and subsystems. Surge capacity, including, for example, particle leach liquor receiver/surge/accountability tanks and equipment units, will be indicated on process flowsheets but not defined in terms of capacity per unit or number of units required. With the exception of several major processing units, e.g., typical operating cycles for primary and secondary burners, similar simplification will be applied to the process equipment for the HRDF head-end system. It should perhaps be pointed out that typical operating cycles which will be described for the burners are not necessarily exhaustive for HRDF conceptual design. For example, the proposed mission for HRDF includes the sporadic processing of atypically small customer lots of certain element types, as well as processing of TRISO-coated FSV fertile particles through the normally fissile-particle-oriented crush - secondary burn - leach sequence. For a number of process-variant reasons similar to these, the process flowsheets will illustrate the flexible baseline processing concept for the HRDF head-end and can serve as a starting point for HRDF conceptual design.

11.1.1.2. HRDF Head-End Operating Mode

The head-end system is designed to operate semicontinuously during processing of a customer spent fuel lot, which typically corresponds to a reactor half-segment [approximately 500 elements for the 1160-MW(e) HTGR]. The half-segment operating mode reduces fuel storage requirements and may be necessary to accommodate refabrication turnaround schedules. Customer accountability requirements are satisfied by campaign processing of a customer's fuel elements, daily sampling of accountability tanks, and a final sweep-down of the head-end system at the completion of each customer spent fuel lot.

The duration of batch operations during processing of a customer spent fuel lot is principally determined by the operating characteristics and cycles of key processing subsystems, such as the crushed fuel element (primary) burner, crushed fuel particle (secondary) burner, and fertile particle leacher. Surge capacity between each subsystem will provide a high degree of flexibility and will make head-end system operation less sensitive to operating upsets or equipment failure.

11.1.1.3. Technical Issues and Resultant Flowsheet Changes

In prior review of the head-end reprocessing flowsheet (Ref. 11-2), a number of technical design issues were highlighted for future study and resolution. Attention during the current flowsheet review activity is being focused on addressing major technical issues which impact on:

1. Head-end processing efficiency, yield, and safety.
2. Reduction of U-233/U-235 crossover.
3. Effect of head-end processing methods on downstream processes and resultant products (specifications).

An objective of the current flowsheet review is the incorporation of the results of recent Thorium Utilization Program technology developments

and design studies, as well as the highlighting of significant flowsheet design issues which require confirmation and resolution by continuing development and engineering studies. Major changes made in the head-end process flowsheet concept are summarized in Table 11-1.

The flowsheet review activity also served to update the prior head-end process system flowsheets by incorporating a number of current operating modes and new design data. The significant changes to the flowsheet include:

1. Addition of screening/oversize roll crusher equipment as an adjunct to the UNIFRAME fuel element crusher subsystem.

2. Utilization of the UNIFRAME CO_2 purge stream as the conveying medium for the crusher subsystem product.

3. A change in the primary burner product discharge/product transport interface.

4. Use of internal direct cooling of particle hoppers by a CO_2 gas coolant stream, starting with the primary burner product and continuing up to the fissile particle crush-secondary burn flowsheet sequence, which will use a helium coolant stream.

5. Application of gravity cascade flow for material transfers from the particle crusher feed hopper to the secondary (particle) burner. Product removal from the secondary burner is accomplished by a vacuum transport method.

11.1.2. Off-Gas Treatment System

The off-gas treatment system process flowsheets were revised extensively in line with (1) conclusions and recommendations which were published in the previous quarterly report (Ref. 11-3) and (2) further off-gas studies pursued at GA during this reporting period.

TABLE 11-1
MAJOR CHANGES IN HEAD-END PROCESS FLOWSHEET CONCEPT

Description of Change	Reason for Change
Deletion of Thorex leaching of the fissile particle fractions of the primary burner product.	1. Minimization of U-235 cross-over to Thorex SX. Cross-over would result from leaching of broken fissile particles. 2. Reduction of adverse HM carbide effects on solvent extraction: a. Formation of organic acids, leading to emulsion problems in SX. b. Possible reduction of Zr-95 DF due to Zr-complex formation. 3. Potential effect of nitrate salts adhering to particles on secondary burner operation.
Incorporation of secondary pneumatic classification for the particle classifier overheads and bottoms.	1. Minimization of U-235/U-233 crossover by: a. Entrainment in overheads/bottoms. b. Particle breakage effects. 2. Need for upgraded classification efficiency because of deletion of fissile fraction leaching.
Recovery of uncrushed fissile/FSV fertile fuel particles from SiC hulls/insols following leaching of secondary burner product. Recovery by pneumatic classification.	This process step was implied but not specifically shown on prior flowsheets.
Recovery of fissile particles from fertile particle leacher/dried insols stream, by pneumatic classification.	Materials balance study shows possible loss of 1.4% of U-235 values in the insols stream.
Incorporation of closed loop helium purge/cooling gas system in fissile particle crush-secondary burn flowsheet	1. Minimization of decay heat constraints on particle hopper operation and design. 2. Assurance of elimination of uncontrolled oxidation reactions with pyrophoric crushed fuel particles.

Proposed major changes in the off-gas treatment are summarized in Table 11-2. In addition to the changes summarized in Table 11-2, the sequence of treatment units within the processing scheme was changed in several instances. Generally, the reason for such changes was (1) to remove certain off-gas species early in the treatment scheme to minimize their interference with the proper performance of downstream off-gas treatment units or (2) to reduce premature and undesirable adsorption of certain off-gas species on beds not intended for their removal. Review of the off-gas treatment system process flowsheets is continuing.

11.2. REPROCESSING YIELDS AND MATERIAL THROUGHPUT

This study defines the basis for material balances to accompany the reprocessing flowsheets described in Section 11.1. HRDF feed material characteristics are being defined, together with the projected paths of material through the reprocessing unit operations and to side streams such as off-gas and waste.

11.2.1. Reprocessing Feed Material - Fuel Element Definitions

The HRDF will be designed to process spent HTGR prismatic fuel elements plus pebble-bed fuel elements (Ref. 11-4). The uncertainties of the pebble-bed expected composition and form upon receipt at HRDF have precluded its inclusion in this brief study.

The average heavy metal and fission product content of various prismatic fuel feed materials is summarized in Table 11-3. "As-loaded," or "fresh," fuel content is also shown since the plant should be capable of handling unirradiated fuel elements, either possibly returned from a reactor or possibly from refabrication scrap recovery. Table 11-3 is only a partial list since initial fuel element loadings will vary from segment to segment for both FSV and Large HTGR fuel. Spent fuel composition will vary

TABLE 11-2
MAJOR CHANGES IN OFF-GAS TREATMENT FLOWSHEET CONCEPT

Description of Change	Reason for Change
Provision of separate off-gas treatment systems for primary (crushed fuel element) and secondary (particle) burners.	Primary burner off-gas represents nearly 95% of total off-gas flow, is high in CO_2, and is relatively low in activation and fission product gases. Secondary burner off-gas contains much higher concentrations of radioactive contaminants and represents a relatively small CO_2 off-gas stream.
Incorporation of sulfur removal unit in primary burner off-gas treatment system.	The presence of sulfur in the off-gas is expected to interfere with proper performance of the downstream CO/HT oxidizer.
Adsorption of iodine on silver zeolite beds, and bed regeneration by iodine stripping as HI gas. The hydrogen iodide is adsorbed on a lead zeolite bed which is periodically loaded out for disposal.	Silver zeolite is a more effective adsorbent for iodine than lead zeolite, which had previously been shown as the primary iodine removal unit. Lead zeolite is, however, an effective adsorber for hydrogen iodide.
Disposal of tritium by stripping from molecular sieve adsorbent, followed by condensation of HTO and tritium immobilization with Portland cement.	Allows regeneration and re-use of molecular sieve beds, minimizes bed load-out, and results in lower treatment cost.
Incorporation of hot air regeneration of the vessel off-gas radon holdup bed (synthetic mordenite molecular sieve).	Destroys adsorbed organic impurities and removes moisture, both of which adversely affect the holdup of radon on synthetic mordenite molecular sieve.
Inclusion of zeolite adsorption bed for moisture removal from the vessel off-gas stream, upstream to the radon holdup bed.	Protects the radon holdup bed (see above) by minimizing moisture break-through to the bed.
Incorporation of internal recycle of the CO/HT oxidizer exhaust.	Limits the incoming gas stream CO concentration to about 1% CO so that the catalyst bed does not reach damaging temperatures.

TABLE 11-3
AVERAGE FUEL ELEMENT DEFINITIONS - HRDF

Fuel Type[a]	Fuel Design[a]	Average kg/Fuel Element (approximate)					
		U Content		Th Content		Fission Products	Other Heavy Metal
		Fresh	Spent	Fresh	Spent		
Average - 6-yr Burnup (Ref. 11-5)							
FSV							
Segment 4	Fissile - TRISO $(Th,U)C_2$	0.62	0.23			0.54	0.02
Standard	Fertile - TRISO ThC_2		0.23	7.49	6.93	0.33	Trace
FSV							
Segment 9	Fissile - TRISO UC_xO_y	0.94	0.24			0.67	0.03
Standard	Fertile - TRISO ThO_2		0.35	11.11	10.26	0.50	Trace
Average - Loaded at Reload 9 - Discharged at Reload 13 - 4-yr Burnup (Ref. 11-6)							
Large HTGR							
Makeup	Fissile - TRISO UC_xO_y	0.83	0.22			0.58	0.02
Standard	Fertile - BISO ThO_2		0.26	8.55	7.94	0.35	Trace
Large HTGR							
23R	Fissile - TRISO UC_xO_y	0.68	0.16			0.50	Trace
Standard	Fertile - BISO ThO_2		0.26	8.55	7.94	0.35	Trace
Large HTGR							
25R	Fissile - TRISO UC_xO_y	2.10	1.40			0.43	0.17
Standard	Fertile - BISO ThO_2		0.26	8.55	7.94	0.35	Trace
Average - Loaded in Initial Core - Discharged at Reload 1 - 1-yr Burnup (Ref. 11-6)							
Large HTGR							
Initial core	Fissile - TRISO UC_xO_y	0.45	0.26			0.18	Trace
Standard	Fertile - BISO ThO_2		0.14	9.50	9.32	0.04	Trace
Average - Loaded at Reload 1 - Discharged at Reload 5 - 4-yr Burnup							
Large HTGR							
Makeup	Fissile - TRISO UC_xO_y	0.74	0.18			0.53	0.02
Standard (Ref. 11-6)	Fertile - BISO ThO_2		0.26	8.55	7.91	0.38	Trace
Large HTGR							
Makeup Top control[a]	Fissile - TRISO UC_xO_y	0.42	0.10			0.30	0.01
	Fertile - BISO ThO_2		0.15	4.87	4.51	0.22	Trace
Large HTGR							
Makeup	Fissile - TRISO UC_xO_y	0.32	0.08			0.23	Trace
Bottom control[a]	Fertile - BISO ThO_2		0.11	3.68	3.40	0.16	Trace

[a] Assumes per-rod loading equivalent to standard element.

depending on reactor loading and operating conditions. Control rod fuel elements are a part of all segments (the two shown at the bottom of the table give only a typical comparison). Special buffer zone elements with specialized fuel loadings are not included.

The averaging effect in Table 11-3 must be realized. A number of factors affect fuel loadings, including variations within allowable ranges in the fresh fuel loading specifications and the use of fuel rod blends to achieve desired loadings (typically 17-18 blends in fresh fuel, 15 blends in refabricated fuel). Spent fuel composition will vary according to core position, years of burnup, and operating history of individual reactors. The averages shown are derived from FSV as-loaded fuel data, and from Large HTGR designs projected for reactors of the Philadelphia Electric Unit type (Ref. 11-6). Owing to the complexity of variables affecting fuel element loadings and burnup, and to possible fuel design changes pending in General Atomic Lead Unit Plant studies, no attempt has been made to predict maximum throughput expected at various unit operations as a result of fuel element variations. Instead, throughput variations resulting from different types of fuel elements with average characteristics are being examined.

Since several processing unit operations in the head-end are dependent on more than the heavy metal and fission product content of the fuel, more detailed definitions have been developed for certain elements as shown by the example in Table 11-4. Fission product, carbon and heavy metal contents are derived from Ref. 11-6, and particle coating characteristics and densities are derived from arithmetic averages of mean value ranges specified in Ref. 11-7.

11.2.2. Reprocessing Feed Material Plant Daily Throughput Definition

HRDF daily throughput will vary depending on the type of fuel elements or mix of types being processed. The effect on different unit operations varies. For example, primary crushing is dependent on the number of fuel

TABLE 11-4
SPENT FUEL ELEMENT DEFINITION -
AVERAGE LARGE HTGR STANDARD MAKEUP ELEMENT:
TRISO-UC_xO_y FISSILE; BISO ThO_2 FERTILE

FUEL ELEMENT COMPOSITION (Refs. 11-6, 11-7)

Component			Weight (kg/FE)
Fissile particles (avg ρ = 2.16 g/cm^3)			6.45
Outer PyC coating		1.80	
Sic coating (1.5 kg Si)		2.10	
Inner PyC coating		0.95	
Buffer coating		0.57	
Kernel (avg ρ = 3.3 g/cm^3)		1.03	
	Fresh	Spent	
U	0.83	0.22	
Oxygen	0.03	0.03	
Carbon	0.18	0.18	
Fission products		0.58	
Other heavy metals (Pu = 0.01)		0.02	
Fertile particles (avg ρ = 3.15 g/cm^3)			15.86
Outer PyC coating		4.38	
Buffer coating		1.75	
Kernel (avg ρ = 9.5 g/cm^3)		9.73	
	Fresh	Spent	
U		0.26	
Th	8.55	7.94	
Oxygen	1.18	1.18	
Fission products		0.35	
Other heavy metals		0.00	
Carbon (including graphite fuel element, plugs, dowels, fuel rod matrix, shim			96.25
Boron			0.01
		Total Weight	118.57

TABLE 11-4 (Continued)

RADIOACTIVITY (Ref. 11-6)

	Ci/FE 180 Days After Discharge
Fissile fraction	35,690
Fertile fraction	48,930
Total	84,620

DECAY HEAT (Ref. 11-8)

	Watts/FE 180 Days Decay
Fissile fraction	156.2
Fertile fraction	182.9

elements and only slightly dependent on their composition (type of graphite, TRISO versus BISO, control element versus standard element). The primary burner operation is more dependent on composition (burnable carbon content, TRISO versus BISO), while secondary crushing and burning throughput is quite dependent on composition (quantities of particles, particle size distribution, coating characteristics). Dissolution and solvent extraction are dependent on heavy metal and fission product content.

In addition, operating efficiency and economic considerations may affect the mix of fuel elements contributing to throughput. For example, in examining the current HRDF schedule (Ref. 11-9), it is apparent that available feed material exceeds processing capacity for many years and hence operating decisions such as postponing the recovery of less valuable fuel will affect throughput. Decisions on reactor processing priorities can also have an effect. Table 11-5 illustrates the effect on types of fuel blocks available for processing when recycle for an individual reactor is delayed (cf. segment 7).

It has also been determined (Ref. 11-10) that in the early years of plant operation when new reactors are contributing to throughput, the U-235 throughput is quite high owing to low burnup of some initial core segments. As the plant becomes fully loaded, the U-235 throughput decreases significantly and is offset by increasing U-233 throughput as recycle U-233 begins returning through the plant.

Owing to all of the above factors, the approach being taken to establish a daily throughput basis for this study is to assume an equilibrium operating state several years after startup when more than 50% of the plant throughput consists of makeup elements initially loaded with fresh U-235. The detailed material balance can then be derived from a single element type, and variations can be projected at crucial process points by comparing the reference single element definition with fuel element definitions of other types and applying appropriate factors to the material balance at that point.

TABLE 11-5
TYPICAL MIX OF SPENT FUEL ELEMENTS
DISCHARGED FROM AN 1160-MW(e) HTGR
(ILLUSTRATIVE DATA ONLY)

	With Recycle at Reload 2			With Recycle at Reload 3		
Segment	IM	23R	25R	IM	23R	25R
1	1064			1064		
2	960			960		
3	960			960		
4	960			960		
5	1064			1064		
6	451	278	230	960		
7	527	346	86	19	624	317
8	497	431	32	602	326	32
9	578	457	29	617	418	29
10	499	431	29	499	431	29

11.2.3. Reprocessing Yields

The separation of HTGR fissile and fertile particles has two goals: (1) to provide a means of purging accumulated U-236 (a neutron poison) from the fuel cycle without undue penalties in loss of fuel values, and (2) to provide maximum recovery of fissile U-233 bred in the reactor to replace the need for fresh makeup U-235. The efficiency of particle separation within the processing plant and the ability to recover a maximum amount of useful fuel value in a purified form for refabrication have a strong bearing on HTGR reactor economics. Early definition of expected process performance is required to properly evaluate HTGR fuel cycles. Alternatively, the lack of representative irradiated HTGR fuel to obtain experimental verification of expected process yields precludes definition at this time. This study therefore is addressed to establishing reasonable goals for fuel separation and recovery and to identifying ongoing experimental plans and target dates for experimental verification. Work completed to date has identified fuel separation (classifier) efficiency goals based in part on particle breakage limit goals established for preceding unit operations. These goals will be used as assumptions in calculating material balances to accompany the flowsheet review (Section 11.1).

Particle breakage assumptions identified to date are summarized in Table 11-6. Experimental verification of these assumptions will come from unirradiated fuel data obtained in cold prototype operations and from comparative unirradiated and irradiated fuel data obtained in the Hot Engineering Tests at ORNL extrapolated to prototype equipment. Such verification will not be available until about 1985 on the present schedule (Ref. 11-5).

Classifier separation efficiency goals for Large HTGR fuel are identified as 1.5% crossover of whole fertile kernels and 75% crossover of broken fertile kernels to the fissile stream and 2% crossover of burned-back fissile particles (unbroken) to the fertile stream. Again, verification of these assumptions must await cold prototype and hot engineering test completion.

TABLE 11-6
PARTICLE BREAKAGE LIMIT GOALS - HRDF

Breakage Mechanism	BISO Fertile (%)	TRISO Fissile (%)	Total Particles (%)
Irradiation damage	0.4	0.7	0.5
Primary crushing	0.8	2.6	1.3
Transport (crush to burn)	0.2	2.0	0.7
Primary burning	0.1	4.5	1.4
Transport (burn to classify)	0.3	2.0	0.8
Classification	-	0.5	0.2
Total	1.8	12.3	4.9

Definition of fuel material loss, process impurity, and decontamination factor assumptions will be completed in the next quarter, and a final report and ccmpleted material balances are scheduled to be released in April 1977.

11.3. SPENT FUEL ELEMENT DECAY HEAT AND SOURCE TERM ANALYSIS

The analytical work on this task was completed and a draft report describing this work (Ref. 11-8) was prepared. This report is expected to be issued in January 1977. A summary from the report is presented below.

Decay heat, gamma dose rate, and neutron source strengths were determined for spent fuel elements from a High-Temperature Gas-Cooled Reactor (HTGR). The calculations were based on curie values reported in Ref. 11-6. Results were obtained for spent fuel elements from the initial core and from representative non-recycle and recycle reloads. The study was performed for fuel element decay times after reactor shutdown from 180 days to 10 yr. Tables of the isotopic results are given for both the fertile and fissile fuel particles in each fuel element type. In addition, ordered tables of the important isotopic contributors are presented with graphical presentations of the results.

11.4. SIMULATION OF REPROCESSING PLANT OPERATING MODES

This work is scheduled to begin in January 1977. The objective is to develop a computerized simulation model of the HRDF reprocessing plant. Specific problems to be studied and reported using the model are:

1. The effects of equipment reliability on system performance.
2. The dependence of system performance on the level of surge capacities available.
3. The effects of batch versus continuous operation on system performance.

11.5. HRDF REQUIREMENTS DOCUMENTS

During the quarter, the following HRDF Draft Requirements documents were reviewed and comments were forwarded to UCC-ND:

1. R-001, Requirements Tree and Traceability System
2. R-003, Level 0 - Plant
3. R-007, Level 1 - Reprocessing Facility
4. R-006, Level 1 - Refabrication Facility

REFERENCES

11-1. Holder, N. D., et al., "Reprocessing Yields and Material Throughput," General Atomic Company, to be published.

11-2. Abraham, L., et al., "Flowsheet Review for Production Reprocessing and Production Refabrication Requirements," General Atomic Company, unpublished data.

11-3. "Thorium Utilization Program Quarterly Progress Report for the Period Ending August 31, 1976," ERDA Report GA-A14085, General Atomic Company, September 30, 1976.

11-4. "HRDF Requirements Document, Level 0 - Plant," UCC-ND, September 2, 1976, unpublished data.

11-5. Criteria Document for HTGR Fuel Recycle Hot Engineering Test, Oak Ridge National Laboratory, UCC-ND, et al., October 1976.

11-6. Hamilton, C. J., et al., "HTGR Spent Fuel Composition and Fuel Element Block Flow," ERDA Report GA-A13886, General Atomic Company, July 1, 1976.

11-7. "HTGR Fuel Product Specification," ERDA Report GA-A13464, Issue B, General Atomic Company, unpublished data.

11-8. "Spent Fuel Decay Heat and Source Term Analysis," General Atomic Company, unpublished data.

11-9. "National Program Plan (Draft)," Appendix A, UCC-ND, October 1, 1976, unpublished data.

11-10. Holder, N., et al., "An Economic Analysis of U-235 Recycle in the HTGR," ERDA Report GA-A13836, General Atomic Company, July 15, 1976.

APPENDIX A
PROJECT REPORTS PUBLISHED DURING THE QUARTER

Wong, H. W., "Thermal Analysis of Reprocessing Particle Hoppers," ERDA Report GA-A14094, October 15, 1976.

APPENDIX B

DISTRIBUTION LIST

L. BROOKS	SV-101	J. F. WATSON	L-640
R. C. DAHLBERG	L-503	B. BAXTER	ORNL*
G. B. ENGLE	L-364	R. D. ZIMMERMAN	E-179
W. V. GOEDDEL	SV-101	M. H. MERRILL	L-510
A. J. GOODJOHN	E-217	H. C. CARNEY	E-086
T. D. GULDEN	L-444	A. H. SCHWARTZ	EA2-211
S. LANGER	TO-559	G. E. BENEDICT	E-249
G. B. MELESE d'HOSPITAL	TO-365	J. W. ALLEN	E-166
C. L. RICKARD	L-205	R. M. BURGOYNE	E-165
O. STANSFIELD	L-440	P. L. WARNER	E-167
H. B. STEWART	L-602	G. CHANDLER	E-161
J. J. SHEFCIK	E-244	N. W. JOHANSON	E-165
R. F. TURNER	L-507	J. S. RODE	E-174
R. C. NOREN	SVB-131	U-S PARK	E-243
B. YALOF	S-117		

LEGAL

WASHINGTON

15 DOCUMENT CENTER

171 TIC

---

*Room 215, Bldg. 4508
ORNL, P. O. Box X
Oak Ridge, Tenn. 37830

1 R. D. Thorne, Manager, SAN
U.S. ERDA
San Francisco Operations Office
1333 Broadway
Oakland, Ca. 94612

1 J. B. Radcliffe
PMRS-SD

1 Assistant Director, Commercial
Fuel Cycle Division of Nuclear
Fuel Cycle and Productions
U.S. ERDA
Washington, D. C. 20545

5 Chief, HTGR Fuel Recycle Branch
Division of Nuclear Fuel Cycle
and Productions
U.S. ERDA
Washington, D. C. 20545

2 Project Manager, HTGR Fuel
Reprocessing Development
Allied Chemical Corp.
P. O. Box 2204
Idaho Falls, Idaho 83401

1 Director, Reactor Division,
Attn: Fred E. Dearing
Oak Ridge Operations Office
U.S. ERDA
P. O. Box E
Oak Ridge, Tennessee 37830

1 Director, Advanced Gas-Cooled
Reactor Programs
Attn: P. R. Kasten
Oak Ridge National Laboratory
P. O. Box X
Oak Ridge, Tennessee 37830

1 C. E. Williams
Office of the Manager
Idaho Operations Office
U.S. ERDA
Idaho Falls, Idaho 83401

1 Barry Smith
Idaho Operations Office
U.S. ERDA
Idaho Falls, Idaho 83401

1 V.C.A. Vaughen
Chemical Technology Division
Union Carbide Co.
P. O. Box X
Oak Ridge, Tennessee 37830

1 W. D. Woods
1 E. E. Fisher
R. M. Parsons Co.
Pasadena, Ca 91124

1 Chong Lewe
Nuclear Utility Services
4 Research Place
Rockville, Maryland 20850

1 W. G. Price
Vice President - Generation
Delmarva Power and Light
800 King St.
Wilmington, Delaware 19899

1 J. D. Hornbuckle
So. Calif. Edison
P. O. Box 351
Los Angeles, Ca. 90053

1 G. F. Daebeler
Branch Head, Safety and
Licensing
1 R. F. Manty
Branch Head, Fuel Management
1 H. D. Honan
Philadelphia Electric
2301 Market St.
Philadelphia, Penn. 19101

1 P. U. Fischer
1 R. Finkbeiner
General Atomic Europe
Weinbergstrasse 109
8006 Zurich
Switzerland

1 Director, Office of Public Affairs,
U.S. ERDA
San Francisco Operations Office
1333 Broadway
Oakland, Ca. 94612

1 California Patent Group
U.S. ERDA
San Francisco Operations Office
1333 Broadway
Oakland, Ca. 94612

1 John Ganley
GAC Fuels Group
France
(via M. H. Merrill)

1 Mr. Claude Moreau
Commissariat a 1'Energie Atomique
Centre d'Etudes Nucleaires de Saclay
BP No. 2
91190 Gif-sur-Yvette
France

1 J. L. McElroy
Battelle Northwest Laboratories
P.O. Box 999
Richland, Washington 99352

1 Dr. K. Hackstein
HOBEG
6450 Hanau/Main
Postfach 787
Germany

1 Dr. D. Stoelzl
Hochtemperatur Reaktorbau Gmbh
Gottlieb-Daimler-Strasse 8
D-68 Mannheim - 1
Postfach 5360
Germany

1 K. Notz
Oak Ridge National Laboratory
Oak Ridge, Tennessee 37830

1 A. L. Lotts, Program Manager
Thorium Utilization Program
Oak Ridge National Laboratory
P.O. Box X
Oak Ridge, Tennessee 37830